The role of synapse-associated protein 102 in postsynaptic signalling, synaptic plasticity and learning

Peter Charles Cuthbert

Wellcome Trust Sanger Institute

Clare Hall

University of Cambridge

Dissertation submitted for the degree of Doctor of Philosophy

2005

Declaration

This dissertation is the result of my own work and includes nothing which is the outcome of work done in collaboration except as detailed in the text and below.

Blastocyst injections of targeted embryonic stem cells were performed by Jane Robinson. Assistance with PCR genotyping was given by Georgina Berry, David Fricker, Amanda Lunney, Elizabeth Sotheran and Emma Stebbings (Wellcome Trust Sanger Institute, Hinxton, Cambridgeshire, UK).

Electrophysiological experiments were performed by Ann Fink, Patricio Opazo and Tom O'Dell (Department of Physiology, University of California, Los Angeles, California, USA). Biochemical experiments on the MAP kinase pathway were performed by Marcelo Coba (Wellcome Trust Sanger Institute).

Mouse body weights were measured by Lianne Stanford, Hayley Cooke and Margaret Green (Wellcome Trust Sanger Institute). SAP102 mutant mice were tested in the water maze by Jamie Ainge (Division of Neuroscience, University of Edinburgh). All other behavioural testing was performed in collaboration with Lianne Stanford. Behavioural data analyses were performed by Lianne Stanford.

Peter Charles Cuthbert
September 2005

Acknowledgements

I owe a debt of gratitude to many people for their generosity in science and in friendship. I warmly and sincerely thank my supervisor, Seth Grant, for the opportunity to be part of an exciting research group and for his unfailing support and enthusiasm throughout my PhD. Noboru Komiyama has been a mentor and advisor like no other, giving freely his time, scientific knowledge and friendship. It has been truly a privilege to work beside him.

Other members of the lab, in Edinburgh and Cambridge, have gone out of their way to help me over the past few years. Doug Strathdee gave much valuable advice on molecular biological techniques and experimental strategies. Kris Dickson was always happy to engage in scientific discussion or help out with an experiment. Lianne Stanford was an enthusiastic collaborator and patient travelling companion. Chris Anderson taught me many aspects of immunohistochemistry and was always up for a laugh. Karen Porter's acerbic wit kept my feet on the ground and ego suitably deflated. Jane Robinson spent many hours looking after the mice. Jane Turner dealt expertly and efficiently with administrative issues. To everyone else in Team 32, thank you for your support, friendship and fond memories.

To my family, thank you for your long-suffering, unfailing support for my endeavours. Finally, to Claire, thank you for everything.

Peter Cuthbert

September 2005.

Abstract

N-methyl-D-aspartate receptors (NMDARs) are found at the postsynaptic membrane of glutamatergic synapses and play essential roles in brain development, plasticity, learning and memory. Synaptic activation of NMDARs is transduced to a large complex of intracellular postsynaptic proteins. Synapse-associated protein 102 (SAP102) is part of the MAGUK protein family whose members, including PSD-95 and PSD-93, interact directly with the NR2 subunits of NMDARs and appear to act as adaptors connecting the receptor to its intracellular signalling network. Truncating mutations in SAP102 in humans are associated with X-linked mental retardation, however the *in vivo* function of SAP102 is unknown.

This dissertation describes a gene targeting approach to elucidate the function of SAP102 in mice. A DNA cloning technique using homologous recombination in bacteria was adapted and found to provide a highly efficient and flexible tool for the production of large numbers of varied mutation types in different loci of the mouse genome. Targeting vectors were generated for the introduction of three different mutations into the SAP102 locus: a constitutive knockout; a reporter gene knock-in and a conditional mutation.

SAP102 knockout mice were generated and found to be viable and fertile with grossly normal adult brain morphology. Behavioural tests uncovered a deficit in spatial learning in the watermaze which, in contrast to PSD-95 mutant mice, could be overcome with training. SAP102 mice exhibited a specific, frequency-dependent deficit in NMDAR-mediated hippocampal synaptic plasticity, a possible physiological mechanism for learning, while basal synaptic function and NMDAR conductance were unaffected. A screen of postsynaptic protein phosphorylation states in SAP102 mutant mice showed a specific increase in phosphorylation of extracellular signal-related kinase (ERK), part of the MAP kinase signalling pathway.

Targeted mutations in SAP102 and PSD-95 were utilised to explore the functional relationship between the two proteins. PSD-95 mutants have evelated hippocampal expression of SAP102, while SAP102 knockouts have increased PSD-95 associated with NMDARs, suggesting a partial compensation in these two targeted strains arising from functional overlap between SAP102 and PSD-95. A SAP102/PSD-95 double mutation was lethal, indicating an important role for these proteins during development.

These data show that SAP102 is crucial for normal postsynaptic signalling, synaptic plasticity and learning and begins to shed light on the differential roles of NMDAR-associated MAGUKs in coordinating intracellular responses to postsynaptic activation. SAP102 null mice may prove a useful tool in discovering and testing treatments for human learning disability.

Abbreviations

A_n	Absorbance at a wavelength of *n* nanometres.
AMPA	α-amino-3-hydroxy-5-methyl-4-isoxazole propionate
AMPAR	AMPA receptor
BAC	Bacterial artificial chromosome
bp	Base pairs
BCA	Bicinchoninic acid
BSA	Bovine serum albumin
Dlg	Discs large protein
dNTP	Deoxynucleoside triphosphate
DAB	Diaminobenzidine
DMSO	Dimethyl sulfoxide
DNA	Deoxyribonucleic acid
DOC	Deoxycholic acid
DTA	Diptheria toxin A fragment
DTT	Dithiothreitol
ECL	Cyclic diacylhydrazide
ELISA	Enzyme-linked immunoassay
EM	Electron microscopy
EPSC	Excitatory postsynaptic current
EPSP	Excitatory postsynaptic potential
ES cells	Embryonic stem cells
FBS	Foetal bovine serum
FRT	Flp recognition target
hr	Hour

g	Gravity
GAP	GTPase activating protein
GAPDH	Glyceraldehyde-3-phosphate dehydrogenase
GEF	Guanine nucleotide exchange factor
GMP	Guanosine monophosphate
HEK	Human embryonic kidney
HRP	Horseradish peroxidase
IRES	Internal ribosome entry site
IQ	Intelligence quotient
Kb	Kilobase pairs
loxP	Locus of recombination in P1
LTP	Long-term potentiation
LTD	Long-term depression
LB	Luria Bertani
MCS	Multiple cloning site
mGluR	Metabotropic glutamate receptor
min	Minute
mRNA	Messenger RNA
NMDA	N-methyl-D-aspartate
NMDAR	NMDA receptor
NR	NMDA receptor subunit
neo	Neomycin phosphotransferase
NS-XLMR	Non-syndromic X-linked mental retardation
pA	PolyA signal sequence
PBS	Phosphate-buffered saline
PCR	Polymerase chain reaction

rpm	Revolutions per minute
PDZ	PSD-95/dlg/zona occludens-1
PGK	Phosphoglycerate kinase
PSD	Postsynaptic density
PVDF	Polyvinyl difluoride
RNA	Ribonucleic acid
RT	Reverse transcription
SAP102	Synapse-associated protein 102
SDS-PAGE	Sodium dodecyl sulphate-polyacrylamide gel electrophoresis
sharm	Short homology arm
SV40	Simian virus 40
SRF	Serum response factor
S-XLMR	Syndromic X-linked mental retardation
YENB	Yeast extract, nutrient broth
U	Units
UV	Ultraviolet
XLMR	X-linked mental retardation

List of figures

List of tables

Table of contents

Chapter 1

Introduction

1.1 Molecular mechanisms of brain function

What is the physiological basis of cognition? The full answer to this question requires nothing less than a detailed understanding of the characteristics of every molecule in the brain, how they interact to form operational signalling pathways, how that signalling impacts on neuronal function, how individual neurons are connected into information-processing networks and, finally, how neuronal networks interact with each other and the rest of the body to produce behaviour.

Among higher order cognitive functions, the ability to acquire, store and recall at will vast quantities of information about ourselves and the world around us is one which possibly contributes the most to our humanity. Memory impairment in human cognitive disorders has a severely deterimental impact on quality of life.

Types of memory

Memory can be divided into declarative and reflexive forms. Reflexive memory has an automatic quality and is not dependent on conscious cognitive processes. It includes storage of specific motor skills such as walking. Declarative memory requires conscious thought and involves cognitive processes such as evaluation, comparison and inference. It encodes specific autobiographical events and associations and can be described using specific declarative statements. For example, the memory of the year astronauts first walked on the moon is declarative (Kandel et al., 2000).

Declarative and reflexive memories are encoded by distinct areas of the brain. Lesions to the temporal lobe, and in particular the hippocampus, disrupt the ability to remember declarative events without affecting reflexive memories. This is demonstrated by the well-known case of patient HM, who, having undergone temporal lobe removal to treat epilepsy, forgets new faces so

rapidly and consistently he introduces himself to the same person hundreds of times over many years, each time as if they are a new acquaintance. He can rapidly learn new motor tasks but although in a later test his performance in the task will be retained he insists he has never performed the task before. The hippocampus seems to store declarative memories only for a limited period of time, after which they are consolidated to other areas of brain, since temporal lobe damage causes anterograde amnesia involving inability to remember new information, while pre-damage memories remain intact (Frankland and Bontempi, 2005; Milner et al., 1998).

The hipppocampus encodes declarative memories

Hippocampus-dependent memory formation is a valuable paradigm for understanding complex cognitive function. There is a wealth of clinical data on the consequences of hippocampal damage in humans (Milner et al., 1998) and there exist also a number of rodent memory tasks which rely on hippocampal function (Gerlai, 2001; Morris et al., 1982). Rodent hippocampal anatomy, including its structure, cell types and circuitry, is very well-characterised, as are physiological manipulations allowing modelling of plastic changes in the area. Decades of research using pharmacological and, more recently, genetic manipulations has provided much information on the biochemical processes underlying hippocampal neuronal network activity and hippocampus-dependent behaviour (Kandel et al., 2000).

1.2 Glutamatergic synaptic transmission

The majority of excitatory synapses in the central nervous system use glutamate as their neurotransmitter. Glutamatergic synaptic transmission is mediated by three types of ionotropic glutamate receptors, classified according to their agonist sensitivity: α-amino-3-hydroxy-5-methyl-4-isoxazole propionate (AMPA), N-methyl-D-aspartate (NMDA) and kainate receptors. AMPA receptors (AMPARs) open in rapid response to glutamate binding, allowing sodium ions

into the postsynaptic cell and mediating fast synaptic transmission. NMDA receptors (NMDARs) are unusual in requiring both ligand binding and membrane depolarisation for activation, the latter necessary to release the magnesium ions which otherwise block the channel (Nowak et al., 1984). This property of 'coincidence detection' makes them an attractive potential mediator for storing information about associated stimuli during learning (Blitzer et al., 2005). Once open, NMDAR channels are permeable not just to sodium and potassium but also to calcium, a crucial aspect of their function in activating intracellular signalling pathways to modify synaptic strength (Lynch et al., 1983; Malenka et al., 1988). Kainate receptors can be expressed both presynaptically and postsynaptically. At some synapses they support synaptic transmission along with AMPARs, while at others they act alone. In the hippocampus, activation of presynaptic kainate receptors in Schaffer collateral axons reduces their transmitter release onto CA1 dendrites (Huettner, 2003). Figure 1.1 shows the structure and operation of a glutamatergic synapse.

NMDAR expression patterns and activation properties

A functional NMDAR consists of two NR1 subunits and two NR2 subunits. There are four NR2 subtypes, designated NR2A, NR2B, NR2C and NR2D, each with their own expression patterns and activation characteristics (Dingledine et al., 1999; Ottersen and Landsend, 1997). NR2A and NR2B are predominantly expressed in the forebrain, particularly in the hippocampus, cortex and olfactory bulb. NR2B is more strongly expressed during the early postnatal period while NR2A is dominant during adulthood. NR2C is specific to the cerebellum and thalamus and NR2D is mainly expressed prior to birth (Wenzel et al., 1997; Wenzel et al., 1995). NR2A and NR2B-containing NMDARs have a stronger voltage-gated Mg^{2+} block than those containing NR2C or NR2D, making them more resistant to activation, and specific comparison between NR2A and NR2B subunits show that NR2A-containing receptors have higher open probability when exposed to a brief, synaptic-like pulse of glutamate (Erreger et al., 2005). The time taken for channel closing following activation also varies between subunits: NR2A-containing receptors

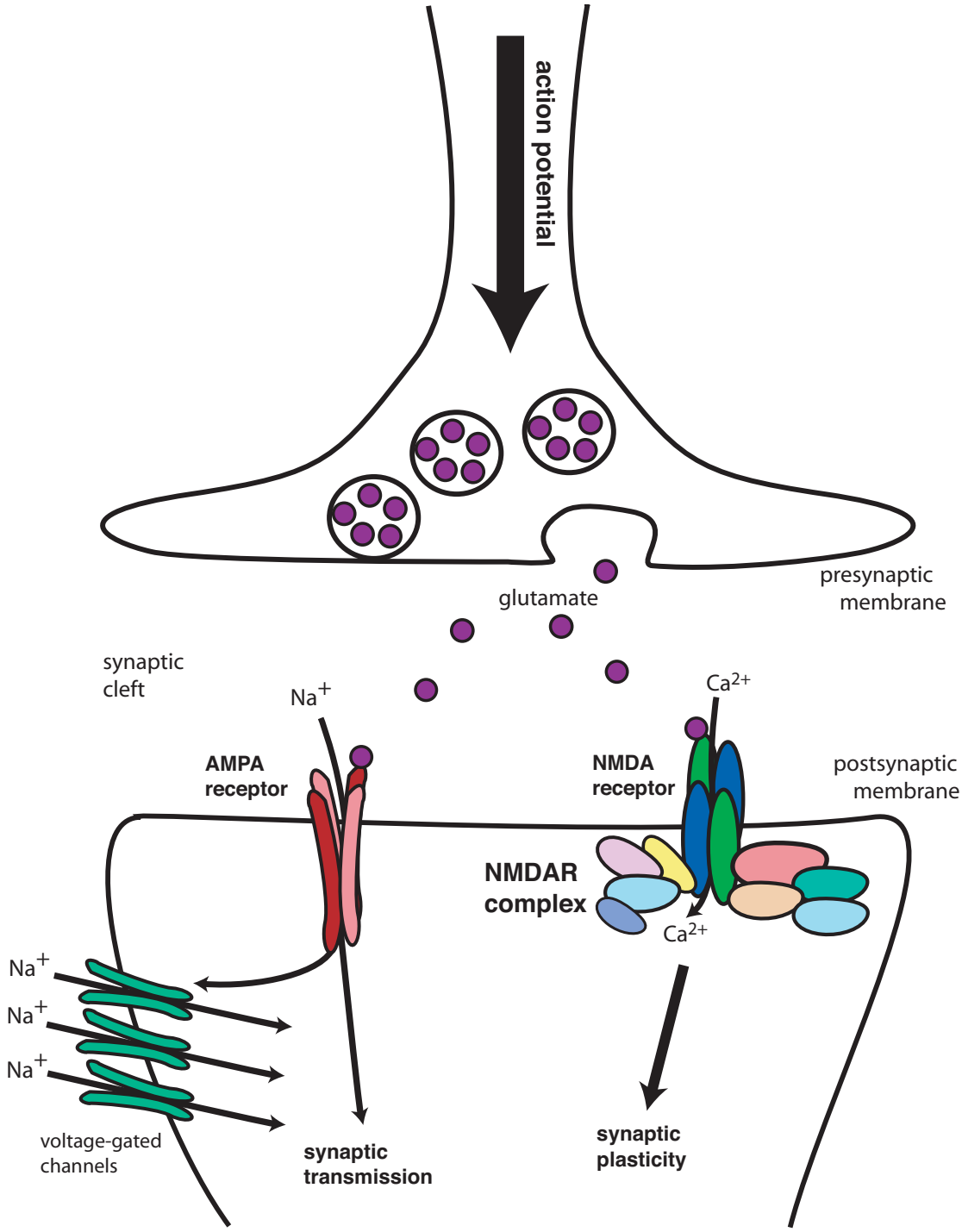

Figure 1.1 The glutamatergic synapse. Arrival of an action potential at the presynaptic terminal stimulates the fusion of synaptic vesicles with the presynaptic membrane and release of glutamate neurotransmitter into the synaptic cleft. Glutamate binding activates AMPA receptor channels, leading to an influx of sodium ions and depolarisation of the postsynaptic membrane. This in turn activates postsynaptic voltage-gated sodium channels further depolarising the membrane and leading to the generation of a new action potential. NMDA receptors are activated preferentially by intense presynaptic activation, since they require both glutamate binding and membrane depolarisation. Activated NMDARs allow an influx of calcium ions which stimulates NMDAR-associated postsynaptic signalling proteins, leading to synaptic plasticity and other modifications of neuronal function.

have the fastest decay time, while those containing NR2B and NR2C have decay time constants around 4-fold greater. NR2D-containing receptors take exceptionally long to close with a decay time constant 40-fold greater than NR2A-containing receptors (Monyer et al., 1994).

1.3 Synaptic plasticity

Information storage in the brain must necessarily be mediated by some persistant physical change in its components. One candidate for such a change is synaptic plasticity, the modification of the strength of a synaptic connection resulting in an increase or decrease in the sensitivity of the postsynapse to presynaptic activation. The origins of modern ideas on the relationship between synaptic plasticity and cognitive function lie in Donald Hebb's 1949 proposal of a physiological mechanism that could potentially translate repeated exposures to associated environmental stimuli into a physical modification of synaptic strength:

When an axon of cell A is near enough to excite a cell B and repeatedly or persistently takes part in firing it, some growth process or metabolic change takes place in one or both cells such that A's efficiency, as one of the cells firing B, is increased' (Hebb, 1949).

Long-term potentiation is a cellular model of synaptic plasticity

Hebb's theory was bereft of solid physiological basis until more than 20 years later, when Bliss and Lømo discovered that intense synaptic stimulation increases the response of those synapses to subsequent stimuli, a phenomenon called long term potentiation or LTP (Bliss and Lømo, 1973). In the decades since, research effort in this area has focussed on elucidating the physiological characteristics of synaptic plasticity, its molecular mechanisms and its relationship to cognitive function.

LTP is now known to occur at excitatory synapses in virtually every region of the brain but is best characterised in the stratum radiatum of the hippocampus at synapses formed between Schaffer collateral axons projecting from neurons in the CA3 area and the dendrites of CA1 pyramidal cells. In a typical experiment, a stimulating electrode is placed among the Schaffer collateral axons and a recording electrode in stratum radiatum. Baseline synaptic strength is determined by measuring field potentials from the recording electrode in response to repeated pulses low-frequency stimulation. Two pulses of 100 Hz tetanic stimulation are then given followed by a return to baseline stimulation. Potentiation of the slope of excitatory postsynaptic potentials (EPSPs) post-stimulation typically reaches around 150 % of the pre-stimulation level and lasts for several hours. The stimulation frequency threshold for LTP induction is around 5 Hz (Mayford et al., 1995). 1 Hz stimulation produces the opposite effect, a lasting reduction in synaptic response known as long term depression or LTD (Dudek and Bear, 1992).

NMDAR-dependent LTP requires calcium influx

An initial clue to the molecular basis of LTP came with the demonstration that its induction by tetanic stimulation in hippocampal CA1 is prevented by NMDAR antagonists (Collingridge et al., 1983). Pharmacological inhibition of NMDARs also prevents hippocampal-dependent spatial learning in the water maze and a role for NMDARs in these processes fits conceptually well with its coincidence-detecting capabilities (Morris et al., 1986). Low-frequency stimulation-induced LTD in hippocampal CA1 is also NMDAR-dependent (Dudek and Bear, 1992).

It is now known that influx of calcium through activated NMDARs is the critical event for inducing LTP. Most research has focussed on elucidating the mechanisms by which calcium entry leads to changes in synaptic strength. Early emphasis on possible presynaptic mechanisms for LTP induction by increasing transmitter release probability have now mostly given way to a focus on modifications to postsynaptic sensitivity to glutamate. Initial postsynaptic attention focussed

on increasing posttranslational modifications of AMPARs. In particular, LTP induction and/or NMDAR activation increases phosphorylation of GluR1 at ser-831 on its C-terminal tail by CaMKII and PKC, increasing its open channel probability, while LTD dephosphorylates ser-845 and produces the opposite effect (Malenka and Bear, 2004).

More recently it has become clear that the insertion and withdrawal of AMPAR subunits in and out of the postsynaptic membrane is a major mechanism for changing synaptic strength. LTP induction stimulates insertion of AMPARs into the membrane, increasing synaptic response, while LTD has the opposite effect (Bredt and Nicoll, 2003; Malenka and Bear, 2004).

1.4 NMDAR complex and signalling

Targeted mutations in mice have shown that NMDAR subunits and other constituents of the complex are crucial for many aspects of cognitive function including brain development, plasticity, addiction, learning and memory as shown in figure 1.2 (Grant and O'Dell, 2001).

The essentiality of NMDARs for neuronal function is highlighted by the phenotypic effects of their loss in mice (Sprengel and Single, 1999). Germline knockout of NR1 results in perinatal lethality, although the gross anatomy of the central nervous system at death appears undisturbed (Forrest et al., 1994). CA1-restricted NR1 conditional knockout produces viable mice which lack CA1 LTP and show spatial learning deficit in the water maze (Tsien et al., 1996b). Mice with a constitutive knockout of NR2A are viable but also display disrupted CA1 LTP and spatial learning (Sakimura et al., 1995). NR2B knockouts die perinatally from lack of a suckling response (Kutsuwada et al., 1996). Deletion of only the intracellular C-terminal of these subunits produces phenotypes similar to the full knockout, suggesting a default in intracellular signalling is responsible (Sprengel et al., 1998).

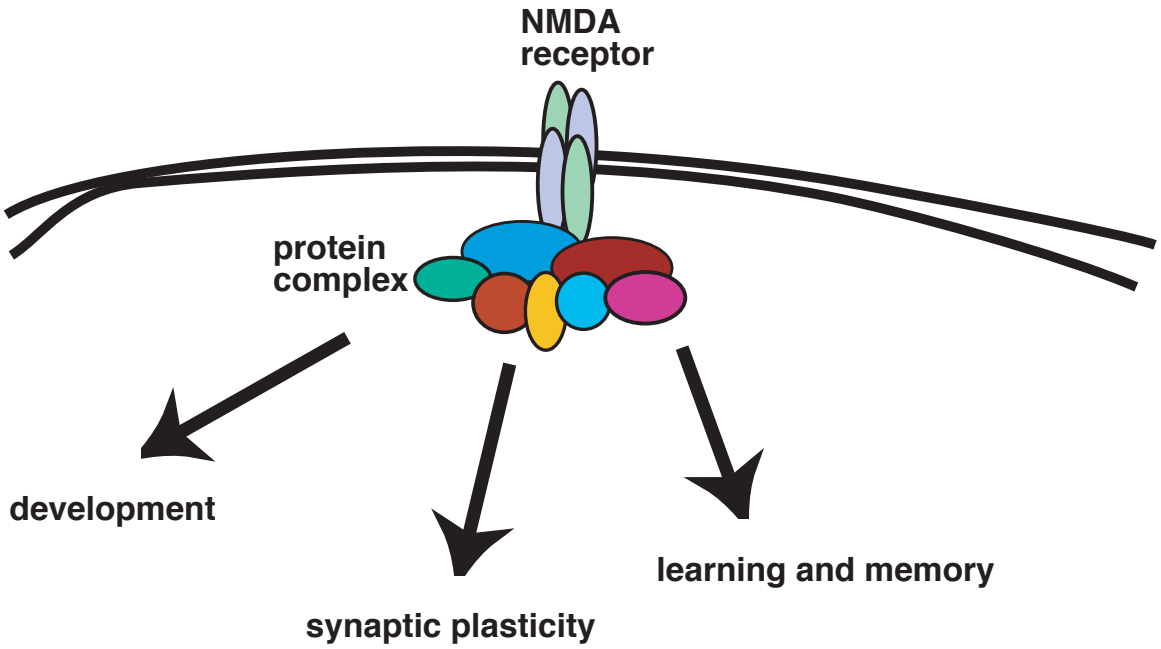

Figure 1.2 NMDA receptors are essential for many aspects of neuronal function. Activation of NMDARs is transduced to a large postsynaptic signalling complex containing adaptors, enzymes and cytoskeletal proteins. Signalling through the receptor and its complex is required for neuronal development, synaptic plasticity and complex cognitive functions.

Purification of NMDARs and their associated proteins show the receptors form part of a large signalling complex of more than 100 adaptors, enzymes and cytoskeletal proteins (Grant and O'Dell, 2001; Husi et al., 2000). The complex connects NMDARs to a multitude of intracellular signalling pathways and, through them, to various mechanisms for changing neuronal properties. The major mechanism by which NMDAR activation impacts on intracellular signalling is by influx of calcium through the open NMDAR channel pore. Calcium activates diverse signalling molecules including cAMP-dependent protein kinase (PKA), calcium/calmodulin-dependent protein kinase II (CaMKII) and the MAP kinase pathway. These changes can modify neuronal properties directly at the synapse, for example by altering postsynaptic sensitivity to glutamate through posttranslational modifications and trafficking of AMPARs, and indirectly through synapse-nucleus signalling to modify the cellular transcriptional programs, for example to alter synaptic structure (Blitzer et al., 2005; Malenka and Bear, 2004).

The interactions and priorities among the plethora of signalling molecules surrounding NMDARs are not well understood. What are the rules governing which pathway responds under what circumstances? The number and complexity of molecules and pathways implies that elucidation of the organising principles surrounding the complex will be a valuable step towards understanding its roles in neuronal function.

Correlations between synaptic plasticity and cognitive function

If the same synaptic plasticity mechanisms that underlie hippocampal LTP were also responsible for hippocampal-dependent spatial learning, manipulations that modified one would also alter the other. This prediction has been extensively explored using mice carrying engineered mutations in postsynaptic proteins. While, it is often the case that such mutations influence performance in both paradigms, no clear correlation has emerged. Null mutations in some genes, such as NR2A

(Tsien et al., 1996b), α-CaMKII (Silva et al., 1992a; Silva et al., 1992b), fyn (Silva et al., 1992a) and synGAP (Komiyama et al., 2002) result in LTP deficits and impaired spatial learning. Overexpression of NR2B produces elevated LTP and enhanced water maze performance (Tang et al., 1999). However, examples also abound in which only one or the other is affected, for example, GluR1 knockout ablates LTP but spares water maze performance (Zamanillo et al., 1999). IP3-kinase(A) knockout mice have enhanced LTP but unaltered spatial learning (Jun et al., 1998). Still other manipulations have apparently opposing effects on the two phenomena, such as mutations in PSD-95 which produce impaired spatial learning but enhanced LTP (Migaud et al., 1998). Clearly the value of LTP is as a model of cellular synaptic plasticity whose underlying mechanisms overlap with, but do not equate with, current spatial learning paradigms.

The MAP kinase pathway in NMDAR-dependent synaptic plasticity and learning

The Mitogen-Activated Protein Kinase (MAPK) pathway was originally described as a cascade inducing cellular division and differentiation in response to extracellular growth signals in non-neuronal cells (Pearson et al., 2001). The discovery of highly-expressed MAPK components in fully differentiated, post-mitotic neurons, however, indicated the pathway must play a somewhat different role in these cells and it is now known to be intimately involved in neuronal signalling in NMDAR-dependent synaptic plasticity, learning and memory (Sweatt, 2004; Thomas and Huganir, 2004).

In classical MAPK signalling, mitogens activate small G proteins like Ras by increasing its GTP-bound state. This is executed by changing the activity of GTPase Activating Proteins (GAPs) which inhibit Ras by enhancing its endogenous GTPase activity and Guanine Nucleotide Exchange Factors (GEFs) which activate Ras by catalysing the production of GTP from GDP. Ras-GTP activates kinases such as the Raf proteins which phosphorylate and activate

MAPK/ERK Kinase (MEK). MEK in turn phosphorylates extracellular signal-related kinase 1 and 2 (ERK1 and ERK2, also called p44 and p42 respectively). The ERKs are themselves serine/threonine kinases whose targets include transcription factors, cytoskeletal proteins, regulatory enzymes and other kinases which mediate cellular growth and differentiation. In neurons, intracellular calcium influx induced by NMDAR activation at glutamatergic synapses activates the MAPK pathway by a currently unknown mechanism (Ghosh and Greenberg, 1995; Thiels et al., 2002; Thomas and Huganir, 2004).

Blum et al. (1999) demonstrated that water maze training increases ERK phosphorylation in hippocampal areas CA1 and CA2 and that administration of the MEK inhibitor P098059 into the hippocampus before or after training impairs retention, but not acquisition, of spatial memories in the maze. Selcher et al. (1999) also found a requirement for hippocampal MAPK activation in water maze learning using the MEK inhibitor S327; in this case the intervention impaired both latency to reach the hidden platform during training and preference for the training quadrant in probe tests, but was only effective when administered prior to training. No impairment was observed during visible platform training. Infusion of P098059 into the entorhinal cortex also impairs spatial learning in the water maze (Hebert and Dash, 2002). SL327 administration one hour prior to training also inhibits hippocampal-dependent contextual fear conditioning (Atkins et al., 1998).

NMDA-dependent synaptic plasticity also requires MAPK activation: P098059 application to hippocampal slices one hour prior to tetanic stimulation greatly reduces both LTP induction and the consequential elevation of phosphorylated ERK levels (Davis et al., 2000; English and Sweatt, 1997). SL327 blocks both NMDAR-dependent LTD in CA1 of the hippocampus and its associated increase in ERK phosphorylation (Thiels et al., 2002).

Studies of the effects of MAPK activation during synaptic plasticity and learning implicate the ERK targets CREB, RSK2 and Elk-1 in activating downstream transcription. LTP induction results in phosphorylation of these targets along with induction of the immediate early genes zif268 and arc. These phosphorylation and transcriptional events are blocked by MEK inhibitor administration (Davis et al., 2000; Impey et al., 1998; Thomas and Huganir, 2004). MEK inhibitors also impair LTP induced by 5 Hz stimulation (Winder et al., 1999).

Opposing roles of NMDAR subunits in synaptic plasticity

Recent evidence suggests the NMDAR subunits NR2A and NR2B may play opposing roles in synaptic plasticity. Treatment of acute hippocampal slices with the NR2B-selective antagonists ifenprodil or Ro25-6981 blocks NMDAR-dependent LTD, but not LTP, in area CA1. In the same region, the NR2A-selective antagonist prevents induction of NMDAR-dependent LTP but has no effect on LTD (Liu et al., 2004; Massey et al., 2004). Biochemically, surface expression of the GluR1 AMPAR subunit is increased by NR2B antagonists and decreased by NR2B overexpression. In contrast, knockdown of NR2A by RNA interference (RNAi) reduces delivery of GluR1 to the cell surface and steady state levels of surface GluR1 (Kim et al., 2005). These results suggest LTP induction preferentially activates NR2A-containing NMDARs, leading to a consequent increase in the number of synaptic AMPAR channels, while LTD-inducing stimuli activate NR2B-containing NMDARs, stimulating AMPAR withdrawal from the synaptic membrane.

A possible mechanism for this phenomenon is provided by the observation that inhibition of NR2B by pharmacological antagonist or RNAi prolongs the NMDA-induced activation of the MAPK pathway constituents Ras and ERK (Kim et al., 2005). SynGAP, which inhibits MAPK signalling through its Ras GTPase activity, interacts with NMDARs through the PSD-95 family of Membrane-Associated Guanylate Kinase (MAGUK) proteins and preferentially associates

with NR2B-containing receptors (Kim et al., 2005; Sans et al., 2000). RNAi knockdown of SynGAP prolongs NMDA-induced ERK activation and reduces GluR1 cell surface expression (Kim et al., 2005). According to these data, then, low-frequency stimulation activates NR2B-containing NMDARs, stimulating synGAP which reduces MAPK activity, leading to synaptic withdrawal of AMPARs. High-frequency stimulation activates NR2A-containing receptors, leading to AMPAR insertion.

Further support for this hypothesis comes from experiments using the known activation characteristics of NMDAR subunits to simulate the responses of NMDARs to different types of synaptic stimulation. Under high-frequency, 100 Hz, tetanic stimulation the greater opening probability and faster rise and decay times of NR1/NR2A receptors means they contribute more to calcium influx than NR1/NR2B receptors, while the reverse is true for low-frequency, 1 Hz stimulation (Erreger et al., 2005).

There remain a number of issues surrounding this model that need explanation, however. Transgenic mice with forebrain-specific overexpression of NR2B display enhanced LTP with unaltered LTD (Tang et al., 1999). Other experiments indicate that robust LTP is possible even under strong pharmacological NR2A inhibition, particularly when induced by multiple tetanic stimuli (Berberich et al., 2005), and LTP can be partially induced in NR2A knockout mice (Sakimura et al., 1995).

1.5 The PSD-95 family of Membrane-Associated Guanylate Kinases

Interacting directly with the intracellular C-terminal tails of NR2 subunits of NMDARs is a family of adaptor proteins whose function may be crucial in organising the response of the plethora of PSD signalling proteins to synaptically-induced calcium influx. This is the PSD-95 family of proteins, which are Membrane-Associated Guanylate Kinases (MAGUKs) localised to

cell-cell junctions. MAGUKs are defined by a common domain structure with one or more PDZ (postsynaptic density-95/discs large/zona occludens-1) domains, a src homology 3 (SH3) domain and a guanylate kinase-like (GK) domain (Funke et al., 2005). The first MAGUK discovered was discs large (dlg) in *Drosophila*, which was initially identified as a recessive oncogenic mutation (Stewart et al., 1972) but not cloned until two decades later (Woods and Bryant, 1991). Its protein, DLG, is the sole *Drosophila* representative of the Postsynaptic Density-95 (PSD-95) family of MAGUKs, which in mammals consists of PSD-95, Postsynaptic Density-93 (PSD-93), Synapse-Associated Protein 102 (SAP102) and Synapse-Associated Protein 97 (SAP97, the mammalian homologue of DLG). PSD-95 family proteins carry three tandem PDZ domains each as shown in figure 1.3.

Domain properties

PDZ domains are modular protein-interaction domains which bind to short peptide motifs at the C-termini of other proteins. They are found in a variety of different proteins and often in tandem in multidomain scaffolding proteins which mediate formation of multiprotein complexes. PSD-95 family proteins carry type 1 PDZ domains which bind the C-terminal motif S/T-X-V (Nourry et al., 2003).

SH3 domains are also protein-interaction domains which occur in proteins of varied function. Unlike canonical SH3 domains, those in MAGUKs rarely bind to polyproline Pro-X-X-Pro motifs. Instead they interact intramolecularly with the GK domain and thus may regulate interactions between MAGUKs and their GK-binding proteins (Masuko et al., 1999).

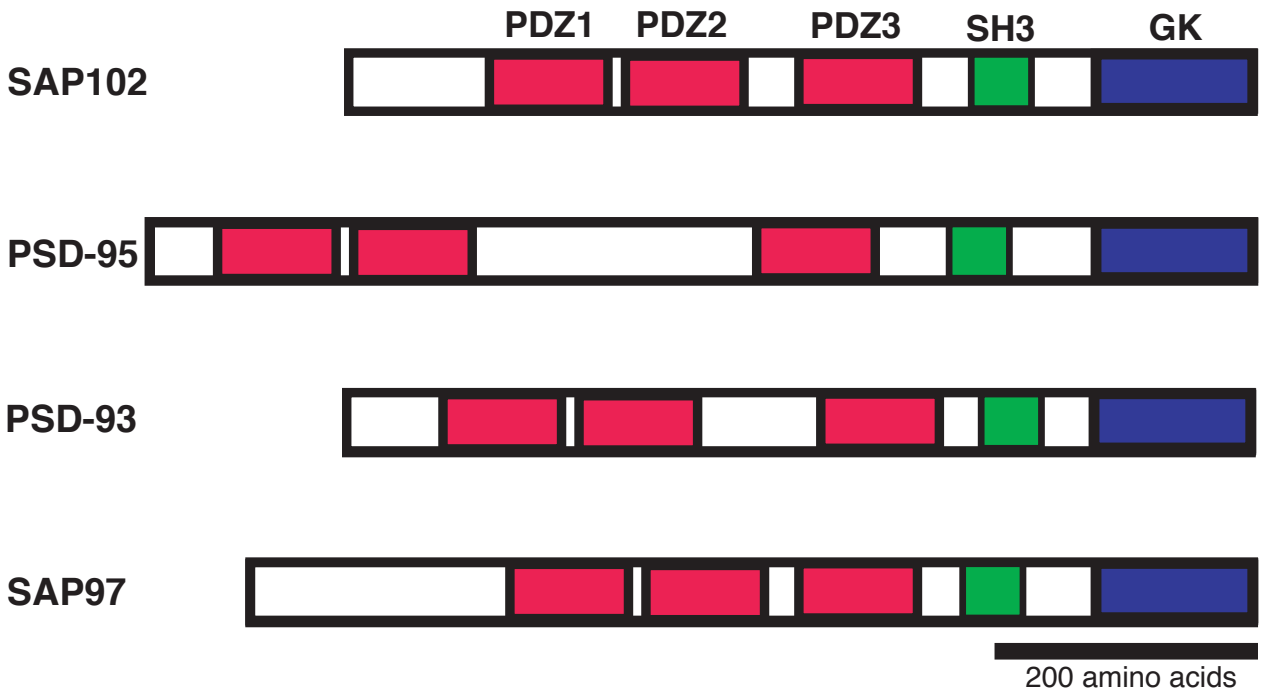

Figure 1.3 Domain structure of the PSD-95 family of Membrane Associated Guanylate Kinase proteins. Each member carries multiple protein-protein interaction domains including three tandem PDZ domains, an SH3 and a GK domain. SAP102, PSD-95 and PSD-93 are associated with NMDA receptors while SAP97 interacts with AMPA receptors. Adapted from Fujita and Kurachi (2000).

The MAGUK GK domain shares only 40 % sequence homology with the true yeast guanylate kinase and has lost its enzymatic capacity to produce guanosine diphosphate. An early study suggested that while the MAGUK GK domain could no longer interact with adenosine triphosphate (the phosphate group donor), it retained some capacity for binding to guanosine monophosphate (the reaction substrate) (Kistner et al., 1995) and there was even some suggestion of a possible role for the nucleotide in regulating GK-dependent PSD-95 protein interactions (Li et al., 2002). Further examination, however, failed to replicate these results and more convincingly showed a lack of GMP binding resulting from the loss of two conserved residues in the GMP-binding pocket of PSD-95 (Olsen and Bredt, 2003).

Regional expression patterns and subcellular localisation

MAGUK proteins are highly expressed in the brain. SAP102, PSD-95 and PSD-93 are most abundant in the hippocampus, cortex and olfactory bulb (Brenman et al., 1996; Fukaya et al., 1999; Fukaya and Watabe, 2000) while SAP97 is more highly expressed in the cerebellum (Muller et al., 1995).

The subcellular localisation of the MAGUKs has historically been the subject of some disagreement. Biochemical fractionation experiments showed a concentration of SAP102, PSD-95 and PSD-93 in the postsynaptic density (Brenman et al., 1998; Cho et al., 1992; Muller et al., 1996) - indeed, PSD-95 was discovered by virtue of its presence in this fraction (Cho et al., 1992) - and electron microscopic (EM) studies showed selective labelling of the postsynaptic junctional membrane (Aoki et al., 2001; Roche et al., 1999; Sans et al., 2000). However, early conventional immunohistochemical experiments presented staining in the cytoplasm of dendritic shafts as well as in neuronal perikayra (Bassand et al., 1999; Hunt et al., 1996; Kim et al., 1996). These data also appeared to contradict regional mRNA expression patterns shown by *in situ* hybridisation (Fukaya et al., 1999). The puzzle was eventually solved by the observation that protease

pretreatment of tissue sections prior to immunohistochemistry resulted in sharp, punctate, synaptic MAGUK staining patterns and empty dendritic shafts, in precise concordance with the EM and mRNA results (Fukaya and Watabe, 2000; Watanabe et al., 1998; Wenzel et al., 1995). The same problem in localising NMDAR subunits had been resolved by this method, suggesting that the inaccessibility of the PSD to antibodies may be to blame (Watanabe et al., 1998; Wenzel et al., 1995). It is now generally agreed that SAP102, PSD-95 and PSD-93 are postsynaptic, while SAP97 occurs both pre- and postsynaptically (Aoki et al., 2001; Funke et al., 2005).

Developmental expression profiles

In a comprehensive examination of the developmental expression patterns of NMDARs and their associated MAGUKs in the mouse hippocampus, Wenthold and his colleagues (Petralia et al., 2005; Sans et al., 2000) found intriguing correlations between NR2A, PSD-95 and PSD-93 on one hand and NR2B and SAP102 on the other. The former group is virtually undetectable by western blot at postnatal day 2 but increase their levels during postnatal development to be robustly expressed at 3 months of age. In contrast, the latter two are both expressed at P2, with NR2B declining during development and SAP102 expression increasing only moderately before levelling off at P35 then declining slightly through adulthood. These patterns are to a greater extent reflected in their respective mRNA levels during development (Fukaya et al., 1999; Monyer et al., 1994; Wenzel et al., 1997). These experiments suggest that SAP102 and PSD-95 may differentially facilitate the function of NR2B- and NR2A-containing NMDARs, respectively, and is consistent with the observations of distinct activation properties, signalling associations and roles in plasticity for the two receptor subunits.

At the synaptic level, immunogold electron microscopy examination reveals the developmental increase in hippocampal PSD-95 is a result of greater numbers of synapses containing the protein, while the number of molecules per synapses remains static. In contrast, both particles per synapse

and number of synapses labelled with SAP102 are at their maximum at P2 and decrease during postnatal development (Sans et al., 2000). This observation is at odds with the total developmental expression levels of SAP102 described above, but could possibly be accounted for by an increase non-synaptic SAP102.

Biochemical associations

Like the NMDAR subunits, SAP102, PSD-95 and PSD-93 are found in the cell membrane fraction of tissue protein extracts (Lau et al., 1996; Sans et al., 2003) and co-immunoprecipitation experiments show that MAGUK proteins associate with their respective glutamate receptors. SAP102, PSD-95 and PSD-93 co-immunoprecipitate with NMDAR but not AMPAR subunits, while the reverse is true for SAP97 (Cai et al., 2002; Garcia et al., 1998; Lau et al., 1996; Leonard et al., 1998; Muller et al., 1996; Sans et al., 2001). The correlated temporal expression patterns of SAP102 and PSD-95 with NR2B and NR2A respectively are recapitulated in their co-immunoprecipitation patterns, that is, more SAP102 co-immunoprecipitates with NR2B and more PSD-95 co-immunoprecipitates with NR2A, lending credence to the idea that each MAGUK supports the function of distinct NMDAR subtypes. The reciprocal experiment, immunoprecipitating each MAGUK and blotting for the receptor subunits, produces a similar result (Sans et al., 2000; Townsend et al., 2003). The C-terminal PDZ binding motif of NR2B also binds SAP102 preferentially over PSD-95 *in vitro* (Lim et al., 2002).

Immunogold double labelling electron microscopy of the NMDAR-associated MAGUKs at CA1 hippocampal synapses suggests it is not the case that distinct populations of synapses carry particular subsets of these proteins. SAP102 and PSD-95 double labelling shows some synapses contain one, some the other, and some both proteins with the proportion of double labelled synapses varies between 10 and 35 % according to their combined abundance at different developmental time points in what appears to be a random distribution of the two proteins.

Similar patterns are seen with other labelling combinations: the maximum proportion of synapses double-labelled for SAP102 and PSD-93 is 16 %, and for PSD-95 and PSD-93 is 33 % (Sans et al., 2000).

Clustering properties

Excitement surrounding the PSD-95 family was first elevated with the observation that PSD-95 possessed a striking ability to cluster the voltage-gated potassium channel Kv1.4 at the cell surface when the two proteins were co-expressed in heterologous cells, suggesting it may function to anchor ionotropic receptors in the synaptic membrane (Kim et al., 1995). This observation was quickly replicated in other laboratories with different cell lines, MAGUKs and membrane-bound receptors and the functional hypothesis was supported by the observation of co-localisation of the receptors and MAGUKs in mammalian neurons (El-Husseini et al., 2000a; El-Husseini et al., 2000b; Imamura et al., 2002).

The general observation is that a MAGUK or ionotropic receptor expressed in isolation in, for example, HEK cells, produces a smooth and uniform staining pattern throughout the cell cytosol. In contrast, co-expression of both the MAGUK and receptor results in co-localisation of the two proteins in clustered staining patterns on the cell surface. The two proteins co-immunoprecipitate with each other and the clustered receptor can be shown to be inserted into the membrane and functional by recording the appropriate ion currents into or out of the cell. Use of mutant receptors lacking the S/TxV binding motif at their C-terminus shows that these phenomena are dependent on interactions between the receptor and the PDZ domains of the MAGUK.

Similar methodologies have been used to show that PSD-95 clusters NR1 (El-Husseini et al., 2000a), the inward rectifying potassium channel Kir4.1 (Horio et al., 1997), the *ShaI* voltage-sensitive potassium channel family member Kv4.2 (Wong et al., 2002), the kainate receptor KA2

(Garcia et al., 1998) and the neuregulin receptor ErbB4 (Huang et al., 2002). PSD-93 clusters NMDA receptors and potassium channels (Kim et al., 1996). SAP102 does not cluster NMDA receptor subunits or potassium channels in heterologous cells, a property attributed to its lack of palmitoylation (El-Husseini et al., 2000b). It has been demonstrated, however, to cluster transfected Kv1.4 at postsynaptic sites in a PDZ interaction-dependent manner in hippocampal neuronal cultures (Firestein et al., 1999).

As will be shown later in this section, however, these results need to be interpreted with caution. A demonstration that two proteins can associate when overexpressed at high levels in a foreign cell by no means proves the interaction occurs endogenously and with functional significance in neurons *in vivo*. Where such a functional interaction does occur it still remains to be proven that the interaction is necessary for the observed phenotype, in this case receptor clustering.

Links with postsynaptic signalling pathways

Links between PSD-95 family proteins and specific postsynaptic signalling pathways currently rely almost exclusively on simple protein interaction data rather than more convincing demonstrations of altered signalling following disruption of MAGUK expression. For example, their association with synGAP implies a role in MAPK signalling. An exception to this is the observation that not only does PSD-95 interact with neuronal nitric oxide synthase (nNOS), but that antisense-mediated PSD-95 knockdown reduces nitric oxide production and NMDA-induced excitotoxicity in culture cortical neurons (Sattler et al., 1999).

Mutations in PSD-95 family proteins *in vivo*

MAGUK expression early in development suggests mice with mutations in these proteins might display developmental phenotypes and there is some evidence of this. SAP97 knockouts are perinatal lethal (Caruana and Bernstein, 2001). PSD-95 homozygous mutants survive but in

reduced numbers and many show delayed postnatal development, catching up in size only upon reaching adulthood at around seven weeks of age (Migaud et al., 1998). In PSD-93 mutant mice viability appears unaffected (McGee et al., 2001).

As a result of their clustering properties in heterologous cells, there has been much interest in whether loss of NMDAR-associated MAGUKs *in vivo* would lead to alterations in NMDAR synaptic localisation. In *Drosophila*, where DLG is the only PSD-95 family protein present, the neuromuscular junction contains two types of glutamate receptors, those containing the GluRIIA subunit and those containing GluRIIB. Dlg colocalises with these glutamate receptors at the postsynapse and flies with a loss-of-function *dlg* mutation exhibit loss of GluRIIB surface expression and concomitant decreases in glutamate receptor currents and spontaneous excitatory junctional currents. They also show an increase in single channel glutamate receptor currents, a phenotype observed in GluRIIB mutant flies (Chen and Featherstone, 2005).

In mammalian cells, however, only PSD-93 has thus far been proven necessary for mammalian ionotropic receptor localisation and then only in specific situations. In the forebrain and spinal cord, loss of PSD-93 results in reduced surface expression of NR2A and NR2B subunits, decreased NMDA component of EPSC amplitudes and lowered sensitivity to NMDAR-dependent neuropathic pain (Tao et al., 2003). In contrast, in cerebellar Purkinje cells, where PSD-93 is the only MAGUK expressed and there is thus no possibility for compensation from other family members, loss of PSD-93 has no effect on EPSCs or short term plasticity measured by paired pulse facilitation or depression, suggesting normal NMDAR localisation and function in these cells (McGee et al., 2001). A truncating mutation in SAP97 in mice which removes the SH3 and GK domains has no apparent effect on AMPAR subunit localisation in cortical neuronal cultures (Klöcker et al., 2002). In the hippocampus of PSD-95 mice no gross disruptions of NMDA receptor subunit distribution are evident at light or electron microscopic levels and NMDA-

induced currents and NMDA component of EPSCs are normal (Migaud et al., 1998). Neither is any disruption of high-density clustering of MAGUK-interacting voltage gated potassium channels Kv1.1, Kv1.2, Kv1.4 or Kvβ2 observed at juxtaparanodes adjacent the nodes of ranvier in the optic nerve where PSD-95 is the only MAGUK expressed (Rasband et al., 2002). These data are not exhaustive, but the emerging picture is that SAP97 and PSD-95 do not function to anchor their respective receptors at the synapse. There is as yet no convincing evidence for a requirement or lack thereof for SAP102 in postsynaptic receptor localisation or function.

MAGUK association with glutamate receptors and other signalling molecules at the postsynapse is also suggestive of involvement in emergent neuronal properties such as synaptic plasticity, learning and memory, however, phenotypic data of this type from mouse mutants is surprisingly patchy. Cerebellar postsynaptic currents and short term synaptic plasticity are normal in PSD-93 knockout mice as described above (McGee et al., 2001). Data on long-term synaptic plasticity is available only for PSD-95, where long-term potentiation (LTP) is strikingly enhanced in stimulation protocols of varied frequency, even with low-frequency (1 Hz) stimulation, such that LTD is effectively abolished (Migaud et al., 1998). The long term synaptic plasticity phenotype of PSD-95 mutant mice is shown in figure 1.4. There is no published data on the involvment of SAP102, PSD-93 or SAP97 in LTP. Data on learning behaviour in MAGUK mutants is available only for PSD-95 mice, which perform normally with a visual cue in the water maze but have impaired spatial learning in the hidden platform version of the task which cannot be improved by overtraining (Migaud et al., 1998).

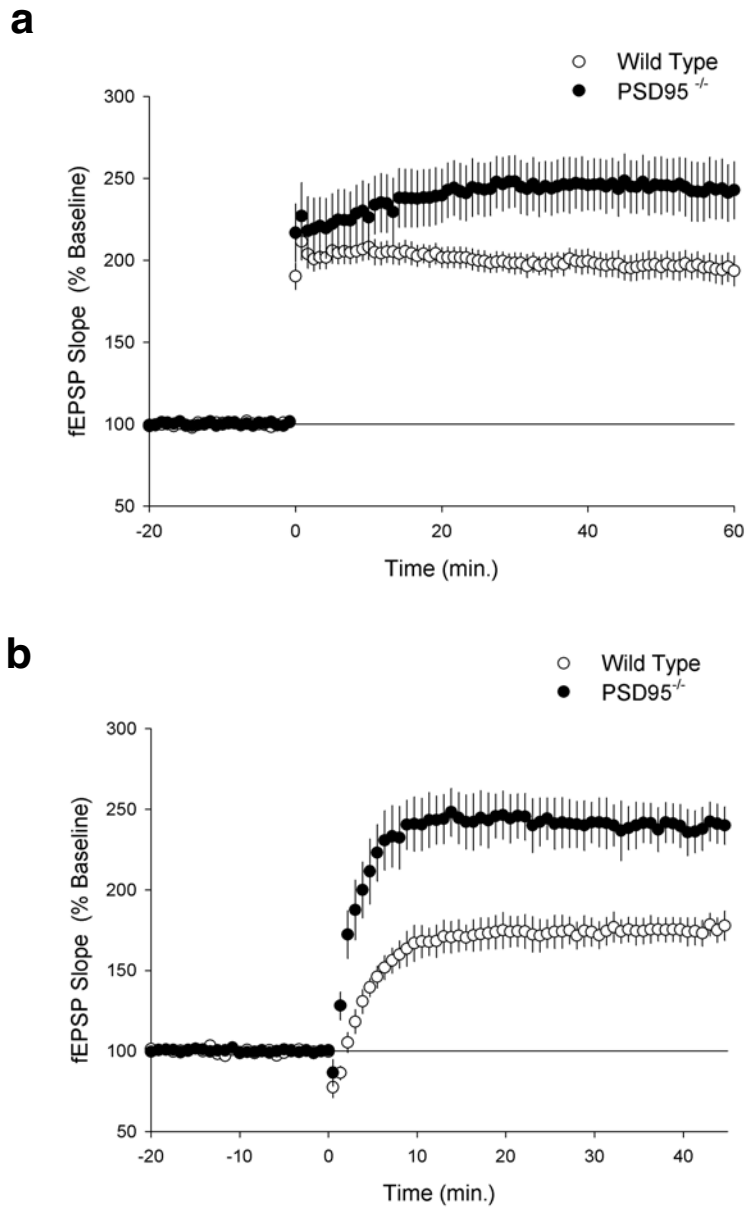

Figure 1.4 Enhanced NMDAR-dependent hippocampal synaptic plasticity in mice with a targeted mutation in PSD-95. Synaptic plasticity is measured here using long term potentiation (LTP), in which the strength of synapses formed between Schaffer collateral axons and CA1 pyramidal cell dendrites is increased following tetanic stimulation delivered at time zero. Potentiation of postsynaptic responses is observed after both **(a)** 100 Hz and **(b)** 5 Hz stimulation. From Migaud et al., 1998.

Hypotheses of the function of PSD-95 family proteins

Current knowledge of the properties of the PSD-95 family of proteins described above has led to two major hypotheses as to their function at the postsynapse (Fujita and Kurachi, 2000; Funke et al., 2005; Montgomery et al., 2004):

1. *Localisation and clustering of postsynaptic transmembrane receptors.*

This hypothesis arises from the observation that the family associates with numerous transmembrane proteins via their PDZ binding motifs and is able to cluster such proteins at the surface of neurons and heterologous cells.

2. *Organisation of intracellular postsynaptic signalling molecules in close proximity to relevant transmembrane receptors to facilitate efficient signal transduction.*

The need for proteins with such a function is suggested by the sheer number of signalling proteins in the postsynaptic density, the array of signalling pathways known to be sensitive to synaptic activation and the rapid response of these pathways to signals such as calcium influx through NMDARs. PSD-95 family proteins, linking multiple signalling molecules with transmembrane receptors, seem ideally placed to fulfill such a role.

1.6 Properties of SAP102

This dissertation focusses on the function of SAP102 (dlg3, neuroendocrine dlg, NE-dlg) as the PSD-95 family protein whose *in vivo* function remains uncharacterised. The following section describes in detail the current knowledge of SAP102 properties.

Expression patterns and localisation

As described above, SAP102 is predominantly expressed in the hippocampus, cortex and olfactory bulb in the brain. Northern and Western blotting of rat tissue fails to detect SAP102

mRNA or protein in liver, heart or muscle (Muller et al., 1996). In humans it has been reported as expressed in trachea, prostate, stomach, spinal cord, cardiac myocytes, islets of Langerhans and cell-cell junctions in the oesophageal epithelium, but absent from lung, liver, skeletal muscle, kidney, placenta, lymph nodes and proliferating cells such as basal oesophageal epithelial cells and cultured cancer cell lines (Makino et al., 1997). SAP102 is also expressed in the retina (Koulen, 1999; Koulen et al., 1998). Developmentally, SAP102 begins to be produced at P2 and increases over the following postnatal week before levelling off into adulthood (Monyer et al., 1994; Petralia et al., 2005; Sans et al., 2000; Wenzel et al., 1997).

Like NMDAR subunits, SAP102 is found in the membrane fraction of tissue protein extracts, being insoluble in Triton X-100, CHAPS and RIPA but soluble in SDS and DOC detergents (Lau et al., 1996; Sans et al., 2003).

Binding partners

SAP102 has numerous and varied interacting protein partners. It is unlikely the following list is complete, however, since many more proteins are known to bind to PSD-95. Most experiments in this area have been performed on only one or two of the three NMDAR-interacting PSD-95 family proteins, thus little is known about the potential differential interaction preferences; such investigations are likely to be valuable in elucidating distinct functions of SAP102, PSD-95 and PSD-93.

Transmembrane receptor binding partners

SAP102 interacts with several postsynaptic transmembrane receptors. These include the NR2A and NR2B subunits of the NMDAR (Garcia et al., 1998; Lau et al., 1996; Lim et al., 2002; Muller et al., 1996; Sans et al., 2003), the 5-HT2c subunit of the serotonin receptor (Becamel et al., 2004), the plasma membrane calcium ATPase 4b which maintains intracellular calcium

homeostasis by pumping calcium out of the cell (DeMarco and Strehler, 2001), the axon guidance molecular semaphorin 4C (de Wit and Verhaagen, 2003; Inagaki et al., 2001), the neuregulin growth factor receptor ErB4 (Garcia et al., 2000; Huang et al., 2002) and the low-density lipoprotein receptor megalin (Larsson et al., 2003). This diverse list is strongly suggestive of a role for SAP102 transmembrane receptor function, for example trafficking them to the cell membrane, anchoring them at particular sites after arrival and/or organising their associated intracellular signalling molecules.

Trafficking and adaptor protein binding partners

SAP102 has been implicated in the trafficking of NMDA receptors via its association with the transport protein Sec8. Sec8 is a member of the exocyst protein complex known to be involved in delivery of vesicles to the cell membrane for exocytosis. It binds to SAP102 via a C-terminal class I PDZ binding motif and co-immunoprecipitates from mouse hippocampal extracts with SAP102 and with NMDAR subunits. This association is formed in the endoplasmic reticulum. Overexpression of sec8 in COS cells, which express endogenous SAP102, results in clustering of NR1 subunits in a manner dependent on the sec8 PDZ binding motif. Sec8 overexpression also amplifies the spontaneous excitoxicity induced by co-expression of NR1 and NR2B; this effect is not observed when the PDZ binding motif of either sec8 or NR2B is mutated. In cultured hippocampal neurons, overexpession of a dominant negative form of sec8 lacking the PDZ binding motif decreases punctate, dendritic NMDAR staining and reduces both whole-cell NMDAR currents and synaptic NMDAR EPSCs. These data suggest that NMDARs are associated with sec8 and the exocyst complex via a mutual interaction with SAP102 and that this complex transports the receptor to the synaptic membrane (Sans et al., 2003).

SAP102 also interacts with stargazin, a protein required for delivery of AMPARs to the cell surface in cerebellar granule cells (Chen et al., 2000). However, since SAP102 is not

biochemically associated with AMPARs (Cai et al., 2002; Lau et al., 1996; Sans et al., 2001), the significance of this interaction is not clear. Cypin, another SAP102 interacting protein, may be involved in trafficking of MAGUKs themselves, since cypin overexpression leads to loss of SAP102 clustering in cultured hippocampal neurons (Firestein et al., 1999; Kuwahara et al., 1999). Cypin also interacts with tubulin and regulates dendritic outgrowth and branching in hippocampal neurons (Akum et al., 2004).

The adaptor proteins guanylate kinase-associated protein (GKAP) and SAP90/PSD-95-associated proteins (SAPAPs) 1-4 interact with SAP102 via its GK domain and may anchor it to the cytoskeleton (Kim et al., 1997; Takeuchi et al., 1997).

Signalling protein binding partners

Direct interactions between SAP102 and a number of postsynaptic signalling proteins suggests the MAGUK may ensure physical proximity between postsynaptic transmembrane receptors and their intracellular signalling networks. This could facilitate rapid signalling responses to receptor activation. Perhaps most intriguingly, SAP102 interacts with the synaptic Ras GTPase activating protein SynGAP, which links NMDARs to the MAP kinase pathway (Kim et al., 1998). Mice with a mutation in SynGAP show a deficit in LTP and spatial learning and enhanced activation of ERK in response to NMDA stimulation (Komiyama et al., 2002), suggesting SAP102 may mediate the physical association between NMDARs and MAPK signalling proteins for synaptic plasticity and cognitive function.

Further suggestion of SAP102 involvement in NMDAR-mediated cognitive function arises from its interaction with the tyrosine kinase Pyk2. Pyk2 activates Src kinase which phosphorylates NR2B. Increases in calcium concentration activate Pyk2 and LTP induction also activates Src and results in increased Src phosphorylation of NR2B. Inhibition of Src can inhibit LTP induction

(Seabold et al., 2003). Thus, SAP102 may hold Pyk2 close to NMDARs, allowing efficient signal transduction for synaptic plasticity.

There is also evidence for interactions between SAP102 and the guanine exchange factor kalirin-7 involved in dendritic morphogenesis (Penzes et al., 2001), the calcium signalling protein calmodulin (Masuko et al., 1999) and the tumour suppressor adenomatous polyposis coli (APC) protein (Makino et al., 1997).

Table 1.1 shows currently known SAP102 binding partners along with the SAP102 domain with which they interact and the experimental paradigm used to demonstrate binding. Only proteins for which there is a evidence for a direct interaction with SAP102 are shown. For example, the kainate receptor subunits GluR6 and KA2 co-immunoprecipitate with SAP102 from rat brain extracts and have been shown to bind the PDZ domains of PSD-95 *in vitro* (Garcia et al., 1998) but have not been shown to bind directly to SAP102.

Mutations in SAP102 cause XLMR

Recently, a large-scale exon-resequencing effort identified four families with NS-XLMR associated with truncating mutations around the second and third PDZ domains of SAP102. Affected males have moderate to severe mental retardation with IQ levels between 31 and 48, developmental delay and learning disabilities. No non-cognitive symptoms are apparent (Tarpey et al., 2004).

Table 1.1 SAP102 interacting proteins. Categories of evidence for interaction with SAP102 are: 1 – yeast 2-hybrid, 2 – co-immunoprecipitation from double-transfected heterologous cells, 3 - in vitro binding assay (3^a - overlay assay, 3^b - GST pulldown, 3^c - ELISA, 3^d - surface plasmon resonance 3^e – affinity chromatography with mass spectrometry or amino acid sequencing), 4 – co-immunoprecipitation of endogenous proteins from brain extracts.

Protein	Description	Function	SAP102 domain	Evidence	References
NR2A	Ionotropic glutamate receptor subunit	Excitatory synaptic transmission, synaptic plasticity	PDZ	3^a, 4	(Lau et al., 1996) (Garcia et al., 1998)
NR2B	Ionotropic glutamate receptor subunit	Excitatory synaptic transmission, synaptic plasticity	PDZ	$3^{a, b, c}$, 4	(Muller et al., 1996) (Sans et al., 2003) (Lim et al., 2002)
5-HT2c	G protein-coupled serotonin receptor subunit	Serotonergic synaptic transmission: mood, sleep, appetite	PDZ	3^e	(Becamel et al., 2004)
Kir2.2	Inward-rectifying potassium channel	Regulation and maintenance of cell excitability	PDZ	3^e	(Leonoudakis et al., 2004)
ErbB4	Neuregulin transmembrane receptor	Growth factor receptor. Regulates expression of voltage- and ligand-gated channels in neurons	PDZ	1	(Garcia et al., 2000) (Huang et al., 2002)
Semaphorin 4C	Transmembrane semaphorin	Axonal guidance	PDZ	1	(Inagaki et al., 2001) (de Wit and Verhaagen, 2003)
PMCA4b	Plasma membrane calcium ATPase	Maintenance of calcium homeostasis	PDZ	1, 2, 3^b	(DeMarco and Strehler, 2001)
Megalin	Low-density lipoprotein membrane receptor	Endocytosis, signalling	PDZ	1, 3^d	(Larsson et al., 2003)
PSD-95	Postsynaptic adaptor protein	Postsynaptic organisation, synaptic plasticity, spatial learning	SH3/GK	1, 3^b	(Masuko et al., 1999)
Sec8	Exocyst complex	Vesicle trafficking and exocytosis	PDZ	1, 3^b, 4	(Sans et al., 2003)
Stargazin	Relative of γ-1 calcium channel	AMPAR trafficking and localisation	PDZ	2	(Chen et al., 2000)
Cypin	guanine deaminase enzyme	Cytoskeleton assembly, regulation of dendritic branching, MAGUK trafficking	PDZ	2, $3^{b, e}$, 4	(Firestein et al., 1999) (Akum et al., 2004) (Kuwahara et al., 1999)
GKAP	Postsynaptic adaptor protein	Assembly of multiprotein complexes, anchoring to cytoskeleton	GK	1	(Kim et al.)
SAPAP	Postsynaptic adaptor protein	Assembly of multiprotein complexes, anchoring to cytoskeleton	GK	1	(Takeuchi et al., 1997)
SynGAP	Synaptic Ras-GTPase activating protein	MAP kinase signalling, synaptic plasticity	PDZ	1, 4	(Kim et al., 1998) (Komiyama et al., 2002)
Kalirin-7	Rac1 guanine nucleotide exchange factor	Dendritic spine morphogenesis	PDZ	1	(Penzes et al., 2001)
Pyk2	Tyrosine kinase	Src activation, synaptic plasticity	SH3	2, 3^b, 4	(Seabold et al., 2003)
Calmodulin	Calcium binding protein	Calcium signalling	SH3/GK	$3^{b, d}$	(Masuko et al., 1999)
APC	Wnt signalling	Tumour suppressor	PDZ	1, 3^b	(Makino et al., 1997)

1.7 Genetic approaches to elucidating gene function

The mouse as a model organism

The best method of analysing the function of a gene is to examine the phenotypic consequences of its loss *in vivo*. The mouse has long been a favoured model organism for such genetic ablation experiments as a result of its small size, short life cycle, prolific breeding capabilities and broad physiological similarity to humans (Capecchi, 2005; van der Weyden et al., 2002). This similarity applies to the brain, where the majority of neuronal structures, cell types and physiological processes found in the human brain are also present in the mouse (Kandel et al., 2000). Equally important for gene function analyses is the genetic similarity between the two organisms, an issue which has recently been become much clearer as a result of genome sequencing projects. The mouse genome contains 2.5 billion base pairs of DNA, slightly smaller than the human at 2.9 billion, but both contain approximately 30,000 genes and the identity of those genes is strikingly similar: 99 % of mouse genes have a human homologue. The broad structure of the two genomes is also similar, with around 90 % of each residing in unambiguously syntenic regions. Coding regions are well conserved at 85 % identity between mouse and human at the DNA level. Untranslated regions have 75 % identity and even introns 69 %. At the protein level, an analysis of nearly 13,000 1:1 orthologues (those with direct equivalents in the other genome which have arisen from the same ancestral gene) have 70.1 % amino acid identity (Consortium, 2001; Consortium, 2002).

Before the advent of mutagenesis technology, geneticists relied on finding naturally-occurring genetic mutations by looking for interesting inherited phenotypes in breeding colonies of mice. In this way the genetic bases of physiological traits such as coat colour, skeletal morphology and behaviour were studied long before the genes involved were cloned and characterised (Morgan et al., 1999; Rakyan et al., 2003; Zeng et al., 1997).

The mid-1980s saw the beginning of a revolution in mouse genetics with the demonstration that a piece of foreign DNA could be inserted into the mouse genome at a predetermined or 'targeted' location by homologous recombination in totipotent embryonic stem (ES) cells (Doetschman et al., 1987; Smithies et al., 1985; Thomas and Capecchi, 1987) and that those targeted ES cells, when injected into an early blastocyst, could contribute to the germline of a mouse (Capecchi, 2005; Schwartzberg et al., 1989; Thompson et al., 1989). With this technology came the ability to ablate any specific murine gene and examine its effect *in vivo*. The most common type of DNA construct now used to target a gene is the replacement vector. This consists of a plasmid containing a positive selectable marker for genomic insertion, flanked by sequences homologous to the site of insertion (homology arms). The plasmid backbone contains a unique restriction site for linearisation and a negative selectable marker such as herpes simplex thymidine kinase (HSVtk) or the diphtheria toxin A fragment (DTA) to discourage integration of the entire construct into a random genomic location. For targeting, the linearised vector is introduced into ES cells and undergoes homologous recombination, replacing the genomic target sequence with the targeting fragment (figure 1.5). Despite their lower targeting efficiency, replacement vectors are now more popular than the alternative insertion vectors for most targeting experiments because they do not involve a duplication of the targeted region, making genotyping and phenotype interpretation more straightforward (Ramirez-Solis et al., 1993).

Current possibilities for manipulating the mouse genome

The past 20 years has seen the efficiency of fundamental targeting technology develop sufficiently that the creation of knockout lines for all 30,000 genes in the mouse genome is now an achievable goal (Adams et al., 2004; Austin, 2004; Valenzuela, 2003). In parallel, expansion of the versatility of genetic manipulations has made available a wide array of strategies for

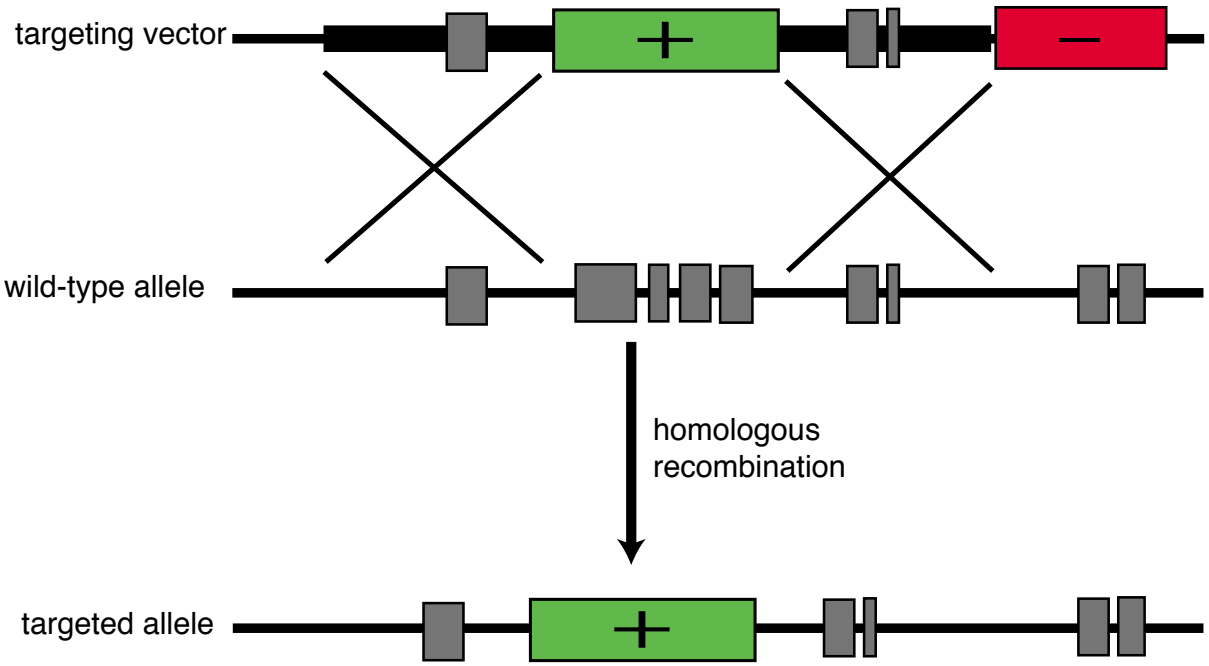

Figure 1.5 Gene targeting with a replacement vector. The replacement vector consists of a positive selectable marker (green box) flanked by regions of homology (thicker black lines) corresponding to the desired site its genomic insertion. Homologous recombination between the homology arms and their endogenous counterparts in the ES cell genome replaces the intervening sequence with the positive marker. Integration of the entire targeting construct at a random location in the genome results in insertion of the negative selectable marker (red box) and the death of the cell.

mutagenisation and it is now possible to make virtually any desired modification to the mouse genome.

Reporter genes such as lacZ can be inserted into a locus and placed under the control of an endogenous promoter to track the transcriptional patterns of a gene (Komiyama et al., 2002; Migaud et al., 1998). BAC transgenesis allows the insertion of an entire structural gene along with its regulatory elements for accurate expression profiles in the new genome (Heintz, 2001). Introduction of a single point mutation or replacement protein domain can be achieved by several different strategies. The double replacement method uses a replacement vector to first introduce positive and negative selectable markers then a second targeting to replace them with the required mutation (Cearley and Detloff, 2001). The hit-and-run method introduces the required mutation in an insertion vector alongside positive and negative selectable markers, then removes the markers and the insertional duplication by intrachromosomal recombination (Dickinson et al., 2000). Finally, a single replacement vector can be used to introduce the required mutation along with an adjacent (intronic) positive selectable marker which is later removed by site-specific recombination (van der Weyden et al., 2002).

The Cre/*loxP* and Flp/*FRT* site-specific recombinase systems allow creation of temporally- and spatially-restricted conditional deletions, described in the following section. Inducible overexpression of a gene can be achieved using the *tet* system, in which a transgenic tetracycline transactivator is driven by a tissue-specific promoter and becomes active upon binding to externally-administered tetracycline. The active transactivator interacts with a tet operator sequence which is located in a second transgene alongside a minimal promoter driving the gene of interest. Thus, the gene is expressed in reversible fashion only upon tetracycline administration and only in the tissue of interest (Gossen and Bujard, 1992; Sakai et al., 2002; Zhu et al., 2001b). Large structural modifications spanning several megabases of DNA can be introduced by

chromosomal engineering to recapitulate rearrangements that cause human cancers and other disorders (Yu and Bradley, 2001). RNA interference reduces, without ablating, the expression of a target gene (Carmell et al., 2002; Elbashir et al., 2001; Paddison et al., 2002; Paddison et al., 2004).

While the reverse genetics approaches above allow functional analysis of a specified gene, forward genetic strategies use random mutagenesis followed by phenotypic screening to identify sets of genes involved in a physiological process of interest. For example, adminstration of the chemical mutagen ethylnitrosurea (ENU) introduces point mutations at random in the genome. Mutagenised mice carrying the phenotype of interest, skeletal deformation for example, are then identified and the causative mutations positionally cloned (van der Weyden et al., 2002). Gene trap strategies involve insertional mutagenesis, where a reporter is introduced into genes at random, disrupting function and placing the reporter under control of the host promoter. Mutagenised cells displaying the phenotype of interest are selected and the disrupted gene identified by rapid amplification of cDNA ends (Stanford et al., 2001).

Engineering conditional mutations in mice using site-specific recombination

The advent of conditional mutations has been an important step in the development of gene function analysis technology. Ablating a gene in the germline and thus removing it from every cell of the animal throughout its lifetime is a valuable method of determining its broad physiological impact and is relevant for creating models of human disease, but it does not allow separation of the gene's function in different tissues or during different periods of development. The most severe example of this problem occurs when loss of a gene causes embyronic or early postnatal lethality, preventing examination of adult phenotypes. A recent example of this is Serum Response Factor (SRF), a neuronally-expressed transcription factor mediating activity-dependent upregulation of many immediate early genes including c-fos and c-jun. Mice with a constitutive knockout of SRF lack mesoderm and die around embryonic day 12.5 (E12.5),

showing the protein is crucial for normal development and survival but precluding an analysis of its role in the adult brain (Arsenian et al., 1998). Even if a constitutive knockout animal is viable, absence of a gene during development will regularly produce morphological or other abnormalities that may complicate examination of the effects of acute absence of the gene during later life. In the brain, a constitutive knockout precludes independent analyses of the function of a protein for the development of normal neuronal networks and synaptic connections and in synaptic transmission and/or plasticity once normal and mature synapses have been formed. The severe disruptions of hippocampal morphology in knockouts of the CREB family of transcription factors are good examples of this phenomenon (Lonze and Ginty, 2002).

Site-specific recombinase systems allow the deletion or rearrangement of DNA between two recombination sites upon the introduction of the appropriate recombinase enzyme. The system most commonly used in mice is Cre-*loxP* from P1 bacteriophage, in which Cre recombinase excises DNA from between two 34 bp *loxP* sequences, leaving only a single *loxP* site behind. A conditional knockout can be created by flanking key exons in the gene of interest with *loxP* sites by standard targeting methods, producing a 'floxed' allele (Kwan, 2002). If *FRT* recombination sites have been included flanking the positive selection cassette used for targeting, crossing the floxed mouse with a line expressing the Flp recombinase from *S. cerevisiae* excises the cassette, preventing its strong promoter from interfering with expression of the target gene and leaving a pseudo-wild-type floxed allele (Farley et al., 2000). Crossing the floxed mouse with a strain expressing Cre results in excision of the flanked exons and ablation of gene function (Dymecki, 2000; Lallemand et al., 1998; Nagy, 2000). Figure 1.6 summarises this strategy, which has recently been used, for example, to circumvent embyronic lethality in SRF knockout mice and show that SRF is required for activity-dependent gene expression and synaptic plasticity but not neuronal survival (Ramanan et al., 2005).

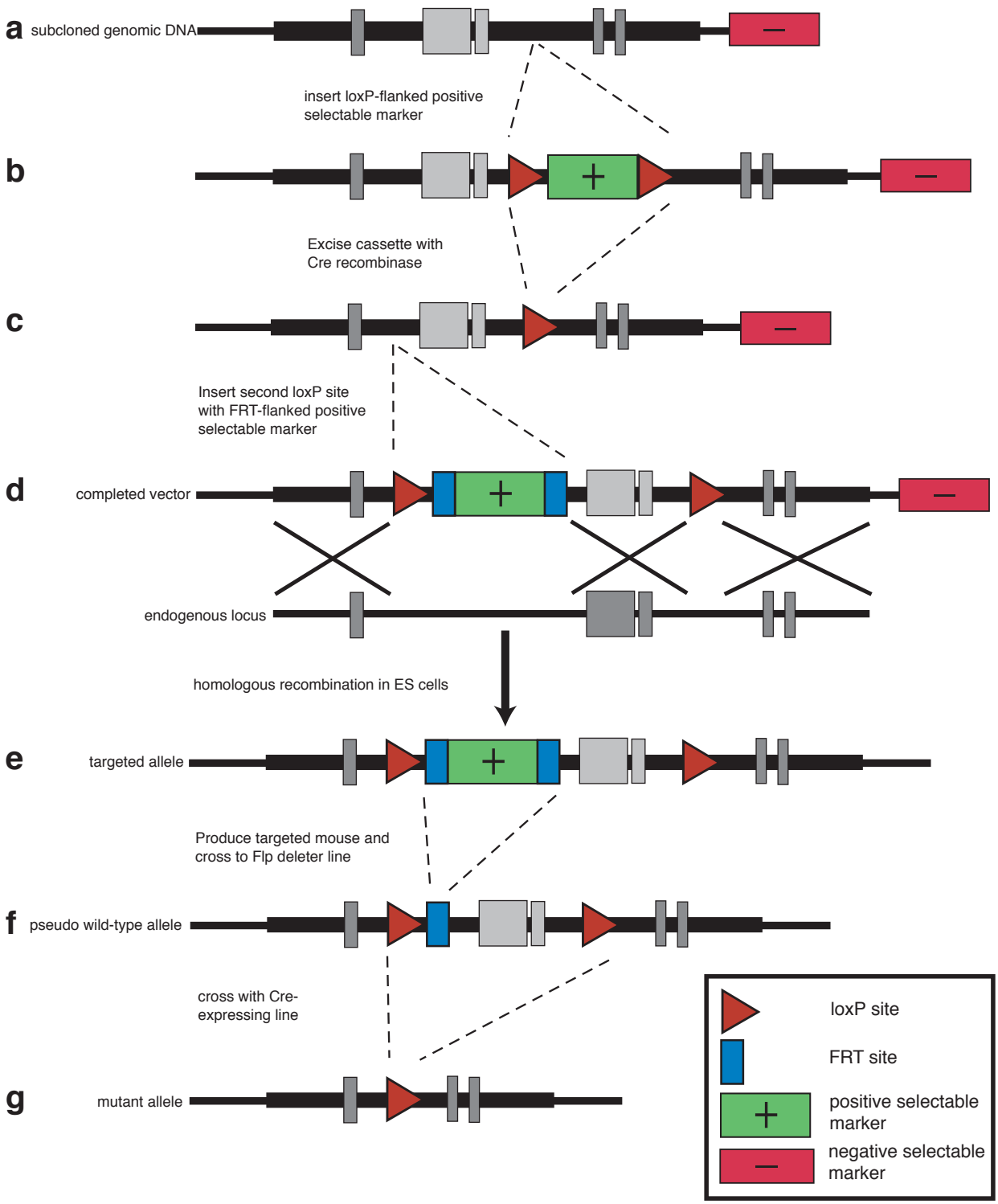

Figure 1.6 Conditional targeted mutagenesis strategy using site-specific recombinases. (a-c) The first loxP site is inserted on one side of the exons of interest in a genomic subclone using a loxP-flanked postive selectable marker followed by excision of the marker in Cre-expressing E.coli. **(d)** The second loxP site is inserted along with an FRT-flanked positive selectable marker. **(e)** The completed targeting construct is introduced into the endogenous locus in ES cells by homologous recombination, the negative selectable marker inhibiting random integration. Targeted ES cells are injected into blastocysts to generate a mouse **(f)** Crossing with a mouse strain ubiquitously expressing Flp recombinase removes the selection cassette along with its strong promoter, leaving a pseudo-wild-type allele containing loxP sites but expressing the gene normally. **(g)** Crossing to a Cre-expressing mouse strain results in recombination between the loxP sites, removing the exons of interest and ablating gene function.

Mouse strains with restricted Cre expression allow conditional gene deletion in a spatially- and/or temporally-controlled fashion. This can be achieved by placing the *cre* gene under the control of a promoter which drives expresion only in the tissue or temporal period of interest. For example, the synapsin-1 promoter drives neuron-specific Cre expression (Zhu et al., 2001a), the D6 promoter/enhancer results in Cre expression only in the neocortex and hippocampus (van den Bout et al., 2002) and the CaMKIIα promoter produces transgenic lines which express Cre postnatally in various regions of the forebrain, the precise specificity varying with each line (Dragatsis and Zeitlin, 2000; Tsien et al., 1996a).

An alternative strategy is to use mice expressing Cre fused with a mutated form of the hormone-binding domain of the oestrogen receptor (Cre-ER^T). The fusion protein can be expressed ubiquitously from a strong promoter but becomes active only with administration of tamoxifen, an oestrogen analog, which can be performed systemically or, for example, stereotaxically injected into a particular brain region (Brocard et al., 1997; Indra et al., 1999; Kellendonk et al., 1999; Vooijs et al., 2001). A third approach is to infect the animal with a virus expressing Cre (Ahmed et al., 2004). Yet another possibility is to produce recombinant Cre fused to a membrane translocation sequence, enabling the protein to be injected directly into the mouse (Chen and Behringer, 2001; Jo et al., 2001).

Caveats in the use of conditional mutagenesis technology

The technologies described above present a wide array of alternative strategies for mouse mutagenesis and other versions and combinations of these methods have also been published. No method is perfect, however, and the limitations of each need to be born in mind when designing a functional analysis strategy. This section focuses on the imperfections of the Cre recombinase system as it is so commonly used and comprises an important part of this dissertation.

The advantages of the Cre/*loxP* system lie in its ability to produce spatially- and temporally-restricted mutations. However, the specificity of expression of Cre transgenes is limited by the availability of an appropriately specific promoter for the purpose in hand. Patterns of Cre expression vary between transgenic lines produced with the same DNA construct (Dragatsis and Zeitlin, 2000) and anecdotal evidence suggests that even a single transgenic line can perform differently in different laboratories and through different generations, possibly as a result of variations in genetic background and/or epigenetic silencing of the transgene. The efficiency of recombinase activity in these lines also varies with the locus being recombined, highlighting the importance of analysing recombination not just with reporter lines but by confirming loss-of-function by immunohistochemistry or similar techniques (Vooijs et al., 2001).

Some of these limitations can be circumvented by delivering Cre virally or by direct injection of the recombinant protein, however these strategies also have disadvantages, notably in relation to achieving efficient recombination in the target population of cells but no others. Finally, high levels of Cre expression in mammalian cells lines causes DNA damage and inhibition of cell proliferation, properties which are dependent upon its endonuclease activity (Loonstra et al., 2001) and may be the result of recombinase activity on cryptic *loxP* sites in the genome (Schmidt et al., 2000; Silver and Livingston, 2001; Thyagarajan et al., 2000).

Targeting vector construction by homologous recombination in bacteria

Targeting vectors have traditionally been constructed using standard manipulation methods, cutting plasmids with restriction enzymes, isolating the required DNA fragments by agarose gel electrophoresis and joining them together using a DNA ligase enzyme. Relying on the presence of unique restriction sites limits the precision with which deletions and insertions can be made in the genome and often requires complicated and time-consuming cloning strategies to build

vectors from large pieces of genomic DNA. The recent development of homologous recombination-based DNA cloning strategies in bacteria ('recombineering'), however, allows insertions and deletions to be made at any position in a target DNA without the need for appropriate restriction sites (Muyrers et al., 2001).

Using recombineering, fragments of DNA can be excised from or inserted into plasmids by a process similar to gene targeting by homologous recombination in ES cells. For insertion, short homologous sequences corresponding to the site of insertion are attached to either end of the DNA fragment. It is then introduced into recombination-competent bacteria harbouring the recipient plasmid and clones carrying the desired recombination event are selected by antibiotic resistance. For an excision, short homology arms defining the ends of the fragment to be excised are attached adjacent to one another in the recipient plasmid. The plasmid is linearised between the homology arms and introduced into recombination-competent bacteria harbouring the donor plasmid and recombinants are selected as before (figure 1.7).

Endogenous homologous recombination activity in *E.coli* relies on the ATP-dependent, dsDNA exonuclease RecBCD, which also degrades linear DNA. To circumvent this problem, recombineering plasmids have been developed which express the λ-bacteriophage *gam* gene, which inhibits RecBCD, along with the Rac prophage genes *recE* and *recT* or the λ-bacteriophage genes *redα* and *redβ* to restore recombination activity. *RecE* and *redα* encode Exo, a 5'-3' exonuclease which acts on linear dsDNA to produce 3' overhangs. Beta, encoded by *recT* or *redβ*, binds to those overhangs and stimulates annealing to a complementary strand. In the plasmid, *gam* and *recT*/*redβ* are constitutively expressed while *RecE*/*redα* is placed under the control of the arabinose-inducible BAD promoter to minimise aberrant recombination (Zhang et al., 1998; Zhang et al., 2000). These plasmids have the advantage of conferring inducible

homologous recombination activity on any host strain, allowing recombineering to be used, for example, in BAC hosts (Copeland et al., 2001; Muyrers et al., 1999).

An alternative system uses a defective λ prophage containing the *redα*, *redβ* and *redγ* genes under the tight control of the temperature-sensitive λ-*cI857* repressor incorporated into the bacterial chromosome of the BAC host strain DH10B, allowing normal culturing at 32ºC and induction of recombination activity at 42ºC (Court et al., 2003; Yu et al., 2000). Cre and Flp recombinase genes have also been introduced, separately and under the control of the BAD promoter, into the chromosome of these cells to produce the new strains EL350 and EL250 respectively (Lee et al., 2001).

Recombineering has been proven an efficient method for inserting and excising DNA fragments into and out of plasmids without the need for restriction enzymes or DNA ligases in situations where positive selectable marker can be used (Zhang et al., 1998; Zhang et al., 2000). Importantly for targeting vector construction, it works efficiently for manipulating large DNA fragments many kilobases in length and has been used to generate deletions of up to 70 kb (Valenzuela, 2003; Zhang et al., 2000). Use of positive selectable marker genes such as neomycin phosphotransferase which confer drug resistance upon both *E.coli* and vertebrate cells, along with dual promoters which drive strong expression in both cell types, means the same selection cassette can be used for homologous recombination in bacteria for targeting vector construction and in ES cells for gene targeting (Angrand et al., 1999). The efficiency, rapidly and flexibility of the technique means it is particularly suited for constructing complex conditional targeting vectors. The EL350 and EL250 strains are especially convenient for vectors utilising the Cre/*loxP* and Flp/*FRT* site-specific recombinase systems (Liu et al., 2003; Muyrers et al., 1999). Recombineering is also useful for inserting reporter genes into BAC clones for producing

transgenic mice (Orford et al., 2000). The efficiency of recombination is such that it can even be used to retrieve a desired DNA fragment or clone from a complex mixture such as a genomic library (Zhang et al., 2001) or fragmented mouse genomic DNA (Zhang et al., 2000).

Recombineering also simplifies the introduction into targeting vectors of fine mutations such as point mutations or very small deletions or replacements spanning only a few base pairs. These modifications can be achieved without positive selection by using single-stranded oligonucleotides consisting of the desired mutation flanked by 35 bp of homology on either side. Because of the low recombination efficiency (1 correct recombinant per several hundred electroporated cells) without a selectable marker a PCR-based screen on pooled DNA is required to select positive clones (Swaminathan et al., 2001). The difficulty of designing efficient PCR primers against such short sequences can be overcome using a double replacement-type strategy (Yang and Sharan, 2003).

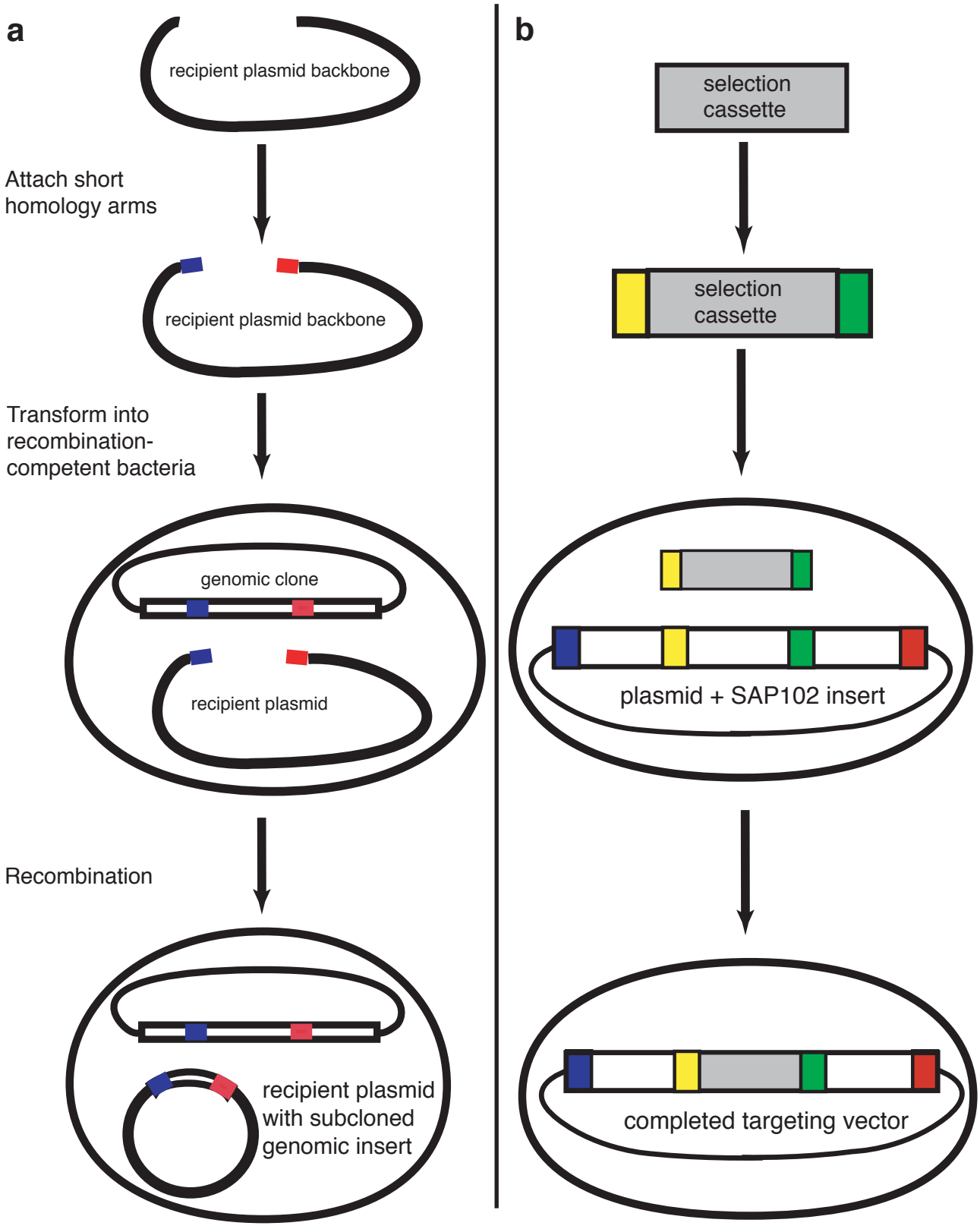

Figure 1.7 Constructing targeting vectors by recombineering. (a) To excise a piece of genomic DNA into the targeting vector backbone, short homology arms (blue and red rectangles) corresponding to the ends of the excision fragment are first attached to the linearised ends of the recipient plasmid. The plasmid is then introduced into recombinaion-competent E.coli harboring the donor vector and resulting antibiotic-resistant clones are screened for correct recombinants. **(b)** To insert a selection cassette into the genomic subclone in the newly-created plasmid, short homology arms (yellow and green rectangles) corresponding to sites of insertion in the subclone are attached to the ends of the cassette. The remainder of the experiment is performed as in (a).

1.8 X-linked mental retardation

The techniques described above allow sophisticated manipulation of the mouse genome. This section examines a genetic, cognitive disorder in humans and how these manipulations are being used to elucidate its causes.

Definition and clinical presentation of X-linked mental retardation

X-linked mental retardation (XLMR) is an inherited cognitive disorder caused by mutations in brain-expressed genes on the X chromosome (Ropers and Hamel, 2005). XLMR primarily affects males as they carry only a single copy of the X chromosome per cell and have thus no backup copy of the majority of their X-linked genes. Females carry two X chromosomes but prevent over-dosage by silencing one, generally at random, in each cell by the process of X inactivation, so that each cell is affected or unaffected depending on whether the wild-type or mutated allele has been silenced.

Mental retardation is clinically defined by three characteristics (American Psychiatric Association, 2000):

1. Sub-average general intellectual functioning, with an intelligence quotient (IQ) of less than 70.
2. Significant limitations in adaptive functioning in at least two of the following skill areas: communication, self-care, ability to live independently, social and interpersonal skills, use of public services, decision making, functional academic skills, work, leisure and health and safety.
3. Onset prior to 18 years of age.

Most investigators distinguish between several levels of severity of XLMR as shown in table 1.2.

Table 1.2 Severity levels of XLMR (Ropers and Hamel, 2005).

Severity of XLMR	IQ level
Mild	50-70
Moderate	35-50
Severe	<35

XLMR is a very heterogeneous disorder. Firstly, it can be divided into two forms: Non-syndromic XLMR (NS-XLMR) has mental retardation as its only symptom, while Syndromic XLMR (S-XLMR) is accompanied by additional abnormalities which often include facial and/or digital dysmorphologies, skeletal abnormalities and macroorchidism, among others (Ropers and Hamel, 2005). Two-thirds of XLMR cases are thought to be non-syndromic, but this is likely to be an underestimate since further symptoms often do not begin until puberty or adulthood. Some forms of the disease originally classed as non-syndromic have since been re-classified following more systematic examination of larger patient cohorts. Even within these two divisions, presentation of the disease can vary widely. IQ can vary from 20 to 70 points (see table 1.2) and syndromic forms can include symptoms as diverse as visual impairment (caused by mutations in *ABCD1* and *NDP*), cleft palate (*PHF8*) and heart defects (*PQBP1*) (Ropers and Hamel, 2005).

Prevalence

Moderate to severe XLMR occurs in around 1 in 2,000 males, although its true frequency is difficult to measure since the genetic basis of many forms of mental retardation remains to be determined and X-linked inheritance patterns are not always clear. Mental retardation in general has a prevalence of 2-3 % in developed countries. The importance of mental handicap as a health issue is highlighted by the fact that it is responsible for 8 % of healthcare expenditure in central

Europe, far greater than that on any other class of disease (Chelly and Mandel 2001, ; Fishburn et al., 1983).

Genes causing XLMR

The heterogeneity in the presentation of XLMR is reflected in its genetic basis. Around 140 syndromic forms of XLMR have been identified so far and causative genetic mutations (including some allelic mutations) have been identified in 66 of these, while partial mapping to distinct regions of the X chromosome has been performed in a further 50. In NS-XLMR mutations in 20 different causative genes have so far been identified, representing approximately 50 % of the total known cases. In total, 59 different genes are currently causatively implicated in XLMR (Ropers and Hamel, 2005).

Current knowledge of the function of XLMR-causing genes indicates heterogeneity but also some common themes emerging. Mutations in Rho GTPase pathways involved in the determination of dendritic spine morphology through actin cytoskeleton remodelling often seem to cause NS-XLMR. Genes in this category are oligophrenin-1 (*OPHN1*), a Rho GTPase activating protein (Billuart et al., 1998); p21-activated kinase (*PAK3*), which links Rho GTPases to the actin cytoskeleton and MAP kinase pathway (Allen et al., 1998); *ARHGEF6* and *FGD1*, both Rho guanine exchange factors (Kutsche et al., 2000; Lebel et al., 2002). The S-XLMR genes *FLNA* and *KIAA1202* are also implicated in this process as a result of their actin-binding properties. Other XLMR genes involved in GTP-based signalling include the Rab3A GTPase effector *SYN1* and the Rab4 and Rab5 GTPase regulator *GDI1* (Chelly and Mandel, 2001). XLMR sufferers often exhibit defects in dendritic spine maturation, resulting in an abundance of long, thin immature spines in the cortex and hippocampus during infancy and low spine density in adulthood (Kaufmann and Moers, 2000). This suggests spine dysgenesis may be a key factor in XLMR cognitive deficits and is consistent with observations that mutations in genes involved in

spine formation cause XLMR. These observations have been linked together in the Rho protein hypothesis of mental retardation (Ramakers, 2002; Renieri et al., 2005).

Transcription and chromatin remodelling forms a second functional theme amongst XLMR genes. *MECP2*, a methyl-binding protein responsible for chromatin condensation, causes the severe mental retardation, including male lethality, observed in Rett's syndrome (Amir et al., 1999). Mutations in *RSK2*, a protein kinase activated by the MAPK pathway which phosphorylates the transcription factor CREB and regulates the histone acetyltransferase CBP, cause a form of S-XLMR called Coffin-Lowry Syndrome whose symptoms include severe mental retardation, dysmorphology of the face and digits and progressive skeletal deformations (Trivier et al., 1996). *ARX* and *FMR2* are other transcriptional regulators which can cause XLMR (Chelly and Mandel, 2001).

Other XLMR genes possess more isolated functions. For example, Neuroligin 4 (*NLGN4*) is localised to the glutamatergic postsynapse and is central in the assembly of presynaptic structures (Yan et al., 2004). *PQBP1* is implicated in RNA splicing (Kalscheuer et al., 2003), *FTSJ1* in translation, *MID1* in protein degradation and *SLC6A8* in energy metabolism (Ropers and Hamel, 2005).

Mouse models of XLMR

Modelling the cognitive deficits of XLMR using genetic engineering in mice is a potentially very valuable method of elucidating the molecular and physiological mechanisms of the disorder. Since the causative genetic mutation is generally loss-of-function, a targeted deletion which knocks out the gene is a relatively straightforward and usually appropriate strategy for generating a mouse model. Cognitive and other behavioural tests can be used to validate the model followed

by morphological, electrophysiological and biochemical analyses to uncover the underlying pathology (Watase and Zoghbi, 2003).

Mouse models generated so far have been generally successful in reproducing some of the phenotypic aspects of the relevant human disorder. By far the most advanced and successful has been the model of Fragile X mental retardation discussed below. Others include a knockout of the NS-XLMR gene *GDI1*, producing mice which display a specific deficit in short-term hippocampal-dependent memory in radial maze and trace fear conditioning tests with normal long-term spatial memory in the water maze. They also exhibit a reduction in aggressive behaviour (D'Adamo et al., 2002). Mice with a deletion in *Fmr2* display impaired contextual fear conditioning and increased pain sensitivity, but none of the syndromic facial dysmorphology observed in the analogous human condition (Gu et al., 2002). Mice with a conditional, neuron-specific mutation in *NF1*, a model for Von Recklinghausen's neurofibromatosis type 1 (NF1), begin to show a growth retardation 3-4 days postnatally which continues into adulthood, where they stabilise at half the weight and size of their wild-type littermates. They also show reduced cortical thickness (Zhu et al., 2001a). *PAK3* mutant mice display normal hippocampal structure and dendritic spine morphology and normal spatial learning in the water maze, but have a deficit in the late phase of hippocampal LTP and more rapid extintion of a learned taste aversion than wild-type controls (Meng et al., 2005).

It is promising that these mutant mice display the types of phenotypes that might be expected in mental retardation. Still lacking, however, is robust demonstration that these phenotypes directly correspond to those observed in the relevant human disorder. This will be an important step in giving confidence that biochemical analyses of the underlying pathologies in these mice may lead to generation of useful therapeutic measures.

Fragile X mental retardation – a case study

The best-characterised XLMR mouse model is the *Fmr1* knockout mouse, a model for Fragile X syndrome. Fragile X is the most common form of mental retardation, accounting for 2-3 % of male retardation (Chelly and Mandel, 2001) and is a syndromic form whose symptoms include mental retardation, developmental delay, facial dysmorphology and macroorchidism (Maes et al., 1994; O'Donnell and Warren, 2002). Fragile X males have abnormally long and thin dendritic spines in cortical neurons without a change in cell density (Hinton et al., 1991; Purpura, 1974).

Fragile X is caused by an expanded CGG trinucleotide repeat in the 5' untranslated region of the *Fmr1* gene on the X chromosome. Presence of the expanded repeat induces methylation of the *Fmr1* promoter region and transcriptional silencing of the gene. Thus, Fragile X is a result of *Fmr1* loss-of-function (Bagni and Greenough, 2005).

The function of the fragile X mental retardation protein (FMRP), the product of *Fmr1*, is also well characterised. FMRP contains several RNA-binding domains including two KH and two RGG box domains. Studies of its RNA-binding properties show that it binds a large number of mRNAs, including its own (Ashley Jr et al., 1993; Brown et al., 2001; Chen et al., 2003; Dolzhanskaya et al., 2003). For example, one study used several approaches including co-immunoprecipitation of RNAs with FMRP followed by identification of the transcripts by microarray hybridisation to show binding of the protein to 432 different transcripts (Brown et al., 2001). The same study used fractionation of translating polyribosomes from human fragile X cells to show that the translational status of 50 % of these transcripts was changed in the absence of FMRP. FMRP is in fact a repressor which binds to mRNAs and prevents their translation, a function mediated via its interaction with microRNAs and the RNA-induced silencing complex (RISC). FMRP's targets include many transcripts localised near synapses and implicated in synaptic plasticity (Bagni and Greenough, 2005).

Fmr1 knockout mice show morphological and behavioural phenotypes mainly consistent with human Fragile X syndrome. 90 % of hemizygous males display macroorchidism, although none have facial dysmorphology. They display mild spatial learning deficits in both the traditional circular water maze and a plus-shaped version, along with a locomotor deficit. No deficit was observed, however, in a contextual fear conditioning test of hippocampus-dependent spatial learning (D'Hooge et al., 1997; Van Dam et al., 2000). Other behavioural abnormalities include increased locomotion in an open field test and reduced anxiety responses in an elevated plus maze. Like fragile X males, *Fmr1* mutant mice have longer and thinner cortical dendritic spines than wild-type controls (Comery et al., 1997).

FMRP is important for normal synaptic function, demonstrated by the observation that synaptic plasticity is disrupted in *Fmr1* knockout mice. Specifically, these mice show enhancement of LTD induced by activation of group 1 metabotropic gluatamate receptors (mGluR) in the CA1 area of the hippocampus. This is observed whether the LTD is induced by low-frequency electrical stimulation or by adminstration of the mGluR agonist DHPG. NMDAR-dependent LTD is unaffected. mGluR-dependent LTD is also dependent on protein synthesis and is associated with increased translation of FMRP protein (Huber et al., 2002).

These observations have led to the mGluR theory of fragile X syndrome, which postulates that mGluR-dependent LTD is a mechanism by which inactive synapses are marked for destruction during brain development, allowing only active, functional synapses to mature. Enhancement of LTD in the absence of FMRP prevents normal synapse maturation leading to developmental delay, aberrant synaptic connections and cognitive deficiency (Bear et al., 2004).

1.9 Aims

The aim of this dissertation was to analyse for the first time the function of the SAP102 protein *in vivo* in the mouse. Several characteristics of the protein suggest it may play crucial roles in fundamental neural processes. It is highly expressed in the hippocampus, a brain region important for memory formation and is localised to the postsynaptic density at glutamatergic synapses and interacts directly with NMDARs that are essential for normal brain development, synaptic plasticity, learning and memory.

SAP102 contains multiple protein-protein interaction domains and is a member of the PSD-95 family of MAGUK proteins which is implicated in the organisation of postsynaptic signalling pathways as well as localisation of postsynaptic transmembrane receptors. Mutations in PSD-95, which has similar domain structure and expression patterns to SAP102, cause enhancement of synaptic plasticity and spatial learning deficits in mice. Targeted mouse mutations have been generated for all PSD-95 family proteins except for SAP102. Mutations in SAP102 cause X-linked mental retardation in humans, providing further evidence for its importance in cognition and adding an urgency to the elucidation of its precise role in neuronal function.

Gene targeting in mice is the most powerful method available for the determination of neuronal gene function since it allows the creation of multiple mutations to assess different functional aspects of the gene in a system sufficiently sophisticated for meaningful analyses of complex cognitive behaviours. Thus, to discover the function of SAP102, a targeted deletion was introduced into the mouse gene with the aim of creating a null allele and assessing its impact on brain development and morphology, postsynaptic signalling, synaptic plasticity and behaviour. In addition to this constitutive knockout mutation, targeting vectors were also constructed for the introduction of a reporter gene knock-in to analyse SAP102 transcriptional patterns and a conditional knockout to facilitate the spatially- and temporally-dependent functions of SAP102.

These targeted mutations will allow a detailed functional analysis of SAP102 in relation to postsynaptic signalling, brain development and morphology, synaptic function and plasticity and behaviour.

A comprehensive understanding of neuronal function requires detailed investigations as to the function of large numbers of brain-expressed genes. To facilitate these types of experiments this dissertation aimed to use the SAP102 gene as a test case for developing a rapid and efficient system for generating mouse targeting constructs utilising recently-developed recombination-based cloning technology in bacteria.

Chapter 2

Materials and methods

2.1 General procedures and materials

Molecular biological procedures were performed as described (Sambrook and Russell, 2001) except as detailed below. All chemicals were analytical grade and purchased from Sigma except where specified.

General cloning was performed in DH10B or XL1Blue *E.coli*. The *dam*$^-$ strain SCS110 was used to prepare plasmids for digestion with *dam*-sensitive restriction endonucleases. Recombineering was performed in JC9604, HS996 or EL350 strains as specified. Cre and Flp recombinase-mediated site-specific recombination was performed in EL350 and EL250 strains respectively.

Mice were treated in accordance with the UK Animals (Scientific Procedures) Act, 1986 and all procedures were approved by the British Home Office Inspectorate.

2.2 Restriction digestion and DNA fragment purification

DNAs were digested with the appropriate type II restriction endonucleases from New England Biolabs. For digestion of DNA vectors for use in ligations with other DNA fragments 1 U of Shrimp Alkaline Phosphatase (USB) was added to the reaction to prevent subsequent self-ligation of the vector. Restriction fragments were size separated by agarose gel electrophoresis on an i-mupid electrophoresis system (Eurogentec) and/or purified from the gel using Spin-X columns (Corning). Synthetic linkers were annealed prior to ligation by combining equimolar amounts of sense and antisense strands in annealing buffer (10mM Tris, 50mM NaCl, 1mM EDTA pH 8.0), heating to 95°C and cooling gradually.

2.3 Ligation and transformation

DNAs were ligated using 1 U of T4 DNA ligase (Roche) at 20ºC for 4 hours or at 16ºC overnight. For transformation of bacteria, 1 µl of ligation reaction was mixed with 40µL electrocompetent *E.coli* which were produced as described by Sharma and Schimke (1996). The mixture was transferred to an ice-cold, 1mm-gap electroporation cuvette (Bio-Rad) and subjected to an exponentially decaying pulse of 1.8kV and 200µF in a Gene Pulser Xcell electroporation unit (Bio-Rad). The cells were then mixed in 1ml room temperature LB medium and incubated at 37ºC for 1hr with shaking at 250 rpm before being spread onto LB agar plates containing the appropriate antibiotic(s) and incubated at the same temperature overnight. Antibiotics were used at the following concentrations:

ampicillin	100µg/ml
kanamycin	30µg/ml
tetracycline	14µg/ml
chloramphenicol	12.5µg/ml

2.4 Plasmid DNA preparation and sequencing

Single *E.coli* colonies from were picked from agar plates into 3ml LB containing the appropriate antibiotic(s) at the concentrations above and incubated at 37ºC overnight with shaking. For general use, DNA was extracted from the liquid cultures using a boiling lysis procedure as follows: 1.5ml of culture was centrifuged at 10,000 x g for 1.5 minutes and the supernatant discarded. The cell pellet was resuspended in 180µl STET (10mM Tris.Cl,100mM NaCl, 1mM EDTA, 0.5% Triton X-100, pH 8.0), lysozyme was added to a final concentration of 1.4mg/ml and the mixture was left at room temperature for 1-5 min before boiling at 100ºC for 1 min. The solution was then centrifuged at maximum speed for 10 min and the plasmid DNA precipitated

from the resulting supernatant by the addition of 0.15 volumes of 4M ammonium acetate and 1 volume isopropanol. Precipitated DNA was washed with 70% ethanol, dried and dissolved in water or 10mM Tris, pH 8.0. RNA was degraded by the addition of 0.6 μg/ml RNase A (Sigma).

For high-quality preparations, DNA was extracted using a Wizard Plus Miniprep system (Promega) or a Qiagen Plasmid Midiprep kit. Routine plasmid sequencing from unique primers was performed by the Wellcome Trust Sanger Institute Plasmid Sequencing Facility using standard dideoxy methods. Full sequencing of *TARGETER* plasmids was performed by David Willey, Wellcome Trust Sanger Institute, using transposon-mediated shotgun sequencing.

2.5 BAC library screen

An adult 129Sv mouse genomic BAC library (ResGen, Release 11, 96021RG) was screened by PCR according to the manufacturer's instructions using the primer pair SAP3'PDZ, slightly 3' of the PDZ-encoding exons of the SAP102 gene. The identity of the positive clone was confirmed using two separate primer pairs, SAP5'PDZ and SAP5'PDZ2 both 5' of the PDZ-encoding exons. PCR reactions are described in section 2.7. The genomic clone was then end-sequenced to further confirm its identity and to establish the extent of the clone's coverage of the SAP102 locus. Multiple restriction digests were used to confirm an absence of structural alterations in the clone for each experiment in which it was used.

2.6 Protein extraction

Mouse tissue was thoroughly homogenised in DOC buffer [1% (w/v) DOC, 50mM Tris, 50mM sodium fluoride, 1mM sodium vanadate, 20μM zinc chloride, 1x Roche Complete protease inhibitor], centrifuged at maximum speed for 15 min at 4ºC and the protein-containing

supernatant retained. Extract concentrations were quantified by BCA assay (Pierce) according to the manufacturer's instructions.

2.7 Polymerase chain reaction

Oligonucleotides for use as PCR primers were designed using the web-based program Primer3 (Rozen and Skaletsky, 2000). Oligonucleotide sequences are listed in appendix 2.

General amplification

PCR for BAC library screening, amplification of DNA probes for Southern blotting and cDNA amplification following RT-PCR was performed using approximately 1ng (plasmid) or 1 μg (genomic) template DNA in a reaction containing 1.5 U *Taq* DNA polymerase (Promega), 1 x amplification buffer (Promega), 200 μM each dNTP, 0.5 μM each primer and 25 mM $MgCl_2$. The cycling protocol is shown in table 2.1. For BAC screening 30-40 amplification cycles were used; for DNA probes 25 cycles were used.

Table 2.1 Cycling protocol for general PCR amplification

Temperature (°C)	Time (s)	Cycle number
94	60	1
94	30	see text
55	30	
72	60/kb	
72	120	1

Mouse genotyping

For SAP102 PCR genotyping, approximately 1 μg of genomic DNA was placed in a reaction containing 1x PCR master mix (Promega), 0.5 μM each primer and an additional 0.25 mM $MgCl_2$ (total $MgCl_2$ concentration 1.25 mM). Amplification was as described in table 2.1 using 33 cycles with an extension time of 60 s. Two separate reactions were performed for each tail, one using primers P4 and P5 to amplify the wildtype allele and the other using primers P4 and P3 to amplify the mutant allele.

The PSD-95 PCR genotyping assay was developed by Karen Porter. Approximately 1 μg of genomic DNA was placed in a reaction containing 1.25 U HotStar *Taq* DNA polymerase (Qiagen), 1x amplification buffer (Qiagen), 0.8 μM each primer, 300 μM each dNTP and 10 % (v/v) DMSO. Each tail was genotyped with a single, multiplex PCR reaction containing primers P6 and P7 to amplify the wildtype allele and P8 and P9 to amplify the mutant allele. Table 2.2 shows the cycling conditions for this assay.

Sex determination PCRs were performed as described (Lambert et al., 2000).

Table 2.2 Cycling protocol for PSD-95 PCR genotyping assay

Temperature (°C)	Time (s)	Cycle number
95	900	1
94	30	35
58	60	
72	60	

ES cell genotyping

Amplification was performed using the Expand Long Template PCR System (Roche), utilising a mixture of thermostable *Taq* DNA polymerase and thermostable *Tgo* proofreading DNA polymerase. Approximately 1 μg of genomic DNA was placed in a reaction containing 1.75 U polymerase mix, 1x Expand amplification buffer 3, 0.2 μM each primer and 200 μM each dNTP. Two separate PCR reactions were performed for each clone, one with primers P1 and P2 to amplify the wildtype allele and the other with primers P1 and P3 to amplify the mutant allele. Table 2.3 shows the cycling conditions for this assay.

Table 2.3 Cycling protocol for SAP102 targeted ES cell genotyping assay

Temperature (°C)	Time (s)	Cycle number
97	120	1
96	10	40
60	30	
68	240	
68	10	1

High fidelity amplification

For amplification of short homology arms and cassettes for recombineering, and of the SV40polyA signal fragment, where accurate replication of the DNA template is essential, high-fidelity Platinum *Pfx* DNA polymerase (Invitrogen) was used. Approximately 50 ng of plasmid DNA was placed in a reaction containing 3 U *Pfx* polymerase, 1x *Pfx* amplification buffer, 0.3 μM each primer, 300 μM each dNTP and 1mM $MgSO_4$. Table 2.4 shows the cycling conditions for this assay.

Table 2.4 Cycling protocol for high-fidelity PCR with Platinum *Pfx* polymerase

Temperature (°C)	Time (s)	Cycle number
94	300	1
94	15	26
53	30	
68	60/kb	
68	120	1

2.8 Reverse Transcription-PCR

Reverse transcription reactions were performed using 1 µg total RNA, 200 U SuperscriptII reverse transcriptase (Invitrogen), 1 x SuperscriptII first-strand buffer, 2 µM oligo dT primer, 500 µM each dNTP, 10 mM DTT and 40 U RNaseOUT RNase inhibitor (Invitrogen). The RNA, oligo dT and dNTPS were first combined and incubated at 65°C for 5 min, then placed on ice while the buffer, DTT and RNase inhibitor was added. The reaction was incubated at 42°C for 2 min, then the reverse transcriptase was added. The incubation then continued at the same temperature for 50 min then the enzyme was inactivated by incubation at 70°C for 15 min. 1-2 µl was used in the PCR reaction (see 'general amplification', section 2.7).

2.9 Recombineering

Short homology arms of up to 70 bp for recombineering were attached to DNA fragments by PCR amplification of the entire fragment using composite synthetic oligonucleotides containing

the homology arm sequence adjacent to the PCR primer sequence (see section 2.7 for PCR conditions and oligonucleotides). PCR products were purified with a Geneclean spin kit (Bio 101), treated with *dam*-sensitive restriction enzyme *Dpn*I to remove residual (*dam*-methylated) template plasmid, purified by organic extraction followed by ethanol precipitation then redissolved in water for electroporation.

Short homology arms of length greater were PCR-amplified individually using primers carrying restriction sites on their ends, then digested and ligated either side of the selection cassette for recombineering. Fragments containing the selection cassette flanked by homology arms were released by restriction digestion, isolated by agarose gel electrophoresis, purified through a Spin-X column (Corning), ethanol precipitated and redissolved in water for electroporation.

JC9604 and HS996 *E.coli*

Recombineering experiments using JC9604 cells, which carry endogenous, constitutive recombination activity, were performed as described (Zhang et al., 1998). Electrocompetent cells carrying the appropriate recipient or donor plasmid for recombination were prepared by incubating a 70ml culture in LB medium at 37ºC with shaking to A_{600} = 0.4 and harvesting by centrifugation for 10 min at 4,000 rpm, -5ºC. Cells were then washed twice in ice-cold water and once in 10 % glycerol, each time resuspending the cells in the wash solution then recovering them with the centrifugation step. After the final wash the cells were resuspended in approximately 100µl 10 % glycerol and immediately transformed with the previously prepared linear DNA fragment.

Recombineering in HS996 cells was performed by first transforming the cells with the p*R6K116/BAD/αβγ* plasmid which confers inducible recombination competence. When preparing

the cells for electroporation, expression of *redα, redβ and redγ* was induced by the addition of arabinose to a final concentration of 0.1 % to the culture at A_{600} = 0.15. The remainder of the protocol was identical to that used for JC9604 cells.

EL350 and EL250 *E.coli*

EL350 and EL250 cells were grown at 32ºC except during induction for recombineering. Recombineering was performed as described (Liu et al., 2003). Electrocompetent cells carrying the appropriate recipient or donor plasmid were prepared by incubating a 20ml culture in LB medium at 32º with shaking to A_{600} = 0.5. At this point *Redα, redβ and redγ* expression was induced by transferring half the culture to 42ºC while the remainder was left at 32ºC. 15 min after the transfer both cultures were chilled in wet ice for 20 min then harvested by centrifugation at 5,000 rpm for 6 min at 2ºC. Cells were washed three times in 1ml water per wash, being recovered after each wash by centrifugation at 10,000 x g for 1 min at 2ºC. After the final wash both induced and uninduced cells were resuspended in an approximate total volume of 50 µl ice-cold water and immediately transformed with the previously prepared linear DNA fragment.

To check for differences in transformation efficiency between the induced and uninduced cells, each recombineering experiment was performed in parallel with an additional experiment in which induced and uninduced cells were transformed with 10 pg supercoiled plasmid. Induced cells were generally around 3-fold more efficient in transformation, however this had little bearing on the interpretation of the results since under transformation with the linear DNA fragment for recombination the induced cells produced thousands of antibiotic-resistant colonies (see table 3.1) while the uninduced cells never produced more than 5 colonies.

To perform Cre or Flp recombinase-mediated site-specific recombination between loxP or FRT sites in plasmids, EL350 or EL250 cells respectively were prepared for electroporation as above, except that when the culture reached A_{600} = 0.3, arabinose was added to a final concentration of 0.1 % to induce recombinase expression.

2.10 DNA cloning strategies

Sequences of oligonucleotide linkers used in DNA cloning are listed in appendix 2. Full sequences of p*TARGETER*, p*IRESlacZneoflox*, p*neoflox* and *ploxPneoflrt* are listed in appendix 3.

p*TARGETER*

A *Bcl*I-*Pvu*II fragment from pACYC184 (New England Biolabs), containing p15A replication origin and tetracycline antibiotic resistance gene, was ligated with a synthetic oligonucleotide containing multiple, unique restriction enzyme sites to form the multiple cloning site (MCS). A *Hind*III-*Xho*I fragment containing MC1-DTA-PGKpA from pMC1DTApA (a gift from Noboru Komiyama) was then ligated into the 3' end of the MCS to complete the plasmid.

IRES-lacZ-polyA plasmids

A synthetic oligonucleotide linker (L1) containing an MCS was ligated between the *Aat*II and *Hpa*I sites of pSP72 (Promega). A *BamH*I-loxP-PGK-EM7-neo-PGKpolyA-loxP-*BamH*I cassette (a gift from Karen Porter) was ligated into the *BamH*I site in the new MCS. A 324 bp *Sca*I-*Ssp*I fragment containing the ampicillin resistance gene (*bla*) was then removed from the plasmid and the remaining fragment self-ligated. Absence of *E.coli* colonies containing the plasmid after plating on ampicillin confirmed the success of this strategy. This plasmid was named p*SP75neoflox*.

A *BamH*I-T3-IRES-lacZ-*BamH*I fragment (a gift from Douglas Strathdee) was ligated into the *Bcl*I site of p*SP75neoflox* to produce p*SP76*. p*SP76* was used for initial recombineering attempts to insert the T3-IRES-lacZ-polyA-neoflox cassette into pBSSK.SAP102 by PCR-amplifying the cassette using PCR primers carrying short homology arms on their ends, and also by cloning longer homology arms either side of the cassette and then releasing the entire construct from the plasmid by restriction digestion.

For further recombineering experiments with only the neo cassette, the T3-IRES-lacZ-polyA section was removed from p*SP76* by digesting the plasmid with *EcoR*I, isolating each fragment other than that containing the T3-IRES-lacZ-polyA cassette and back together.

To construct p*IRESlacZneoflox*, an *EcoR*V-*Hpa*I fragment containing the cassette PGK polyA signal was removed from p*SP75neoflox* and, by blunt-end ligation, was replaced with an SV40 polyA fragment which had been PCR-amplified from p*CAGGS* (a gift from Noboru Komiyama) using the primer pair AAC+SV40pA (see appendix 1) to create p*SP75SV40pA*. A *BamH*I-T3-IRES-lacZ-polyA-*BamH*I fragment was then ligated into the *Bcl*I site 5' of the neo cassette to produce p*IRESlacZneoflox*.

<u>p*neoflox* and p*loxPneoflrt*</u>

p*neoflox* was constructed by ligating the *BamH*I-loxP-PGK-EM7-neo-SV40pA-loxP-*BamH*I cassette from p*SP75SV40pA* into the *BamH*I site of p*SP72*.

p*loxPneoflrt* was constructed using a *BamH*I-loxP-FRT-PGK-EM7-neo-PGKpolyA-FRT-*BamH*I cassette in a p*Bluescript* backbone (a gift from Noboru Komiyama). The PGK polyA signal in this cassette was replaced with and SV40 polyA using the same strategy as in p*SP75SV40pA*, then the new cassette was ligated into the *Bgl*II site of p*SP72L*.

SAP102 constitutive targeting vector

A 13 kb section of the SAP102 locus extending from 1 kb upstream of exon 1 to 3.2 kb downstream of exon 10 was excised from the SAP102 BAC clone into p*BSSK.DTA* (a gift from Noboru Komiyama) by recombineering. First the entire p*BSSK.DTA* plasmid was amplified by high-fidelity PCR using primers (SAP1A, SAP1B) containing a short sequence hybridising to the plasmid to prime the reaction adjacent to 70 bp of sequence corresponding to the ends of the SAP102 genomic section to be cloned. The purified PCR product was transformed into recombination-competent bacteria containing the BAC clone and a clone carrying the correctly recombined plasmid (p*BSSK.DTA.SAP102*) isolated as described in section 2.9.

Attempts to insert a selection cassette into the SAP102 fragment in *pBSSK.DTA.SAP102* by recombineering were first performed by PCR-amplifying the cassette from p*SP76* using primers, SAP2A (911 bp product) and SAP2B (863 bp product), containing short homology arms matching the sequence flanking the site of insertion in exon 4. After that, 5' and 3' homology arms were amplified by PCR using primers SAP2Afwd/rev and SAP2Bfwd/rev and ligated into the *Not*I-*Asc*I and *Pme*I-*Pac*I sites either side of the p*SP76* cassette respectively. The construct was then released with *Not*I and *Pac*I for recombination.

When the recombineering strategy failed, the cassette was instead inserted by tradition cloning methods. The *BamH*I-loxP-PGK-EM7-neo-PGKpA-loxP-*BamH*I fragment from p*SP75neoflox* (see above) was isolated and ligated into a *Bam*HI site flanked by *Ssp*I sites in a synthetic linker (L2) previously inserted between the *Pst*I and *EcoR*I sites of p*SP72*. The new plasmid was digested with *Ssp*I and the blunt-ended fragment containing the selection cassette isolated for insertion into the SAP102 targeting vector. p*BSSK.DTA.SAP102* was digested with *Afl*II, removing a fragment of SAP102 sequence from exon 2 to 8 inclusive. The remaining, larger fragment was isolated and treated with mung bean nuclease (New England Biolabs) to cleave the

single strand overhangs left by the restriction enzyme, then blunt-end ligated with the cassette fragment. For targeting, the completed vector was linearised with a unique *Not*I restriction site in the plasmid backbone.

SAP102 reporter knock-in vector

To build this vector a 10.9 kb SAP102 genomic fragment extending from 350 bp downstream of exon 1 to 3.2 kb downstream of exon 10 was excised from the SAP102 BAC clone into p*TARGETER* by recombineering. To do this, 2 short homology arms, aa1 and aa2, each 643 bp in length and matching the 5' and 3' ends respectively of the genomic fragment to be excised, were PCR-amplified using primers aa1fwd/rev and aa2fwd/rev and cloned adjacent to each other, separated only by an *Asc*I site, between the *Kpn*I and *Pme*I restriction sites in p*TARGETER*. The plasmid was linearised with *Asc*I and transformed into recombination-competent *EL350 E.coli* carrying the SAP102 BAC clone. Clones from antibiotic-resistant colonies were purified and analysed for the correct recombination event by restriction digestion and DNA sequencing. The recombined plasmid was named p*TARGETER.SAP102*.

To insert the T3-IRES-lacZ-pA-neoflox cassette into the vector, the same SAP2A and SAP2B short homology arms as were used in the first attempt to produce this vector (see 'SAP102 constitutive targeting vector', section 2.10) were re-amplified and cloned into the *Not*I-*Asc*I and *Pme*I-*Sal*I sites either side of the cassette in p*IRESlacZneoflox*. The cassette was released by digestion with *Not*I and *Sal*I, isolated and recombined into p*TARGETER.SAP102* to complete the targeting vector.

SAP102 conditional targeting vector

This vector used the p*TARGETER.SAP102* plasmid generated above as its base. To insert the first loxP site, short homology arms matching the sequence flanking the required site of insertion in

intron 5 were PCR-amplified using primers SAPneoflox5'fwd/rev (402 bp product) and SAPneoflox3'fwd/rev (420 bp product) and cloned into the *Xba*I-*Xho*I and *Kpn*I-*Bgl*II sites either side of the loxP-PGK-EM7-neo-pA-loxP cassette in p*neoflox*. The construct was released by *Xba*I and *Bgl*II digestion and recombined into p*TARGETER.SAP102*. Cre recombinase expression was induced by arabinose exposure in *EL350* cells carrying the new plasmid to remove the neo cassette, leaving only a single loxP site in intron 5. This plasmid was named p*TARGETER.SAP102.loxP*.

To insert the second loxP and selection cassette for targeting, short homology arms matching the sequence flanking the required site of insertion in intron 1 were PCR-amplified using primers SAPloxPneoflrt5'fwd/rev (601 bp product) and SAPloxPneoflrt3'fwd/rev (485 bp product) and cloned into the *Not*I-*Asc*I and *Pme*I-*Sal*I sites either side of the loxP-FRT-PGK-EM7-neo-pA-FRT cassette in p*loxPneoflrt*. The construct was released by *Not*I and *Sal*I digestion and recombined into p*TARGETER.SAP102.loxP* to complete the targeting vector.

2.11 Genomic DNA extraction

Extraction from ES cells

For extraction of DNA from ES cells in a 24-well plate, the culture medium was removed and replaced with 300µl DNA lysis solution (50mM Tris pH 8.0, 100mM EDTA, 100mM NaCl, 1% SDS) containing 0.7mg/ml proteinase K (Sigma) and thoroughly triturated. The solution was incubated at 55ºC for 2 hours with occasional mixing by inversion. 3µg RNase A (Sigma) was then added and the solution was incubated at 37ºC for 30 min.

For use in PCR, 20µl was removed and the genomic DNA precipitated by the addition of 0.8 volumes of isopropanol. The solution was centrifuged at maximum speed for 10 min and the

DNA pellet retained, washed in 70% ethanol, dried and dissolved in 10µl TE (10mM Tris, 1mM EDTA, pH 8.0). 1 µl was used per PCR reaction.

For use in restriction digestions, the remaining proteinase K- and RNase-treated DNA was extracted once with an equal volume of phenol, once with an equal volume of phenol:chloroform:isoamyl alcohol (25:24:1) and once with chloroform:isoamyl alcohol (24:1). The DNA was precipitated with isopropanol as above and dissolved in 50µl TE

Extraction from mouse tissue

Mouse tissue was digested overnight at 55ºC in 500µl DNA lysis solution containing 1.6mg/ml proteinase K and then treated with 3µg RNase A for 30 min at 37ºC. For PCR the solution was incubated in dry ice for 1 min then centrifuged at maximum speed for 15 min at 4ºC. A small amount of supernatant was removed from the surface and diluted between 5- and 15-fold with water. 1ul of the diluted solution was used per PCR reaction. For restriction digestion the proteinase K- and RNase-treated DNA solution was thrice organically extracted, precipitated and dissolved in TE as described for the ES cell DNA above.

2.12 Southern blot

DNA probes were amplified by PCR and cloned into pGEM-T Easy vectors (Promega). The 5' probe (784 bp) was amplified using primer pair SAP5'probe and the 3' probe (886 bp) with SAP3'probe. The internal probe (969 bp) used for verification of the Ensembl SAP102 genomic sequence was amplified with primer pair SAP5'PDZ3. For hybridisation, probes were released from their vectors by restriction digestion, purified by agarose gel electrophoresis and radiolabelled with ^{32}P-deoxycytosine using a Rediprime II random priming kit (Amersham Biosciences).

Genomic DNA for hybridisation were digested overnight with the appropriate restriction endonuclease and resolved by electrophoresis through a 0.6% agarose gel. Separated DNAs were UV-nicked by subjecting the gel with 0.08 J/cm^2 ultraviolet radiation in a UV crosslinker (Stratagene) and transferred to Hybond-N$^+$ nylon membrane (Amersham Biosciences) by capillary transfer using alkaline transfer buffer (1.5M NaCl, 0.5M NaOH). Membranes were hybridised with radiolabelled probe overnight in 0.1ml phosphate-SDS hybridisation buffer [0.5M sodium phosphate, 1mM EDTA, 7% (w/v) SDS, 1% (w/v) fraction-V BSA, pH 7.2]. Excess probe was removed by washing at 65ºC with phosphate-SDS wash solution I [40mM sodium phosphate, 1mM EDTA, 5% (w/v) SDS, 0.5% (w/v) fraction-V BSA, pH 7.2] followed by phosphate-SDS wash solution II [40mM sodium phosphate, 1mM EDTA, 1% (w/v) SDS, pH 7.2]. The membrane was then exposed to a phosphor screen and developed in a Typhoon imager (Amersham Biosciences).

2.13 Protein extraction

Mice were killed by cervical dislocation. They were then decapitated, the skin and top of the skull removed and the brain extracted from the resulting opening. For forebrain protein extracts, the hindbrain, cerebellum, midbrain and olfactory bulbs were dissected away. For hippocampal extracts, bilateral hippocampii were further dissected from the forebrain.

Adult forebrain was homogenised in 4 ml DOC buffer [1 % (w/v) DOC, 50 mM Tris pH 9.0, 50 mM NaF, 20 μM ZnCl, 1 mM sodium orthovanadate, 0.5 mM PMSF, 2 μg/ml aprotinin, 2 μg/ml leupeptin] in a 5 ml manual homogeniser. Adult hippocampus was homogenised in 1.5 ml DOC buffer in a 2 ml homogeniser and P6 forebrain was homogenised in 2 ml DOC buffer in a 5 ml homogeniser. The homogenised tissue was centrifuged at 32,000 rpm for 20 min at 4ºC and the supernatant retained. Extracts were quantified using a bicinchoninic acid assay (Pierce).

2.14 Western blot

15 μg protein extract was diluted in Laemmli sample buffer (Bio-Rad) and subjected to SDS-PAGE using Tris-HCl Polyacrylamide ReadyGels (Bio-Rad) in Tris/Glycine/SDS buffer [25 mM Tris, 192 mM Glycine, 20% (v/v) SDS, pH 8.3] in a mini-Protean cell (Bio-rad). Proteins were transferred onto Hybond-P membrane (Amersham Biosciences) in a mini trans-blot cell electroblotter (Bio-Rad) at 400mV for 1 hour in Tris/Glycine buffer (25mM Tris, 192mM Glycine, pH 8.3). Membranes were stained in Ponceau S (Sigma) then incubated overnight at 4ºC in PBS/Tween (PBS with 0.1% (v/v) Tween 20) containing 5% (w/v) skimmed milk powder (Marvel). Membranes were washed 5 times in PBS/Tween and then incubated with primary antibody in PBS/Tween for 2 hours at room temperature. Membranes were washed again 5 times then incubated with secondary antibody in PBS/Tween for 1 hour at RT. Secondary antibodies were anti-mouse or anti-rabbit IgG HRP-linked whole antibody (Amersham Biosciences). Binding of the secondary antibody was detected with an ECL Plus kit (Amersham Biosciences) followed by exposure to Hyperfilm (Amersham Biosciences). Primary antibodies are listed in appendix 2.

For repeated probing, the primary antibodies were stripped from membranes by incubation in stripping buffer [1.5% (w/v) glycine, 0.05% (w/v) Tween 20, pH 2.5] at 80ºC for 1.5 hrs with one change of solution. They were then washed 3 times in PBS/Tween at room temperature, 5 min per wash, and then blocked as normal with 5% milk before incubation with the new primary antibody.

2.15 Co-immunoprecipitation

Protein extracts in DOC buffer were incubated with 5 μg of the precipitating antibody with rotation at 4ºC for 1 hour in a total volume of 400 μl. 15 μl Protein G Sepharose beads (Amersham Biosciences) were equilibrated in DOC buffer and added to the mixture before incubating for further hour under the same conditions. Precipitated complexes were washed 3 times in DOC buffer, resuspended in Laemmli sample buffer, boiled at 85ºC for 5 minutes, centrifuged and the supernatant subjected to Western blotting as described above.

2.16 Phosphorylation screen and sandwich ELISAs

These experiments were performed by Marcelo Coba (Wellcome Trust Sanger Institute). Hippocampal protein extracts were subjected to a KPSS-1.3 phosphorylation screen (Kinexus Bioinformatics Corporation). Extracts were prepared by homogenising dissected hippocampi in 20 mM MOPS pH 7.4, 2 mM EDTA, 5 mM EGTA, 0.5% Triton X-100, 30 mM NaF, 40 mM β-glycerophosphate, 20 mM sodium pyrophosphate, 1 mM sodium orthovanadate, 1mM PMSF, 3mM benzamidine, 5 μM pepstatin and 10 μM leupeptin and quantifying the protein concentrations using a BCA assay (Pierce).

Sandwich ELISAs were performed according to the manufacturer's instructions to determine endogenous levels of ERK1/2 (Biosurce total ERK1/2) and phospho-ERK1/2 T202/Y204 (Pathscan Cell Signaling).

2.17 ES cell culture and targeting

Culture and targeting was largely performed as described (Nagy et al., 2003). Reagents were purchased from Gibco-BRL except where indicated. HM-1 mouse ES cells were cultured on

0.1% gelatin in ES cell medium consisting of BHK-21 (Life Technologies) supplemented with 10% FBS (Stem Cell Technologies), 2mM L-glutamine, 100U pencillin, 100µg/ml streptomycin, 1x non-essential amino acids (Gibco-BRL 11140-035), 1mM sodium pyruvate, 100µM 2-mercaptoethanol and 700U/ml ESGRO leukemia inhibitory factor (Chemicon International).

For targeting, 1 x 10^7 cells were electroporated with 100 µg linearised, purified targeting vector in a 0.4mm gap electroporation cuvette (Bio-Rad) at 0.8kV, 3µF using a Gene Pulser Xcell electroporation unit (Bio-Rad). Cells were plated into 10cm petri dishes and selection with 300µg/ml G418 sulphate was begun 24 h after plating. Single G418-resistant colonies were picked 5-7 days later for expansion, analysis and freezing.

Colonies were expanded gradually into 2 wells of a 24-well plate, of which one was used for DNA extraction and analysis and the other stored at –80ºC in ES cell medium containing 10% DMSO and 20% FBS. For blastocyst injection, frozen positive clones were thawed and further expanded, then passaged a final time into medium without G418 before trypsinising, washing and resuspending into fresh G418-free medium for injection. Blastocyst injection was performed as described (Ramirez-Solis et al., 1993).

To test the functionality of the SV40 polyA signal for targeting, approximately 1 x 10^6 cells were electroporated with 5 µg linearised plasmid and subjected to G418 selection as above. After 5 days of selection, drug-resistant colonies were fixed and permeabilised in methanol then stained with Giemsa for analysis.

2.18 Histology

Histological experiments were performed essentially as described (Bancroft et al., 1996). Mice were deeply anaesthetized with sodium pentobarbitone and perfused intracardially with 4 % paraformaldehyde. The whole brain was then dissected and placed in 4 % paraformaldehyde overnight, then impregnated with wax using a Shandon Exelsior tissue processor (Thermo Electron Coorporation). This consisted of dehydration in increasing ethanol concentrations over 6 hrs following by 3 hrs of xylene incubation with fresh solution each hour, then 3 hrs of incubation in molten paraffin wax at 60ºC with fresh solution each hour. The brains were then embedded in paraffin wax blocks and cut into 5 μm sections.

For Nissl staining, slides were incubated for 10 min in xylene then 10 min in ethanol, each with one change of solution, then rehydrated sequentially in 90 %, 70 %, 50 % and 30 % ethanol, 30 s per incubation. The slides were washed briefly in PBS then placed in Nissl stain [0.4 % (w/v) cresyl violet, 80 mM sodium acetate, 120 mM acetic acid, 29 % (v/v) methanol] for 15 min. They were then sequentially dehydrated to 100 % ethanol, cleared in xylene and immediately coverslipped.

Immunohistochemistry was performed on a Ventana Discovery machine according to the manufacturer's instructions. For NR1, NR2A, NR2B, SAP102, PSD-95 and PSD-93 staining, slides were pretreated with Ventana Cell Conditioning 1 followed by 10 min of Protease 1. For MAP2B staining, slides were pretreated with Ventana Mild Cell Conditioning 1 only. Primary antibodies are listed in appendix 1. Secondary antibodies were biotin-conjugated rabbit anti-mouse (Dako Cytomation) or biotin-conjugated donkey anti-rabbit (Jackson). Antibody binding was detected by chromogenic oxidation of diaminobenzidine (DAB) by streptavidin-conjugated

HRP enzyme. Images were captured using a Zeiss Axioplan 2 microscope with Axiovision 4.2 software.

2.19 Electrophysiology

Electrophysiological experiments were performed by Anne Fink, Patricio Opazo and Tom O'Dell (Department of Physiology, University of California, Los Angeles) as described (Mayford et al., 1995). Experimenters were blind to the genotypes of the mice. 400 μm-thick slices of mouse hippocampus were maintained at 30ºC in an interface-type recording chamber perfused with a murine artificial cerebrospinal fluid (ACSF) containing 124 mM NaCl, 4.4 mM KCl, 25 mM Na_2HCO_3, 1 mM NaH_2PO_4, 1.2 $MgSO_4$, 2 mM $CaCl_2$ and 10 mM glucose. EPSPs were elicited once every 50 s (0.02 Hz, 0.01 – 0.02 ms duration pulses) using tungsten wire bipolar stimulation electrodes in stratum radiatum of the CA1 region. The resulting potentials were measured using low resistance glass microelectrodes (5-10MΩ, filled with ACSF), also in CA1 stratum radiatum.

For basal synapse function experiments, fibre volleys in Schaffer collateral axons and field excitatory postsynaptic potential (fEPSP) slopes were measured at stimulation intensities inducing 25 %, 50 %, 75 % and 100 % maximum fEPSP amplitude. Postsynaptic currents were measured using whole-cell voltage-clamp recordings at postsynaptic membrane potentials of –80 and +40 mV. The AMPAR-mediated component of the excitatory postsynaptic current (EPSC) was determined by the peak amplitude of the EPSC at 5 ms after EPSC onset. The NMDAR-mediated component was determined by the amplitude of the EPSCs 50 ms after EPSC onset. For long term potentiation, the 100 Hz stimulation protocol consisted of two trains of 100 Hz stimulation, each 1 s in duration and separated by 10 s. The 5 Hz protocol consisted of continuous 5 Hz stimulation for 3 min (900 pulses delivered in total).

2.20 Behaviour

Two cohorts of mice were used for behavioural testing. The first cohort was tested only in the water maze at eight weeks of age. A second cohort of mice was tested at seven weeks of age in the T-maze and olfactory habituation tasks. Four weeks later they were tested in the elevated plus maze and another four weeks later they were tested in the open field, grip strength and elevated plus maze tasks. All behavioural experiments were performed blind with respect to the genotypes of the mice.

Water maze

This experiment was performed and analysed by Jamie Ainge (Division of Neuroscience, University of Edinburgh) and Lianne Stanford. The water maze was 2 m in diameter with opaque water of temperature 25 ± 1 ºC. The escape platform was 30 cm in diameter and was made visible when required by lowering the water level in the pool and adding a flag to the centre of the platform. A black curtain was drawn around the maze when required to eliminate the visible cues from within the room. Data analysis was performed with automated swim path analysis software (Actimetrics).

The testing protocol was adapted from Migaud et al. (1998) and Komiyama et al. (2002). Each training trial began when the mouse was placed in the water and ended when it climbed onto the platform or after 90 s had elapsed, whichever was shorter. If the mouse had not reached the platform after 90 s it was led to the platform and allowed to climb onto it. Average swimming speed, distance travelled and latency to reach the platform were calculated for each trial. Mice were first trained with a visible platform for three days, then with a hidden platform for five days and finally to the opposite platform location for five days. Four training trials were given per day. In probe tests, each mouse was placed in the pool without the platform present and its swim path recorded for 60 s. Time spent in each quadrant of the pool and number of crossings of the

platform site were recorded for each test. Probe tests were performed 10 min (H1) and 24 hrs (H2) after the final hidden platform training trial, 10 min after the final trial on each day of reversal training (R1-5) and 1, 7, 14 and 56 days after the final reversal training trial (M1, M7, M14 and M56 respectively).

Two-way (genotype x day) mixed ANOVAs were completed for latency, distance and swim speed. For the probe trials, 2-way (genotype x quadrant) mixed ANOVAs were completed. Single mean *t*-tests with the null mean set to 15 s were also performed to assess whether the mean 'training quadrant' times for each genotype were above chance (15 s).

T-maze

This experiment was performed in collaboration with Lianne Stanford. T-maze design and testing protocols were adapted from Gerlai (Gerlai, 1998). The maze was constructed by the maintenance department of the Wellcome Trust Sanger Institute. The floor was a single piece of black acrylic sheet mounted onto plywood. The T was created by a 90º bisection of a 102 cm x 12 cm alley with a second alley of 45 cm x 12 cm. Walls of clear acrylic sheet of height 20 cm were attached to the sides with All Purpose clear adhesive (Bostick Findley Ltd, Stafford, UK) and screws. 10 cm from the end of the bottom arm of the 'T', vertical aluminium guides of length 15 cm were attached to the walls. These held a clear acrylic door which separated the end of the arm from the remainder of the maze, creating a start box. Similar guides were placed close to the T-intersection in the other two arms so that access to either or both arms could be prevented. Thin white lines, 12 cm into each of the right and left arms, were added to the floor of the maze. A second set of lines was drawn 25 cm from the entrance of the two arms. The maze was placed on the floor in a room containing a number of spatial landmarks including a bin, table, chair and door. The room was dark except for some dim white light entering though the slightly opened door.

The T-maze test was run in continuous, non-rewarded fashion (Gerlai, 1998). Each mouse completed one forced-choice followed by 10 choice trials. In the forced-choice trial, entrance to one of the two goal arms (chosen at random) was blocked and the mouse was placed in the start box with the starting gate closed. The starting gate was then raised to begin the trial and closed once the animal had left the start box. Once both rear paws of the mouse had crossed the first white line in the unblocked goal arm, the starting gate was again raised. When the mouse re-entered the main arm of the maze the forced-choice arm was closed behind it. The trial ended when the mouse re-entered the start box and the starting gate was closed. The remaining 10 choice trials were performed the same way except both goal arms were unblocked and available. Arm choice in each trial and total time taken to complete the 11 trials (session duration) was recorded.

Olfactory habituation-dishabituation task

This experiment was performed in collaboration with Lianne Stanford. The habituation-dishabituation protocol was adapted from those previously published (Brown et al., 1987; Wrenn et al., 2003). Mice were tested individually in translucent, empty, housing cages, of dimensions 13 x 30 x 15 cm, with metal lids. The test was performed under dim lighting with only one animal in the room at any one time. Urine samples for use as olfactory stimuli were collected separately from male C57BL/6J and CD-1 strain mice. The experimenter changed gloves between trials and used separate pipettes for each urine type. Mice were placed in an empty cage for 30 minutes prior to the test for acclimatisation. A cotton bud (Sainsbury's Safety Buds, London, UK) containing 9.5 μl urine on its lower end was then suspended from the cage lid so that the urine-soaked tip hung 65 mm below the lid. The cotton bud was removed after 120 s. Each mouse was presented with seven stimuli in this fashion, with an inter-trial interval of 60 s. The first stimulus was distilled water only (vehicle), followed by three presentations of urine from one donor strain,

then three presentations of urine from the other strain. Half the mice received the C57BL/6J urine first and half received the CD-1 urine first in a randomized manner. Time spent sniffing each stimulus was recorded.

Grip strength

This experiment was performed in collaboration with Lianne Stanford. The protocol was adapated from published experiments (Lalonde et al., 2004). The apparatus consisted of a trapeze bar made by bending a 5 cm, 21 g syringe needle, attached to a force displacement transducer (FT03C, Grass Instruments, Mass, USA) transmitting through a Mac Lab Bridge amplifier to a Powerlab/4SP and then into a computer running Powerlab ADInstruments Chart v 4.12. Each mouse was held by its tail and its front paws placed on the trapeze bar. Once the mouse had grasped the bar with both paws, it was pulled horizontally backwards in a continuous motion until the mouse lost its grip. This was performed seven times and the trials with the greatest and least peak force discarded. The score for each mouse consisted of the mean of the peak generated force in the remaining five trials.

Rotorod

This experiment was performed in collaboration with Lianne Stanford. The rotorod was a fixed-speed, Series 8, Model 755 (IITC Life Science, Harvard Apparatus UK) apparatus with a rod diameter of 32 mm. The test was performed during the light period of the light-dark cycle in a brightly-lit testing room adjacent to the vivarium. Each trial consisted of the mouse being placed on the stationery rod which then began to rotate at a constant speed. The trial continued until the mouse fell off the rod or until 60 s had elapsed. Latency to fall was recorded for each trial. Mice were given three trials at each of 4, 16 and 32 rpm on each of three days. Trials were given in order of increasing speed on each day. An additional set of three trials at 2 rpm were given prior

to the 4 rpm trial on the first day only, to habituate the animals to the apparatus. The results were analysed using a three-way (genotype x trial x day) mixed ANOVA.

Open field

This experiment was performed in collaboration with Lianne Stanford. The open field test was performed during the light period of the light-dark cycle. Each mouse was transported alone from its home cage in a small container and placed directly into a clean, opaque, plastic box of dimensions 45 cm x 28 cm x 13 cm with no lid in a brightly-lit room for 15 min. Behaviour was recorded by camcorder for later analysis. Analysis was performed using Hindsight 1.5 behavioural scoring software. The field was divided into thirds along its length and width and the resulting inner rectangle denoted the inner zone (see figure 6.5). The behaviour of the mice was scored for the following measures: Latency to enter inner zone, number of times entering inner zone, duration in inner zone, incidence and duration of immobility, line crosses, supported (against the wall) and unsupported rearing (Crusio, 2001).

Elevated plus maze

This experiment was performed in collaboration with Lianne Stanford. It was designed in accordance with published protocol (Lister, 1987). The elevated plus maze consisted of a black perspex cross with four arms and a central, square platform. The arms of the cross were 5 cm wide and 30 cm long. Two opposite arms had clear perspex walls of height 15 cm and the remaining two arms were open with only a 3 mm lip around the edge. The entire apparatus was supported 45 cm above the floor. The test was performed during the light period of the light-dark cycle in a room lit with dim red light. The behaviour of the mice was recorded using a Sony video camera fitted with an infra-red filter and the data was analysed using Ethovision 3.0 tracking software.

Each mouse was given a single trial in which it was released on the centre square facing an open arm and allowed to explore for 5 minutes. A trained observer recorded the number of times the mouse dipped its head over the edge of the open arms of the maze (head dips) and the number of times it assumed a stretch-attend posture. The maze was cleaned with alcohol-free disinfectant wipes (Trigene Antiseptic Wipes, Medichem UK) between trials.

Chapter 3

Construction of targeting vectors and a novel vector system for recombination-based DNA cloning

This chapter describes the construction of three different targeting vectors for the introduction of a constitutive knockout, a lacZ knock-in and a conditional mutation into the SAP102 locus. It also presents the construction and validation of a novel set of plasmids to facilitate rapid and flexible targeting vector construction using homologous recombination in bacteria.

3.1 SAP102 constitutive targeting vector

Advantages of a constitutive SAP102 knockout mouse

A constitutive knockout strategy for SAP102 was initially used because a germline deletion results in every cell of the targeted mouse lacking SAP102 throughout its lifetime, the most comprehensive method of determining SAP102 function in the whole organism. This is also the situation for human males with inherited mutations in SAP102, thus a constitutive knockout makes the best model of the human disorder. A simple deletion of part of the gene also means rapid generation of the mutant mouse and an uncomplicated targeting vector for testing recombineering-based construction strategies.

SAP102 is not expressed in ES cells

To design a targeting strategy, the mouse HM-1 ES cells to be used for targeting were first tested for SAP102 expression using RT-PCR. If a gene is expressed in ES cells it can be targeted by insertion of a positive selectable marker with no promoter but only a splice acceptor sequence and an internal ribosome entry site (IRES) to drive independent translation, so that the marker is expressed only when integrated into an active locus. This enhances targeting efficiency by greatly reducing random genomic integration of the targeting construct (Hasty et al., 2000). Figure 3.1a shows that SAP102 mRNA is present in total RNA extract from whole brain but not from ES cells, therefore a promoter needed to be included in the selection cassette for targeting.

Targeting vector construction

The constitutive targeting vector was constructed using SAP102 genomic sequence ENSMUSG00000000881 in the Ensembl repository (Birney et al., 2004) and cDNA sequence NM_016747 in the NCBI Entrez Nucleotide database (www.ncbi.nlm.nih.gov). The accuracy of the sequence was verified by PCR and Southern blot analyses. Multiple primer pairs through the target region amplified PCR products of the expected sizes and on Southern blots three unique, intronic, DNA probes from the target region hybridised to genomic DNA fragments of the expected sizes following a variety of restriction enzyme digestions (figures 4.1, 4.2 and data not shown).

To obtain a genomic SAP102 clone, a 129Sv genomic BAC library was screened using PCR primer pairs at each end of the targeting region. The identity and structure of the SAP102 locus in the clone was verified by end-sequencing, restriction digestion, PCR and Southern blot using the known genomic sequence and the experimental results from analyses of the genomic locus above (data not shown).

The targeting vector was constructed by first excising a SAP102 genomic fragment containing the targeting region from the BAC clone into a pBluescript vector containing a DTA negative selectable marker (pSKDTA). This was performed by recombination-based cloning in JC9604 strain *E.coli*, using short homology arms of 70 bp each which were attached to the ends of pSKDTA by PCR amplification (Zhang et al., 2000). This recombineering step was successful but inefficient, producing eight antibiotic-resistant colonies of which only one carried the correct clone (table 3.1, row 1).

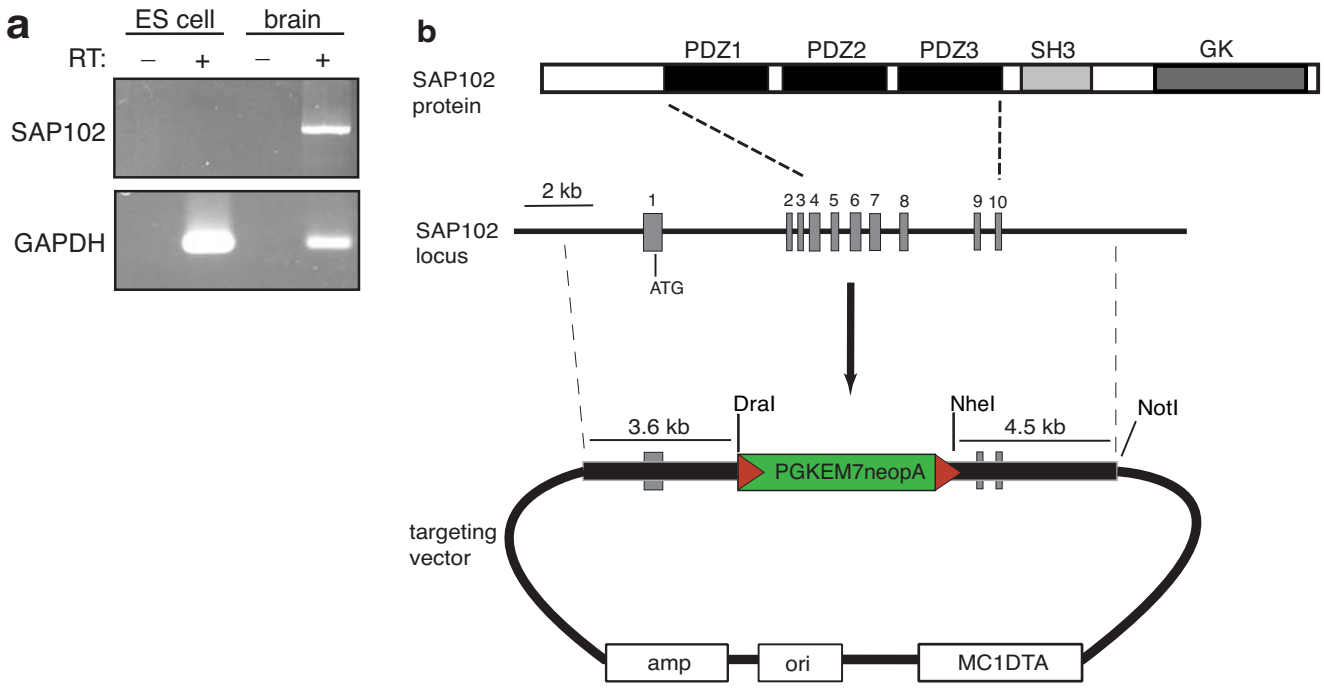

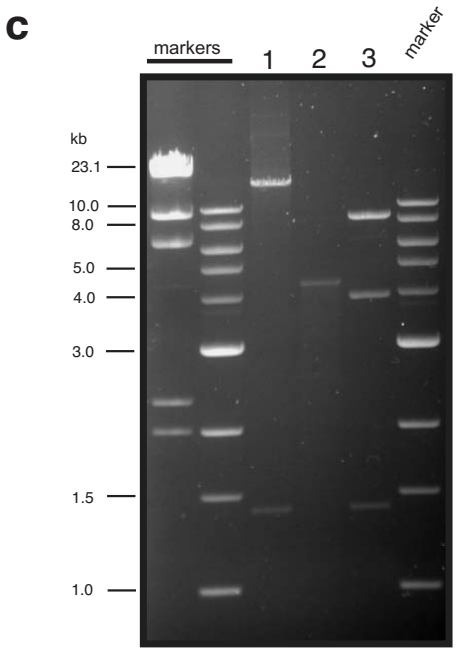

Expected NheI fragment sizes (kb)

1	2	3
15.3	4.3	8.3
1.4		3.9
		1.4

Figure 3.1 SAP102 constitutive targeting vector. (a) SAP102 is not expressed in ES cells. RT-PCR using primers for SAP102 cDNA produces a 1 kb band from RNA from whole brain but not from mouse ES cells. Amplification of GAPDH shows the integrity of the cDNA in each sample. **(b)** Targeting vector design and construction. The PDZ domains of SAP102 are encoded by exons 4 to 10 inclusive. The targeting construct consists of a genomic fragment containing this region with exons 2 to 8 inclusive replaced by a loxP-flanked selection cassette (green box with red triangles). A unique NotI restriction site allows for linearisation of the vector and DraI and NheI restriction sites are included at the ends of the cassette to facilitate genotyping. The vector backbone carries a diphtheria toxin A (DTA) fragment negative marker to discourage random integration. **(c)** Restriction digestion confirms the structure of the targeting vector. Shown are NheI digestions of the targeting vector backbone with SAP102 genomic subclone only (1), the parental plasmid containing the selection cassette (2) and the completed targeting vector with the cassette inserted (3).

An attempt was then made to produce a lacZ knock-in targeting vector by inserting an T3-IRES-lacZ-polyA-*loxP-neo-loxP* cassette into the cloned SAP102 genomic fragment by recombineering. Insertion of this cassette into the coding region of a gene results in a fusion mRNA containing both the endogenous cDNA and cassette sequences. The IRES allows cap-independent ribosome binding and lacZ translation independently of the remainder of the mRNA transcript. This experiment was repeatedly unsuccessful even after increasing the length of the short homology arms from 70 to 800 bp (Liu et al., 2003), shortening the cassette by removing the IRES-lacZ marker and trying a number of different recombination-competent *E.coli* strains (table 3.1, rows 2-6). Further experiments attempting to repeat the original BAC excision or to excise different genomic fragments from the same BAC also failed (data not shown).

To facilitate rapid construction of the targeted mouse a traditional restriction-ligation strategy was then used to introduce a mutation into the SAP102 genomic fragment. No suitable exonic restriction sites were available for insertion of the lacZ cassette so instead a simple *loxP*-flanked antibiotic resistance (*neo*) cassette was used. Figure 3.1b shows the targeting strategy and completed constitutive targeting vector. The cluster of exons encoding the PDZ domains were targeted since they mediate interaction with NMDARs and are close to the 5' end of the gene, minimising the possibility of a functional N-terminal peptide being produced upstream of the mutation. A deletion of exons 2-8 inclusive was engineered as shown (figure 3.1b), removing the coding sequence for amino acids 120 – 400, deleting PDZ domains 1 and 2 and introducing a frameshift mutation between exons 1 and 9. The deleted section was replaced with a selection cassette containing the mouse neomycin phosphotransferase (*neo*) gene driven by a compound phosphoglycerate kinase (PGK) and EM7 promoter for kanamycin resistance in bacterial and G418 resistance in vertebrate cells respectively. The integrity of the completed targeting vector was confirmed by extensive restriction digestion and by sequencing of the junctions of ligated

DNAs. Figure 3.1c shows a restriction digest of the completed targeting vector and its two parental plasmids.

3.2 Construction of an improved system for flexible and efficient targeting vector production

Because of the power and flexibility offered by recombineering as a method for building targeting vectors and because of its successful use by others (Copeland et al., 2001; Liu et al., 2003; Zhang et al., 2000), attempts were made to devise a reliable recombineering strategy that would be effective in producing many different types of mutations in a large number of different mouse loci.

To improve recombineering efficiency and facilitate engineering of a variety of types of mutations in many different genes, a new set of plasmids for recombineering-based targeting vector construction was constructed (figure 3.2). The vectors were designed to minimise intra- and inter-plasmid sequence homology, thereby reducing the risk of aberrant recombination between plasmid backbones and selection cassettes during homologous recombination in bacteria. Donor and recipient vectors carry different antibiotic markers to allow independent selection and further minimise inter-plasmid sequence homology. Each vector contains multiple cloning sites (MCS) for insertion of PCR-amplified homology arms to mediate recombination. All insertion cassettes carry the *neo* gene driven by dual promoters for positive selection in both *E.coli* and ES cells. Each plasmid was verified by extensive restriction digestion followed by full sequencing using a transposon-mediated shotgun method. The verified sequence of each plasmid is shown in appendix 3.

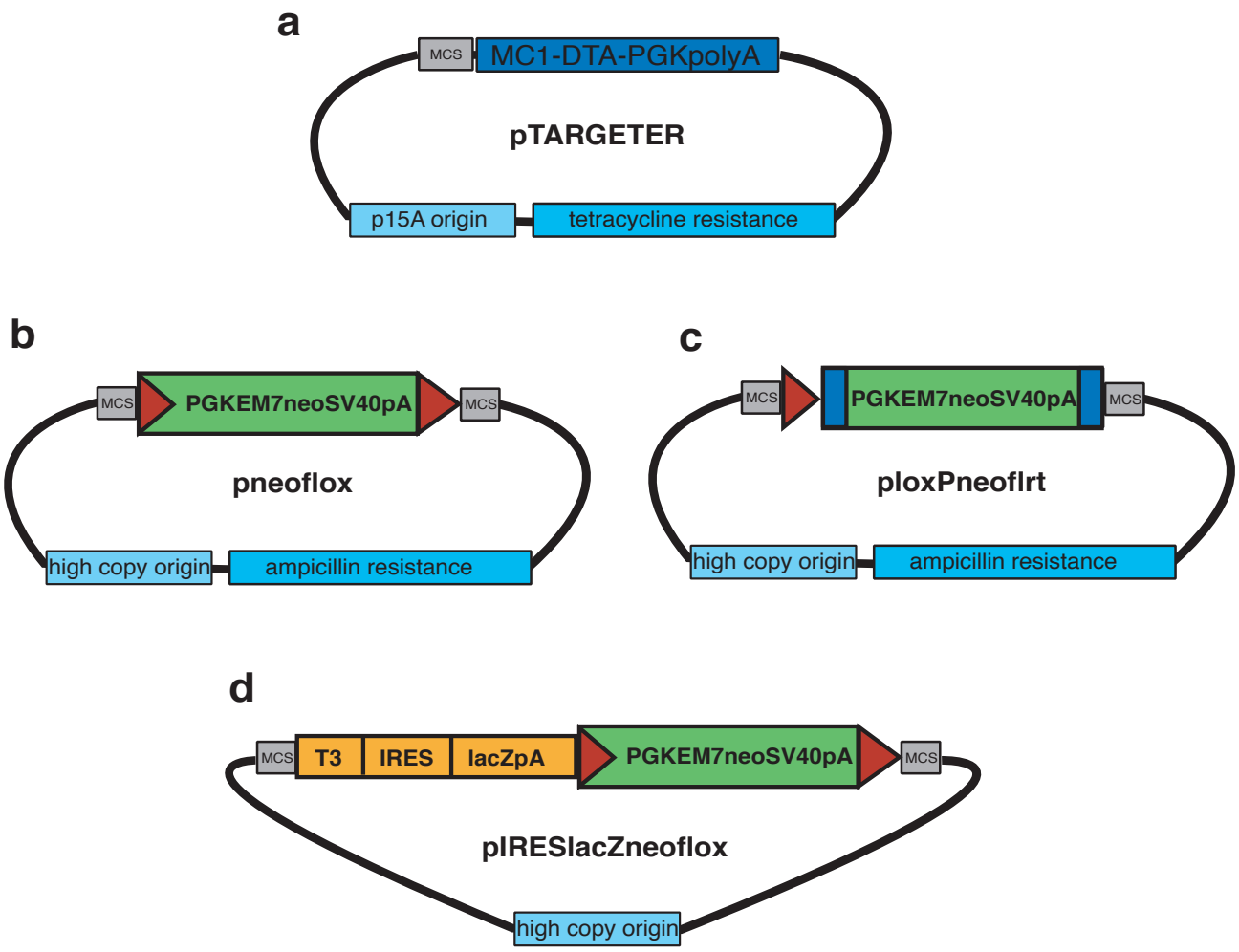

Figure 3.2 The TARGETER vector system for recombination-based construction of targeting vectors. (a) pTARGETER is the targeting vector backbone. It carries a low-copy p15A replication origin to facilitate insertion of large genomic fragments and a DTA negative marker with PGK polyadenylation signal to discourage random integration of the vector into the ES cell genome. **(b)** pneoflox allows introduction of a single loxP site via insertion of a loxP-flanked antibiotic resistance (neo) cassette followed by Cre recombinase-mediated excision of the cassette. **(c)** ploxPneoflrt facilitates insertion of a second loxP site into the same genomic fragment using a loxP site adjacent to an FRT-flanked antibiotic resistance cassette which is subsequently removed by Flp recombinase-mediated excision. **(d)** pIRESlacZneoflox allows insertion of a lacZ marker to track transcriptional activity. The cassette carries termination codons in all three frames (T3) to interrupt translation of the endogenous protein. The selection cassette can be subsequently excised by Cre recombinase. All vectors carry multiple cloning sites (MCS) to facilitate the insertion of short homology arms for recombineering. Red triangles - loxP sites; dark blue boxes - FRT sites.

a

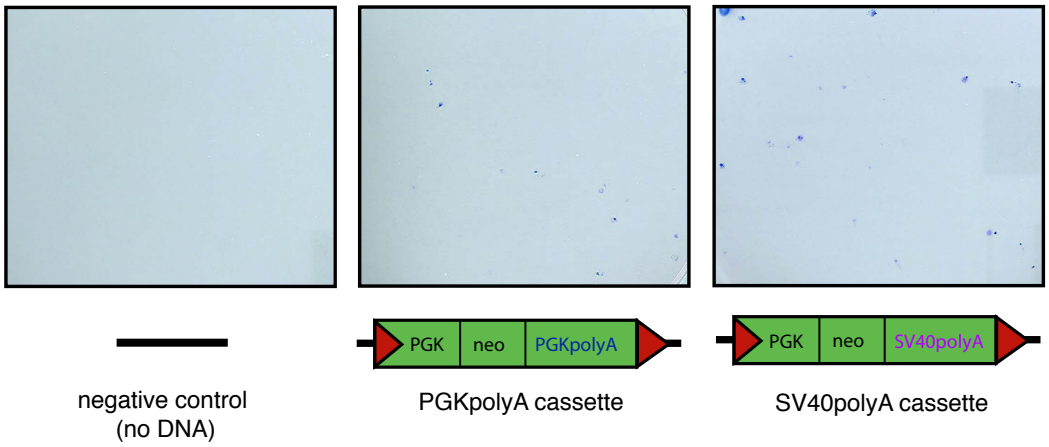

b

plasmid	G48-resistant colonies
none	0
PGKpolyA	33
SV40polyA 1	47
SV40polyA 2	51
SV40polyA 3	33

Figure 3.3 The SV40 polyA signal sequence in TARGETER cassettes mediates efficient expression of a drug resistance marker in mouse ES cells. (a) ES cells were electroporated with linearised plasmid vectors containing neo antibiotic resistance gene with a PGK promoter and either a PGK or SV40 polyA signal sequence. Electroporated cells were subjected to G418 selection for five days, after which drug-resistant colonies were stained with Giemsa for counting. Representative images of Giemsa-stained colonies are shown. **(b)** Colony counting shows that the SV40 polyA in three different plasmids is at least as effective at conferring drug resistance as the PGK polyA.

The targeting vector backbone is p*TARGETER* (figure 3.2a), with a low-copy p15A replication origin to allow incorporation of large genomic fragments. As a negative selection marker for gene targeting, the plasmid carries a Diphtheria Toxin A (DTA) fragment driven by an MC1 promoter with a mouse phosphoglycerate kinase (PGK) polyA signal. DTA is more effective and convenient than thymidine kinase in reducing random genomic integration of the targeting construct (Yagi et al., 1993; Yanagawa et al., 1999).

p*neoflox* (figure 3.2b) is a vehicle for insertion of a *loxP*-flanked selection cassette into a genomic fragment. Exposure to Cre recombinase excises the cassette, leaving a single *loxP* site behind. p*loxPneoflrt* (figure 3.2c) enables insertion of a second *loxP* site as its selection cassette can be excised by Flp recombinase without interference from the *loxP* sites. These plasmids can be used to construct targeting vectors for simple deletions, conditional mutations and point mutations.

p*IRESlacZneoflox* carries a knock-in cassette consisting of the lacZ reporter gene preceded by an IRES to drive reporter expression following integration into a target exon (figure 3.2d). Translation termination codons in three different frames are included at the front of the cassette to ensure truncation of the endogenous protein. *LoxP* sites flanking the selection cassette allow its removal following homologous recombination, preventing interference between the strong PGK promoter in the cassette and that of the endogenous SAP102 gene (Dymecki, 2000).

Since the DTA negative selection marker in *pTARGETER* uses the PGK polyA signal, this sequence was removed from the insertion cassettes and replaced with the SV40 polyA signal to further minimise sequence homology. The efficacy of the SV40 polyA in mediating expression of the selectable marker was tested by electroporation of the new plasmids into mouse ES cells, shown in figure 3.3. SV40 polyA-containing selection cassettes produced at least as many G418-

resistant colonies as the original, PGK polyA-containing vectors, demonstrating that the SV40 polyA is effective for use in gene targeting in ES cells.

3.3 SAP102 targeting vector construction using the *TARGETER* vector system

To test the efficacy of the *TARGETER* system and to produce additional useful SAP102 mutations in mice, lacZ knock-in and conditional targeting vectors for SAP102 were constructed. Each step was performed by recombination-based cloning in EL350 *E.coli* (Liu et al., 2003), using PCR-amplified homology arms ligated into multiple cloning sites in the *TARGETER* vectors.

SAP102 lacZ knock-in targeting vector

This vector inserts a lacZ reporter gene into the SAP102 locus, allowing cell-specific analysis of SAP102 transcriptional activity along with a constitutive knockout mutation. In addition to its use in analysing spatial and temporal SAP102 expression patterns, it provides a simple, high-resolution means to track X-inactivation in heterozygous targeted female mice. Skewed X-inactivation is often associated with mental retardation in heterozgous human females (Ropers and Hamel, 2005) and there is some evidence for impaired cognitive function in female carriers of SAP102 mutations (Tarpey et al., 2004).

To construct the targeting vector, a 10.9 kb genomic fragment encompassing the SAP102 targeting region was excised from the SAP102 BAC clone into p*TARGETER* by recombineering. The IRES-lacZ-polyA-neoflox cassette from p*IRESlacZneoflox* was then inserted into this fragment, again by recombineering, deleting part of exon 4 and all of exons 5-10 inclusive. An in-frame myc epitope was incorporated in front of the cassette to allow tracking of any truncated SAP102 peptide produced using an anti-myc antibody (van der Weyden et al., 2002). Figure 3.4a shows the SAP102 lacZ knock-in targeting vector, the integrity of which was confirmed by

extensive restriction digestion and by DNA sequencing across each recombination junction. The functionality of the *loxP* sites was confirmed by Cre-mediated recombination in arabinose-induced EL350 *E.coli.* Figure 3.4b shows a restriction digest confirming the structure of the parental plasmids, the completed targeting vector and the same vector following Cre-mediated cassette excision.

SAP102 conditional targeting vector

Flanking essential exons of SAP102 with *loxP* sites by gene targeting allows the use of Cre recombinase-expressing mouse lines to generate spatially- and temporally-restricted ablation of SAP102 function (Dymecki, 2000). SAP102 begins to be expressed soon after birth in mice (Sans et al., 2000) and may be required for postnatal viability. Mutations in SAP97, another early-expressing PSD-95 family protein, are lethal. If SAP102 constitutive knockout mice do not survive then a conditional mutation will be necessary to generate live adult mice for experimental analyses. The fact that SAP102 is expressed early postatally and that humans carrying SAP102 mutations experience developmental delay (Tarpey et al., 2004), as well as the known developmental role of SAP102-interacting proteins such as NMDARs (Sprengel and Single, 1999) strongly suggests that SAP102 plays a role in mouse postnatal development. Ablation of SAP102 in adulthood would provide a means for distinguishing between its developmental function and an acute role in synaptic transmission, synaptic plasticity and cognitive function in the adult. Restriction of the mutation to specific brain regions, such as the hippocampus or cerebellum, would make possible a specific analysis of SAP102 function in those areas.

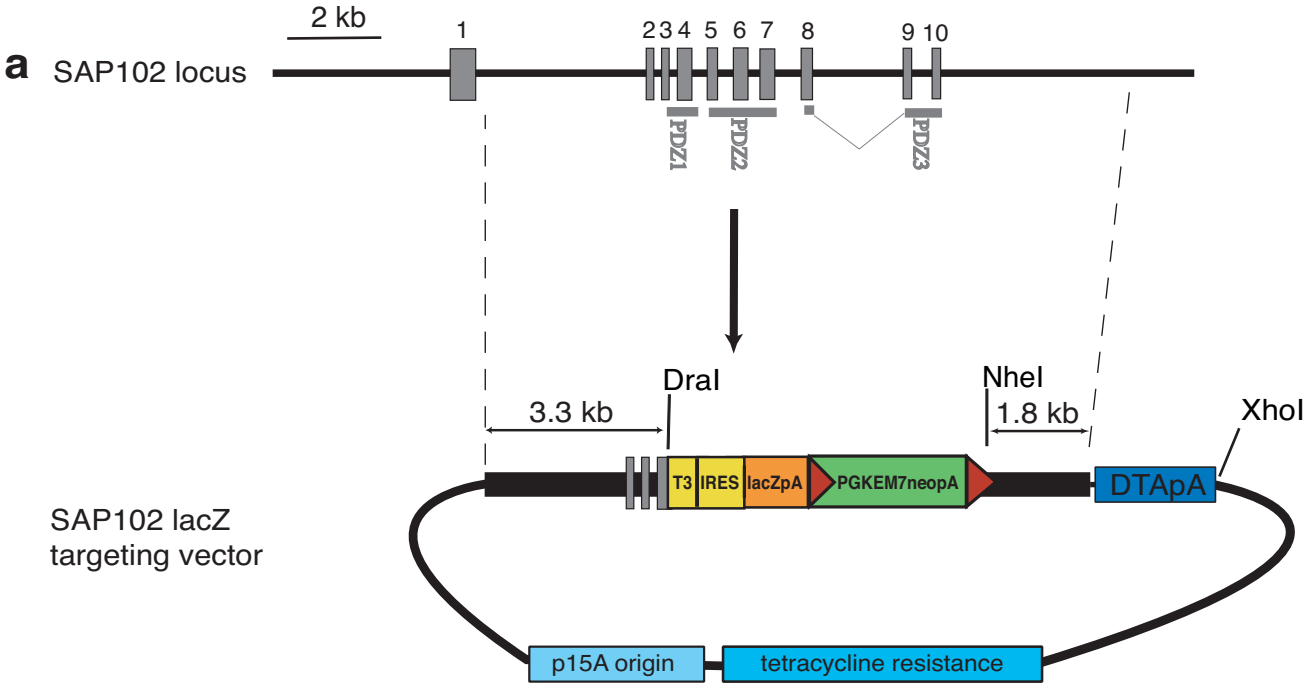

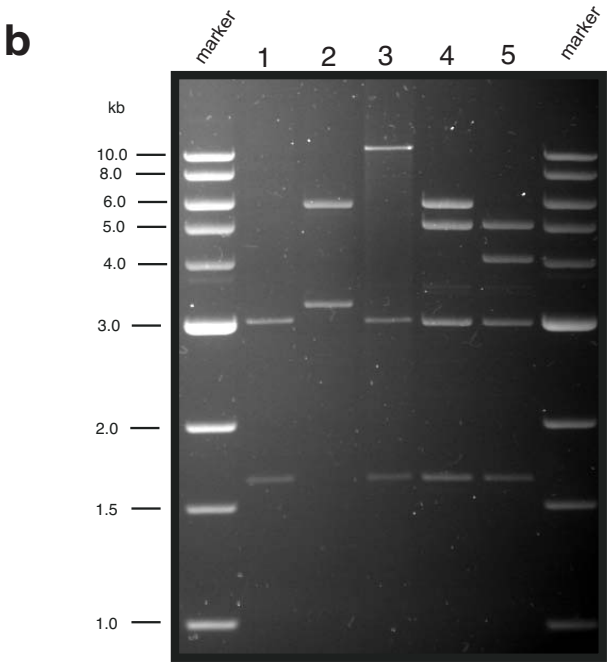

Expected BamHI fragment sizes (kb)

1	2	3	4	5
3.0	5.9	10.9	5.9	5.0
1.6	3.3	3.0	5.0	4.1
		1.6	3.0	3.0
			1.6	1.6

Figure 3.4 SAP102 lacZ knock-in targeting vector. (a) The T3-IRES-lacZ-neo cassette replaces part of exon 4 and all of exons 5-10 inclusive. SAP102 genomic fragments of 3.3 and 1.8 kb mediate homologous recombination. The vector backbone is pTARGETER, containing the DTApolyA negative marker against random integration. DraI and NheI sites in the selection cassette allow genotyping and a unique XhoI site is included for vector linearisation. **(b)** Restriction digestion confirms the structure of the targeting vector. Shown are BamHI digestions of pTARGETER (1), pIRESlacZneoflox with short homology arms for recombination (2), pTARGETER with SAP102 genomic subclone (3), the completed lacZ targeting vector (4) and the same vector following Cre recombinase-mediated recombination to remove the selection cassette (5).

The conditional targeting vector was built using the same SAP102 genomic fragment in p*TARGETER* as was used in constructing the lacZ knock-in vector. Into intron 5 of SAP102 in this subclone was inserted the *loxP*-flanked selection cassette from p*neoflox*, which was then excised in arabinose-induced, Cre-expressing, EL350 *E.coli*, leaving a single *loxP* site behind. A second *loxP* with an adjacent, *FRT*-flanked selection cassette was then inserted from p*loxPneoflrt* into SAP102 intron 1 in the same fragment, completing the targeting vector (figure 3.5a). Extensive restriction digestion and sequencing across the recombination junctions confirmed the vector's integrity (figure 3.5b) and the functionality of the *loxP* and *FRT* sites was confirmed by Cre- and Flp-mediated recombination in arabinose-induced EL350 and EL250 *E.coli* respectively.

Recombineering efficiency using *TARGETER* vectors

In contrast to previous attempts, each recombineering step performed using the *TARGETER* vectors worked with striking efficiency, as shown in table 3.1, rows 7-10. The system worked effectively in excising and inserting a variety of DNA fragments of sizes from 1.9 to 10.9 kb. Sequencing across junctions confirmed that this was accomplished with precise control, to a single nucleotide, over the sites of recombination and without the need for restriction enzyme sites in the genomic sequence. Each step produced at least 1,000 antibiotic-resistant bacterial colonies of which, in the majority of cases, 90 % or more carried the desired recombinant plasmid. The lowest proportion of correct recombinants achieved was 25 %, in the BAC excision step (table 3.1).

These vectors have now been used to produce targeting vectors, exclusively by recombineering, for six other brain-expressed genes with recombination efficiencies of 59.5 +/- 33% for the BAC excision and 51.2 +/- 45 % for the selection cassette insertion step (Noboru Komiyama, personal communication), demonstrating the reliability of the system and its applicability to different loci. One of these vectors has been used for targeting ES cells with a targeting efficiency of 8 %.

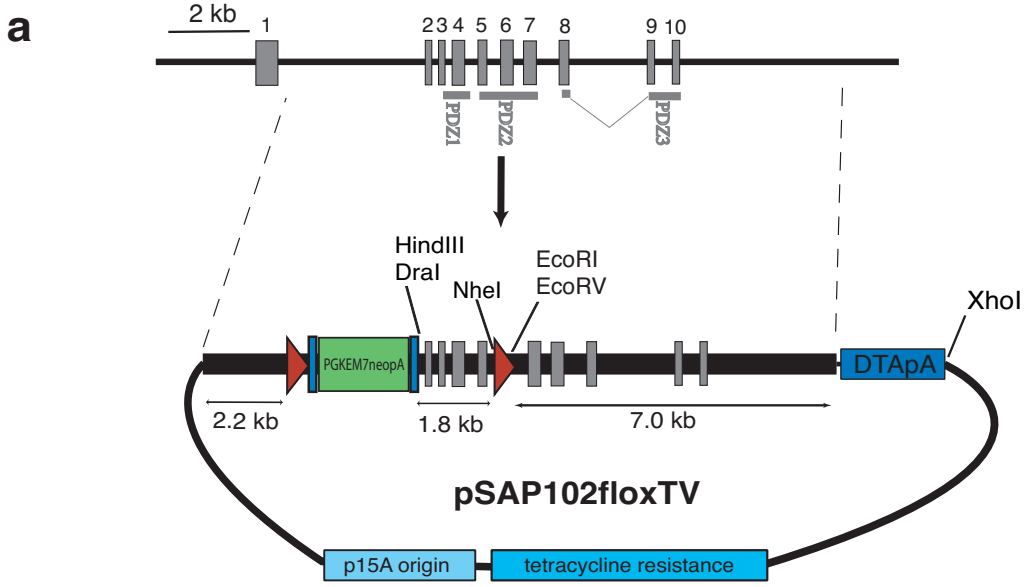

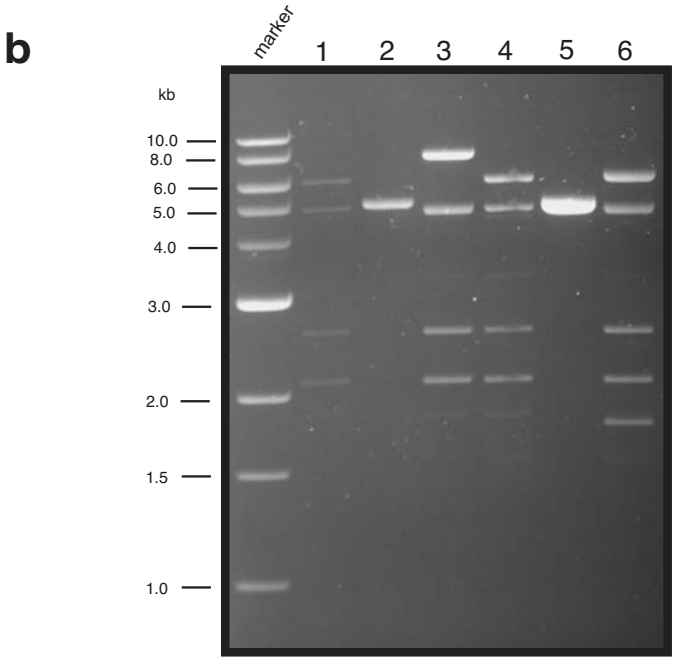

Expected HindIII fragment sizes (kb)

1	2	3	4	5	6
6.0	5.1	7.9	6.1	4.6	6.2
4.9		4.9	4.9	0.5	4.9
2.6		2.6	2.6		2.6
2.1		2.1	2.1		2.1
					1.8

Figure 3.5 SAP102 conditional targeting vector. (a) The vector consists of a loxP site and FRT-flanked selection cassette in intron 1 and a second loxP site in intron 5 of a SAP102 fragment in the pTARGETER backbone. Restriction sites were introduced along with the mutations as shown to facilitate genotyping. Arms for homologous recombination are 7.0 and 2.2 kb. Red triangles - loxP sites; blue boxes - FRT sites; green box - selection cassette. **(b)** Restriction digestion confirms the structure of the targeting vector. Shown are HindIII digests of pTARGETER with the SAP102 genomic subclone (1), pneoflox with short homology arms for recombination (2), pTARGETER.SAP102 with neoflox cassette inserted (3), the same plasmid after Cre recombinase-mediated removal of the cassette, leaving a single loxP site (4), ploxPneoflrt with short homology arms for recombination (5) and the completed targeting vector with the loxPneoflrt cassette inserted (6).

Table 3.1 Efficiency of recombineering in construction of SAP102 targeting vectors

	Cloning step	Size of excision/ insertion fragment (kb)	Donor vector	Recipient vector	*E.coli* strain	length per homology arm (bp)	Antibiotic -resistant colonies	% correct (from at least 20 analysed)
1.	BAC excision	13.0	SAP102 BAC clone	pBSSK.DTA	HS996 + pBADαβγ	70	8	12.5
2.	IRESlacZneoflox insertion	6.0	pSP76IRESlacZneoflox	pBSSK.DTA.SAP102	JC9604	70	120	0
3.	IRESlacZneoflox insertion	6.0	pSP76IRESlacZneoflox	pBSSK.DTA.SAP102	HS996 + pBADαβγ	70	75	0
4.	IRESlacZneoflox insertion	6.0	pSP76IRESlacZneoflox	pBSSK.DTA.SAP102	JC9604	70	150	0
5.	IRESlacZneoflox insertion	6.0	pSP76IRESlacZneoflox	pBSSK.DTA.SAP102	HS996 + pBADαβγ	800	160	0
6.	neoflox insertion	1.9	pSP77neoflox	pBSSK.DTA.SAP102	EL350	800	100	0
7.	BAC excision	10.9	SAP102 BAC clone	pTARGETER	EL350	650	1,000	25
8.	neoflox insertion	1.9	pneoflox	pTARGETER.SAP102	EL350	400	3,000	100
9.	neoflrt insertion	1.9	ploxPneoflrt	pTARGETER.SAP102.loxP	EL350	500	1,000	90
10.	IRESlacZneoflox insertion	6.0	pIRESlacZneoflox	pTARGETER.SAP102	EL350	800	8,000	100

3.4 Discussion

These results show that the *TARGETER* vectors combined with recombineering technology provide a rapid and powerful method for constructing targeting vectors for introducting of a variety of mutations into the mouse genome, including simple deletions, knock-ins and conditional mutations. This strategy works with high efficiency and allows precise control over insertion and excision points in the DNA without the need for restriction sites. The system is effective for constructing targeting vectors for numerous loci and should be broadly useful for targeting almost any location in the genome.

The construction of three different targeting vectors for the SAP102 locus provides a basis for a detailed genetic analysis of SAP102 *in vivo* in the mouse. The constitutive knockout vector will allow analysis of SAP102 function across all organ systems and will provide a model for NS-XLMR in humans. The lacZ knock-in vector will facilitate high-resolution examination of SAP102 transcriptional activity and X-inactivation in heterozygous female mice. The conditional targeting vector will help determine the role of SAP102 in specific brain regions during distinct developmental periods.

Chapter 4

Generation and verification of SAP102 targeted mice

4.1 Production of SAP102 targeted mice

To engineer a loss-of-function mutation in SAP102 in mice, the constitutive targeting vector generated in the previous chapter (see figure 3.1) was used to target the SAP102 locus in HM-1 mouse embryonic stem cells. These cells originate from 129P2 strain mice, formerly known as 129/OlaHsd (Festing et al., 1999; Ledermann, 2000; Selfridge et al., 1992). Cells electroporated with the linearised vector were cultured with G418 to select those carrying the *neo* selection cassette.

DNAs from G418-resistant colonies were analysed for the desired homologous recombination event with two independent long-range PCR reactions, one using a reverse primer (P2) hybridising to the region deleted by the mutation and the other using a reverse primer (P3) in the selection cassette. The two reactions use a common forward primer (P1) upstream of the 5' homology arm. Figure 4.1a shows the location of these primers in the SAP102 targeted region. Since the ES cells are male and carry only a single X chromosome, homologous recombination of the targeting vector with the endogenous SAP102 locus will convert the cell from wild-type (+/Y) to hemizygous (-/Y). As expected, genomic DNA from wild-type ES cells and most G418-resistant clones produced a 3.85 kb PCR amplification product from primers P1 and P2 but nothing from P1 and P3. DNA from a small number of clones, however, produced a 3.9 kb product from primers P1 and P3 but no 3.85 kb wild-type band. The genotype of the putatively targeted clones was confirmed by southern blot using probes outside the region of homology. Figure 4.1a shows the location of the 5' probe and *Dra*I restriction sites used in the Southern blot. Genomic DNA from wild-type ES cells, adult mouse tail and the G418-resistant but untargeted ES clones produced the expected 12.2 kb wild-type band when digested with *Dra*I and hybridised with the 5' probe. In targeted clones, the probe hybridised only with a 4.8 kb band as predicted by the restriction sites, as shown in figure 4.1c. These results were confirmed using *Nhe*I-digested genomic DNA hybridised with a probe 3' of the targeted region (data not shown).

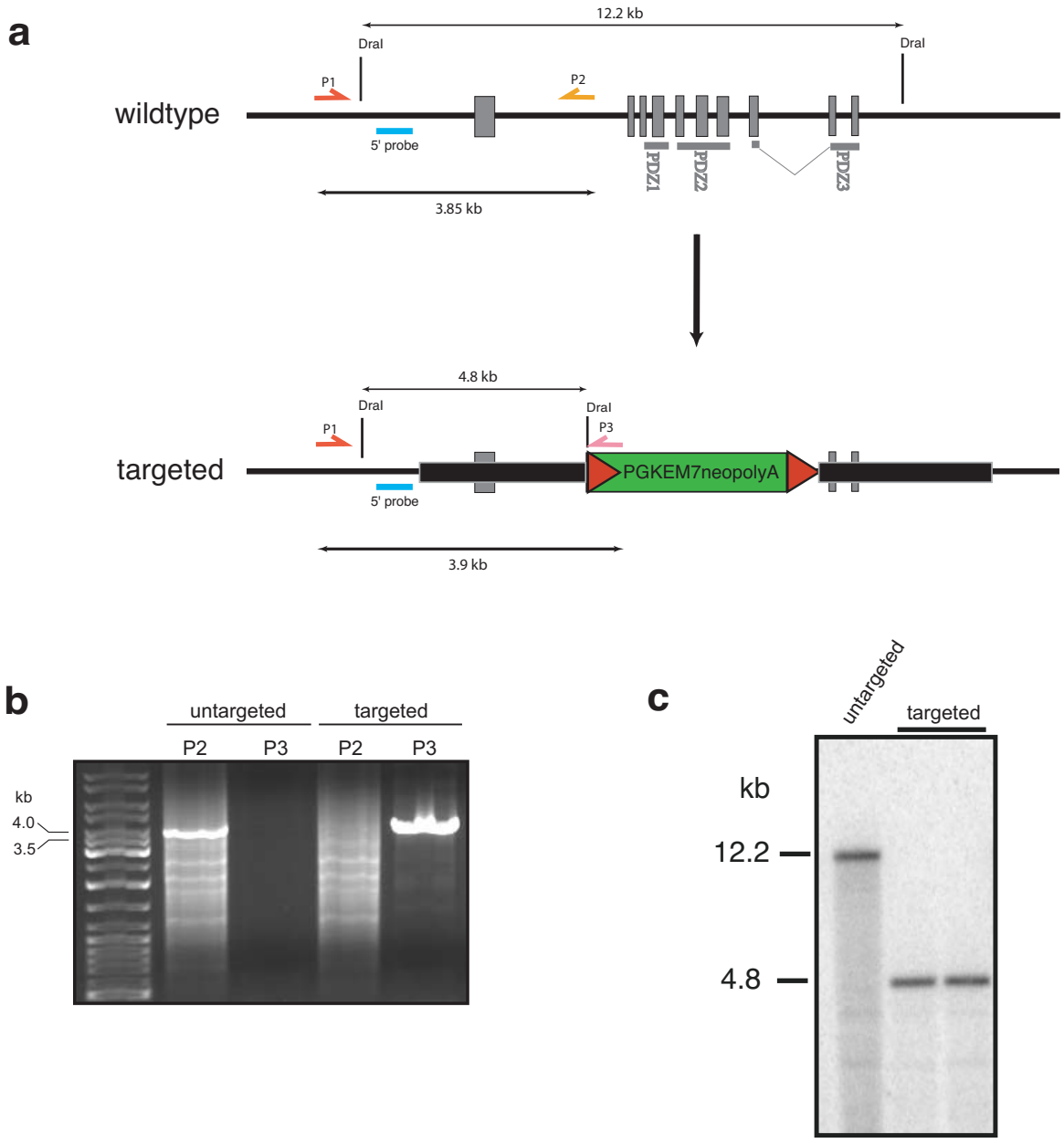

Figure 4.1 Targeting SAP102 in mouse ES cells. (a) The SAP102 deletion encompasses exons 2-8 inclusive, including PDZ domains 1 and 2, and creates a frameshift mutation between exons 1 and 9. PCR primers, restriction sites and the DNA probe used for genotyping are shown. Filled black boxes show the extent of homology arms used for targeting. **(b)** Following electroporation of the targeting construct and antibiotic selection, resistant ES cells are screened by long-range PCR using a forward primer 5' of the targeted region (P1) and two reverse primers, one hybridising to the deleted section of wild-type sequence (P2) and the other hybridising to the selection cassette (P3). Random integration of the targeting construct leaves the SAP102 locus intact so that a PCR reaction using P1 and P2 produces a 3.85 kb band while P1 and P3 generated no product. Conversely, targeted clones produce a 3.9 kb amplification fragment from P1 and P3 but generate no wild-type product. **(c)** The genomic structure of the mutation in targeted clones is confirmed by Southern blot. The 5' DNA probe is radiolabelled and hybridised to DraI-digested genomic DNA. The 12 kb wild-type fragment is reduced to 5 kb in the targeted allele by a DraI site in the selection cassette.

Of 304 G418-resistant colonies analysed, seven were positive for the mutation and two contained both wild-type and targeted DNA, probably the result of two clones, one having undergone homologous recombination and the other random integration of the construct, growing together as one colony in the dish. No unexpected DNA rearrangements were observed in any of the tested clones. These figures give an overall targeting efficiency of approximately 3%.

Two different targeted clones were injected into C57BL6/J mouse blastocysts which were then implanted into pseudopregnant mice. Among the resulting offspring, chimeras carrying cells derived from the targeted (129 strain) ES cells identified by coat colour.

Generation of hemizygous male mice for experimental analyses

Male chimeras from one of the two targeted lines were crossed with wild-type, MF1 strain females. Female (XX) offspring from these crosses inherit an X chromosome from each parent, while male offspring (XY) receive their single X chromosome from their mother and the Y chromosome of their father. Thus, passing of the targeted cells through the male germline produces SAP102 heterozygous (+/-) female and wild-type male (+/Y) offspring.

The heterozygous female offspring were bred with wild-type male offspring from the same crosses to produce hemizygous (-/Y) and wild-type male littermates (see figure 5.1b). Mice were weaned, ear-marked and tail tipped at 3-4 weeks of age and the tail tissue used for genotyping. Genotypes of mice used for further experiments were confirmed by a second PCR assay on tail tissue taken at the end-point of the experiment. All experiments were performed on male littermate pairs. Where females were used as well, they were wild-type and heterozygous littermate pairs. Experimental mice were at least six weeks old unless otherwise indicated and all conclusions are based on results from at least four pairs of mice of the same sex.

4.2 Genotyping of SAP102 targeted mice

Genotypes of targeted mice were initially confirmed with the same Southern blot analyses used to identify positive ES cell clones. DNA from wild-type, heterozygous and hemizygous targeted mice produced the expected patterns of wild-type and targeted bands when digested and hybridised with the 5' (figure 4.2 and b) and 3' (data not shown) probes. Mice inherited the targeted allele in approximately mendelian ratios and no unexpected DNA rearrangements were observed.

Having confirmed the fidelity of the mutation, subsequent mice were genotyped using two short PCR reactions, one amplifying the wild-type allele with a reverse primer (P5) in the deleted region and a forward primer (P4) a short way upstream, and a second reaction amplifying the mutant allele using the same forward primer along with reverse primer P3 in the cassette. The location of these primers is shown in figure 4.2a. Wild-type DNA produced only the 535 bp P4-P5 band, hemizygous DNA produced only the 215 bp P3-P5 band while heterozygous DNA produced both bands, as shown in figure 4.2c.

4.3 SAP102 protein is absent in targeted mice

To examine the effect of the targeted mutation on SAP102 protein production, total protein was extracted from dissected forebrains of adult wild-type and hemizygous male mice and analysed by western blot using an antibody raised against the N-terminal (undisturbed) region of SAP102 (see appendix 1 for a full list of primary antibodies). Figure 4.3a shows a band of approximately 100 kDa is robustly present in wild-type but undetectable in hemizygous mutant forebrains. An additional, non-specific band appears at approximately 60 kDa in both wild-type and mutant extracts, showing equal loading in each lane of the blot. Stripping the blot and re-probing with an antibody against PSD-95 confirmed equal loading (figure 4.3a).

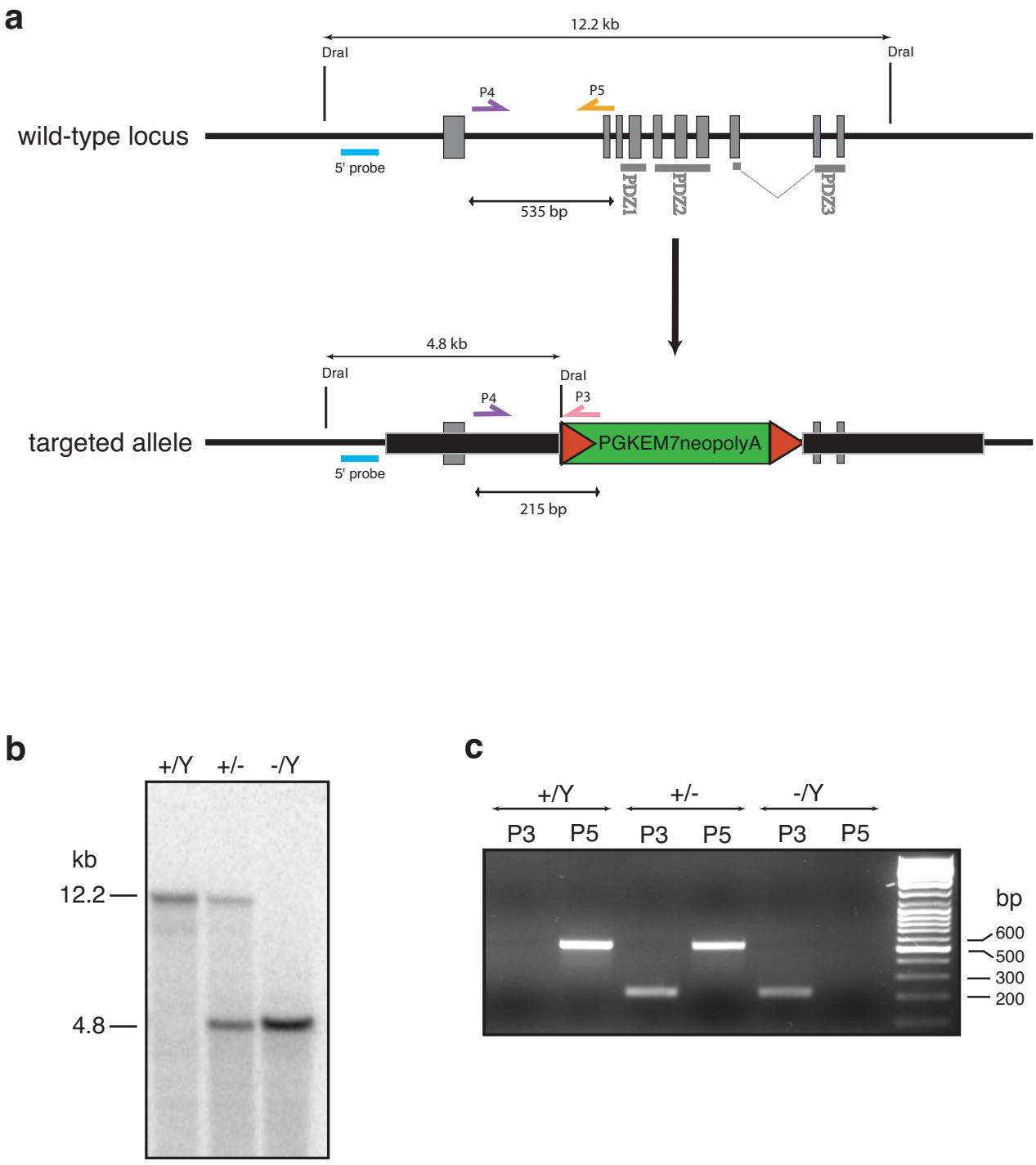

Figure 4.2 Genotyping SAP102 targeted mice. (a) Diagram of the targeted SAP102 genomic locus showing PCR primers, restriction sites and the DNA probe used for genotyping. **(b)** Southern blot confirms the structure of the SAP102 targeted locus, using the same assay as in ES cells (see figure 4.1). DraI-digested DNAs from wild-type (+/Y), heterozygous (+/-) and hemizyous (-/Y) mice produce the expected combinations of wild-type 12.2 kb and mutant 4.8 kb DraI fragments when hybridised with the 5' probe. **(c)** Short-range PCR genotyping assay using a common forward primer, P4, and two reverse primers, P3 and P5, hybridising to the targeted and wild-type alleles respectively. DNA from wild-type, heterozygous and hemizygous mice produce the expected combinations of the 215 bp P4-P3 and 535 bp P4-P5 fragments.

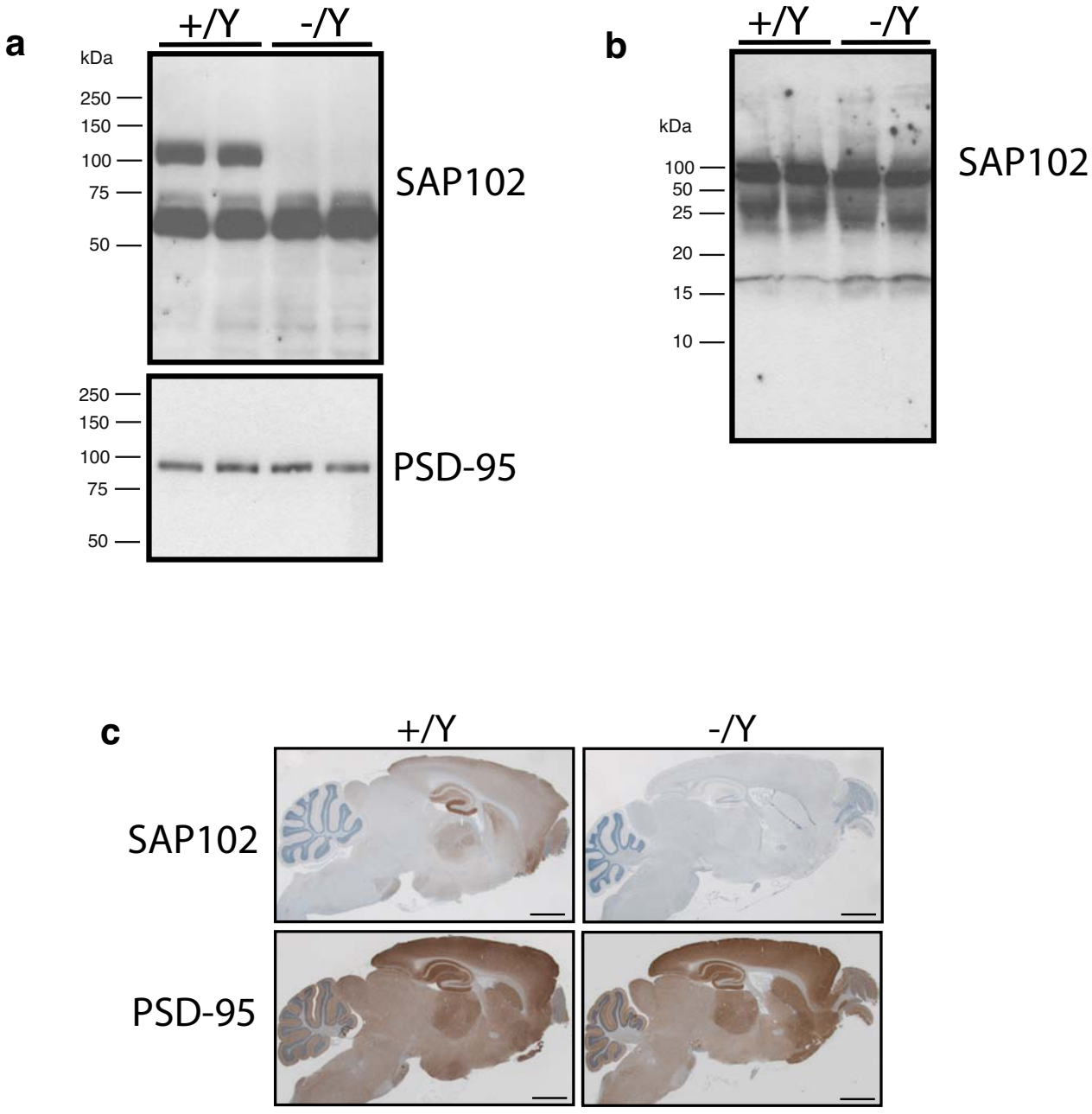

Figure 4.3 SAP102 protein is absent from targeted mice. (a) Western blot analysis of whole forebrain protein extracts shows a strong band at approximately 100 kDa in wild-type mice which is undetectable in hemizgyous mutants. PSD-95 levels are unaffected in the mutants. **(b)** No truncated SAP102 peptide is detectable in forebrain protein extracts from hemizygous mutant mice. The truncated product is expected to be 13 kDa in size. **(c)** Immunohistochemical staining of SAP102 (brown) in parasagittal sections shows the protein is absent from all regions of the brain in hemizygous mice while PSD-95 staining is unaffected. Sections are counterstained with haemotoxylin (blue). For both (a) and (b) antibodies were raised against the N-terminal, unaffected section of SAP102 protein. Scale bars are 2 mm.

The targeted mutation leaves intact the coding sequence for the N-terminal 120 amino acids of SAP102, which could potentially produce a 13 kDa truncated peptide. Such a peptide could not be detected in western blots even when 18 % polyacrylamide gels were loaded with three times the usual amount of protein extract and the blots were exposed for 30 minutes, as shown in figure 4.3b.

Immunohistochemical staining of parasagittal sections from wild-type and hemizygous adult brains was then undertaken to see whether any full-length or truncated protein remained in any part of the brain. For these experiments a different antibody, raised against the N-terminus of SAP102, was used that recognises only a single 102 kDa band on western blots (Fukaya and Watabe, 2000), a generous gift from Masahiko Watanabe (see appendix 1). As figure 4.3c shows, strong staining was observed in wild-type but no signal was detectable from mutant brain sections. These results strongly suggest that no full-length or truncated SAP102 protein is produced in hemizygous mice.

4.4 Discussion

No structural anomalies were observed in PCR or Southern blot analyses of the targeted allele in either ES cells or mice and the mutation was inherited by successive generations in the expected X-linked fashion, suggesting that the SAP102 mice carry the desired homologous recombination event without any other disruption to the genome. Similar analyses of the second, independently targeted line along with a partial phenotypic analysis to ensure agreement with the first line, will need to be performed to further reduce the slight possibility of a linked genomic rearrangement that remains undetected by the methods above.

The brains of male mice hemizygous for the targeted deletion have no detectable SAP102 protein, indicating that the mutation likely produces a null allele.

Chapter 5

Viability and brain morphology of SAP102 mutant mice

Several lines of evidence indicate roles for PSD-95 family proteins in neural development. They are expressed early postnatally during synaptogenesis and their domain structure and interaction partners suggest a potential synapse-assembly function (Funke et al., 2005). *Drosophila* dlg mutants have abnormal synapse structure (Lahey et al., 1994) and mice with a truncating mutation in SAP97 die soon after birth (Caruana and Bernstein, 2001). In contrast, synaptic structure appears normal in both PSD-95 and PSD-93 mutant mice, with a mild decrease in viability in PSD-95 -/- mice but not in PSD-93 -/- (McGee et al., 2001; Migaud et al., 1998). This chapter describes the characterisation of the viability, fertility and brain structure of SAP102 mutant mice.

5.1 SAP102 mutant mice are viable and fertile

To examine the effect of loss of SAP102 on viability and fertility, the results of crosses between 12 heterozygous females and 4 wild-type males were analysed. These matings produced litters of approximately normal size and frequency, suggesting that the mutation does not affect female viability in the heterozygous state, although for ethical and practical reasons the equivalent wild-type litters required for a formal comparison could not be produced. Male hemizygous and female heterozygous offspring had no apparent gross abnormalities at weaning and were indistinguishable from their wild-type littermates in appearance (figure 5.1a). Figure 5.1b shows the percentage of hemizygous adult male offspring (19 %) in these litters was slightly lower than that of wild-type males (27 %), wild-type females (26 %) or heterozygous females (28 %), however a chi-squared test for goodness-of-fit indicated these proportions were not statistically different from those expected under normal mendelian inheritance ($\chi^2 = 5.95$, n = 346, p = 0.11).

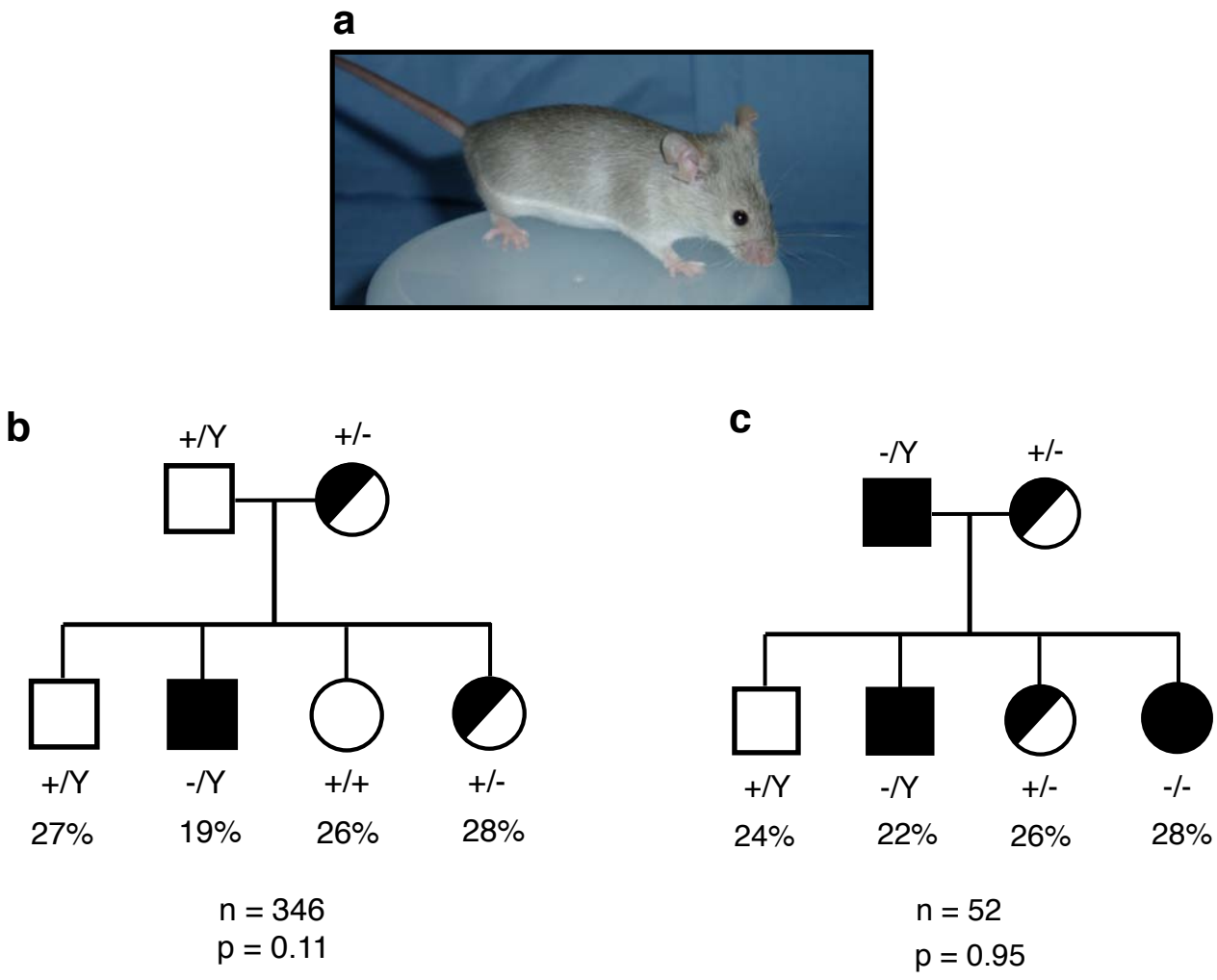

Figure 5.1 SAP102 mutant mice are viable and fertile. (a) Hemizygous males appear grossly normal with no obvious abnormalities. **(b)** Crosses between heterozygous females and wild-type males produce offspring of all expected genotypes in proportions not significantly different from those expected under mendelian inheritance inheritance (χ^2 = 5.95, n = 346, p = 0.11). **(c)** Crosses between hemizygous males and heterozygous females also produce mendelian ratios of the expected offspring genotypes including hemizygous males and homozygous females (χ^2 = 0.37, n = 52, p = 0.95).

Crosses between 3 hemizygous males and 6 heterozygous females also produced litters of approximately normal size and frequency, indicating no obvious effect of SAP102 loss on male fertility. Figure 5.1c shows that wild-type and hemizygous males, heterozygous and homozygous females were produced from these crosses at 24, 22, 26 and 28% respectively, proportions also no different from those expected under mendelian inheritance ($\chi^2 = 0.37$, n = 52, p = 0.95), showing that the null mutation does not affect the survival of either male or female mice. Preliminary crosses between 2 male hemizygous and 2 female homozygous mice were also fertile, producing one litter each within 4 weeks of being placed together. The first litter consisted of 8 male and 6 female pups. The second consisted of 4 males and four females. PCR genotyping confirmed that all the male pups were hemizygous and all the females homozygous for SAP102. Thus, the SAP102 null mutation affects neither survival nor fertility in mice of either sex.

5.2 Expression patterns of NMDAR-associated MAGUKs in the adult mouse brain

To inform the planned phenotypic analysis of the SAP102 mice and to search for possible differences in expression patterns between the three NMDAR-associated MAGUK proteins that could provide clues as to their differential function, an immunohistochemical study of SAP102, PSD-95 and PSD-93 expression was undertaken in the mouse brain. Four formalin-fixed, paraffin-embedded wild-type brains were sectioned parasagittally and stained separately for the three proteins of interest. Figure 5.2 shows the regional staining patterns of SAP102, PSD-95 and PSD-93 adult mouse brain (Paxinos and Franklin, 2001). The proteins display similar staining patterns with strongest expression in the hippocampus, cortex, olfactory bulb and olfactory tubercle, followed by the striatum, nucleus accumbens and pontine nuclei with the signal in remaining regions being weak or undetectable. Some regional differences were apparent, however. In the thalamus SAP102 and PSD-95 show moderate staining, while PSD-93 is weak.

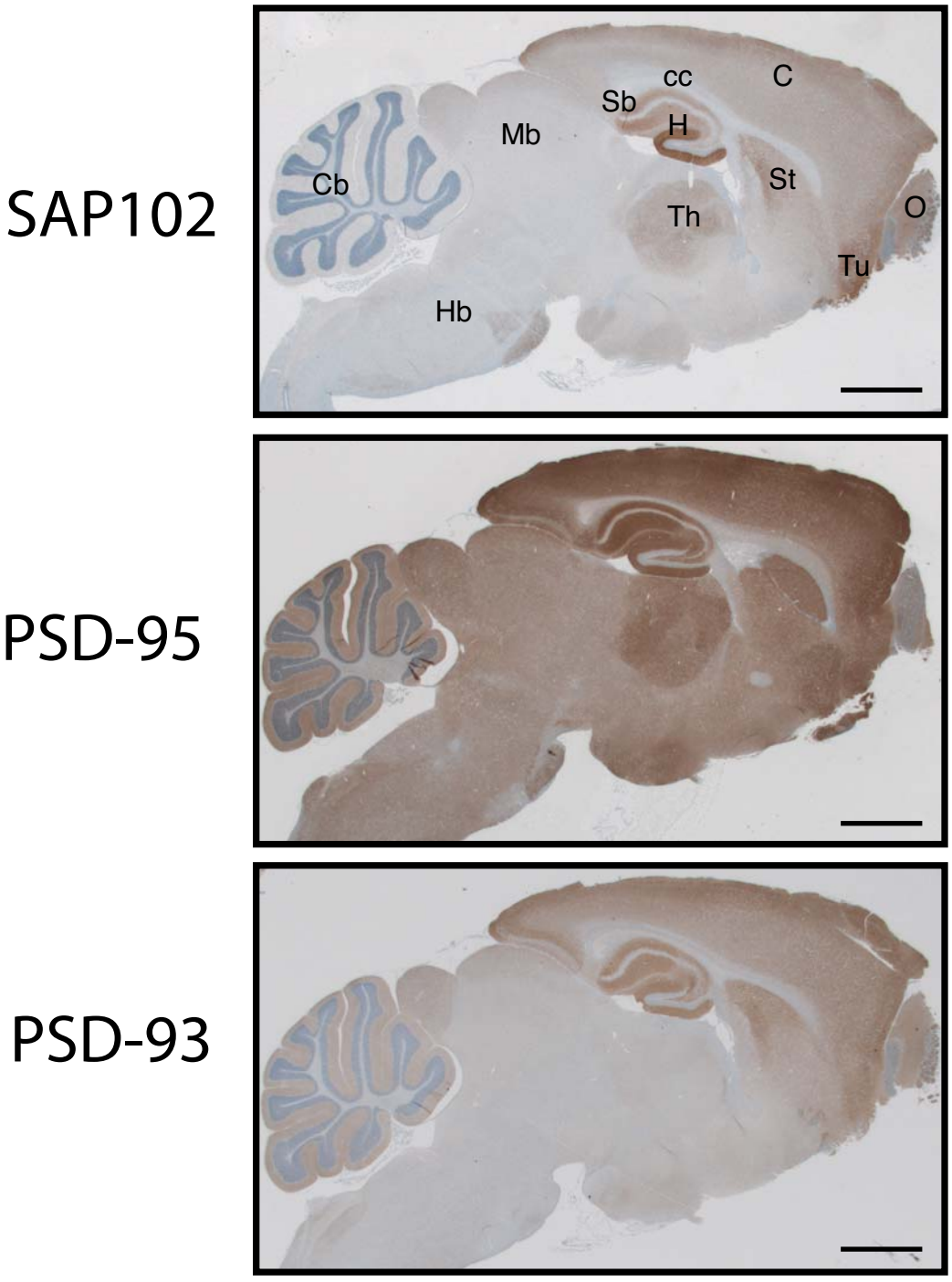

Figure 5.2 Expression patterns of NMDAR-associated MAGUK proteins in the wild-type adult mouse brain. Parasagittal sections are stained immunohistochemically for each MAGUK as shown (brown) and counterstained with haemotoxylin (blue). C - cortex; cc - corpus callosum; H - hippocampus; St - striatum; Sb - subiculum; O - olfactory bulb; T - olfactory tubercle; Th - thalamus; Mb - midbrain; Hb - hindbrain; Cb - cerebellum. Scale bars are 2 mm.

Within the hippocampus SAP102 is strikingly stronger in the dentate gyrus than in other subregions. PSD-95 shows a mild bias towards CA1 while PSD-93 stains at approximately equal intensity in each subregion, as shown in figure 5.3a. In the cerebellum, SAP102 and PSD-95 show strong staining in the granular layer while PSD-93 is weak. In the molecular layer, PSD-95 and PSD-93 display moderate staining, with only weak signal from SAP102. SAP102 and PSD-95 are undetectable in Purkinje cells while PSD-93 is strongly expressed (figure 5.3b).

At a subcellular level, the three MAGUKs were undetectable in cell bodies throughout the brain (see figures 5.3, 5.5 and 5.6). Staining was also weak or undetectable in fibre tracts such as the corpus callosum, anterior commissure and cerebellar white matter (figure 5.2). All three MAGUKs display striated staining patterns in the dendritic layers of the hippocampus and cortex (figures 5.3a and 5.6). These staining patterns are consistent with those previously reported (Fukaya et al., 1999; Fukaya and Watabe, 2000) and with their synaptic localisation. Table 5.1 summarises the regional expression levels of the three MAGUKs.

5.3 Brain morphology and postsynaptic protein expression in SAP102 mutant mice

The brain structure of SAP102 targeted mice was examined using histochemical and immunohistochemical staining of parasagittal and coronal sections from formalin-fixed, paraffin-embedded adult brain samples.

Whole brain

Whole brain morphology was examined by staining parasagittal brain sections from hemizygous and wild-type control mice with antibodies against the postsynaptic proteins PSD-95, PSD-93, NR1, NR2A, NR2B and MAP2B as shown in figure 5.4. Like the NMDAR-associated MAGUKs and consistent with published data (Watanabe et al., 1998; Wenzel et al., 1995), NMDAR

Table 5.1 Regional expression patterns of NMDAR-associated MAGUK proteins in the adult mouse brain

Structure			Expression level		
			SAP102	**PSD-95**	**PSD-93**
hippocampus	dentate gyrus	granular layer	-	*	*
		molecular layer	*****	***	***
		lacunosum moleculare layer	**	***	**
		polymorph layer	**	**	**
	stratum radiatum		***	***	***
	pyramidal cell layer		-	*	*
	stratum oriens		***	***	***
	stratum lucidem		**	**	**
cerebellum	white matter		-	*	-
	granular layer		***	***	*
	purkinje layer		-	-	***
	molecular layer		*	**	**
Subiculum			**	**	*
fimbria			-	*	*
thalamus			**	**	*
caudate putamen (striatum)			**	**	***
nucleus accumbens			**	**	**
olfactory bulb			***	***	**
olfactory tubercle			***	***	**
cortex			***	***	***
inferior colliculus			**	*	*
superior colliculus			**	*	*
hindbrain			*	*	*
midbrain			*	*	*
corpus callosum			-	*	*
anterior commissure			-	*	-

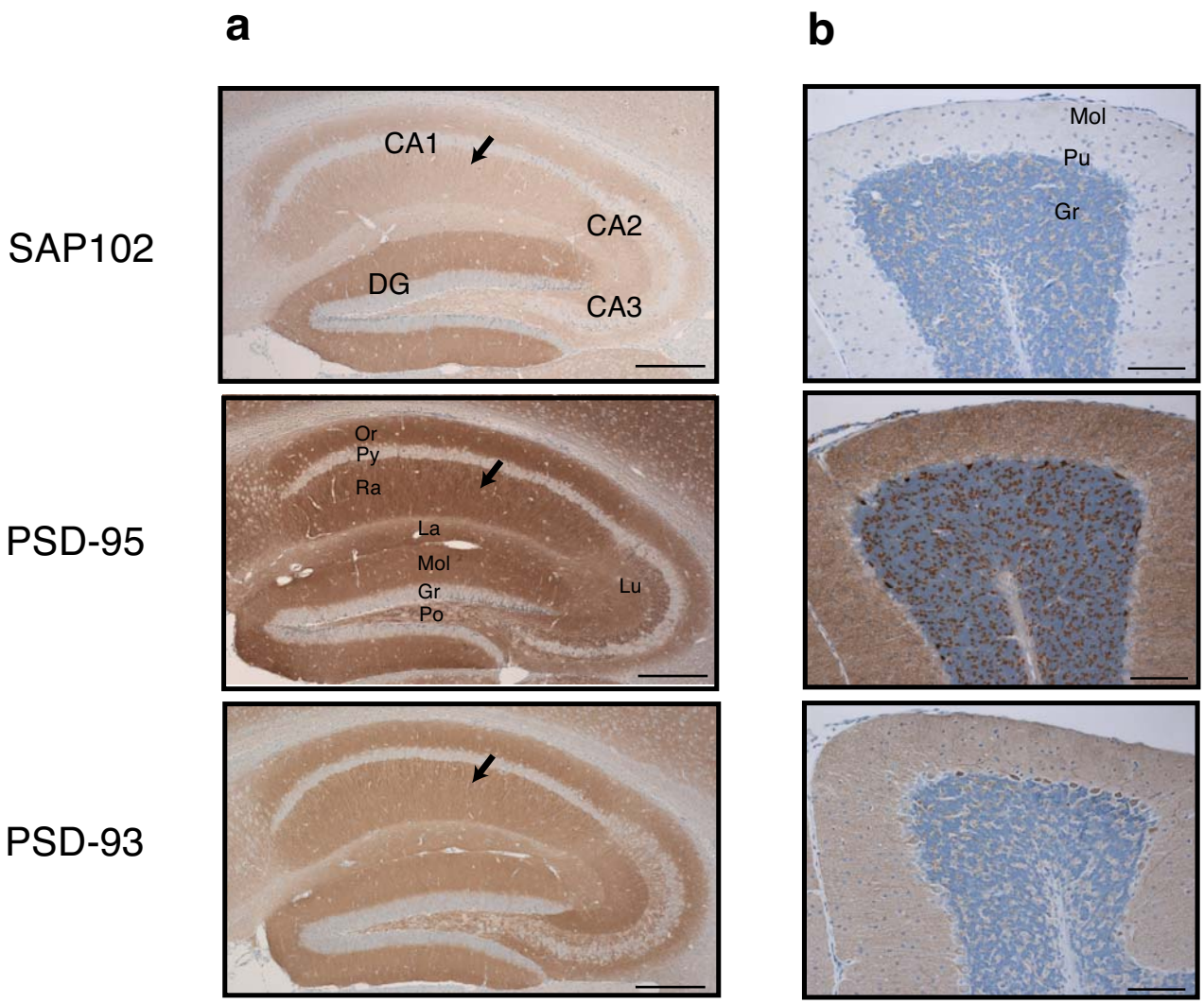

Figure 5.3 Subregional expression patterns of NMDAR-associated MAGUK proteins in the adult mouse brain. Parasagittal sections are stained immunohistochemically for each MAGUK as shown (brown) and counterstained with haemotoxylin (blue). **(a)** hippocampus, **(b)** cerebellum. DG - dentate gyrus; Or - stratum oriens; Py - pyramidal cell layer; Ra - stratum radiatum; La - lacunosum moleculare layer; Mol - molecular layer; Gr - granular layer; Po - polymorph layer; Lu - stratum lucidem, Pu - Purkinje cell layer. Arrow heads in (a) indicate striated dendritic staining patterns. Scale bars: (a) 500 μm, (b) 100 μm.

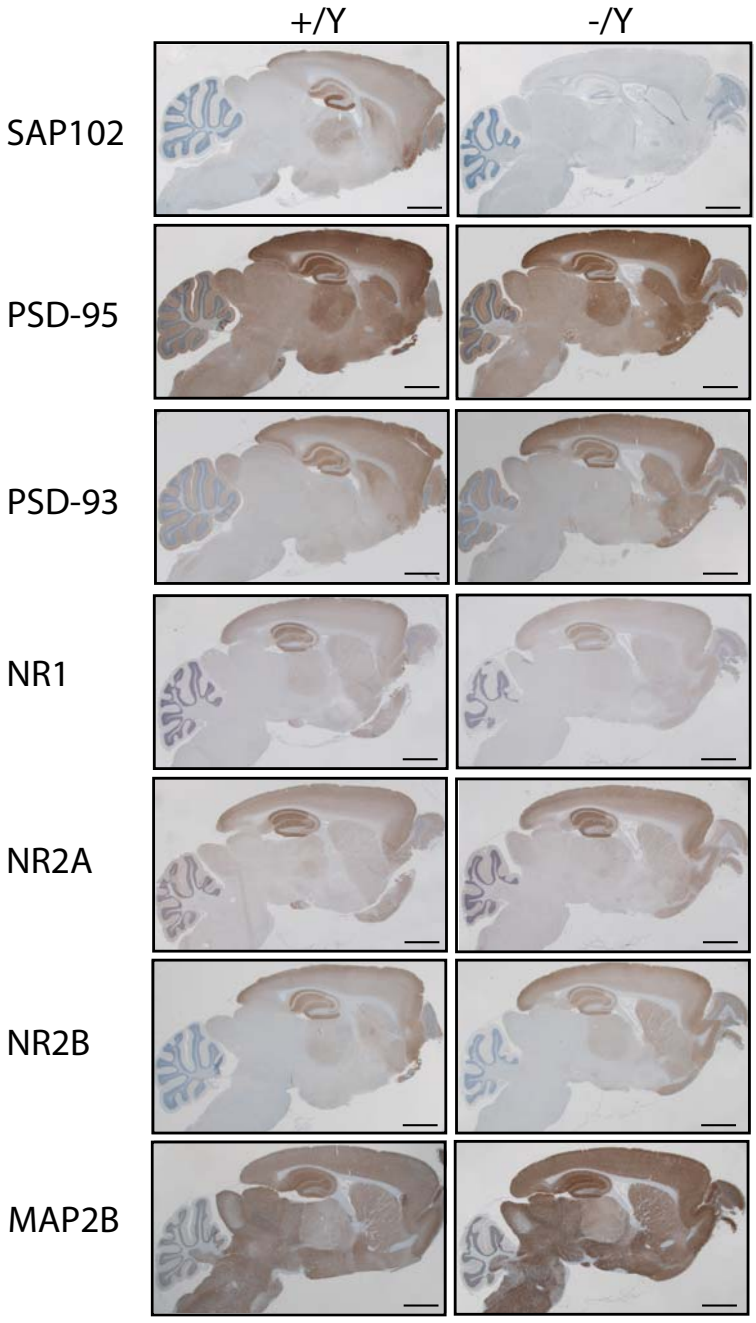

Figure 5.4 Brain morphology and postsynaptic protein expression patterns are normal in SAP102 mutant mice. Morphology and postsynaptic expression patterns in wild-type and SAP102 hemizygous mice in whole brain. Parasagittal sections are stained immunohistochemically (brown) as indicated and counterstained with haemotoxylin (blue). Scale bars are 2 mm.

subunits exhibited strong staining in the hippocampus, cortex and olfactory bulb in both mutant and wild-type sections. Microtubule-associated protein 2B (MAP2B), a dendritic marker (Huber and Matus, 1984), produced robust staining in dendrites throughout the brain. No alterations in levels of expression or regional distributions of these proteins was observed between mutant and wild-type sections.

Hippocampus

To examine more closely the structure of the hippocampus in SAP102 mutant mice, higher-magnification images of the region were captured as shown in figure 5.5a. In addition to the immunohistochemical stains used above, coronal sections were stained with Nissl, a cell-body stain. Hippocampal morphology appeared normal with no detectable differences between wild-type and control sections and no changes in postsynaptic protein expression levels or distribution were observed under any of the immunohistochemical stains.

Hippocampal expression levels of postsynaptic proteins were also analysed by western blot, using antibodies against the PSD-95 family proteins SAP97, PSD-95 and PSD-93, the NMDAR subunits NR1, NR2A and NR2B, the voltage-gated potassium channel Kv1.4, the AMPAR subunits GluR1 and GluR2, the kainate receptors GluR6/7, the neuregulin receptor ErbB4 and intracellular MAGUK-interacting signalling proteins SynGAP, Sec8, Pyk2, Kalirin-7 and Stargazin. Figure 5.5b shows that no differences in expression levels in these proteins were observed between hippocampal protein extracts from SAP102 hemizygous and wild-type mice.

The ultrastructure of the hippocampus was then examined using high-power light microscopy in the CA1 area. SAP102 immunohistochemical staining confirmed that even at high magnification no protein could be detected in mutant sections (figure 5.6, top panel). Despite the loss of SAP102, however, no differences were observed in the morphology or density of cell bodies in

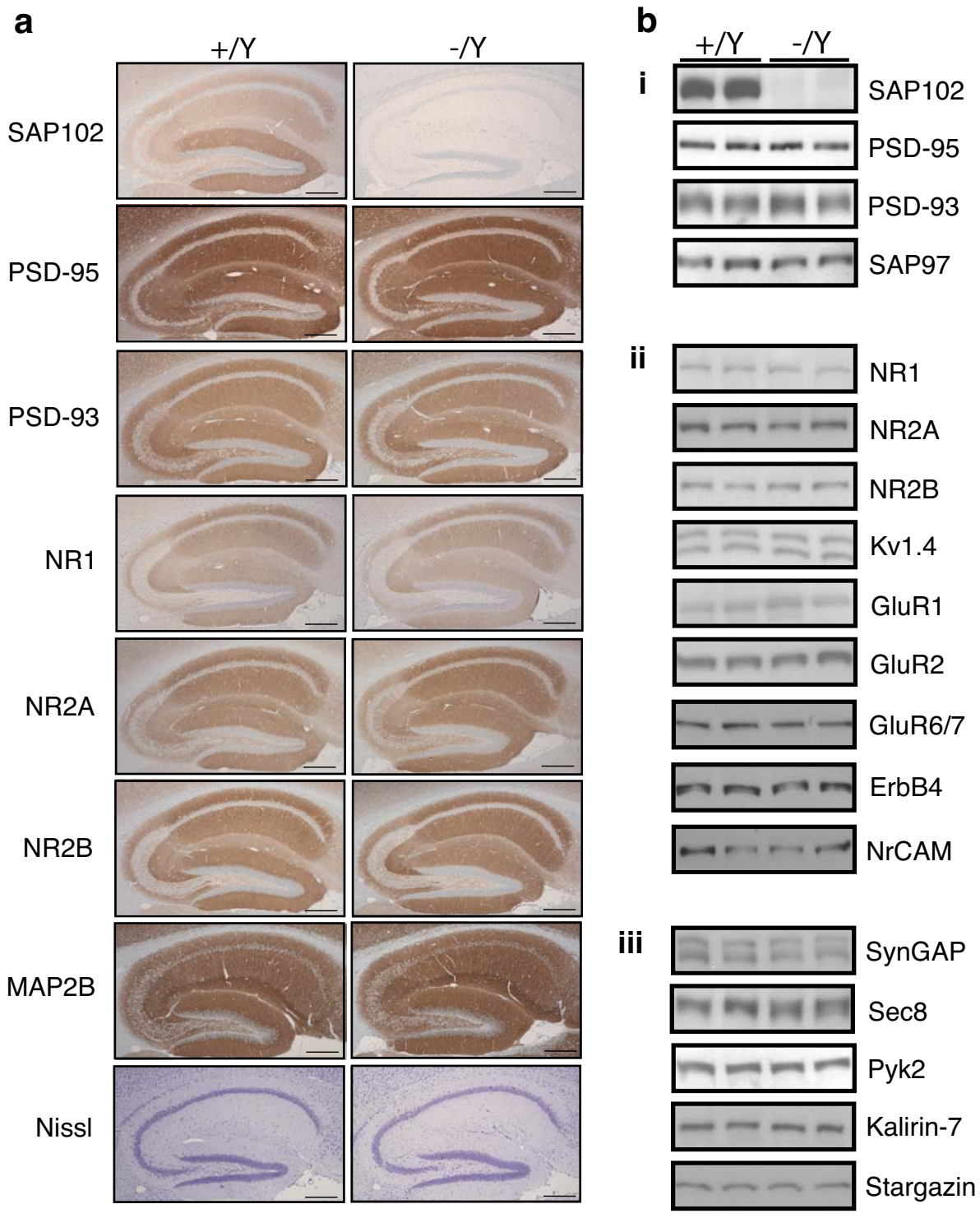

Figure 5.5 Hippocampal morphology and postsynaptic protein expression are normal in SAP102 mutant mice. (a) Morphology and postsynaptic expression patterns in the hippocampus of wild-type and SAP102 hemizygous mice. Parasagittal sections are stained immunohistochemically (brown) and counterstained with haemotoxylin (blue) or stained with cresyl violet (Nissl) only as indicated. Scale bars are 500 μm. **(b)** Normal levels of postsynaptic protein expression in the hippocampus of SAP102 mutant mice. Shown are western blots of hippocampal protein extracts for **(i)** PSD-95 family MAGUKs, **(ii)** transmembrane proteins and **(iii)** intracellular MAGUK-interacting proteins.

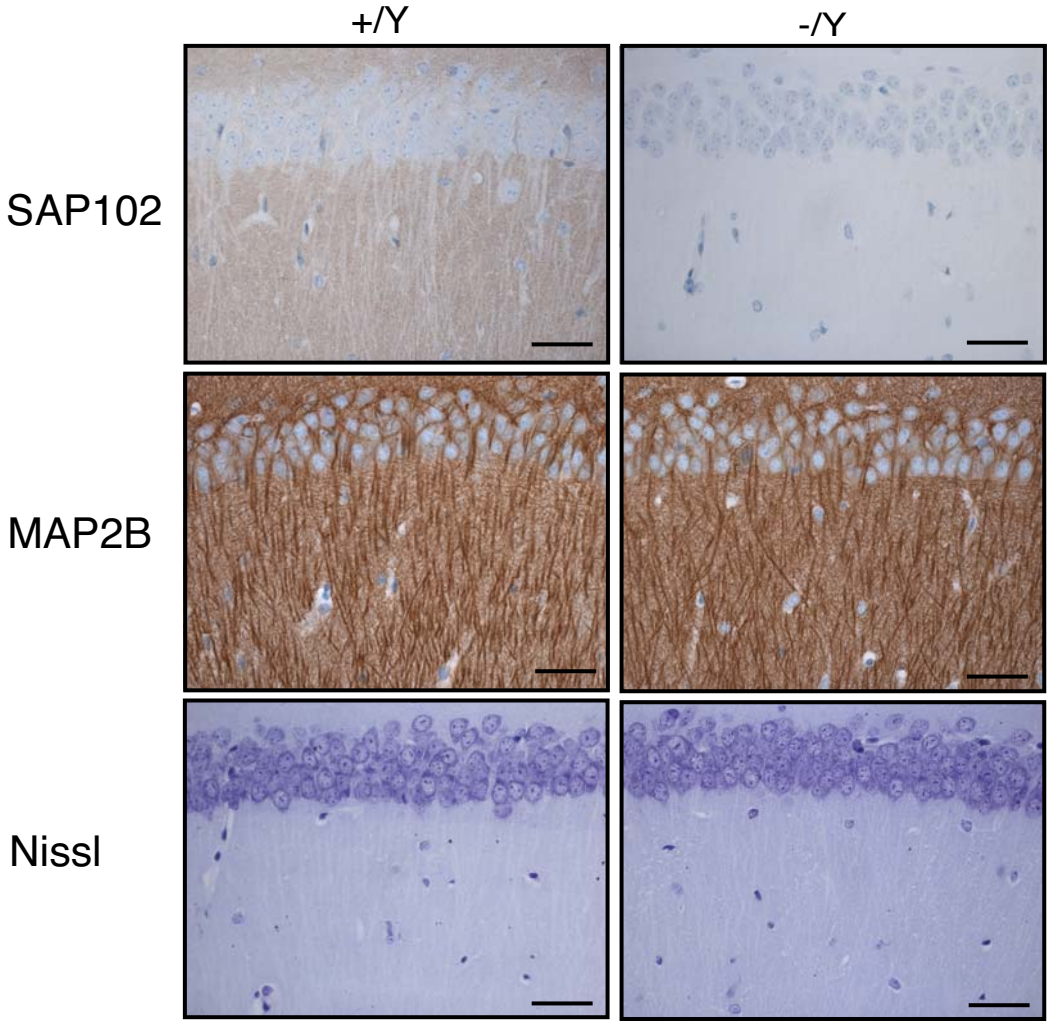

Figure 5.6 Normal hippocampal morphology under high magnification in SAP102 mutant mice. Sections show the CA1 pyramidal cell layer with the dendritic stratum radiatum layer below. No SAP102 staining is detectable in hemizygous brain sections even at high magnification, however dendrites stained with MAP2B and cell bodies stained with Nissl appear normal. SAP102 and MAP2B sections are counterstained with haemotoxylin. Scale bars are 50 μm.

the CA1 pyramidal area or dendrites in stratum radiatum when stained with Nissl or MAP2B respectively (figure 5.6, middle and lower panels). Finally, neuronal cell density in the hippocampus was quantified by counting columns of Nissl-stained cell bodies in pyramidal layer of CA1 and the granular layer of the dentate gyrus, shown in figure 5.7. No significant differences in mean cell density between wild-type and SAP102 mutant mice were observed in either region.

5.4 SAP102 mutant mice experience a postnatal developmental delay

In humans truncating SAP102 mutations cause developmental cognitive delay (Tarpey et al., 2004). To see if the same effect was observed in mice lacking SAP102, offspring born from matings between SAP102 heterozygous females and wild-type males were weighed every day from birth to postnatal day 14 (P14) and then every six days from P18 to P48. This experiment was performed by Lianne Stanford, Hayley Cooke and Margaret Green (Wellcome Trust Sanger Institute). Male and female pups increased in weight from approximately 1 g on the day of their birth to 9-10 g at P10 after which the sexes diverged, with males reaching 23-25 g and females 17-18 g by P48 (figure 5.8).

Analysis of body weight development of hemizygous versus wild-type male pups revealed a significant difference over the first 10 postnatal days [$F(1, 22) = 5.98$, $p = 0.023$] but not over the entire developmental period from P1 to P48 [$F(1, 33) = 1.29$, $p = 0.26$], as shown in figures 5.8a and 5.8c. Amongst female pups there was no significant difference in the body weights of heterozygous and wild-type individuals either during the first two postnatal weeks [$F(1, 32) = 0.25$, $p = 0.62$] or over the entire period [$F(1, 43) = 0.05$, $p = 0.83$], as shown in figures 5.8b and 5.8d.

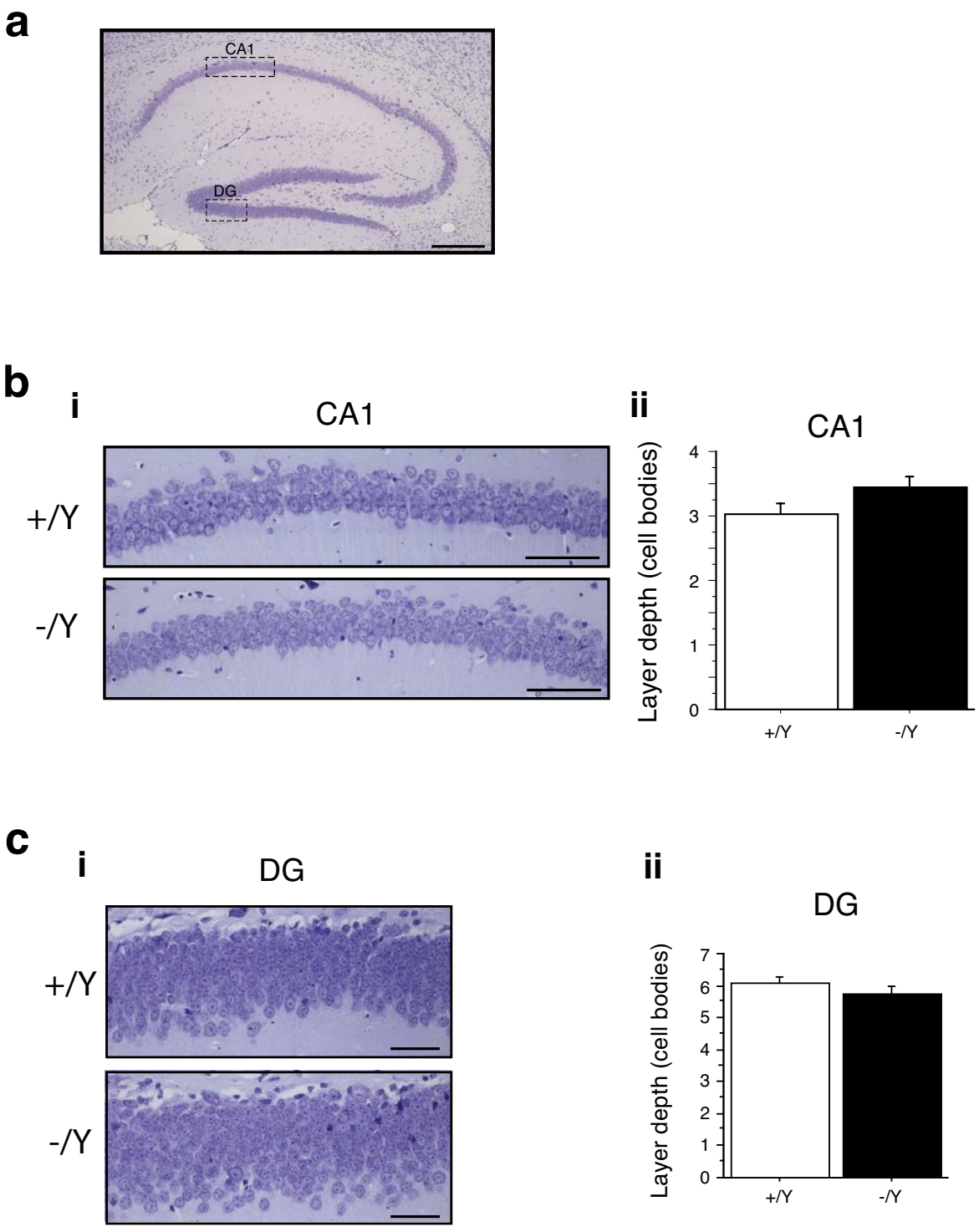

Fig 5.7 Loss of SAP102 does not affect hippocampal cell density. (a) Dashed rectangles indicate regions of CA1 and dentate gyrus (DG) in which cell numbers were quantified. Scale bar: 500 μm. **(b)** Cell numbers in CA1. **(i)** Cells were quantified by counting the number of Nissl-stained cell bodies between the dorsal and ventral boundaries of the CA1 pyramidal layer at 50 μm-intervals along the most dorsal part of the layer. Representative sections are shown. Scale bars: 100 μm. **(ii)** No difference in cell numbers were observed between wild-type and hemizygous animals [$F(1,4) = 1.23$, $p = 0.33$]. **(c)** Cell numbers in the dentate gyrus. **(i)** Cells were quantified using the same counting method at the caudal end of the lower arm of the pyramidal layer of the dentate gyrus. Scale bars: 50 μm. **(ii)** No difference between wild-type and hemizygous cell numbers was observed [$F(1,4) = 0.36$, $p = 0.58$].

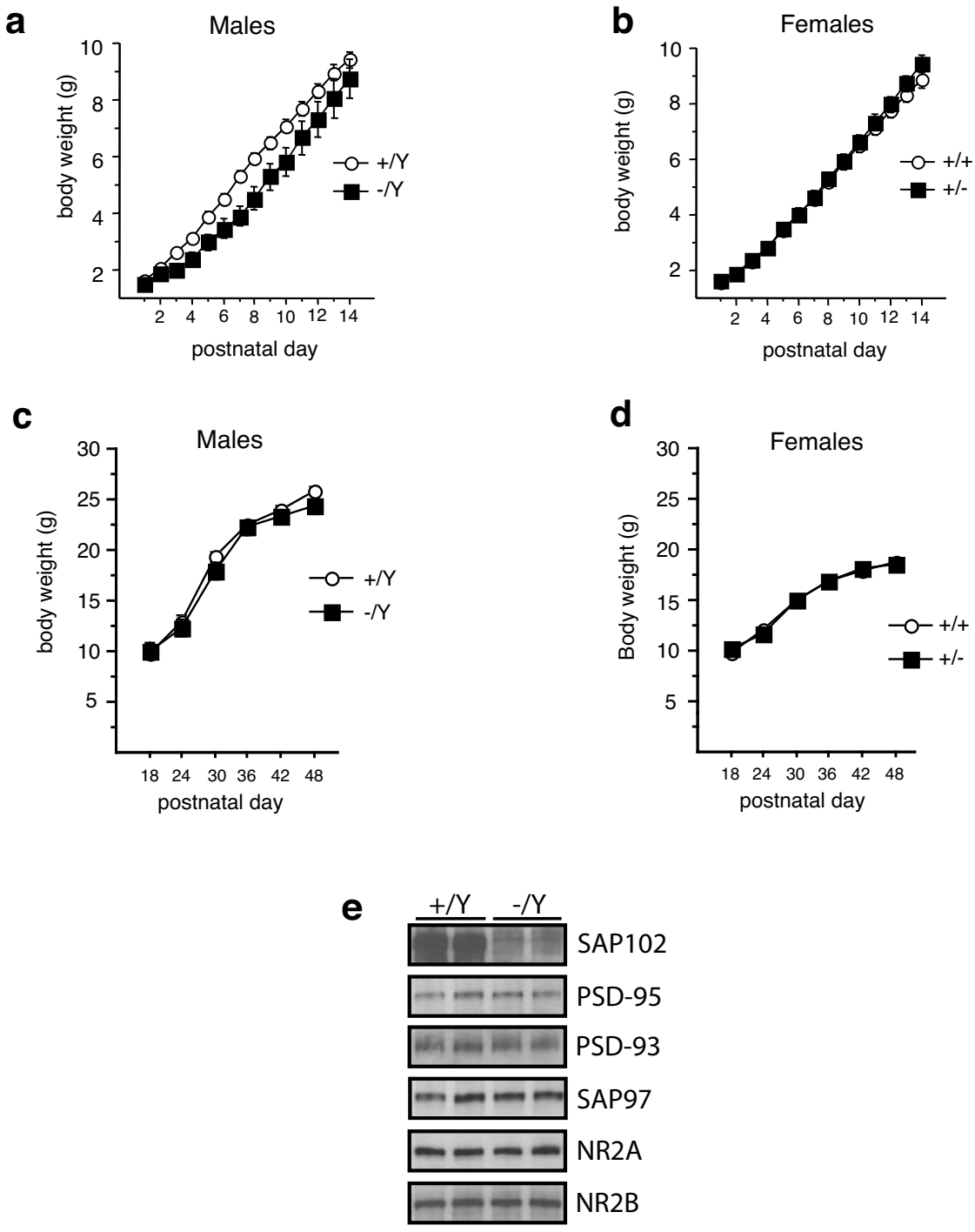

Figure 5.8 Loss of SAP102 causes developmental delay. **(a)** Body weights of male hemizygous and wild-type pups from postnatal day 1 (P1) to P14. Statistical analysis shows a significant effect of genotype on body weight [$F(1, 22) = 5.98$, $p = 0.023$]. **(b)** Body weights of heterozygous females remain normal throughout the first two postnatal weeks [$F(1, 32) = 0.25$, $p = 0.62$]. **(c)** No differences in body weight between wild-type and hemizygous male mice are observed between P18 and P48. Statistical analysis of body weights over the entire developmental period (P1-48) showed no effect of genotype [$F(1, 33) = 1.29$, $p = 0.26$]. **(d)** No differences in body weight between wild-type and heterozygous female mice are observed between P8 and P48 [$F(1, 43) = 0.05$, $p = 0.83$ for P1-48]. **(e)** Expression of MAGUKs and NMDA receptor subunits at P6 in the hippocampus of SAP102 mutant mice. All four MAGUKs as well as NR2A and NR2B are present and no changes in expression are observed as a result of the mutation.

Figure 5.8a shows that the weight of SAP102 -/Y pups diverges after P2 and remains below that of wild-type controls until regaining parity after P12. Published data of temporal expression patterns in the mouse suggest that SAP102 is robustly expressed from P2, while PSD-95 and PSD-93 levels are almost undetectable until their expression increases around P11 (Sans et al., 2000). This provides a possible reason for the requirement of SAP102 for normal development during this period, since no other MAGUK would be available to compensate for its function. The absence of all three MAGUKs during early development in SAP102 mutant mice would also provide a valuable opportunity to test the necessity of these proteins for NMDA receptor localisation and function during this period. To examine this possibility directly, MAGUK expression was analysed using western blots of protein extracts from forebrains of wild-type and SAP102 hemizygous male mice at P6 (figure 5.8e). Surprisingly, all four MAGUK proteins were present, although PSD-95 and PSD-93 appeared to be at lower levels than in adult tissue. No changes in MAGUK levels or NMDAR subunit expression was observed as a result of SAP102 mutation at this developmental time point.

5.5 Discussion

SAP102, PSD-95 and PSD-93, the three NMDAR-associated MAGUK proteins, display similar regional expression patterns in the adult mouse brain with strongest expression in the hippocampus, cortex and olfactory bulb. They are absent from neuronal cell bodies but strongly stain dendritic layers where they exhibit a distinctive striated pattern, suggesting they are preferentially localised to dendritic spines and present only at low levels or are absent from dendritic shafts. These results are consistent with their known enrichment in PSD fractions (Brenman et al., 1998; Cho et al., 1992; Muller et al., 1996), their postsynaptic localisation in electron microscopic studies (Aoki et al., 2001; Roche et al., 1999; Sans et al., 2000) and previously published immunohistochemical data (Fukaya and Watabe, 2000). These regional and

subcellular staining patterns match well with those observed for their associated NMDAR subunits NR1, NR2A and NR2B.

Despite broad similarities, some differences in expression patterns are apparent and may be used to make predictions as to the differential functions of individual NMDAR-associated MAGUKs. Perhaps the most striking difference is the strong expression of SAP102 in the dendritic layer of the dentate gyrus, contrasting with PSD-95's preference for CA1. It seems likely that any disruption of synaptic plasticity in SAP102 knockout mice will be most prominent in the dentate gyrus, while the disruption in PSD-95 mutants should be strongest in CA1.

Loss of SAP102 has no apparent effect on the survival, appearance or fertility of male or female constitutively targeted mice, so a full phenotypic analysis of the consequences of germline SAP102 loss upon adulthood should be possible. This is consistent with the human disorder, in which male hemizygous and female heterozygous individuals live to adulthood and can be fertile (Tarpey et al., 2004).

Neither does the SAP102 null mutation have any observable effect upon brain morphology or postsynaptic protein expression. Whole brain sections appear structually normal when examined under light microscopy with immunohistochemical staining, as does the general morphology and ultrastructure of the hippocampus. Hippocampal neuronal cell density is also normal and there is no evidence of disruption to expression levels or distribution patterns of postsynaptic proteins in the hippocampus either by immunohistochemical staining or western blot. Normal localisation of NMDAR subunits to hippocampal dendrites in these brain sections indicates that SAP102 may not be required for transport of this receptor to the synapse.

This result is encouraging with respect to human mental retardation, since therapeutically it is likely to be easier to compensate for an acute lack of adult SAP102 function in specific postsynaptic signalling pathways than to repair a gross structural dysmorphology. This does not preclude, however, the possibility of microscopic disruption to dendritic spine morphology which is a common mental retardation phenotype both in humans and mouse models (Comery et al., 1997; Kaufmann and Moers, 2000; Ropers and Hamel, 2005) and which could not be detected without more sophisticated microscopic techniques than have been employed here.

Loss of SAP102 does result in a postnatal developmental delay in growth from P2 to P11, corresponding closely with the period when, according to published data, SAP102 expression is strong while PSD-95 and PSD-93 expression is weak (Sans et al., 2000). Western blots showed however, that the latter two proteins were easily detectable at P6. Loss of SAP102 could cause delayed growth via several potential mechanisms. For example, impaired suckling ability could arise from lack of motor coordination as a result of cerebellar SAP102 loss. Alternatively SAP102 deficiency in the olfactory bulb could lead to olfactory impairment and a concomitant inability of a pup to find its siblings and mother for warmth and food.

Chapter 6

Behavioural analyses of SAP102 mutant mice

In humans, loss of SAP102 function has significant behavioural consequences. This chapter presents the results of a battery of tests to determine the effect of SAP102 loss on behaviour in the mouse.

6.1 Loss of SAP102 causes a deficit in spatial learning

Male patients with truncating SAP102 mutations have learning difficulties and SAP102 is highly expressed in the hippocampus, where functioning NMDA receptors are required for normal spatial learning. To see whether SAP102 is required for spatial learning the mice were tested in a water maze, a widely used task in which performance is both hippocampal- and NMDAR-dependent (Frankland and Bontempi, ; Morris et al., 1986; Morris et al., 1982). The apparatus consists of a large circular pool of opaque liquid with a small platform hidden just below its surface. To escape from the water, the mouse must use distal spatial cues to navigate its way to the platform. To facilitate direct comparisons with the spatial learning capabilities of the PSD-95 mutant mice, the SAP102 mice were tested using the same water maze apparatus and experimental protocol (Migaud et al., 1998). These experiments were performed and analysed by Jamie Ainge (Division of Neuroscience, University of Edinburgh) and Lianne Stanford (Wellcome Trust Sanger Institute).

Figure 6.1a shows a timeline of the water maze experiment. SAP102 hemizygous mice and wild-type littermate controls were initially tested with a raised, visible platform for three days with four trials per day, to habituate them to the apparatus and tested for differences in visual or motor abilities which could confound the spatial learning aspect of the task. Performance of the mice in the visible platform training is shown in the left panels of the plots in figure 6.1b, c and d.

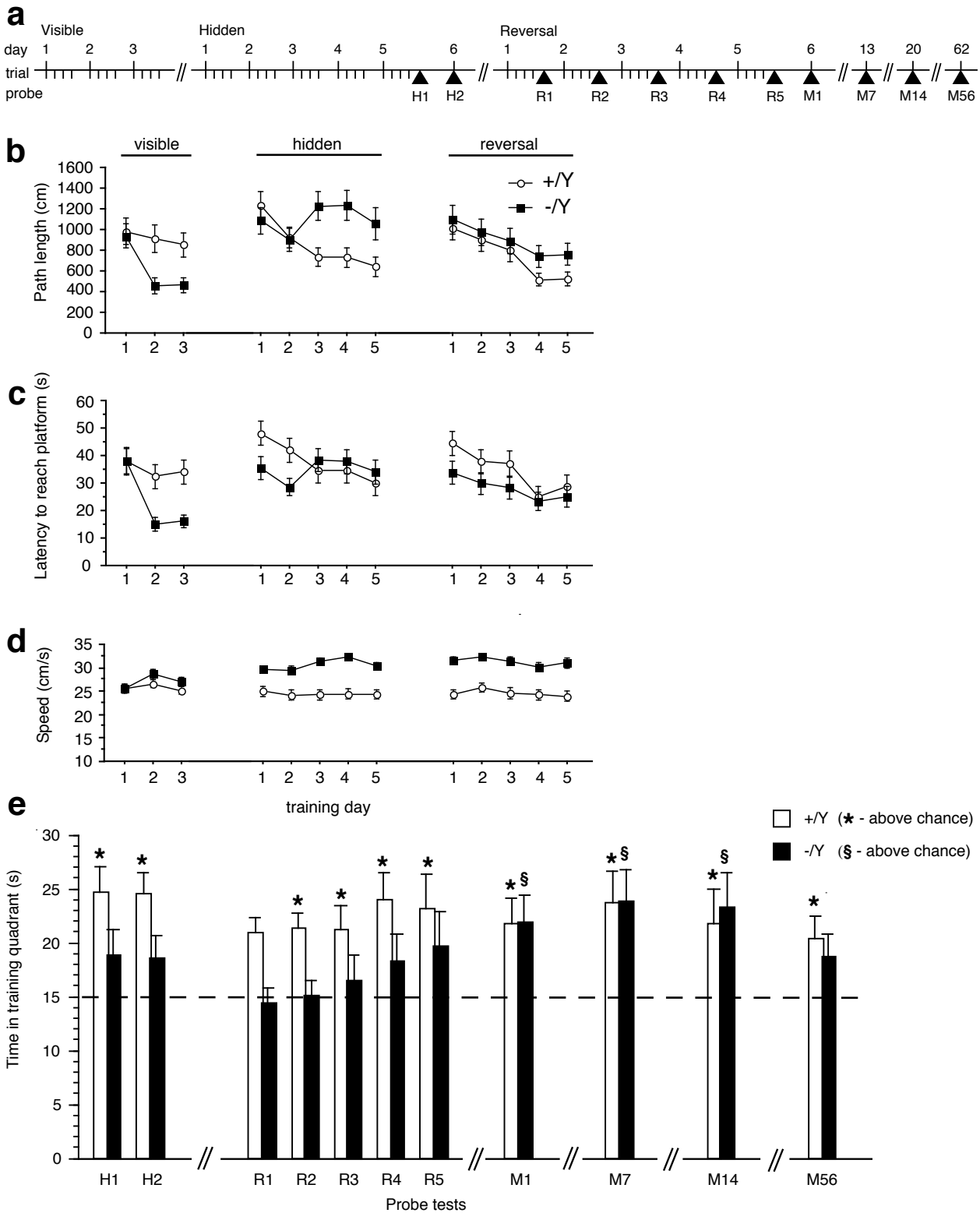

Figure 6.1 SAP102 mice display a spatial learning deficit in the water maze. (a) Mice were given three days training with a visible platform, followed by five days training with a hidden platform, followed by five more days of training with the hidden platform in the opposite location. Probe tests, in which mice were placed in the pool for 60 s without the platform present, were performed immediately (H1) and 24 hrs (H2) after the final hidden platform training trial, after every day of reversal training (R1-5) and 1 day (M1), one week (M7), two weeks (M14) and eight weeks (M56) after the final reversal training trial. **(b)** Mean path length to reach the platform during each day of training. **(c)** Mean latency to reach the platform during each day of training. **(d)** Mean swimming speed during each day of training. **(e)** Time spent in training quadrant during each transfer test.

The overall path length taken by the mice decreased across the three days of visible training [$F(2,48) = 6.64$, $p = 0.003$] indicating that they learnt the task, but there was no significant difference between wild-type and SAP102 -/Y mice [$F(1,24) = 2.83$, $p = 0.11$]. The plot (figure 6.1b) shows that mutant mice improved more rapidly over the three days than wild-type controls and the interaction between genotype and day approaches significance [$F(2,48) = 3.00$, $p = 0.06$].

Consistent with the path length data, the latency to reach the platform (figure 6.1c) decreased across all mice during the visible platform training [$F(2,48) = 8.50$, $p = 0.0007$]. Again there was no overall effect of genotype [$F(1,24) = 2.91$, $p = 0.10$] but the plot shows that mutant mice improved more than the wild-types over the three days, producing a significant genotype x day interaction [$F(2,48) = 3.41$, $p = 0.041$]. The average swimming speed of the mice in the visible platform training stayed constant over the three days [$F(2,48) = 2.58$, $p = 0.086$] and there was no difference between mutant and wild-type individuals [$F(1,24) = 1.55$, $p = 0.23$]. In summary, overall the mice improved their performance in reaching the visible platform with three days of training. There was no evidence of any SAP102-related motor or vision deficit - indeed, the mutant mice swam at the same speed as wild-types but rapidly learnt to take a more direct line to the platform, reducing their path length and latency over that of the controls.

The spatial learning ability of the mice was tested over five days of training with a platform hidden beneath the liquid surface. Performance during these trials is shown in the middle parts of the plots in figure 6.1b, c and d. Figure 6.1b shows that wild-type, but not mutant, mice reduced their path lengths with training and this was confirmed by the presence of a day x genotype interaction [$F(4,100) = 3.06$, $p = 0.02$] and separate statistical analysis of the two groups [$F(4,46) = 3.06$, $p = 0.03$ for wild-types]. A similar pattern was observed in latencies to reach the platform (figure 6.1c) with wild-type but not mutant mice improving with training [$F(4,46) = 3.36$, $p = 0.017$ for wild-types]. However the strikingly longer path lengths taken by mutants in the last

three days of training interestingly did not produce longer latencies on those days. This is explained by the fact that the mutants swam faster than wild-types throughout the training period [$F(1,24) = 19.73$, $p = 0.0002$] as shown in figure 6.1d. In summary, it appears that, unlike wild-types, SAP102 -/Y mice are unable to learn to swim more directly towards the hidden platform. However they swim faster than wild-type mice so that their latency to reach the platform is unimpaired.

Mice were subjected to probe tests 10 min and 24 hrs after the final hidden platform training trial. In a probe test, each mouse is placed in the pool without a platform for one minute. The proportion of time spent in the quadrant of the pool where the platform used to be (the 'target' quadrant) is a good measure of its spatial ability (Gerlai, 2001). The results of these tests are shown in figure 6.1e (H1 and H2). No differences were observed between mutant and wild-type mice in amount of time spent in each quadrant [$Fs(3,78) < 1.4$, $ps > 0.25$)], however, analysis of each genotype separately showed that wild-types spent more time in the training quadrant in both tests than chance would predict [$ts(13) > 2.87$, $ps < 0.013$), while mutants did not ($ts(13) < 1.36$, $ps > 0.20$). This suggests the mutant mice may have a mild deficit in spatial learning.

To examine the spatial abilities of the knockout mice in more detail they were then trained to find a hidden platform in the reverse position, that is, on the opposite side of the pool to its previous location. For this task, the process of acquisition of spatial knowledge by the mice was tracked by performing a probe test at the end of each of the five days of reversal training. Performance during this training period is shown in the right-most panels of figures 6.1b, c and d. Overall the path lengths [$F(4,100) = 5.60$, $p = 0.0004$] and latencies [$F(4,100) = 4.62$, $p = 0.002$] of the mice improved during this training period. There was no effect of genotype on either measure [$F(1,24) = 0.67$, $p = 0.42$ for path length; $F(1,24) = 0.65$, $p = 0.43$ for latency] but a general tendency towards the mutants having longer path lengths but lower latencies was present (figures 6.1b and

c). Again the mutants swam faster than wild-types throughout [$F(1,24) = 12.10$, $p = 0.002$], as shown in figure 6.1d.

Mice were subject to a probe test at the end of each day of reversal training (R1 – R5). as well as 1 day (M1), one week (M7), two weeks (M14) and 8 weeks (M56) after the last day of training. The time spent in the training quadrant by wild-type and mutant mice for each of these tests is shown in figure 6.1e. A full mixed ANOVA showed that there was no significant difference between the two groups of mice during any of these tests [$Fs(3,75) < 2.165$, $ps > .099$]. To examine this further, t-tests were performed for each probe test, comparing time spent in the training quadrant to chance level (15 s). Wild-type mice performed better than chance from the second day of reversal training (R2) and maintained this differential for the remainder of the tests. In contrast the mutant mice did not perform above chance level until 24 hours after the last training trial (M1). They maintained their above-chance performance in the 1-week (M7) and 2-week (M14) probe tests but after 8 weeks (M56) were again no better than chance. These results indicate that SAP102 loss causes an initial mild deficit in spatial learning which can be overcome by training. Once spatial information has been encoded it can be retained for a period but decays more rapidly than in wild-type mice.

6.2 SAP102 knockout mice display an activity deficit in T-maze and olfactory habituation dishabituation tasks

The spatial learning abilities of SAP102 null mice were further tested using spontaneous alternations in an unrewarded T-maze task. This experiment was performed in collaboration with Lianne Stanford and the results analysed by her. Each mouse was placed in the bottom arm of a T-shaped maze and allowed to make repeated choices between entering the left and right arms upon reaching the T-junction. Exploratory tendencies mean the mice tend to choose the less

familiar arm on each trial, resulting in a series of spatially-related choice alternations which are dependent on the hippocampus (Gerlai, 1998).

Figure 6.2 shows the results of the T-maze test. There was no difference in the number of choice alternations performed by hemizygous and wild-type mice [$t(19) = 0.42$, $p = 0.67$, figure 6.2a], however, SAP102 mice took significantly longer to complete the 11 trials [$t(19) = 2.6$, $p = 0.02$, figure 6.2b].

In a third, non-spatial, learning task, SAP102 mice were given three presentations of the same olfactory stimulus followed by three presentations of different olfactory stimulus. Since mice use urine as a means of identification and territorial marking and are very sensitive to slight variations in its odour, urine samples from two different strains of inbred mice were used as the olfactory stimuli. Learning the identity of each stimulus would result in a gradual reduction in time spent sniffing as each odour became familiar over repeated presentations (Brown et al., 1987; Wrenn et al., 2003). This experiment was performed in collaboration with Lianne Stanford and the results analysed by her.

The results of the olfactory habituation-dishabituation task are shown in figure 6.3. A log transformation of the data was performed prior to statistical analyses to satisfy the requirement of a normal distribution. There was a significant genotype effect on sniffing time across the whole experiment [$F(1, 37) = 8.24$, $p = 0.007$]. Simple effects analyses showed that wild-type mice spent different amounts of time sniffing each stimulus [$F(6,132) = 17.49$, $p < 0.0001$]. Post-hoc analyses showed that the time they spent sniffing the blank was different from that of the first presentation of odour A and the three presentations of that odour were different from one another.

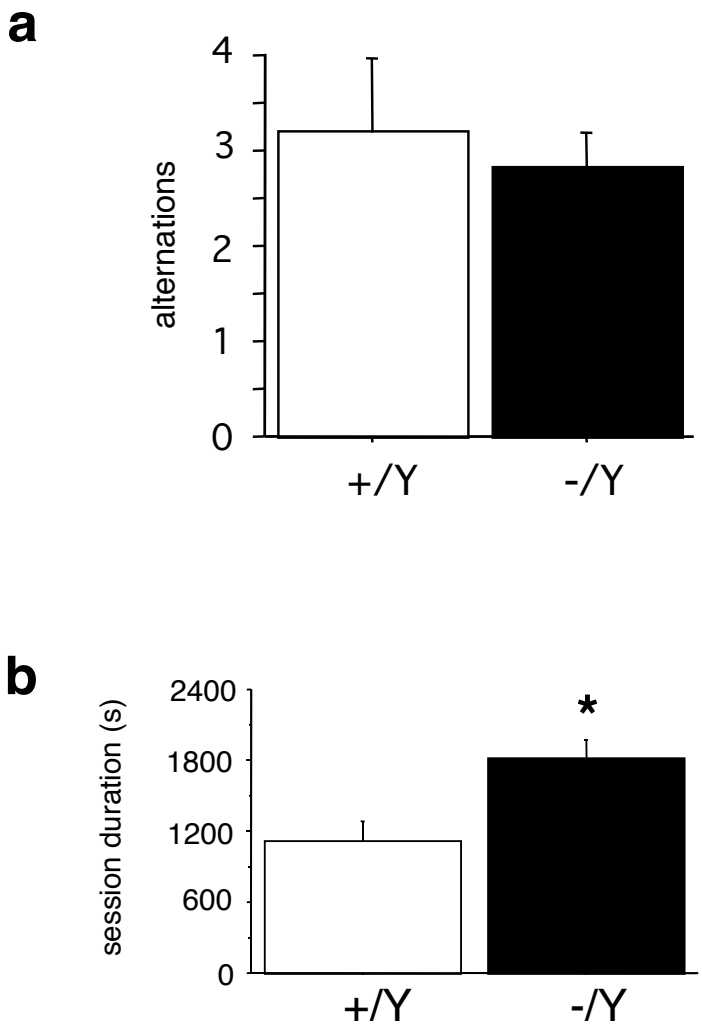

Figure 6.2 SAP102 mutant mice take longer to complete a T-maze task. Mice performed one forced choice trial followed by 10 trials of free choice between the unrewarded left and right arms of the maze. **(a)** No difference in spontaneous alternations in direction choice at the T-junction between wild-type and hemizygous SAP102 mice [$t(18) = 0.65$, $p = 0.67$]. **(b)** Hemizygous mice take longer to complete the 11 trials [$t(18) = 2.6$, $p = 0.02$].

The third presentation of odour A was different to the first presentation of odour B and the three presentations of the latter were different to one another. These analyses confirm that the wild-type mice distinguished between the two odours and habituated to each one, as shown in figure 6.3.

In contrast, the simple effects analysis showed that there was no difference in time spent sniffing each odour stimulus by the mutant mice [$F(6,90) = 1.05$, $p = 0.39$] and this was confirmed by post-hoc analyses. Since they spent no more time sniffing any of the odour stimuli than the vehicle their learning ability in this task could not be assessed.

In both the T-maze and habituation-dishabituation tasks SAP102 mice displayed a reduction in activity levels. The remainder of this chapter describes attempts to elucidate the cause of this phenotype.

6.3 Motor ability in SAP102 mutant mice

The performance of SAP102 mutant mice in the visual platform task in the water maze suggested their swimming ability was unimpaired (see figure 6.1a). However, since SAP102 is expressed in the cerebellum, an important centre for motor control, and motor impairment is an obvious potential cause of an activity deficit, the mice were subjected to a grip strength test for muscular strength and a rotorod task for motor coordination. Mice with targeted mutations in genes involved in motor control show poor performance on these tasks (Aiba et al., 1994; Chen et al., 1995).

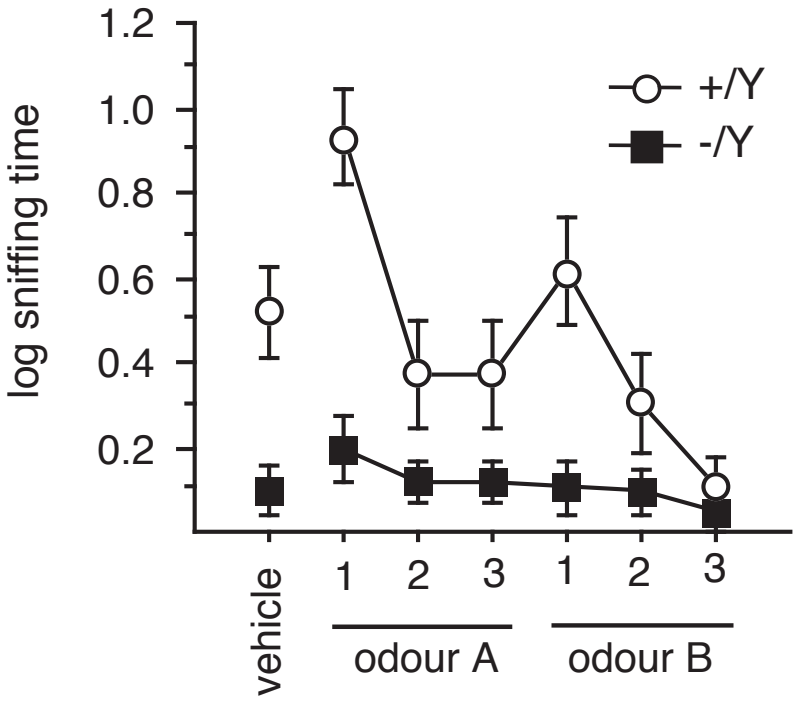

Figure 6.3 SAP102 mutant mice display impaired performance in an olfactory habituation-dishabituation task. Male hemizygous mice and wild-type littermate controls were subject to repeated exposures to two different odours. Wild-type mice initially spent more time sniffing the first odour than they did the vehicle but rapidly habituated and spent less time sniffing on its second and third presentations. Sniffing time increased upon presentation of the second odour but again rapidly decreased upon the second and third presentations. In contrast, SAP102 -/Y mice spent no more time sniffing any of the odour stimuli than they did the vehicle. See section 6.2 for statistical analyses.

The grip strength test was performed and analysed in collaboration with Lianne Stanford. Mice were held by the base of the tail and placed with their front paws gripping a horizontal, elevated bar. They were then drawn horizontally and smoothly backwards until they released their grip, while the maximum force exerted on the bar was measured by means of an attached force transducer. Mice with inherited neuromuscular deficits show impairment on this task (Levedakou et al., 2004). However, figure 6.4a shows there was no difference in the force exerted by SAP102 mutants and wild-type mice in this test, suggesting loss of SAP102 does not result in a deficit in muscular strength.

The motor coordination test was performed in collaboration with Lianne Stanford and the results analysed by her. In this test mice were given a series of trials on a non-accelerating rotorod. Each mouse was subjected to three trials at each of 4, 16 and 32 rpm, in that order, every day for three days. The results are shown in figure 6.4b. Both wild-type and mutant mice rapidly mastered the 4 rpm trials and by the third day could stay on the rotating rod for nearly the maximum 60 s. There was a main effect of day at this speed [$F(2,38) = 13.01$, $p < 0.0001$], suggesting performance improved with training, but no effect of genotype [$F(1,39) = 0.42$, $p = 0.52$] and no interaction between day and genotype [$F(2,78) = 1.08$, $p = 0.34$], indicating the mutation had no effect on performance at this speed. At 16 rpm both groups of mice performed considerably less well but improved with training, producing an effect of day [$F(2,35) = 22.19$, $p < 0.0001$]. Again there was no effect of genotype [$F(1,36) = 3.93$, $p = 0.06$] or day x genotype interaction [$F(2,72) = 2.37$, $p = 0.10$]. At 32 rpm both genotypes performed poorly, consistently falling off the rod after approximately 10 s, but there was still a significant day effect [$F(2,38) = 6.94$, $p = 0.002$]. There was no main genotype effect [$F(1,39) = 0.28$, $p = 0.60$] but an interaction between genotype and day was present [$F(2,78) = 3.26$, $p = 0.04$]. Analysis of the two genotypes

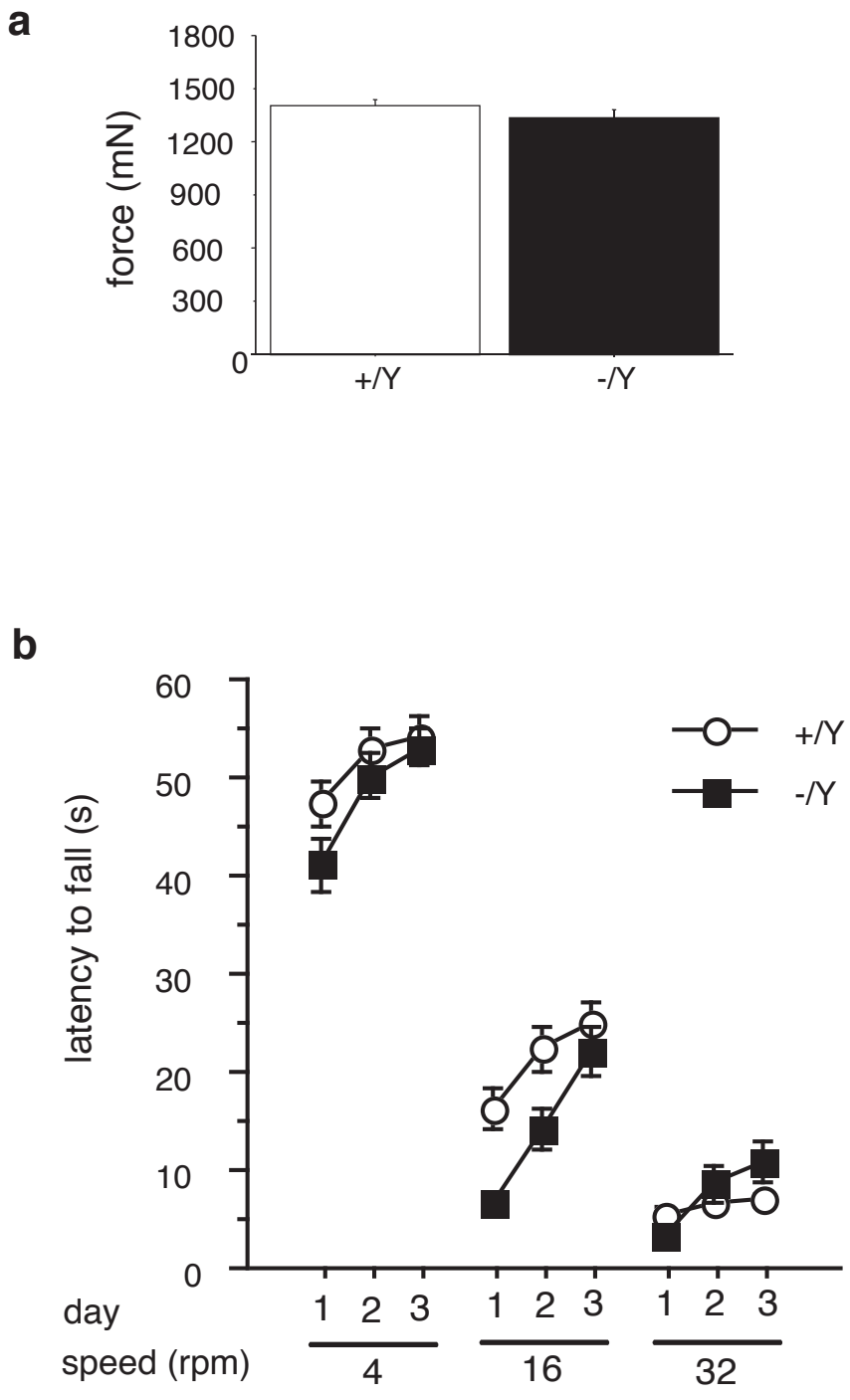

Figure 6.4 Motor abilities in SAP102 mutant mice. (a) A grip strength test shows loss of SAP102 has no effect on muscle strength ($t = 1.55$, $p = 0.12$, $n = 20$). **(b)** Rotorod test for motor coordination. Mice were given one trial at each of 4, 16 and 32 rpm each day for three days. Latency to fall from the rotating cylinder was recorded. See section 6.3 for statistical analyses.

separately showed a significant day effect in hemizygous mice [$F(2,38) = 5.9$, $p = 0.006$] but not in wild-type controls [$F(2,40) = 0.95$, $p = 0.40$]. Figure 6.4b shows that this effect is the result of mutant mice improving over time while wild-type performance remains static.

6.4 No change in anxiety behaviour following loss of SAP102

Another potential cause of reduced activity levels in SAP102 null mice is elevated anxiety levels. To examine this possibility the behaviour of the mice during a 15 min exposure to an open field was analysed, the results of which are shown in figure 6.5. This experiment was performed in collaboration with Lianne Stanford and the results analysed by her, Hayley Cooke and Magaret Green. For the analysis, the field was divided into three rows of three equal-sized rectangles. The centre rectangle was denoted the inner zone and the remainder the outer zone (figure 6.5a). Mutant mice were no different to wild-types in their latency to enter the inner zone (figure 6.5b), total time spent in the inner zone (figure 6.5c), number of stretch-attend postures (figure 6.5d) or time spent grooming (figure 6.5e), all important anxiety related behaviours (Gerlai et al., 2002; Gordon and Hen, 2004; Parks et al., 1998). They did, however, display differences consistent with a more general deficit in activity, including more time spent immobile (figure 6.5f), fewer crossings of the lines defining the nine rectangles (figure 6.5g) and fewer incidents of rearing, both supported (against a wall, figure 6.5h) and unsupported (figure 6.5i).

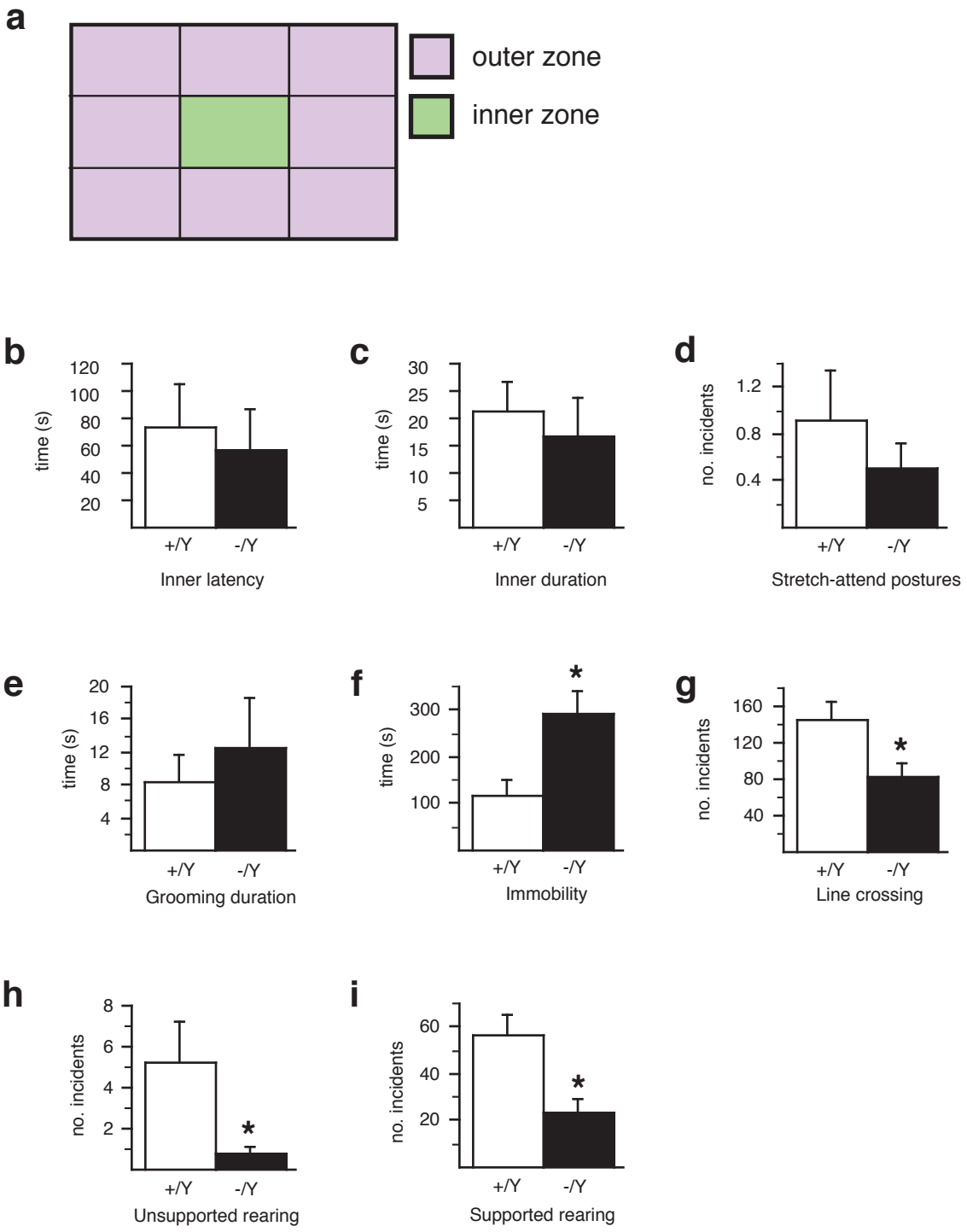

Figure 6.5 SAP102 mutant mice display decreased locomotion but no elevated anxiety in an open field. **(a)** Diagram of the open field layout. Limits of the inner and outer areas of the field are shown. **(b) - (e)** No difference in anxiety-related behaviours in SAP102 hemizygous males compared to wild-type controls, including **(b)** Latency to enter the inner zone [$t(38) = 0.35$, $p = 0.73$], **(c)** total time spent in inner zone [$t(38) = 0.5$, $p = 0.62$], **(d)** number of stretch-attend postures [$t(38) = 0.81$, $p = 0.43$] or **(e)** grooming behaviour [$t(38) = 0.63$, $p = 0.53$]. **(f) - (i)** SAP102 mutants show significantly decreased locomotion in several behavioural measures, including **(f)** increased time spent immobile [$t(38) = 3.05$, $p = 0.004$], **(g)** reduced crossings of internal dividing lines [$t(38) = 2.52$, $p = 0.02$], **(h)** less frequent unsupported rearing [$t(38) = 2.1$, $p = 0.04$] and **(i)** less frequent supported rearing [$t(38) = 3.12$, $p = 0.003$]. Asterixes above -/Y columns indicate $p < 0.05$ compared to wild-type.

The open field data were suggestive of an activity deficit without a change in anxiety levels, but many of the behavioural measures used in its analyses are equally indicative of both these phenotypes (Weiss et al., 2000), making the results somewhat ambiguous. To obtain a clearer distinction between anxiety and activity the mice were further examined in an elevated plus maze test, in which the animals spent 5 min exploring a plus-shaped maze supported 45 cm above the floor, with two arms shielded by high, vertical, opaque sides and the other two arms open (figure 6.6a). This experiment was performed in collaboration with Lianne Stanford and the results analysed by her.

There was no difference between wild-type and SAP102 hemizygous mice in their preference for the closed arms of the maze (figure 6.6b), the crucial measure of anxiety behaviour in this test (Rodgers and Johnson, 1995). In addition, both genotypes performed equal numbers of stretch-attend postures (figure 6.6c) and head-dips over the sides of the open arms (figure 6.6d). The only measure on which mutant and wild-type mice differed in the task was the total distance travelled, the mutants covering less distance than their wild-type counterparts (figure 6.6e), confirming that SAP102 loss causes an activity deficit which is not the result of a change in anxiety levels.

It appears that the observed differences in locomotor activity in the SAP102 mutants is not a consequence of changes in musculoskeletal ability or anxiety levels and may instead be a result of motivational changes caused by the mutation.

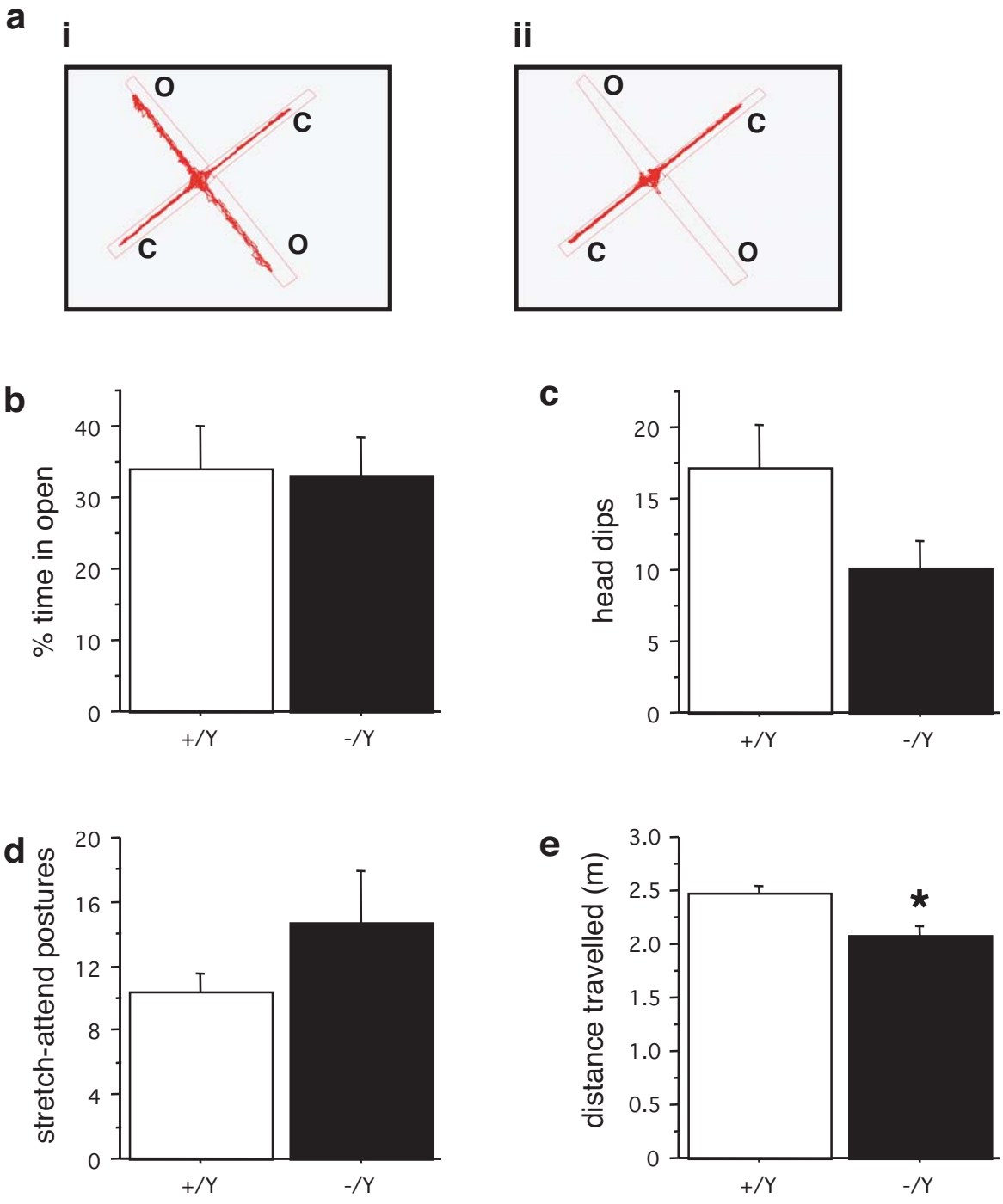

Figure 6.6 SAP102 mutant mice display no alterations in anxiety levels in an elevated plus maze. (a) The maze is an elevated, cross-shaped configuration in which two arms are covered by high, opaque side walls (c) and two are open (o). The red traces show the movement of two wild-type mice during 5 min in the maze, one spending approximately equal time each arm **(i)** and one staying exclusively in the closed arms **(ii)**. **(b)** The proportion of time spent in the open arms, a measure of anxiety, is no different between wild-type and hemizygous mice [$t(21) = 0.14$, $p = 0.90$]. **(c)** No difference between wild-type and hemizygous mice in the number of head dips over the sides of the open arms [$t(21) = 1.67$, $p = 0.11$], **(d)** nor in the number of stretch-attend postures [$t(21) = 1.40$, $p = 0.18$]. **(e)** Hemizygous mice travelled less total distance in the maze than wild-type controls [$t(21) = 2.71$, $p = 0.01$].

6.5 Discussion

The results of the water maze task show that loss of SAP102 causes a deficit in spatial learning that can be overcome with training. This contrasts with PSD-95 mutant mice, whose performance is severely impaired and cannot be improved by overtraining (Migaud et al., 1998). This is first evidence of an *in vivo* distinction between the functional roles of NMDAR-associated MAGUK proteins. The success of additional training in improving the learning performance of SAP102 mutant mice is also an encouraging result for treatment strategies in the human disorder, suggesting that patients may be able to minimise their cognitive impairment with additional practice or tuition. Knowledge of this property of SAP102 could be usefully broadened by examining whether it applies to memory in other tasks, for example retention of motor learning on the rotorod.

In contrast to the approximately 30 % alternation level observed here in mice of both genotypes, previously published experiments on inbred mouse strains have found wild-type 129S6 mice perform at chance level (50 % alternations), while various substrains of C57 mice perform at or above chance (Spowart-Manning and van der Staay, 2004). A study of targeted mice carrying an I213T substitution in presenilin 1 in a hybrid B6 x 129X1/SvJ background found wild-type controls displayed 68 % while mutant mice displayed 58 % alternations, both above chance level (Spowart-Manning and van der Staay, 2004). The former study reported a mean duration of approximately 60 s per trial across most inbred strains tested, while our wild-type mice on average took 110 s and the SAP102 mutants 164 s. It is possible that the low alternation levels seen in the 129P2 x MF1 background are creating a ‘floor’ effect, masking a deficiency in this task caused by loss of SAP102.

It is interesting to note that SAP102 knockout mice had a faster average swim speed than wild-types on every day of the hidden platform and reversal training, while their distance travelled was

often greater and their latency to reach the platform similar to wild-type. This suggests the mutant mice may be using a different search strategy which results in a less direct path to the platform but not in latency because the mutants are swimming more quickly.

SAP102 mutant mice display a deficit in activity which manifested itself in longer latency to complete the T-maze task, severe lack of response to olfactory stimuli and reduced movement in both an open field and an elevated plus maze. Grip strength and rotorod tests show this deficit is not the result of a lack of muscle strength or motor coordination. SAP102 mice also display what could be interpreted as enhanced motor performance when swim speed is measured in the water maze task. While the mutants' impairment in the habituation-dishabituation task in isolation could be attributed to loss of olfactory ability resulting from lack of SAP102 in the olfactory bulb, this would not explain the results of the other three tests which do not depend on olfaction. Results from the open field and elevated plus maze show that neither is the activity deficit the result of elevated anxiety levels in SAP102 mutants.

A further, as yet untested, possibility is that loss of SAP102 modifies activity by altering motivation levels. In relation to this it is interesting to note that the lowered activity was observed in passive, exploratory-type tasks, but not in tasks requiring active movement to avoid or escape from a negative stimulus – water in the water maze, hanging by the tail in the grip strength test, falling off the rotorod. In the visual platform training in the water maze and 32 rpm trials of the rotorod, mutants even displayed enhanced performance compared to wild-type controls. It may be that SAP102 mutants have a greater-than-normal range of motivation levels: lower than wild-type in passive situations, manifested as a reluctance to move, but increasing to levels higher than wild-type mice in situations requiring action to avoid or escape from unpleasant circumstances.

Whatever its cause, the activity phenotype clearly poses problems when assessing the mice on certain behavioural tasks, as seen in the results of the olfactory habituation test where no conclusions on the learning ability of the mice could be drawn. Further behavioural tests need to be carefully chosen and/or modified to allow analysis of the ability of interest independently of any altered activity level. For example, contextual and cued fear conditioning could be used to examine hippocampal-dependent and hippocampal-independent associative learning respectively, with freeze time prior to conditioning subtracted from freeze time after conditioning to adjust for any tendency of the mutant mice to remain immobile.

Chapter 7

Synaptic plasticity and postsynaptic signalling in SAP102 mutant mice

SAP102 is localised to synapses and is greatly enriched in the postsynaptic density. It interacts directly with NMDAR subunits, ionotropic glutamate receptors that are crucial for synapse function. It also interacts with other proteins with play essential roles at the synapse. Among these are the AMPAR and NMDAR synaptic delivery proteins stargazin and sec8 respectively, the ubiquitous calcium-binding protein calmodulin, the MAPK inhibitor and synaptic plasticity regulator synGAP and the controller of synaptic plasicity and complex cognitive function PSD-95 (see sections 1.5 and 1.6). Mutations in SAP102 disrupt cognitive function in humans (Tarpey et al., 2004). It therefore seems likely that SAP102 plays an important role in some aspect of synaptic communication and the first part of this chapter describes experiments performed to test this hypothesis. These electrophysiological experiments were performed by Ann Fink, Patricio Opazo and Tom O'Dell (Department of Physiology, University of California, Los Angeles).

An understanding of the role of SAP102 in postsynaptic signalling is a prerequisite for detailed knowledge of its role in neuronal function. The second part of this chapter begins to examine the biochemical consequences of loss of SAP102 in relation to synaptic function, with emphasis on potentially differing roles of SAP102 and PSD-95.

7.1 SAP102 mutant mice have normal basal synaptic function

Normal synaptic responses in SAP102 mice

To analyse basal synaptic function in the absence of SAP102, the responses of pyramidal cells in CA1 to synaptic stimulation via Schaffer collateral axons projecting from CA3 were recorded in acute, adult, hippocampal slices. Axonal firing, measured by the amplitude of fibre volleys in Schaffer collateral projections, was induced by electrical stimulation eliciting 25 %, 50 %, 75 % and 100 % of maxium fEPSP amplitude. Synaptic responses were measured by the slope of field excitatory postsynaptic potentials (fEPSPs) in the stratum radiatum layer of CA1. Figure 7.1a shows that no differences were observed in the postsynaptic responses of SAP102 mutant slices

compared to wild-type controls at any of the stimulation intensities used, suggesting that basal hippocampal function is undisturbed by the mutation.

Normal AMPAR and NMDAR conductance in SAP102 mutant mice

The conductance of AMPARs and NMDARs in SAP102 mutant mice was next examined. CA1 pyramidal cells were subjected to whole-cell voltage clamp while induced excitatory postsynaptic currents (EPSCs) were recorded. Since AMPAR channels open rapidly in response to glutamate but also close quickly afterwards, while NMDAR channels take longer to respond but remain open open for longer, the relative contributions of the two receptor subtypes can be determined using the ratio of the EPSC amplitude 5 ms after onset, when mainly AMPARs are active, and 50 ms after onset, when mainly NMDARs are open. Furthermore, when the experiment is performed with membrane potential held at –80 mV, EPSC is mediated almost exclusively by AMPARs since NMDAR channels are subject to the magnesium block, while at +40 mV both AMPARs and NMDARs can be activated (Nowak et al., 1984). Figure 7.1b shows that absence of SAP102 had no effect on relative contribution of AMPARs and NMDARs to CA1 EPSCs at either membrane potential. Figure 7.1c shows representative EPSC traces from wild-type (top) and SAP102 mutant (bottom) slices. To analyse the subunit composition of NMDARs at these synapes, the EPSC decay constant was calculated by fitting a single exponential curve to the decaying phase of the synaptic currents measured at +40 mV. Different NMDAR subunits have differing decay characteristics, so a change in NMDAR composition in SAP102 mutants would be reflected in a change in the decay constant. However, figure 7.1d shows that this was not the case.

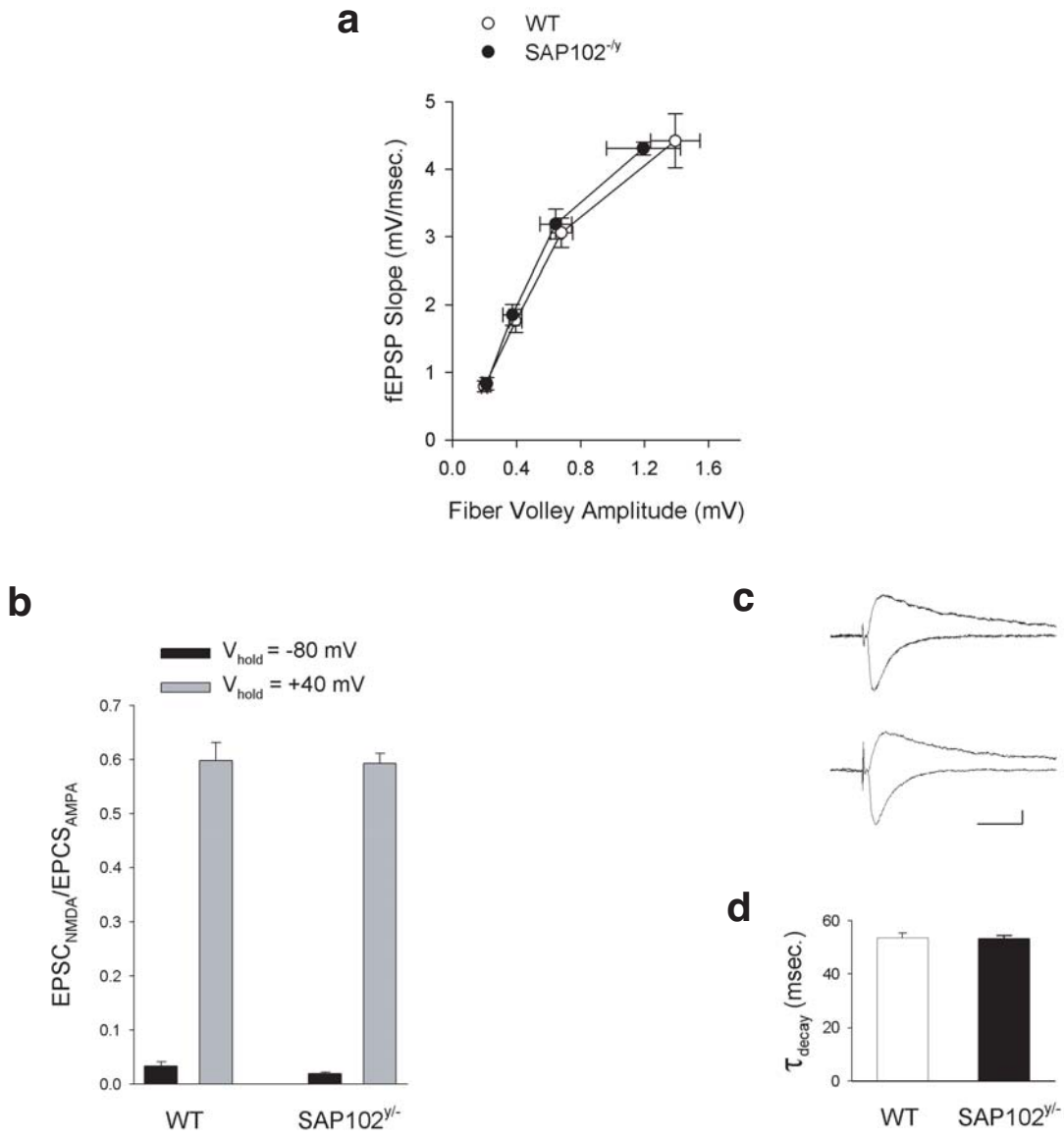

Figure 7.1 Basal hippocampal synaptic function is undisturbed in SAP102 mutant mice. (a) Basal synaptic responses were measured by recording field excitatory postsynaptic potentials (fEPSPs) from CA1 stratum radiatum in following Shaffer collateral axonal fibre volleys induced by stimulation at levels which invoked 25 %, 50 %, 75 % and 100 % of the maximum fEPSP amplitude. There were no differences between wild-type and SAP102 -/Y fEPSP responses at any of the four stimulation intensities. **(b)** Synaptic glutamate receptor function in SAP102 mutant mice. AMPAR and NMDAR conductance was measured using excitatory postsynaptic currents (EPSCs) at membrane potentials of -80 and +40 mV under whole-cell voltage clamp conditions in CA1. The AMPAR ($EPSC_{AMPA}$) and NMDAR ($EPSC_{NMDA}$) contributions to EPSCs were determined by the EPSC amplitude 5 and 50 ms after onset respectively. No differences between wild-type and mutant responses were observed at either membrane potential. **(c)** Representative EPSC traces recorded at -80 and +40 mV in wild-type (top) and SAP102 -/Y (bottom) slices. Horizontal and vertical calibration bars are 20 ms and 50 pA respectively. **(d)** NMDAR subunit composition was examined by fitting a single exponential curve to the decaying phase of the synaptic currents recorded at +40 mV. A change in the time course of the delay would be indicative of a change in NMDAR subunit composition. Again, no difference between wild-type and SAP102 -/Y cells was observed.

7.2 SAP102 loss enhances synaptic plasticity induced by low-frequency stimulation

Synaptic plasticity is often hypothesised to be a mechanism underlying information storage in the brain. Some types of synaptic plasticity, including tetanus-induced long term potentiation (LTP) in hippocampal CA1, require functional NMDARs, as does hippocampal-dependent spatial learning (Collingridge et al., 1983; Morris et al., 1986). SAP102 interacts directly with NMDAR subunits and is strongly expressed the hippocampus. Loss of SAP102 or PSD-95 causes spatial learning deficits in the water maze and PSD-95 mice have enhanced hippocampal long term potentiation.

To analyse the consequences of SAP102 loss on synaptic plasticity, NMDAR-dependent hippocampal long term potentiation was examined in the CA1 area of SAP102 mutant mice using a stimulating electrode in the Schaffer collateral projections and a field recording electrode in stratum radiatum. Figure 7.2 shows the results of these experiments. Tetanic stimulation at a frequency of 100 Hz resulted in potentiation of CA1 fEPSP slope to approximately 200 % of baseline in both wild-type and SAP102 mutant slices (figure 7.2a). There was no significant difference in fEPSP slope between the genotypes at 60 min post-tetanus [$t(5) = 0.72$, $p = 0.51$].

When LTP was induced with 3 min of continuous stimulation at 5 Hz, a striking enhancement of potentiation was observed in mutant slices compared to wild-type controls (figure 7.2b), the statistical significance of which was confirmed by comparing fEPSP slopes 45 min post-tetanus [$t(8) = 4.68$, $p = 0.005$].

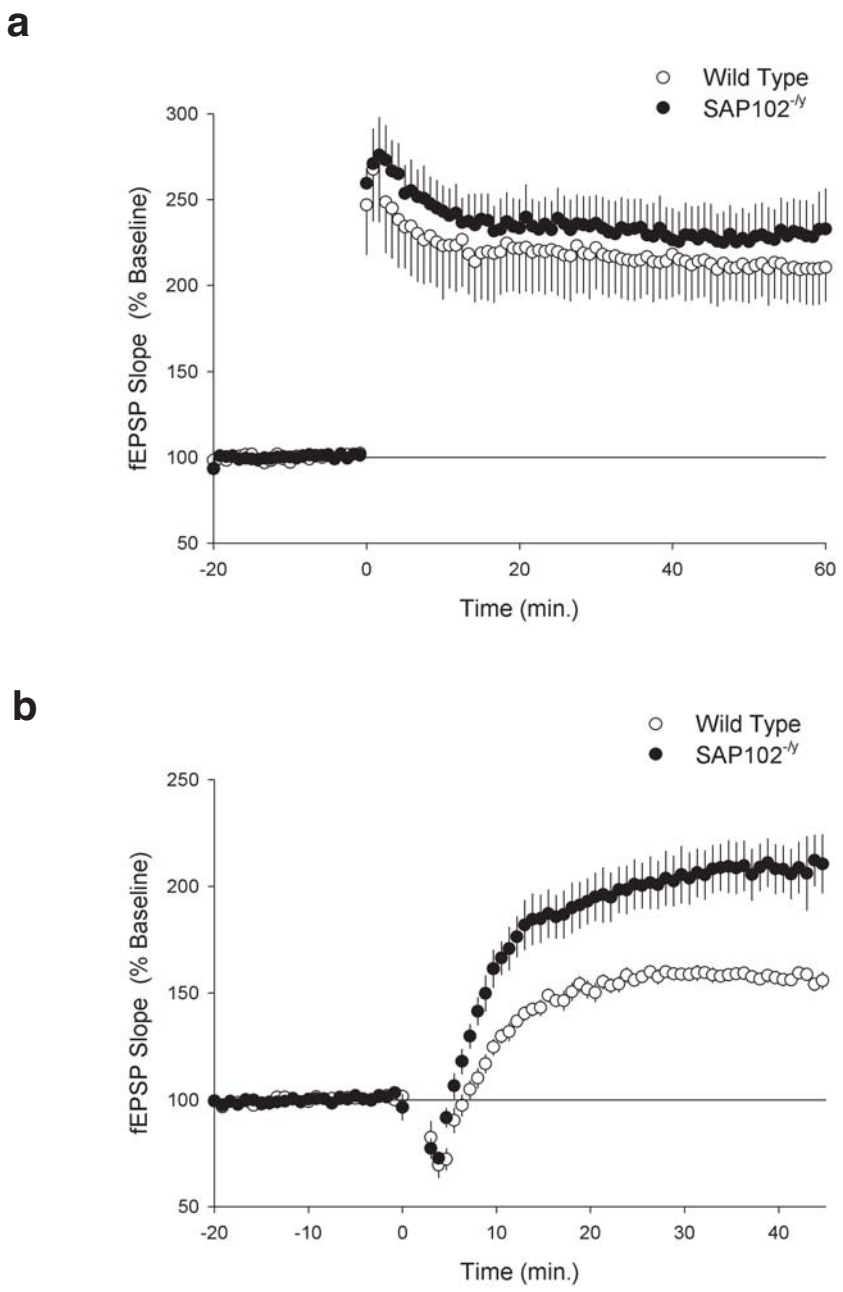

Figure 7.2 Enhanced hippocampal long-term potentiation induced by low-frequency stimulation in SAP102 mutant mice. (a) Loss of SAP102 does not affect potentiation of fEPSP slope in CA1 pyramidal cells induced by 100 Hz tetanic stimulation of Schaffer collateral axons. At 60 min post-tetanus: wild-type = 209 +/- 20% of baseline, n = 3 mice (5 slices); SAP102 -/Y fEPSPs = 230 +/- 20% of baseline, n = 4 mice (9 slices). t (5) = 0.72, p = 0.51. **(b)** Potentiation is enhanced in SAP102 mutant mice compared to wild-type controls when induced by 3 min of 5 Hz stimulation. At 45 min post-tetanus: wild-type = 156 +/- 3% of baseline, n = 6 mice (12 slices); SAP102 -/Y = 207 +/- 12% of baseline, n = 4 mice (10 slices). t(8)=4.68, p = 0.005.

7.3 Upregulation of MAP kinase activity in SAP102 mutant mice

The experiments in this section were performed by Marcelo Coba (Wellcome Trust Sanger Institute). To identify potential signalling changes that may underlie the SAP102 mutant phenotype, a differential proteomics strategy was adopted. Since phosphorylation is a common post-translational modification in postsynaptic signalling molecules (Collins et al., 2005), is an important modulator of activity in numerous signalling NMDAR-related signalling pathways and is associated with changes in signalling and LTP induction (Atkins et al., 1998; Blitzer et al., 2005; Collins et al., 2005; Davis et al., 2000; English and Sweatt, 1997), an analysis of protein kinase function was used. Hippocampal protein extracts from two wild-type and two SAP102 -/Y mice are subjected to a Kinexus screen of postsynaptic phosphorylation sites. This commercial screen uses phospho-specific antibodies to quantify phosphorylation states of the following proteins (phospho-sites shown in parentheses): ADD1 (S724), ADD3 (S693), B23 (S4), CDK1/2 (T14/Y15), CREB1 (S133), ERK1 (T202/Y204), ERK2 (T185/Y187), GSK3α (S21, 279), GSK3β (S9, Y216), JNK (T183/Y185), Jun (S73), MEK1 (S217/S221), MEK3 (S218), MEK6 (S207), MSK1 (S375), NR1 (S896), p38α MAPK (T180/Y182), PKBα (T308, S473), PKCα (S657), PKCα/β2 (T638/T641) PKCδ (T505) PKCε (S729), PKR1 (T414), Raf1 (S259), Rb (S773, S800/S804), RSK1/2 (T359/T365), S6Kα (T412), Smad1/5/9 (S463/S465/S428/S430), Src (Y423, Y543) STAT1 (Y701), STAT3 (S727) and STAT5A (Y694).

Of the 32 proteins only extracellular signal-related kinase 2 (ERK2), a component of the MAP kinase signalling pathway, showed a change in phosphorylation state in both pairs of samples, being more phosphorylated in SAP102 -/Y than in wild-type extracts. To confirm this result, ERK phosphorylation levels were determined in additional hippocampal extracts from wild-type and mutant animals using western blotting and ELISA assays. Western blots of hippocampal extracts

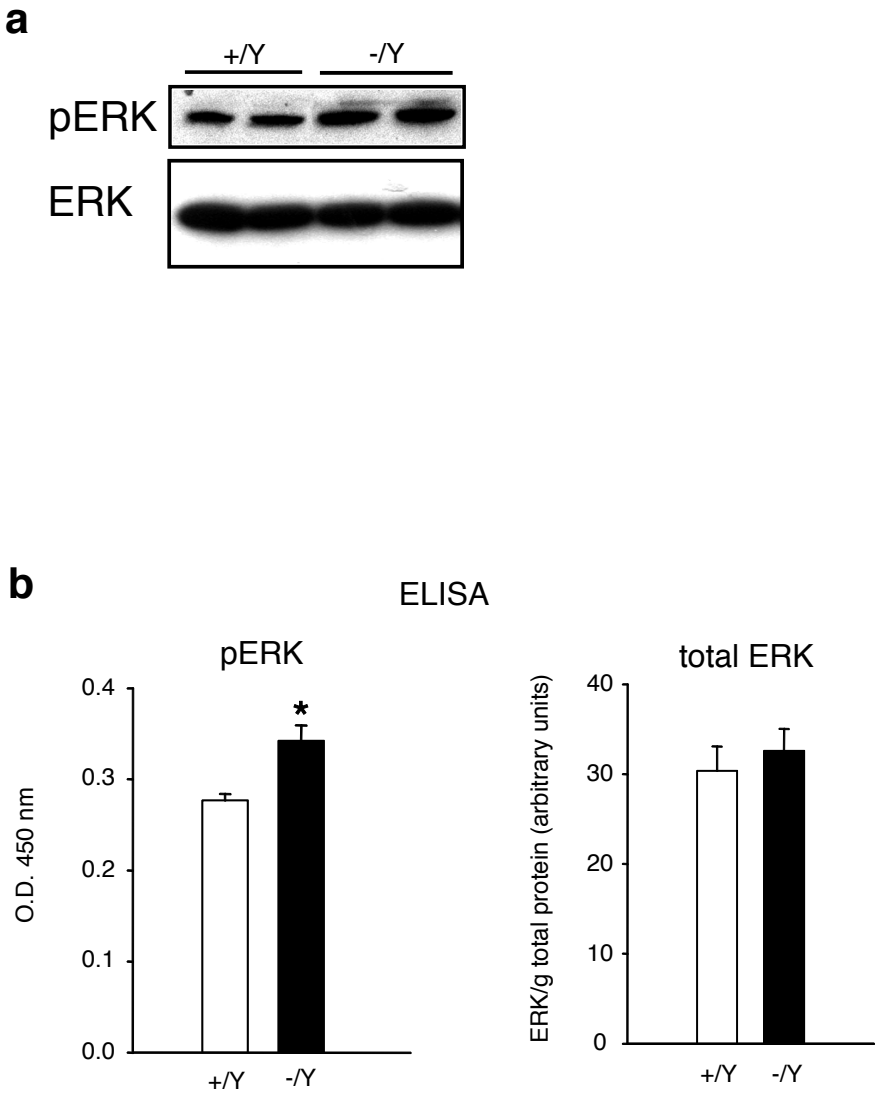

Figure 7.3 Elevated ERK phosphorylation in SAP102 mutant mice. (a) Western blotting of hippocampal protein extracts with an antibody against phospho-ERK (pERK) shows a consistent elevation of the phosphorylated form with no change in levels of total ERK. Representative samples from 15 wild-type and 15 SAP102 -/Y animals are shown. **(b)** A sandwich ELISA assay on 9 wild-type and 9 SAP102 -/Y animals confirms the increase in ERK phosphorylation [$t(16) = 3.38$, $p = 0.004$] without a change in total ERK [$t(28) = 0.06$, $p = 0.95$].

showed a consistently reproducible increase in phospho-ERK (pERK) in 15 mutant animals compared to 15 wild-type controls as shown in figure 7.3a. A sandwich ELISA experiment on 9 wild-type and 9 SAP102 -/Y animals further confirmed the increase, showing an approximately 25 % elevation of pERK in mutant extracts over controls but no significant change in total ERK levels (figure 7.3b).

7.4 SAP102 and PSD-95 perform distinct yet overlapping functions

SAP102 and PSD-95 have similar protein domains, binding partners, subcellular localisation and regional expression patterns (Fukaya and Watabe, 2000; Cho et al., 1992; Fujita and Kurachi, 2000; Muller et al., 1996), yet their functional relationship *in vivo* remains undefined. This issue was examined using biochemical and genetic strategies in the SAP102 mice along with previously generated PSD-95 mutant mice (Migaud et al., 1998).

First, it was asked whether SAP102 expression is altered in PSD-95 mutant mice. Western blots of hippocampal extracts from 10 wild-type and 10 mutant animals showed a robust and reproducible elevation of SAP102 (figure 7.4a), suggesting a partial compensation for loss of PSD-95 in these mice. We had already found no change in PSD-95 protein levels in SAP102 mice (see figure 5.5b), however, this did not preclude a change in localisation of PSD-95 as a compensatory mechanism. Co-immunoprecipitation was used to determine the amount of PSD-95 associated with NMDARs. More PSD-95 co-immunoprecipitated with NR1 in forebrain extracts from 10 SAP102 mutant mice than from 10 of their wild-type littermates as shown in figure 7.4b.

These results suggest that SAP102 and PSD-95 have partial functional overlap and that the phenotypes observed in the two mutant mouse strains may be tempered by compensation from the other MAGUK. If this was the case, mice with mutations in both proteins should display a more

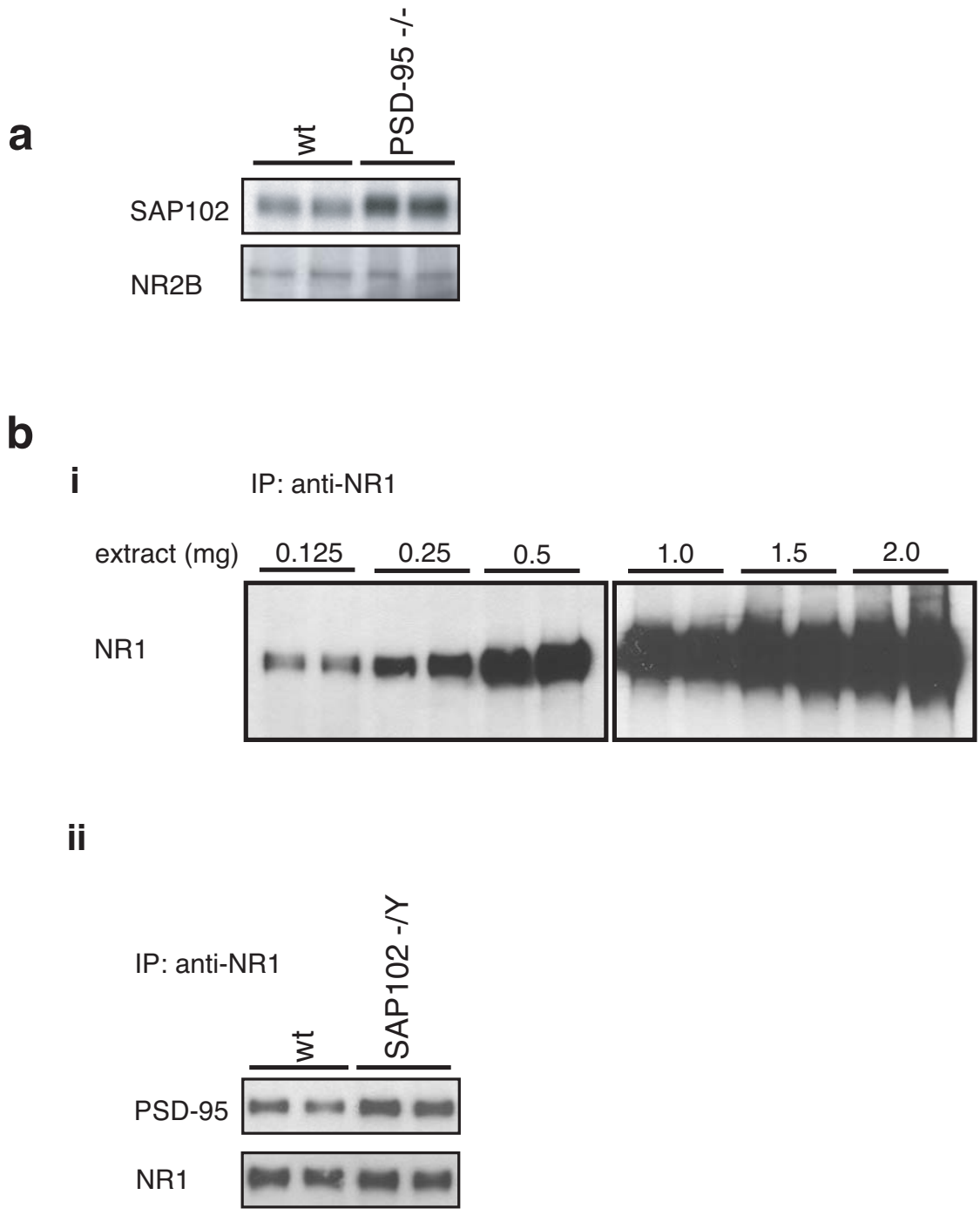

Figure 7.4 Changes in MAGUK expression and localisation in SAP102 and PSD-95 mutants **(a)** Western blot shows SAP102 protein levels are elevated in the hippocampus of PSD-95 mutant mice. **(b)** Co-immunoprecipitation of NR1 and PSD-95 from forebrain extracts of SAP102 mutant mice. **(i)** NR1 immunoprecipitations are quantitative over a range of wild-type input amounts. **(ii)** Increased PSD-95 co-immunoprecipitating with NR1 in SAP102 mutants (0.5 mg extract per IP).

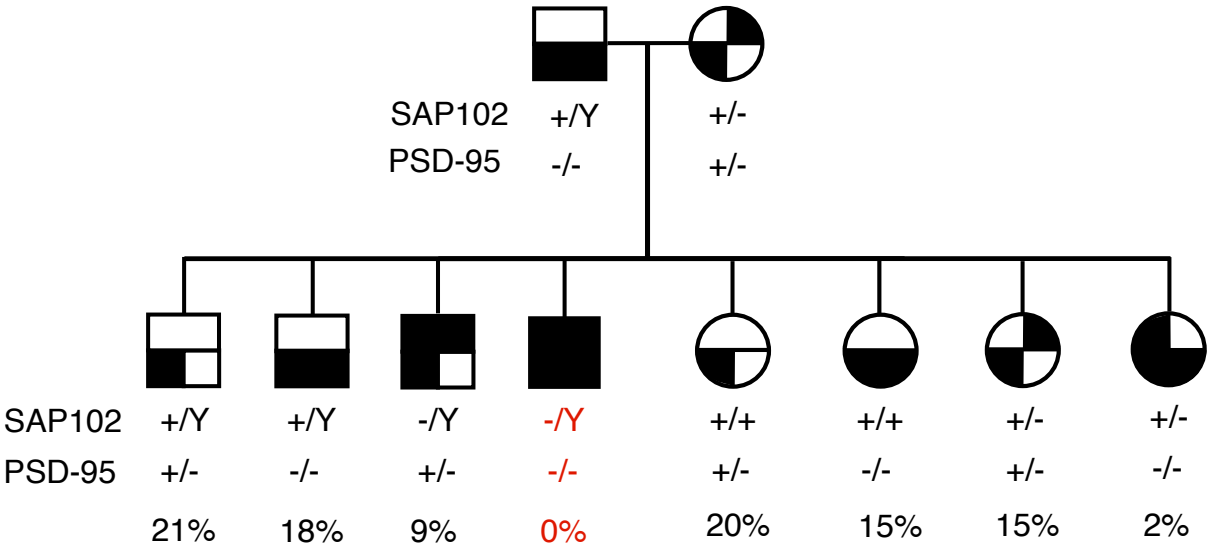

Figure 7.5 SAP102/PSD-95 double mutation is lethal. Pups from crosses between SAP102 +/Y, PSD-95 -/- males and SAP102 +/-, PSD-95 +/- females were weaned and genotyped at 4 weeks of age. The distribution of genotypes among weaned pups differed significantly from that expected under mendelian inheritance (χ^2 = 34.37, n = 94, p = 0.000014). No viable double knockout (SAP102 -/Y, PSD-95 -/-) pups and only a small proportion (2 %) of SAP102 +/-, PSD-95 -/- pups were produced.

severe phenotype than that of the individual mutations. To examine this prediction we crossed the SAP102 and PSD-95 strains. Of 94 weaned pups from these crosses none were double null and only two were heterozygous for SAP102 and homozygous for PSD-95, reflecting a severely skewed distribution of genotypes among the offspring (figure 7.5, $\chi^2 = 34.37$, $p = 0.000014$). These data show that SAP102 and PSD-95 have partial functional overlap and that the presence of at least one is necessary for viability.

7.5 Discussion

Despite localisation of SAP102 at the glutamatergic postsynapse and its interaction with numerous proteins implicated in synaptic communication and postsynaptic signalling, SAP102 does not appear to be necessary for basal synaptic transmission, since evoked synaptic responses in hipppocampal CA1 are normal in its absence.

The amplitude and time course of ion influx through AMPARs and NMDARs at these synapses in response to presynaptic stimulation is also unaffected in the mutant mice, suggesting lack of SAP102 does not alter the number of these receptors in the postsynaptic membrane, their activation properties or their conductance characteristics upon activation. SAP102 does not therefore appear to be required for trafficking of AMPARs or NMDARs to the synaptic membrane under these circumstances. Absence of a deficit in NMDAR-dependent LTP in the mice further implies normal localisation of the receptor. This result is surprising because SAP102 is often presented as an adaptor responsible for trafficking postsynaptic proteins (Fujita and Kurachi, 2000) and in one study has been directly implicated in trafficking of NMDARs in association with sec8, in experiments overexpressing a dominant negative form of sec8 lacking its C-terminal PDZ interaction motif in heterologous cells and cultured hippocampal neurons (Sans et al., 2003). Synaptic delivery of AMPARs requires an indirect interaction with a PDZ protein,

possibly SAP102, mediated by stargazin, a protein which contains a PDZ interaction motif and interacts directly with the AMPAR GluR1 subunit (Chen et al., 2000). It is possible that PDZ proteins other than SAP102 perform these functions or that they are at least able to functionally compensate when SAP102 is absent. Growing evidence from postsynaptic receptor localisation studies using targeted mutations in situations where other MAGUKs are not present, however, suggests that in fact, with occasional exceptions (Tao et al., 2003), the family does not function in this capacity at all (Klöcker et al., 2002; Migaud et al., 1998; Rasband et al., 2002).

Enhancement of 5 Hz LTP in the mutant mice, however, demonstrates that SAP102 has an essential role in regulating hippocampal synaptic plasticity. The presence of this phenotype in the absence of a disruption of basal synaptic transmission or NMDAR activation or conductance implies that SAP102 controls the intracellular signalling response to NMDAR stimulation, an observation in keeping with SAP102's intracellular location and interactions with multiple postsynaptic signalling proteins.

As with spatial learning, the effect of SAP102 loss on hippocampal synaptic plasticity is distinct from that of PSD-95 (compare figures 1.5 and 7.2). The comparison can be made with confidence since LTP experiments on the two targeted strains have been performed by the same research group, using the same protocol and experimental conditions. Enhancement of LTP in both mutants is consistent with the similarity of function suggested by the proteins' common localisations, domain structures and interaction partners. While the enhancement in PSD-95 mice is seen across a number of stimulation protocols, for SAP102 it is present mainly when potentiation is induced by low-frequency stimulation. Intriguingly, this may indicate that each of the MAGUKs mediates postsynaptic response to different patterns synaptic activation. Indeed, ERK activation is required for 5 Hz but not 100 Hz LTP (Winder et al., 1999).

An alternative explanation is that the differential involvement of the two proteins in different forms of LTP is amplitude- rather than frequency-dependent. That is, loss of PSD-95 may have a greater effect on LTP amplitude, while the smaller effect of SAP102 can be seen only following stimulation protocols, like 5 Hz, which induce a greater amount of potentiation. This would be consistent with the slight but non-significant enhancement of LTP under 100 Hz induction (see figure 7.2a) and could be further investigated by using saturating stimulation protocols to determine the maximum possible potentiation in each strain (Migaud et al., 1998). The effect of SAP102 mutation on LTD also remains to be investigated.

Initial biochemical investigations presented here on the consequences of SAP102 loss have focussed on two aspects: the identification of disruptions to postsynaptic signalling pathways which may underlie the observed synaptic plasticity and spatial learning deficits in mice and cognitive impairments in humans, and potential functional overlap between SAP102 and PSD-95. In relation to postsynaptic signalling, several different experimental protocols demonstrate that lack of SAP102 leads to a steady state elevation of phosphorylation of ERK, a member of the MAP kinase signalling pathway required for hippocampal LTP and spatial learning. This change is likely a result of modified NMDAR-dependent intracellular signalling – this could be confirmed using NMDAR agonists in acute hippocampal slices or neurons in primary culture. It will be important to determine the proteins mediating the link between SAP102 and ERK as well as the consequences for downstream MAPK signalling and how these may underlie the observed effects on plasticity and cognitive function.

The observation that mutations in either SAP102 or PSD-95 result in compensatory-like changes in the expression or localisation of the other supports the notion that partial functional overlap between the two proteins may limit the extent of phenotypic impairment in the individually targeted mouse strains. Indeed, absence of both MAGUKs resulted in loss of viability, a far more

severe phenotype, demonstrating a requirement for at least one of these proteins for postnatal survival.

Chapter 8

General discussion

8.1 Summary of results

This dissertation demonstrates for the first time the function of the postsynaptic adaptor protein SAP102 *in vivo* in the mouse. SAP102 allows efficient hippocampal-dependent learning of spatial information. Despite its early postnatal onset of expression and postsynaptic location, SAP102 is not required for the development of normal brain structures, nor for normal operation of basal excitatory synaptic transmission or NMDAR localisation or activation even at synapses where SAP102 is robustly expressed. Instead it controls potentiation amplitude during NMDAR-dependent plasticity induced by specific types of stimulation, a role consistent with its close association with NMDARs at the postsynapse. Biochemically, SAP102 governs basal activation levels of the MAPK pathway.

In addition, a novel vector system has been developed and shown to be broadly useful for constructing targeting vectors by bacterial homologous recombination for the introduction of a variety of mutations into different loci in the mouse. In particular its use to construct additional targeting vectors for SAP102 will facilitate more detailed analysis of the protein's expression patterns and its function in distinct brain regions during specific developmental periods.

8.2 Future directions for recombineering-based targeting vector construction

DNA cloning by homologous recombination in bacteria has been shown here as well as previously in the literature to be a significant step forward in technology for constructing targeting vectors, allowing rapid modification of large DNA fragments with precise control over excision and insertion points and without the need for appropriate restriction sites in those fragments.

This means that simple targeting vectors, such as replacement of one or more key exons of an endogenous gene with a lacZ marker, can be constructed using an almost identical cloning

strategy independent of the locus being targeted. The process can thus be partially automated for the construction of large collections of simple mouse mutations. The process is being further facilitated by improvements in associated areas, such as the availability of end-sequenced BAC clones to alleviate the need for library screening, quantitative PCR for genotyping of targeted ES cell clones and automated procedures for cell culturing and colony picking (Valenzuela, 2003). These technological advances are driving a paradigm shift in gene targeting, away from single genes and individual proteins towards gene families, signalling pathways and entire protein complexes.

As well as the capacity to produce large numbers of mutations, recombineering facilitates construction of sophisticated targeting vectors for detailed *in vivo* analysis of multiple functional aspects of a single gene. *LoxP* and *FRT* sequences for site-specific recombination can be introduced at precisely the required genomic location in a single cloning step for deletion of key exons with minimal disruption to the surrounding genomic sequence. Introduction of point mutations can be performed by recombination using single-stranded oligonucleotides without the use of a selectable marker, although this approach is inefficient and requires several cloning steps in the context of targeting vector construction. A better strategy may be to include the selectable marker in intronic sequence adjacent to the exonic point mutation and insert both elements in a single recombination step mediated by flanking homology arms.

8.3 SAP102 function

Normal hippocampal NMDAR expression levels, distribution patterns and postsynaptic currents suggests that SAP102 is not required for synaptic delivery of these receptors. Instead, changes to postsynaptic signalling and synaptic plasticity in SAP102 mice, together with SAP102's ability to bind numerous postsynaptic proteins support the hypothesis that it mediates the postsynaptic

signalling response to calcium influx through synaptically activated NMDARs to control cellular mechanisms for synaptic plasticity and information encoding in the hippocampus.

What is the causal relationship between the biochemical, synaptic plasticity and behavioural phenotypes in mice lacking SAP102? We have seen that there is no clear correlation between disruption of LTP and disruption of spatial learning by genetic maniupation in mice, but these two processes share many common molecular mechanisms. Although the phosphorylation screen results suggest that basal activity of most postsyaptic signalling pathways is unaffected by the mutation, the screen is not exhaustive and other biochemical effects may be present. Demonstration that disruption of MAPK activity is responsible for the electrophysiological and behavioural phenotypes in SAP102 mice would require rescue of those phenotypes by artificial dampening of the pathway by pharmacological or genetic means.

Elevation of ERK activation in SAP102 knockout mice is consistent with published data suggesting preferential linking of NR2B-containing NMDARs with SAP102 and the MAPK pathway (Kim et al., 2005; Sans et al., 2000). SAP102 interactors and MAPK regulators synGAP or kalirin could mediate this link. Also consistent is the observation that synGAP regional expression patterns correspond more closely with those of SAP102 than PSD-95 (Porter et al., 2005). MAPK activation by NMDARs is necessary for normal hippocampal synaptic plasticity and spatial learning.

Enhancement of LTP in the mutant mice suggests that, as expected, SAP102 has some association with NR2A-containing NMDARs despite its preference for those containing NR2B. It will be important to determine whether MAPK signalling is also disturbed in PSD-95 mutant mice. Preferential association of SAP102 with NR2B predicts that mice lacking SAP102 will show greater disturbance of LTD induced by low-frequency stimulation than of LTP. Changes in

synaptic delivery of GluR1 following NMDAR activation by LTP-inducing stimuli should also be evident.

Developmental versus acute SAP102 function

While germline deletion gives a reliable indication of the effect of SAP102 loss on the entire animal and provides the most genetically accurate model of the equivalent human disorder, it means that the temporal origins of the observed phenotypes cannot always be determined. For a synaptic protein, changes in synaptic plasticity and learning could result from disruption to synapse structure arising from lack of SAP102 during development, or acute alterations in protein trafficking or signalling during each behavioural or electrophysiological experiment. No chronic modifications to gross brain morphology or basal synaptic transmission were observed in SAP102 mutant mice, but this does not preclude ultrastructural changes that are beyond the scope of the current investigation, such as changes in dendritic spine morphology which can be associated with XLMR. Interestingly, both SynGAP and PSD-95 mutant mice display changes in dendritic spine morphology (Vazquez et al., 2004; Cathy Vickers, personal communication). A distinction could be made between developmental and acute roles for SAP102 using mice with floxed SAP102 alleles crossed with Cre-ER^{T} mice followed by stereotaxic tamoxifen administration to ablate the gene solely in the adult hippocampus.

8.4 Distinct roles of PSD-95 family proteins in postsynaptic signalling, plasticity and learning

Elevelated hippocampal expression of SAP102 in PSD-95 mutants and increased association of PSD-95 with NMDARs in the absence of SAP102 suggest that these two proteins may be able to partially compensate for loss of the other. One would expect, then, that loss of both proteins would produce a more severe phenotype, a prediction confirmed by the loss of viability in

SAP102/PSD-95 double mutants. This observation further highlights the importance of these proteins for normal development.

It is unlikely, however, that these two molecules are completely redundant; indeed, several observations here provide the first evidence of distinct functions for SAP102 and PSD-95 at the postsynapse. Without SAP102, mice have difficulty encoding spatial information in the water maze but can acquire the information with additional training. Once acquired, the information is retained and recalled without impairment. In contrast, PSD-95 mutant mice display severe disruption of spatial learning which cannot be improved with overtraining. The observation that spatial learning impairments resulting from deletion of SAP102 and synGAP can be improved with overtraining provides further circumstantial evidence that these two proteins are operate in the same signalling pathway. PSD-95 mice exhibit enhancement of LTP in area CA1 with a variety of induction protocols, while loss of SAP102 elevates potentiation at 5 Hz but has little effect at 100 Hz.

Comprehensive analyses of the protein partners of each of the three NMDAR-associated MAGUKs may link each to distinct postsynaptic signalling pathways and provide further clues as to their individual functions. A bioinformatic search of the human genome sequence in 2002 revealed 54 proteins with a canonical C-terminal class I PDZ binding motif (Lim et al., 2002), suggesting there remain further MAGUK interactions to be characterised.

Further examination of the collective roles of SAP102, PSD-95 and PSD-93 in NMDAR function awaits the generation of mice lacking all three MAGUK proteins as well as double knockout combinations. The SAP102 floxed targeting vector will probably be useful in preventing developmental lethality in some of these combinations.

8.5 Mental retardation

SAP102 mutant mice as a model of XLMR

Several phenotypic observations already made on the SAP102 mice are relevant to the human disorder. Enouragingly, the mice show no apparent gross disruptions to brain morphology, the caveats already discussed notwithstanding. Cognitive deficits in mental retardation sufferers carrying SAP102 mutations may thus be a result of acute alterations in postsynaptic signalling which could be more easily corrected by pharmaceutical intervention. Pharmacological MAPK inhibitors may be a rewarding therapeutic avenue to explore in this regard. Further biochemical characterisation of the mutant mice will inform these investigations. The mice will also provide a useful means for testing promising drug candidates.

Improvement of cognitive performance with additional training in the mutant mice suggests that additional tutoring and assistance for human sufferers may be successful in improving their quality of life. More detailed examination of the cognitive consequences of SAP102 loss using analogous tasks in humans and mice may be valuable.

Future directions in XLMR research

How many different genes have the potential to cause XLMR in humans? The answer to this question is valuable not only because of its clinical implications for the diagnosis and treatment of the disorder but also because its implied insight into the fundamental biology of the brain. Indeed, the question could be rephrased: how many proteins are there in the human brain that are essential for normal cognitive function? Around 350 of the approximately 1,000 genes on the X chromosome are expressed in the brain (Ropers and Hamel, 2005; Ross, 2005) and it seems reasonable to assume the majority of these will impact on cognition. Even if the phenotypic effects of loss-of-function are on occasion masked because of redundancy or environmental

factors, it seems likely that mutations in many of these genes would result in cognitive deficits including, in many cases, mental retardation.

Technology is now sufficiently advanced to make realistic the prospect of analysing the function of every brain-expressed, X-linked gene by targeting in ES cells. Unlike their autosomal counterparts, generation of null ES cell lines for each X chromosome gene requires only a single targeting experiment. Such lines could then be differentiated into neurons for cell-based analysis and only the more interesting of them initially used to generate mutant mice.

Such wide variability in the genetic causes of XLMR presents potential problems for its treatment. If different causative genes impact on cognition through independent molecular mechanisms it will be difficult to design pharmacological interventions to be effective across the different disease forms. On the other hand, if the neuronal function of XLMR genes converges on a limited number of signalling pathways which are crucial for cognitive function, it may be possible to design drugs only against these ‘master’ cognitive pathways.

References

Adams, D. J., Biggs, P. J., Cox, T., Davies, R., van der Weyden, S., Jonkers, J., Smith, J., Plumb, B., Taylor, R., Nishijima, I., *et al*. (2004). Mutagenic insertion and chromosome engineering resource (MICER). Nature Genetics *36*, 867-871.

Ahmed, B. Y., Cahkravarthy, S., Eggers, R., Hermens, W. T., Zhang, J. Y., Niclou, S. P., Levelt, C., Sablitzky, F., Anderson, P. N., Lieberman, A. R., and Verhaagen, J. (2004). Efficient delivery of Cre-recombinase to neurons in vivo and stable transduction of neurons using adeno-associated and lentiviral vectors. BMC Neuroscience *5*, 4.

Aiba, A., Kano, M., Chen, C., Stanton, M. E., Fox, G. D., Herrup, K., Zwingman, T. A., and Tonegawa, S. (1994). Deficient cerebellar long-term depression and impaired motor learning in mGluR1 mutant mice. Cell *79*.

Akum, B. F., Chen, M., Gunderson, S. I., Riefler, G. M., Scerri-Hansen, M. M., and Firestein, B. L. (2004). Cypin regulates dendrite patterning in hippocampal neurons by promoting microtubule assembly. Nature Neuroscience *7*, 145-152.

Allen, K. M., Gleeson, J. G., Bagrodia, S., Partington, M., MacMillan, J. C., Cerione, R. A., Mulley, J. C., and Walsh, C. A. (1998). *PAK3* mutation in nonsyndromic X-linked mental retardation. Nature Genetics *20*, 25-30.

Amir, R. E., Van den Vayver, I. B., Wan, M., Tran, C. Q., Francke, U., and Zoghbi, H. Y. (1999). Rett syndrome is caused by mutations in X-linked MECP2, encoding methyl-CpG-binding protein 2. Nature Genetics *23*, 185-188.

Angrand, P. O., Daigle, N., van der Hoeven, F., Scholer, H. R., and Stewart, A. F. (1999). Simplified generation of targeting constructs using ET recombination. Nucleic Acids Research *27*, e16.

Aoki, C., Miko, I., Oviedo, H., Mikeladze-Dvali, T., Alexandre, L., Sweeney, N., and Bredt, D. S. (2001). Electron microscopic immunocytochemical detection of PSD-95, PSD-93, SAP-102 and SAP-97 at postsynaptic, presynaptic and nonsynaptic sites in the adult and neonatal rat visual cortex. Synapse *40*, 239-257.

Arsenian, S., Ruther, U., and Nordheim, A. (1998). Serum response factor is essential for mesoderm formation during mouse embryogenesis. EMBO Journal *17*, 6289-6299.

Ashley Jr, C. T., Wilkinson, K. D., Reines, D., and Warren, S. T. (1993). FMR1 protein: conserved RNP family domains and selective RNA binding. Science *262*, 563-566.

Association, A. P. (2000). Diagnostic and Statistical Manual of Mental Disorders, 4-Tr edn (Washington D.C., American Psychiatric Publishing Inc).

Atkins, C. M., Selcher, J. C., Petraitis, J. J., Trzaskos, J. M., and Sweatt, D. (1998). The MAPK cascade is required for mammalian associative learning. Nature Neuroscience *1*, 602-609.

Austin, C. P. (2004). The knockout mouse project. Nature Genetics *36*, 921-924.

Bagni, C., and Greenough, T. (2005). From mRNP trafficking to spine dymorphogenesis: the roots of fragile X syndrom. Nature Reviews Neuroscience *6*, 376-387.

Bancroft, J. D., Stevens, A., and Turner, D. R. (1996). Theory and practice of histological techniques, 4th edn (London, Churchill Livingstone).

Bassand, P., Bernard, A., Rafiki, A., Gayet, D., and Khrestchatisky, M. (1999). Differential interaction of the tSXV motifs of the NR1 and NR2A NMDA receptor subunits with PSD-95 and SAP97. European Journal of Neuroscience *11*, 2031-2043.

Bear, M. F., Huber, K. M., and Warren, S. T. (2004). The mGluR theory of fragile X mental retardation. Trends in Neurosciences *27*, 370-377.

Becamel, C., Gavarini, S., Chanrion, B., Alonso, G., Galeotti, N., Dumuis, A., Bockaert, J., and Marin, P. (2004). The serotonin 5-HT_{2A} and 5-HT_{2C} receptors interact with specific sets of PDZ proteins. Journal of Biological Chemistry *279*, 20257-20266.

Berberich, S., Punnakkal, P., Jensen, V., Pawlak, V., Seeburg, P. H., Hvalby, O., and Kohr, G. (2005). Lack of NMDA receptor subtype selectivity for hippocampal long-term potentiation. Journal of Neuroscience *25*, 6907-6910.

Billuart, P., Bienvenu, T., Ronce, N., des Portes, V., Vinet, M. C., Zemni, R., Crollius, H. R., Carrie, A., Fauchereau, F., Cherry, M., *et al*. (1998). Oligophrenin-1 encodes a rhoGAP protein involved in X-linked mental retardation. Nature *392*, 923-926.

Birney, E., Andrews, T. D., Bevan, P., Caccamo, M., Chen, Y., Clarke, L., Coates, G., Cuff, J., Curwen, V., Cutts, T., *et al*. (2004). An Overview of Ensembl. Genome Res *14*, 925-928.

Bliss, T. V., and Lømo, T. (1973). Long-lasting potentiation of synaptic transmission in the dentate area of the anaesthetized rabbit following stimulation of the perforant path. Journal of Physiology *232*, 331-356.

Blitzer, R. D., Iyenger, R., and Landau, E. M. (2005). Postsynaptic signaling networks: cellular cogwheels underlying long-term plasticity. Biological Psychiatry *57*, 113-119.

Blum, S., Moore, A. N., Adams, F., and Dash, P. K. (1999). A mitogen-activated protein kinase cascade in the CA1/CA2 subfield of the dorsal hippocampus is essential for long-term spatial memory. Journal of Neuroscience *19*, 3535-3544.

Bredt, D. S., and Nicoll, R. A. (2003). AMPA receptor trafficking at excitatory synapses. Neuron *40*, 361-379.

Brenman, J. E., Christopherson, K. S., Craven, S. E., McGee, A. W., and Bredt, D. S. (1996). Cloning and characterization of postsynaptic density 93, a nitric oxide synthase interacting protein. J Neurosci *16*, 7407-7415.

Brenman, J. E., Topinka, J. R., Cooper, E. C., McGee, A. W., rosen, J., Milroy, T., Ralston, H. J., and Bredt, D. S. (1998). Localization of postsynaptic density-93 to dendritic microtubules and interaction with microtubule-associated protein 1A. Journal of Neuroscience *18*, 8805-8813.

Brocard, J., Warot, X., Wendling, O., Messaddeq, N., Vonesch, J. L., Chambon, P., and Metzger, D. (1997). Spatio-temporally controlled site-specific somatic mutagenesis in the mouse. Proceedings of the National Academy of Sciences of the United States of America *94*, 14559-14563.

Brown, R. E., Singh, P. B., and Roser, B. (1987). The major histocompatibility complex and the chemosensory recongition of individuality in rats. Physiology and Behavior *40*, 65-73.

Brown, V., Jin, P., Ceman, S., Darnell, J. C., O'Donnell, W. T., Tenenbaum, S. A., Jin, X., Feng, Y., Wilkinson, K. D., Keene, J. D., *et al*. (2001). Microarray identification of FMRP-associated brain mRNAs and altered mRNA translational profiles in fragile X syndrome. Cell *107*, 477-487.

Cai, C., Coleman, S. K., Niemi, K., and Keinanen, K. (2002). Selective binding of synapse-associated protein 97 to GluR-A α-amino-5-hydroxy-3-methyl-4-isoxazole propionate receptor subunit is determined by a novel sequence motif. Journal of Biological Chemistry *227*, 31484-31490.

Capecchi, M. (2005). Gene targeting in mice: functional analysis of the mammalian genome for the twenty-first century. Nature Reviews Genetics *6*, 507-512.

Carmell, M. A., Zhang, L., Conklin, D. S., Hannon, G. J., and Rosenquist, T. A. (2002). Germline transmission of RNAi in mice. Nature Structural Biology *10*, 91-92.

Caruana, G., and Bernstein, A. (2001). Craniofacial dysmorphogenesis including cleft palate in mice with an insertional mutation in the *discs large* gene. Molecular and Cellular Biology *21*, 1475-1483.

Cearley, J. A., and Detloff, P. J. (2001). Efficient repetitive alteration of the mouse Huntington's disease gene by management of background in the tag and exchange gene targeting strategy. Transgenic Research *10*, 479-488.

Chelly, J., and Mandel, J.-L (2001). Monogenic causes of X-linked mental retardation. Nature Reviews Genetics *2*, 669-680.

Chen, C., Kano, M., Abeliovich, A., Chen, L., Bao, S., Kim, J. J., Hashimoto, K., Thompson, R. F., and Tonegawa, S. (1995). Impaired motor coordination correlates with persistent multiple climbing fiber innervation in PKCγ mutant mice. Cell *83*, 1233-1242.

Chen, C. M., and Behringer, R. R. (2001). CREating breakthroughs. Nature Biotechnology *19*, 921-922.

Chen, K., and Featherstone, D. E. (2005). Discs-large (DLG) is clustered by presynaptic innervation and regulates postsynaptic glutamate receptor subunit composition in *Drosophila*. BMC Biology *3*, 1.

Chen, L., Chetkovich, D. M., Petralia, R. S., Sweeney, N. T., Kawasaki, Y., Wenthold, R. J., Bredt, D. S., and Nicoll, R. A. (2000). Stargazin regulates synaptic targeting of AMPA receptors by two distinct mechanisms. Nature *408*, 936-943.

Chen, L., Yun, S.-W., Seto, J., Lui, W., and Toth, M. (2003). The fragile X mental retardation protein binds and regulates a novel class of mRNAs containing U rich target sequences. Neuroscience *120*, 1005-1017.

Cho, K. O., Hunt, C. A., and Kennedy, M. B. (1992). The rat brain postsynaptic density fraction contains a homolog of the drosophila discs-large tumor suppressor protein. Neuron *9*, 929-942.

Collingridge, G. L., Kehl, S. J., and McLennan, H. (1983). The antagonism of amino acid-induced excitations of rat hippocampal CA1 neurones in vitro. Journal of Physiology *334*, 19-31.

Collins, M. O., Yu, L., Coba, M. P., Husi, H., Campuzano, I., Blackstock, W. P., Choudhary, J. S., and Grant, S. G. N. (2005). Proteomic analysis of *in vivo* phosphorylated synaptic proteins. Journal of Biological Chemistry *280*, 5972-5982.

Comery, T. A., Harris, J. B., Willems, P. J., Oostra, B. A., Irwin, S. A., Weiler, I. J., and Greenough, W. T. (1997). Abnormal dendritic spines in fragile X knockout mice: maturation and pruning deficits. Proceedings of the National Academy of Sciences of the United States of America *94*, 5401-5404.

Consortium, I. H. G. S. (2001). Intitial sequencing and analysis of the human genome. Nature *409*, 860-921.

Consortium, M. G. S. (2002). Intitial sequencing and comparative analysis of the mouse genome. Nature *420*, 520-562.

Copeland, N. G., Jenkins, N. A., and Court, D. L. (2001). Recombineering: A powerful new tool for mouse functional genomics. Nature Reviews Genetics *2*, 769-779.

Court, D. L., Swaminathan, S., Yu, D., Wilson, H., Baker, T., Bubunenko, M., Sawitzke, J., and Sharan, S. K. (2003). Mini-λ: a tractable system for chromosome and BAC engineering. Gene *315*, 63-69.

Crusio, W. E. (2001). Genetic dissection of mouse exploratory behaviour. Behavioural Brain Research *125*, 127-132.

D'Adamo, P., Welzl, H., Papadimitriou, S., Raffaele di Barletta, M., Tiveron, C., Tatangelo, L., Pozzi, L., Chapman, P. F., Knevett, S. G., Ramsay, M. F., *et al.* (2002). Deletion of the mental retardation gene *Gdi1* impairs associative memory and alters social behavior in mice. Human Molecular Genetics *11*, 2567-2580.

D'Hooge, R., Nagels, G., Franck, F., Bakker, C. E., Reyniers, E., Storm, K., Kooy, R. F., Oostra, B. A., Willems, P. J., and De Deyn, P. P. (1997). Mildly impaired water maze performance in male *Fmr1* knockout mice. Neuroscience *76*, 367-376.

Davis, S., Vanhoutte, P., Pages, C., Caboche, J., and Laroche, S. (2000). The MAPK/ERK cascade targets both Elk-1 and cAMP response element-binding protein to control long-term potentiation-dependent gene expression in the dentate gyrus *in vivo*. Journal of Neuroscience *20*, 4563-4572.

de Wit, J., and Verhaagen, J. (2003). Role of semaphorins in the adult nervous system. Progress in Neurobiology *71*, 249-267.

DeMarco, S. J., and Strehler, E. E. (2001). Plasma membrane Ca^{2+}-ATPase isoforms 2b and 4b interact promiscuously and selectively with members of the membrane-associated guanylate kinase family of PDZ (PSD95/Dlg/ZO-1) domain-containing proteins. Journal of Biological Chemistry *276*, 21594-21600.

Dickinson, P., Kimber, W. L., Kilanowski, F. M., Webb, S., Stevenson, B. J., Porteous, D. J., and Dorin, J. R. (2000). Enhancing the efficiency of introducing precise mutations into the mouse genome by hit and run gene targeting. Transgenic Research *9*, 55-66.

Dingledine, R., Borges, K., Bowie, D., and Traynelis, S. F. (1999). The glutamate receptor ion channels. Pharmacological Reviews *51*, 7-51.

Doetschman, T., Gregg, R. G., Maeda, N., Hooper, M. L., Melton, D. W., Thompson, S., and Smithies, O. (1987). Targeted correction of a mutant HPRT gene in mouse embryonic stem cells. Nature *330*, 576-578.

Dolzhanskaya, N., Sung, Y. J., Conti, J., Currie, J. R., and Denman, R. B. (2003). The fragile X mental retardation protein interacts with U-rich RNAs in a yeast three-hybrid screen. Biochemical and Biophysical Research Communications *205*, 434-441.

Dragatsis, I., and Zeitlin, S. (2000). *CaMKIIα-cre* transgene expression and recombination patterns in the mouse brain. Genesis *26*, 133-135.

Dudek, S. M., and Bear, M. F. (1992). Homosynaptic long-term depression in area CA1 of hippocampus and effects of N-methyl-D-aspartate receptor blockade. Proceedings of the National Academy of Sciences of the United States of America *89*, 4363-4367.

Dymecki, S. M. (2000). Site-specific recombination in cells and mice. In Gene targeting: a practical approach, A. L. Joyner, ed. (Oxford, Oxford University Press), pp. 37-96.

El-Husseini, A. E., Craven, S. E., Chetkovich, D. M., Firestein, B. L., Schnell, E., Aoki, C., and Bredt, D. S. (2000a). Dual palmitoylation of PSD-95 mediates its vesiculotubular sorting, postsynaptic targeting and ion channel clustering. Journal of Cell Biology *148*, 259-271.

El-Husseini, A. E., Topinka, J. R., Lehrer-Graiwer, J. E., Firestein, B. L., Craven, S. E., Aoki, C., and Bredt, D. S. (2000b). Ion channel clustering by membrane-associated guanylate kinases. Differential regulation by N-terminal lipid and metal binding motifs. Journal of Biological Chemistry *275*, 23904-23910.

Elbashir, S. M., Harborth, J., Lendeckel, W., Yalcin, A., Weber, K., and Tuschl, T. (2001). Duplexes of 21-nucleotide RNAs mediate RNA interference in cultured mammalian cells. Nature *411*, 494-498.

English, J. D., and Sweatt, D. (1997). A requirement for the mitogen-activated protein kinase cascade in hippocampal long term potentiation. Journal of Biological Chemistry *272*, 19103-19106.

Erreger, K., Dravid, S. M., Banke, T. G., Wyllie, D. J., and Traynelis, s. F. (2005). Subunit-specific gating controls rat NR1/NR2A and NR1/NR2B NMDA channel kinetics and synaptic signalling profiles. Journal of Physiology *563*, 345-358.

Farley, F. W., soriano, P., Steffen, L. S., and Dymecki, S. M. (2000). Wide-spread recombinase expression using FLPeR (flipper) mice. Genesis *28*, 106-110.

Festing, M. F. W., Simpson, E. M., Davisson, M. T., and Mobraaten, L. E. (1999). Revised nomenclature for strain 129 mice. Mammalian Genome *10*, 836.

Firestein, B., Brenman, J., Aoki, C., Sanchez-Perez, A., El-Husseini, A., and Bredt, D. (1999). Cypin: a cytosolic regulator of PSD-95 postsynaptic targeting. Neuron *24*, 659-672.

Fishburn, J., Turner, G., Daniel, A., and Brookwell, R. (1983). The diagnosis and frequency of X-linked conditions in a cohort of moderately retarded males with affected brothers. American Journal of Medical Genetics *14*, 713-724.

Forrest, D., Yuzaki, M., Soares, H. D., Ng, L., Luk, D. C., Sheng, M., Stewart, C. L., Morgan, J. I., Connor, J. A., and Curran, T. (1994). Targeted disruption of NMDA receptor 1 gene abolishes NMDA response and results in neonatal death. Neuron *13*, 325-338.

Frankland, P. W., and Bontempi, B. (2005). The organization of recent and remote memories. Nature Reviews Neuroscience *6*, 119-130.

Fujita, A., and Kurachi, Y. (2000). SAP family proteins. Biochemical & Biophysical Research Communications *269*, 1-6.

Fukaya, M., Ueda, H., Yamauchi, K., Inoue, Y., and Watanabe, M. (1999). Distinct spatiotemporal expression of mRNAs for the PSD-95/SAP90 protein family in the mouse brain. Neuroscience Research *33*, 111-118.

Fukaya, M., and Watabe, A. M. (2000). Improved immunohistochemical detection of postsynaptically located PSD-95/SAP90 protein family by protease section pretreatment: a study in the adult mouse brain. Journal of Comparative Neurology *426*, 572-586.

Funke, L., Dakoji, S., and Bredt, D. S. (2005). Membrane-associated guanylate kinases regulate adhesion and plasticity at cell junctions. Annual Review of Biochemistry *74*, 219-245.

Garcia, E. P., Mehta, S., Blair, L. A. C., Wells, D. G., Shang, J., Fukushima, T., Fallon, J. R., Garner, C. C., and Marshall, J. (1998). SAP90 binds and clusters kainate receptors causing incomplete desensitization. Neuron *21*, 727-739.

Garcia, R. A. G., Vasudevan, K., and Buonanno, A. (2000). The neuregulin receptor ErbB-4 interacts with PDZ-containing proteins at neuronal synapses. PNAS *97*, 3596-3601.

Gerlai, R. (1998). A new continuous alternation task in T-maze detects hippocampal dysfunction in mice: a strain comparison and lesion study. Behavioural Brain Research *95*, 91-101.

Gerlai, R. (2001). Behavioral tests of hippocampal function: simple paradigms, complex problems. Behavioural Brain Research *125*, 269-277.

Gerlai, R., Fitch, T., Bales, K. R., and Gitter, B. D. (2002). Behavioral impairment of APP^{V717F} mice in fear conditioning: is it only cognition? Behavioural Brain Research *136*, 503-509.

Ghosh, A., and Greenberg, M. E. (1995). Calcium signaling in neurons: molecular mechanisms and cellular consequences. Science *268*, 239-247.

Gordon, J. A., and Hen, R. (2004). Genetic approaches to the study of anxiety. Annual Review of Neuroscience *27*, 193-222.

Gossen, M., and Bujard, H. (1992). Tight control of gene expression in mammalian cells by tetracycline-responsive promoters. Proceedings of the National Academy of Sciences of the United States of America *89*, 5547-5551.

Grant, S. G. N., and O'Dell, T. J. (2001). Multiprotein complex signaling and the plasticity problem. Current Opinion in Neurobiology *11*, 363-368.

Gu, Y., McIlwain, K. L., Weeber, e. J., Yamagata, T., Xu, B., Antalffy, B. A., Reyes, C., Yuva-Paylor, L., Armstrong, D., Zoghbi, H., *et al.* (2002). Impaired conditioned fear and enhanced long-term potentiation in *Fmr2* knockout mice. Journal of Neuroscience *22*, 2753-2763.

Hasty, P., Abuin, A., and Bradley, A. (2000). Gene targeting, principles and practice in mammalian cells. In Gene targeting: a practical approach, A. L. Joyner, ed. (Oxford, Oxford University Press), pp. 1-34.

Hebb, D. O. (1949). The organization of behavior: a neuropsychological theory (New York, Wiley).

Hebert, A. E., and Dash, P. K. (2002). Extracellular signal-regulated kinase activity in the entorhinal cortex is necessary for long-term spatial memory. Learning & Memory *9*, 156-166.

Heintz, N. (2001). BAC to the future: The use of BAC transgenic mice for neuroscience research. In Nature Reviews Neuroscience, pp. 861-870.

Hinton, V. J., Brown, W. T., Wisniewski, K., and Rudelli, R. D. (1991). Analysis of neocortex in three males with the fragile X syndrome. American Journal of Medical Genetics *41*, 289-294.

Horio, Y., Hibino, H., Inanobe, A., Yamada, M., Ishii, M., Tada, Y., Satoh, E., Hata, Y., Takai, Y., and Kurachi, Y. (1997). Clustering and enhanced activity of an inwardly rectifying potassium channel, Kir4.1, by an anchoring protein, PSD-95/SAP90. Journal of Biological Chemistry *272*, 12885-12888.

Huang, Y. Z., Wang, Q., Won, S., Luo, Z. G., Xiong, W. C., and Mei, L. (2002). Compartmentalized NRG signaling and PDZ domain-containing proteins in synapse structure and function. International Journal of Developmental Neuroscience *20*, 173-185.

Huber, G., and Matus, A. (1984). Differences in the cellular distributions of two microtubule-associated proteins, MAP1 and MAP2, in rat brain. Journal of Neuroscience *4*, 151-160.

Huber, K. M., Gallagher, S. M., Warren, S. T., and Bear, M. F. (2002). Altered synaptic plasticity in a mouse model of fragile X mental retardation. Proceedings of the National Academy of Sciences of the United States of America *99*, 7746-7750.

Huettner, J. E. (2003). Kainate receptors and synaptic transmission. Progress in Neurobiology *70*, 387-407.

Hunt, C. A., Schenker, L. J., and Kennedy, M. B. (1996). PSD-95 is associated with the postsynaptic density and not with the presynaptic membrane at forebrain synapses. Journal of Neuroscience *16*, 1380-1388.

Husi, H., M.A., W., Choudhary, J. S., Blackstock, W. P., and Grant, S. G. N. (2000). Proteomic analysis of NMDA receptor-adhesion protein signaling complexes. Nature Neuroscience *3*, 661-669.

Imamura, F., Maeda, S., Doi, T., and Fujiyoshi, Y. (2002). Ligand binding of the seond PDZ domain regulates clustering of PSD-95 with the Kv1.4 potassium channel. Journal of Biological Chemistry *277*, 3640-3646.

Impey, S., Obrietan, K., Wong, S. T., Poser, S., Yano, S., Wayman, G., Deloulme, J. G., Chan, G., and Storm, D. R. (1998). Cross talk between ERK and PKA is required for Ca^{2+} stimulation of CREB-dependent transcription and ERK nuclear translocation. Neuron *21*, 869-883.

Inagaki, S., Ohoka, Y., Sugimoto, H., Fukioka, S., Amazaki, M., Kurinami, H., Miyazaki, N., Tohyama, M., and Furuyama, T. (2001). Sema4C, a transmembrane semaphorin, interacts with a postsynaptic density protein, PSD-93. Journal of Biological Chemistry *276*, 9174-9181.

Indra, A. K., Warot, X., Brocard, J., Bornert, J. M., Xiao, J. H., Chambon, P., and Metzger, d. (1999). Temporally-controlled site-specific mutagenesis in the basal layer of the epidermis: comparison of the recombinase activity of the tamoxifen-inducible Cre-ER(T) and Cre-ER(T2) recombinases. Nucleic Acids Res *27*, 4324-4327.

Jo, D., Nashabi, A., Doxsee, C., Lin, Q., Unutmaz, D., Chen, J., and Ruley, H. E. (2001). Epigenetic regulation of gene structure and function with a cell-permeable Cre recombinase. Nature Biotechnology *19*, 929-933.

Jun, K., Choi, G., Yang, S.-G., Choi, K. Y., Kim, H., Chang, G. C. K., Storm, D. R., Albert, C., Mayr, G. W., Lee, C.-J., and Shin, H.-S. (1998). Enhanced hippocampal CA1 LTP but normal spatial learning in inositol 1,4,5-trisphosphate 3-kinase(A)-deficient mice. Learning & Memory *5*, 317-330.

Kalscheuer, V. M., Freude, K., Musante, L., Jensen, L. R., Yntema, H. G., Gecz, J., Sefiani, A., Hoffmann, K., Moser, B., Haas, S., *et al*. (2003). Mutations in the polyglutamine binding protein 1 gene cause X-linked mental retardation. Nature Genetics *35*, 313-315.

Kandel, E. R., Schwartz, J. H., and Jessell, T. M. (2000). Principles of neural science, 4 edn (New York, McGraw-Hill).

Kaufmann, W. E., and Moers, H. W. (2000). Dendritic anomalies in disorders associated with mental retardation. Cerebral Cortex *10*, 981-991.

Kellendonk, C., Tronche, F., Casanova, E., Anlag, K., Opherk, C., and Schutz, G. (1999). Inducible site-specific recombination in the brain. Journal of Molecular Biology *285*, 175-182.

Kim, E., Cho, K. O., Rothschild, A., and Sheng, M. (1996). Heteromultimerization and NMDA receptor-clustering activity of chapsyn-110, a member of the PSD-95 family of proteins. Neuron *17*, 103-113.

Kim, E., Naisbitt, S., Hsueh, Y.-P., Rao, A., Rothschild, A., Craig, A. M., and Sheng, M. (1997). GKAP, a novel synaptic protein that interacts with the guanylate kinase-like domain of the PSD-95/SAP90 family of channel clustering molecules. Journal of Cell Biology *136*, 669-678.

Kim, J. H., Liao, D., Lau, L. F., and Huganir, R. L. (1998). SynGAP: a synaptic RasGAP that associates with the PSD-95/SAP90 protein family. Neuron *20*, 683-691.

Kim, M. J., Dunah, A. W., Wang, Y. T., and Sheng, M. (2005). Differential roles of NR2A- and NR2B-containing NMDA receptors in Ras-ERK signaling and AMPA receptor trafficking. Neuron *46*, 745-760.

Kistner, U., Garner, C. C., and Linial, M. (1995). Nucleotide binding by the synapse associated protein SAP90. FEBS Letters *359*, 159-163.

Klöcker, N., Bunn, R. C., Schnell, E., Caruana, G., Bernstein, A., Nicoll, R. A., and Bredt, D. S. (2002). Synaptic glutamate receptor clustering in mice lacking the SH3 and GK domains of SAP97. European Journal of Neuroscience *16*, 1517-1522.

Komiyama, N. H., Watabe, A. M., Carlisle, H. J., Porter, K., Charlesworth, P., Monti, J., Strathdee, D. J. C., O'Carroll, C. M., Martin, S. J., Morris, R. G. M.*, et al.* (2002). SynGAP regulates ERK/MAPK signaling, synaptic plasticity and learning in the complex with postsynaptic density 95 and NMDA receptor. Journal of Neuroscience *22*, 9721-9732.

Koulen, P. (1999). Localization of synapse-associated proteins during postnatal development of the rat retina. European Journal of Neuroscience *11*, 2007-2018.

Koulen, P., Garner, C. C., and Wassle, H. (1998). Immunoctyochemical localization of the synapse-associated protein SAP102 in the rat retina. Journal of Comparative Neurology *397*, 326-336.

Kutsche, K., Yntema, H., Brandt, A., Jantke, I., Nothwang, H. G., Orth, U., Boavida, M. G., david, D., Chelly, J., Fryns, J.-P.*, et al.* (2000). Mutations in *ARHGEF6*, encoding a guanine

nucleotide exchange factor for Rho GTPases, in patients with X-linked mental retardation. Nature Genetics *26*, 247-250.

Kutsuwada, T., Sakimura, K., Manabe, T., Takayama, C., Katakura, N., Kushiya, E., Natsume, R., Watanabe, M., Inoue, Y., Yagi, T., *et al.* (1996). Impairment of suckling response, trigeminal neuronal pattern formation and hippocampal LTD in NMDA receptor ε2 subunit mutant mice. Neuron *16*, 333-344.

Kuwahara, H., Araki, N., Makino, K., Masuko, N., Honda, S., Kaibuchi, K., Fukunaga, K., Miyamoto, E., Ogawa, M., and Saya, H. (1999). A novel NE-dlg/SAP102-associated protein, p51-nedasin, related to the amidohydrolase superfamily, interferes with the association between NE-dlg/SAP102 and *N*-methyl-D-aspartate receptor. In Journal of Biological Chemistry, pp. 32204-32214.

Kwan, K.-M. (2002). Conditional alleles in mice: practical considerations for tissue-specific knockouts. Genesis *32*, 49-62.

Lahey, T., Gorczyca, M., Jia, X.-X., and Budnik, V. (1994). The drosophila tumor suuppressor gene *dlg* is required for normal synaptic bouton structure. Neuron *13*, 823-835.

Lallemand, Y., Luria, V., Haffner-Kausz, R., and Lonai, P. (1998). Maternally expressed PGK-Cre transgene as a tool for early and uniform activation of the Cre site-specific recombinase. Transgenic Research *7*, 105-112.

Lalonde, R., Kim, H. D., and Fukuchi, K. (2004). Exploratory activity, anxiety and motor coordination in bigenic *APP*swe + *PS1*E9 mice. Neuroscience Letters *269*, 156-161.

Lambert, J.-F., Benoit, B. O., Colvin, G. A., Carlson, J., Delville, Y., and Quesenberry, P. J. (2000). Quick sex determination of mouse fetuses. Journal of Neuroscience Methods *95*, 127-132.

Larsson, M., Hjalm, G., Sakwe, A. M., Hoglund, A.-S., Larsson, E., Roninson, R. C., Sundberg, C., and Rask, L. (2003). Selective interaction of megalin with postsynaptic density-95 (PSD-95)-like membrane-associated guanylate kinase (MAGUK) proteins. Biochemical Journal *373*, 381-391.

Lau, L. F., Mammen, A., Ehlers, M. D., Kindler, S., Chung, W. J., Garner, C. C., and Huganir, R. L. (1996). Interaction of the N-methyl-D-aspartate receptor complex with a novel synapse-associated protein, SAP102. Journal of Biological Chemistry *271*, 21622-21628.

Lebel, R. R., May, M., Pouls, S., Lubs, H. A., Stevenson, R. E., and Schwartz, C. E. (2002). Non-syndromic X-linked mental retardation associated with a missense mutation (P312L) in the FGD1 gene. Clinical Genetics *61*, 139-140.

Ledermann, B. (2000). Embryonic stem cells and gene targeting. Experimental Physiology *85*, 603-613.

Lee, E.-C., Yu, D., Martinez, J. L., Tessarollo, L., Swing, D. A., Court, D. L., Jenkins, N. A., and Copeland, N. G. (2001). A highly efficient *Escherichia coli*-based chromosomee engineering system adapted for recombinogenic targeting and subcloning of BAC DNA. Genomics *73*, 56-65.

Leonard, A. S., Davare, M. A., Horne, M. C., Garner, C. C., and Hell, J. W. (1998). SAP97 is associated with the α-amino-3-hydroxy-3-methylisoxazole-4-propionic acid receptor GluR1 subunit. J Biol Chem *273*, 19518-19524.

Leonoudakis, D., Conti, L. R., Anderson, S., Radeke, C. M., McGuire, L. M. M., Adams, M. E., Froehner, S. C., Yates, J. R., and Vandenberg, C. A. (2004). Protein trafficking and anchoring complexes revealed by proteomic analysis of inward rectifier poteassium channel (Kir2.x)-associated proteins. Journal of Biological Chemistry *279*, 22331-22346.

Levedakou, E. N., Chen, X.-J., Soliven, B., and Popko, B. (2004). Disruption of the mouse *Large* gene in the *enr* and *myd* mutants results in nerve, muscle and neuromuscular junction defects. Molecular and Cellular Neuroscience *28*, 757-769.

Li, Y., Spangenberg, O., Paarmann, I., Konrad, M., and Lavie, A. (2002). Structural basis for nucleotide-dependent regulation of membrane-associated guanylate kinase-like domains. Journal of Biological Chemistry *277*, 4159-4165.

Lim, I. A., Hall, D. D., and Hell, J. W. (2002). Selectivity and promiscuity of the first and second PDZ domains of PSD-95 and synapse-associated protein 102. Journal of Biological Chemistry *277*, 21697-21711.

Lister, R. G. (1987). The use of a plus-maze to measure anxiety in the mouse. Psychopharmacology *92*, 180-185.

Liu, L., Wong, T. P., Pozza, M. F., Lingenhoehl, K., Wang, Y. X., Sheng, M., Auberson, Y. P., and Wang, Y. T. (2004). Role of NMDA receptor subtypes in governing the direction of hippocampal synaptic plasticity. Science *304*, 1021-1024.

Liu, P., Jenkins, N. A., and Copeland, N. G. (2003). A highly efficient recombineering-based method for generating conditional knockout mutations. Genome Res *13*, 476-484.

Lonze, B. E., and Ginty, D. D. (2002). Function and regulation of CREB family transcription factors in the nervous system. Neuron *35*, 605-623.

Loonstra, A., Mooijs, M., Beverloo, H. B., Al Allak, B., van Drunen, E., Kanaar, R., Berns, A., and Jonkers, J. (2001). Growth inhibition and DNA damage induced by Cre recombinase in mammalian cells. Proceedings of the National Academy of Sciences of the United States of America *98*, 9209-9214.

Lynch, G. S., Larson, J., Kelso, S., Barrionuevo, G., and Schottler, F. (1983). Intracellular injections of EGTA block induction of hippocampal long-term potentiation. Nature *305*, 719-721.

Maes, B., Fryns, J.-P., Van Walleghem, M., and Van den Berghe, H. (1994). Cognitive functioning and information processing of adult mentally retarded men wiith Fragile X syndrome. American Journal of Medical Genetics *50*, 190-200.

Makino, K., Kuwahara, H., Masuko, N., Nishiyama, Y., Morisaki, T., Sasaki, J., Nakao, M., Kuwano, A., Nakata, M., Ushio, Y., and Saya, H. (1997). Cloning and characterization of NE-dlg: A novel human homolog of the *Drosophila* discs large (dlg) tumor suppressor protein interacts with the APC protein. Oncogene *14*, 2425-2433.

Malenka, R. C., and Bear, M. F. (2004). LTP and LTD: an embarrassment of riches. Neuron *44*, 5-21.

Malenka, R. C., Kauer, J. A., Zucker, R. S., and Nicoll, R. A. (1988). Postsynaptic calcium is sufficient for potentiation of hippocampal synaptic transmission. Science *242*, 81-84.

Massey, P. V., Johnson, B. E., Moult, P. R., Auberson, Y. P., Brown, M. W., Molnar, E., Collingridge, G. L., and Bashir, Z. I. (2004). Differential roles of NR2A and NR2B-containing NMDA receptors in cortical long-term potentiation and long-term depression. Journal of Neuroscience *24*, 7821-7828.

Masuko, N., Makino, K., Kuwahara, H., Fukunaga, K., Sudo, T., Araki, N., Yamamoto, H., Yamada, Y., Miyamoto, E., and Saya, H. (1999). Interaction of NE-dlg/SAP102, a neuronal and endocrine tissue-specific membrane-associated guanylate kinase protein, with calmodulin and PSD-95/SAP90. A possible regulatory role in molecular clustering at synaptic sites. Journal of Biological Chemistry *274*, 5782-5790.

Mayford, M., Wang, J., Kandel, E. R., and O'Dell, T. J. (1995). CaMKII regulates the frequency-response function of hippocampal synapses for the production of both LTD and LTP. Cell *81*, 891-904.

McGee, A. W., Topinka, J. R., Hashimoto, K., Petralia, R. S., Kakizawa, S., Kauer, F., Aguilera-Moreno, A., Wenthold, R. J., Kano, M., and Bredt, D. S. (2001). PSD-93 knock-out mice reveal that neuronal MAGUKs are not required for development of function of parallel fiber synapses in cerebellum. Journal of Neuroscience *21*, 3085-3091.

Meng, J., Meng, Y., Hanna, A., Janus, C., and Zhengping, J. (2005). Abnormal long-lasting synaptic plasticity and cognition in mice lacking the mental retardation gene *PAK3*. Journal of Neuroscience *25*, 6641-6650.

Migaud, M., Charlesworth, P., Dempster, M., Webster, L. C., Watabe, A. M., Makhinson, M., He, Y., Ramsay, M. F., Morris, R. G. M., Morrison, J. H., *et al.* (1998). Enhanced long-term

potentiation and impaired learning in mice with mutant postsynaptic density-95 protein. Nature *396*, 433-439.

Milner, B., Squire, L. R., and Kandel, E. R. (1998). Cognitive neuroscience and the study of memory. Neuron *20*, 445-468.

Montgomery, J. M., Zamorano, P. L., and Garner, C. C. (2004). MAGUKs in synapse assembly and function: an emerging view. Cellular and Molecular Life Sciences *61*, 911-929.

Monyer, H., Burnashev, N., Laurie, D. J., Sakmann, B., and Seeburg, P. H. (1994). Developmental and regional expression in the rat brain and functional properties of four NMDA receptors. Neuron *12*, 529-540.

Morgan, H. D., Sutherland, H. G. E., Martin, D. I. K., and Whitelaw, E. (1999). Epigenetic inheritance at the agouti locus in the mouse. Nature Genetics *23*, 314-318.

Morris, R. G. M., Anderson, E., Lynch, G. S., and Baudry, M. (1986). Selective impairment of learning and blockade of long-term potentiation by an *N*-methyl-D-aspartate receptor antagonist, AP5. Nature *319*.

Morris, R. G. M., Garrud, P., Rawlins, J. N. P., and O'Keefe, J. (1982). Place navigation impaired in rats with hippocampal lesions. Nature *297*, 681-683.

Muller, B., Kistner, U., Veh, R. W., Cases-Langhoff, C., Becker, B., Gundelfinger, E. D., and Garner, C. C. (1995). Molecular characterization and spatial distribution of SAP97, a novel

presynaptic protein homologous to SAP90 and the *Drosophila* discs-large tumor suppressor protein. Journal of Neuroscience *15*, 2354-2366.

Muller, B. M., Kistner, U., Kindler, S., Chung, W. J., Kuhlendahl, S., Fenster, S. D., Lau, L. F., Veh, R. W., Huganir, R. L., Gundelfinger, E. D., and Garner, C. C. (1996). SAP102, a novel postsynaptic protein that interacts with NMDA receptor complexes in vivo. Neuron *17*, 255-265.

Muyrers, J. P., Zhang, Y., and Stewart, A. F. (2001). Techniques: Recombinogenic engineering - new options for cloning and manipulating DNA. Trends in Biochemical Sciences *26*, 325-331.

Muyrers, J. P., Zhang, Y., Testa, G., and Stewart, A. F. (1999). Rapid modification of bacterial artificial chromosomes by ET-recombination. Nucleic Acids Research *27*, 1555-1557.

Nagy, A. (2000). Cre recombinase: the universal reagent for genome tailoring. Genesis *26*, 99-109.

Nagy, A., Gertenstein, M., Vintersten, K., and Behringer, R. (2003). Manipulating the mouse embryo: a laboratory manual, 3rd edn (New York, Cold Spring Harbor Press).

Nourry, C., Grant, S. G. N., and Borg, J.-P. (2003). PDZ domain proteins: plug and play! Science STKE *179*, re7.

Nowak, L., Bregestovski, P., and Ascher, P. (1984). Magnesium gates glutamate-activated channels in mouse central neurones. Nature *307*, 462-465.

O'Donnell, W. T., and Warren, S. T. (2002). A decade of molecular studies of fragile X syndrome. Annual Review of Neuroscience *25*, 315-338.

Olsen, O., and Bredt, D. S. (2003). Functional analysis of the nucleotide binding domain of membrane-associated guanylate kinases. Journal of Biological Chemistry *278*, 6873-6878.

Orford, M., Nefedov, M., Vadolas, J., Zaibak, F., Williamson, R., and Loannou, P. A. (2000). Engineering EGFP reporter constructs into a 200 kb human β-globin BAC clone using *GET recombination*. Nucleic Acids Res *28*, e84.

Ottersen, O. P., and Landsend, A. S. (1997). Organization of glutamate receptors at the synapse. European Journal of Neuroscience *9*, 2219-2224.

Paddison, P. J., Caudy, A. A., Bernstein, E., Hannon, G. J., and Conklin, D. S. (2002). Short hairpin RNAs (shRNAs) induce sequence-specific silencing in mammalian cells. Genes & Development *16*, 948-958.

Paddison, P. J., Silva, J. M., Conklin, D. S., Schlabach, M., Li, M., Aruleba, S., Balija, V., O'Shaughnessy, A., Gnoj, L., Scobie, K., *et al*. (2004). A resource for large-scale RNA-interference-based screens in mammals. Nature *428*, 427-431.

Parks, C. L., Robinson, P. S., Sibille, E., Shenk, T., and Toth, M. (1998). Increased anxiety of mice lacking the serotonin$_{1A}$ receptor. Proceedings of the National Academy of Sciences of the United States of America *95*, 10734-10739.

Paxinos, G., and Franklin, K. B. J. (2001). The mouse brain in stereotaxic coordinates, 2nd edn (London, Academic Press).

Pearson, G., Robinson, F., Gibson, T. B., Xu, B.-E., Karandikar, M., Berman, K., and Cobb, M. H. (2001). Mitogen-activated protein (MAP) kinase pathways: regulation and physiological functions. Endocrine Reviews *22*, 153-183.

Penzes, P., Johson, R. C., Sattler, R., Zhang, X., Huganir, R. L., Kambampati, V., Mains, R. E., and Eipper, B. A. (2001). The neuronal Rho-GEF kalirin-7 interacts with PDZ domain-containing proteins and regulates dendritic morphogenesis. Neuron *29*, 229-242.

Petralia, R. S., Sans, N., Wang, Y.-X., and Wenthold, R. J. (2005). Ontogeny of postsynaptic density proteins at glutamatergic synapses. Molecular and Cellular Neuroscience *29*, 436-452.

Porter, K., Komiyama, N. H., Vitalis, T., Kind, P. C., and Grant, S. G. (2005). Differential expression of two NMDA receptor interacting proteins, PSD-95 and SynGAP, during mouse development. European Journal of Neuroscience *21*, 351-362.

Purpura, D. P. (1974). Dendritic spine 'dysgenesis' and mental retardation. Science *186*, 1126-1128.

Rakyan, V. K., Chong, S., Champ, M. E., Cuthbert, P. C., Morgan, H. D., Luu, K. V. K., and Whitelaw, E. (2003). Transgenerational inheritance of epigenetic states at the murine *Axin*^{Fu} allele occurs after maternal and paternal transmission. Proceedings of the National Academy of Sciences of the United States of America *100*, 2538-2543.

Ramakers, G. J. A. (2002). Rho proteins, mental retardation and the cellular basis of cognition. Trends in Neurosciences *25*, 191-199.

Ramanan, N., Shen, Y., Sarsfield, S., Lemberger, T., Schutz, G., Linden, D. J., and Ginty, D. D. (2005). SRF mediates activity-induced gene expression and synaptic plasticity but not neuronal viability. Nature Neuroscience *8*, 759-767.

Ramirez-Solis, R., Davis, A. C., and Bradley, A. (1993). Gene targeting in embryonic stem cells. Methods in Enzymology *225*, 855-878.

Rasband, M. N., Park, E. W., Zhen, D., Arbuckle, M. I., Poliak, S., Peles, E., Grant, S. G. N., and Trimmer, J. S. (2002). Clustering of neuronal potassium channels is independent of their interaction with PSD-95. Journal of Cell Biology.

Renieri, A., Pescucci, C., Longo, I., Ariani, F., Mari, F., and Meloni, I. (2005). Non-syndromic X-linked mental retardation: from a molecular to a clinical point of view. Journal of Cellular Physiology *204*, 8-20.

Roche, K. W., Ly, C. D., Petralia, R. S., Wang, Y.-X., McGee, A. W., Bredt, D. S., and Wenthold, R. J. (1999). Postsynaptic density-93 interacts with the δ2 glutamate receptor subunit at parallel fiber synapses. Journal of Neuroscience *19*, 3926-3934.

Rodgers, R. J., and Johnson, N. J. T. (1995). Factor analysis of spatiotemporal and ethological measuures in the murine elevated plus-maze test of anxiety. Pharmacology Biochemistry and Behaviour *52*, 297-303.

Ropers, H. H., and Hamel, B. C. J. (2005). X-linked mental retardation. Nature Reviews Genetics *6*, 46-57.

Ross, M. T. (2005). The DNA sequence of the human X chromosome. Nature *434*, 325-337.

Rozen, S., and Skaletsky, H. (2000). Primer3 on the WWW for general users and for biologist programmers. In Bioinformatics methods and protocols: methods in molecular biology, S. Krawetz, and S. Misener, eds. (Totowa, NJ, Humana Press), pp. 365-386.

Sakai, N., Thome, J., Newton, S. S., JChen, J., Kelz, M. B., Steffen, C., Nestler, E. J., and Duman, R. S. (2002). Inducible and brain region-specific CREB transgenic mice. Molecular Pharmacology *61*, 1453-1464.

Sakimura, K., Kutsuwada, T., Ito, I., Manabe, T., Takayama, C., Kushiya, E., Yagi, T., Aizawa, S., Inoue, Y., Sugiyama, H., and Mishina, M. (1995). Reduced hippocampal LTP and spatial learning in mice lacking NMDA receptor ε1 subunit. Nature *373*, 151-155.

Sambrook, J., and Russell, D. (2001). Molecular cloning: a laboratory manual, 3rd edn (New York, CSHL Press).

Sans, N., Petralia, R. S., Wang, Y. X., Blahos, J., 2nd, Hell, J. W., and Wenthold, R. J. (2000). A developmental change in NMDA receptor-associated proteins at hippocampal synapses. Journal of Neuroscience *20*, 1260-1271.

Sans, N., Prybylowski, K., Petralia, R. S., Chang, K., Wang, Y.-X., Racca, C., Vicini, S., and Wenthold, R. J. (2003). NMDA receptor trafficking through an interaction between PDZ proteins and the exocyst complex. Nat Cell Biol *5*, 520-530.

Sans, N., Racca, C., Petralia, R. S., Wang, Y. X., McCallum, J., and Wenthold, R. J. (2001). Synapse-associated protein 97 selectively associates with a subset of AMPA receptors early in their biosynthetic pathway. Journal of Neuroscience *21*, 7506-7516.

Sattler, R., Xiong, Z., Lu, W.-Y., Hafner, M., MacDonald, J. F., and Tymianski, M. (1999). Specific Coupling of NMDA Receptor Activation to Nitric Oxide Neurotoxicity by PSD-95 Protein. Science *284*, 1845-1848.

Schmidt, E. E., Taylor, D. S., Prigge, J. R., Barnett, S., and Capecchi, M. R. (2000). Illegitimate Cre-dependent chromosome rearrangements in transgenic mouse spermatids. Proceedings of the National Academy of Sciences of the United States of America *97*, 13702-13707.

Schwartzberg, P. L., Goff, S. P., and Robertson, E. J. (1989). Germ-line transmission of a c-abl mutation produced by targeted gene disruption in ES cells. Science *246*, 799-803.

Seabold, G. K., Burette, A., Lim, I. A., Weinberg, R. J., and Hell, J. W. (2003). Interaction of the tyrosine kinase Pyk2 with the *N*-methyl-D aspartate receptor complex via the Src homology 3 domains of PSD-95 and SAP102. Journal of Biological Chemistry *278*, 15040-15048.

Selcher, J. C., Atkins, C. M., Trzaskos, J. M., Paylor, R., and Sweatt, J. D. (1999). A necessity for MAP kinase activation in mammalian spatial learning. Learning & Memory *6*.

Selfridge, J., Pow, A. M., McWhir, J., Magin, T. M., and Melton, D. W. (1992). Gene targeting using a mouse HPRT minigene/HPRT-deficient embryonic stem cell system: inactivation of the mouse ERCC-1 gene. Somatic Cell and Molecular Genetics *18*, 325-336.

Sharma, R. C., and Schimke, R. T. (1996). Preparation of electrocompetent *E.coli* using salt-free growth medium. Biotechniques *20*, 42-44.

Silva, A. J., Paylor, R., Wehner, J. M., and Tonegawa, S. (1992a). Impaired spatial learning in α-calcium-calmodulin kinase II mutant mice. Science *257*, 206-211.

Silva, A. J., Stevens, C. F., Tonegawa, S., and Wang, Y. (1992b). Deficient hippocampal long-term potentiation in α-calcium-calmodulin kinase II mutant mice. Science *257*, 201-206.

Silver, D. P., and Livingston, D. M. (2001). Self-excising retroviral vectors encoding the Cre recombinase overcome Cre-mediated cellular toxicity. Molecular Cell *8*, 233-243.

Smithies, O., Gregg, R. G., Boggs, S., Koralewski, M. A., and Kucherlapati, R. S. (1985). Insertion of DNA sequences into the human chromsomal β-globin locus by homologous recombination. Nature *317*, 230-234.

Spowart-Manning, L., and van der Staay, F. J. (2004). The T-maze continuous alternation task for assessing the effects of putative cognition enhancers in the mouse. Behavioural Brain Research *151*, 37-46.

Sprengel, R., and Single, F. N. (1999). Mice with genetically modified NMDA and AMPA receptors. Annals of the New York Academy of Sciences *868*, 494-501.

Sprengel, R., Suchanek, B., Amico, C., Brusa, R., Burnashev, N., Rozov, A., Hvalby, O., Jensen, V., Paulsen, O., Andersen, P., *et al*. (1998). Importance of the intracellular domain of NR2 subunits for NMDA receptor function in vivo. Cell *92*, 279-289.

Stanford, W. L., Cohn, J. B., and Cordes, S. P. (2001). Gene-trap mutagenesis: Past, present and beyond. Nature Reviews Genetics *2*, 756-768.

Stewart, M., Murphy, C., and Fristrom, J. W. (1972). The recovery and preliminary characterization of X chromosome mutants affecting imaginal discs of drosophila melanogaster. Developmental Biology *27*, 71-83.

Swaminathan, S., Ellis, H. M., Waters, L. S., Yu, D., Lee, E.-C., Court, D. L., and Sharan, S. K. (2001). Rapid engineering of bacterial artificial chromsoomes using oligonucleotides. Genesis *29*, 14-21.

Sweatt, D. (2004). Mitogen-activated protein kinases in synaptic plasticity and memory. Current Opinion in Neurobiology *14*, 311-317.

Takeuchi, M., Hata, Y., Hirao, K., Toyoda, A., Irie, M., and Takai, Y. (1997). A family of PSD-95/SAP90-associated proteins localized at postsynaptic density. Journal of Biological Chemistry *272*, 11943-11951.

Tang, Y.-P., Shimizu, E., Dube, G. R., Rampon, C., Kerchner, G. A., Zhuo, M., Liu, G., and Tsien, J. Z. (1999). Genetic enhancement of learning and memory in mice. Nature *401*, 63-69.

Tao, Y.-X., Rumbauggh, G., Wang, G.-D., Petralia, R. S., Zhao, C., Kauer, F. W., Tao, F., Zhuo, M., Wenthold, R. J., Raja, S. N., *et al*. (2003). Impaired NMDA receptor-mediated postsynaptic function and blunted NMDA receptor-dependent persistant pain in mice lacking postsynaptic density-93 protein. Journal of Neuroscience *23*, 6703-6712.

Tarpey, P., Parnau, J., Blow, M., Woffendin, H., Bignell, G., Cox, C., Cox, J., Davies, H., Edkins, S., Holden, S., *et al*. (2004). Mutations in the *DLG3* gene cause non-syndromic X-linked mental retardation. The American Journal of Human Genetics *75*, 318-324.

Thiels, E., Kanterewicz, B. I., Norman, E. D., Trzaskos, J. M., and Klann, E. (2002). Long-term depression in the adult hippocampus *in vivo* involves activation of extracellular signal-regulated kinase and phosphorylation of Elk-1. Journal of Neuroscience *22*, 2054-2062.

Thomas, G. M., and Huganir, R. L. (2004). MAPK cascade signalling and synaptic plasticity. Nature Neuroscience *5*, 173-183.

Thomas, K. R., and Capecchi, M. (1987). Site-directed mutagenesis by gene targeting in mouse embyro-derived stem cells. Cell *51*, 503-512.

Thompson, S., Clarke, A. R., Pow, A. M., Hooper, M. L., and Melton, D. W. (1989). Germ line transmission and expression of a corrected HPRT genne produced by gene targeting in embryonic stem cells. Cell *56*, 313-321.

Thyagarajan, B., Guimaraes, M. J., Groth, A. C., and Calos, M. P. (2000). Mammalian genomes contain active recombinase recognition sites. Gene *244*, 47-54.

Townsend, M., Yoshii, A., Mishina, M., and Constantine-Paton, M. (2003). Developmental loss of miniature N-methyl-D-aspartate receptor currents in NR2A knockout mice. Proc Natl Acad Sci U S A *100*, 1340-1345.

Trivier, E., De Cesare, D., Jacquot, S., Pannetier, S., Zackai, E., Young, I., Mandel, J.-L., Sassone-Corsi, P., and Hanauer, A. (1996). Mutations in the kinase Rsk-2 associated with Coffin-Lowry syndrome. Nature *384*, 567-570.

Tsien, J. Z., Chen, D. F., Gerber, D., tom, C., Mercer, E. H., Anderson, D. J., Mayford, M., Kandel, E. R., and Tonegawa, S. (1996a). Subregion- and cell type-restricted gene knockout in mouse brain. Cell *87*, 1317-1326.

Tsien, J. Z., Huerta, P. T., and Tonegawa, S. (1996b). The essential role of hippocampal CA1 NMDA receptor-dependent synaptic plasticity in spatial memory. Cell *87*, 1327-1338.

Valenzuela, D. M. (2003). High-throughput engineering of the mouse genome coupled with high-resolution expression analysis. Nature Biotechnology *21*, 652-659.

Van Dam, D., D'Hooge, R., Hauben, E., Reyniers, E., Gantois, I., Bakker, C. E., Oostra, B. A., Kooy, R. F., and De Deyn, P. P. (2000). Spatial learning, contextual fear conditioning and conditioned emotional response in *Fmr1* knockout mice. Behavioural Brain Research *117*, 127-136.

van den Bout, C. J., Machon, O., Rosok, O., Backman, M., and Krauss, S. (2002). The mouse enhancer element D6 directs Cre recombinase activity in the neocortex and the hippocampus. Mechanisms of Development *110*, 179-182.

van der Weyden, L., Adams, D. J., and Bradley, A. (2002). Tools for targeted manipulation of the mouse genome. Physiological Genomics *11*, 133-164.

Vazquez, L. E., Chen, H.-J., Sokolova, I., Knuesel, I., and Kennedy, M. B. (2004). SynGAP regulates spine formation. Journal of Neuroscience *24*, 8862-8872.

Vooijs, M., Jonkers, J., and Berns, A. (2001). A highly efficient ligand-regulated Cre recombinase mouse line shows that *LoxP* recombination is position dependent. EMBO Reports *2*, 292-297.

Watanabe, M., Fukaya, M., Sakimura, K., Manabe, T., Mishina, M., and Inoue, Y. (1998). Selective scarcity of NMDA receptor channel subunits in the stratum lucidum (mossy fibre-recipient layer) of the mouse hippocampal CA3 subfield. European Journal of Neuroscience *10*, 478-487.

Watase, K., and Zoghbi, H. (2003). Modelling brain diseases in mice: the challenges of design and analysis. Nature Reviews Genetics *4*, 296-307.

Weiss, S. M., Lightowler, S., Stanhope, K. J., Kennet, G. A., and Dourish, C. T. (2000). Measurement of anxiety in transgenic mice. Reviews in the Neurosciences *11*, 59-74.

Wenzel, A., Fritschy, J. M., Mohler, H., and Benke, D. (1997). NMDA receptor heterogeneity during postnatal development of the rat brain: differential expression of the NR2A, NR2B, and NR2C subunit proteins. J Neurochem *68*, 469-478.

Wenzel, A., Scheurer, L., Kunzi, R., Fritschy, J. M., Mohler, H., and Benke, D. (1995). Distribution of NMDA receptor subunit proteins NR2A, 2B, 2C and 2D in the rat brain. Neuroreport *29*, 47-48.

Winder, D. G., Martin, K. C., Muzzio, I. A., Rohrer, D., Chruscinski, A., Kobilka, B., and Kandel, E. R. (1999). ERK plays a regulatory role in induction of LTP by theta frequency stimulation and its modulation by β-adrenergic receptors. Neuron *24*, 715-726.

Wong, W., Newell, E. W., Jugloff, D. G. M., Jones, O. T., and Schlichter, L. C. (2002). Cell surface targeting and clustering interactions between heterologously expressed PSD-95 and the *ShaI* voltage-gated potassium channel, Kv4.2. Journal of Biological Chemistry *277*, 20423-20430.

Woods, D. F., and Bryant, P. J. (1991). The discs-large tumor suppressor gene of drosophila encodes a guanylate kinase homolog localized at septate junctions. Cell *66*, 451-464.

Wrenn, C. C., Harris, A. P., Saavedra, M. C., and Crawley, J. N. (2003). Social transmission of food preference in mice: methodology and application to galanin-overexpressing transgenic mice. Behavioral Neuroscience *117*, 21-31.

Yagi, T., Nada, S., Watanabe, N., Tamemoto, H., Kohmoura, N., Ikawa, Y., and Aizawa, S. (1993). A novel negative selection for homologous recombinants using diphtheria toxin A fragment gene. Analytical Biochemistry *214*, 77-86.

Yan, J., Oliveira, G., coutinho, A., Yang, C., Feng, J., Katz, C., Sram, J., Bockholt, A., Jones, I. R., Craddock, N., *et al*. (2004). Analysis of the neuroligin 3 and 4 genes in autism and other neuropsychiatric patients. Molecular Psychiatry *10*, 329-332.

Yanagawa, Y., Kobayashi, T., Ohnishi, M., Kobayashi, T., Tamura, S., Tsuzuki, T., Sanbo, M., Yagi, T., Tashiro, F., and Miyazaki, J. (1999). Enrichment and efficient screening of ES cells containing a targeted mutation: The use of DT-A gene with the polyadenylation signal as a negative selection marker. Transgenic Research *8*, 215-221.

Yang, Y., and Sharan, S. K. (2003). A simple two-step, 'hit and fix' method to generate subtle mutations in BACs using short denatured PCR fragments. Nucleic Acids Res *31*, e80.

Yu, D., Ellis, H. M., Lee, E.-C., Jenkins, N. A., Copeland, N. G., and Court, D. L. (2000). An efficient recombination system for chromosome engineering in *Escherichia coli*. Proc Natl Acad Sci U S A *97*, 5978-5983.

Yu, Y., and Bradley, A. (2001). Engineering chromosomal rearrangements in mice. Nature Reviews Genetics *2*, 780-790.

Zamanillo, D., Sprengel, R., Hvalby, O., Jesen, V., Burnashev, N., Rozov, A., Kaiser, K. M. M., Koster, H. J., Borchardt, T., Worley, P., *et al*. (1999). Importance of AMPA receptors for hippocampal synaptic plasticity but not for spatial learning. Science *284*, 1805-1816.

Zeng, L., Fagotto, f., Zhang, T., Hsu, W., Vasicek, T. J., Perry, W. L., Lee, J. J., Tilghman, S. M., Gumbiner, B. M., and Costantini, F. (1997). The mouse Fused locus encodes Axin, an inhibitor of the Wnt signaling pathway that regulates embryonic axis formation. Cell *90*, 181-192.

Zhang, P., Li, M. Z., and Elledge, S. J. (2001). Towards genetic genome projects: genomic library screening and gene-targeting vector construction in a single step. Nature Genetics *30*, 31-39.

Zhang, Y., Buchholz, F., Muyrers, J. P., and Stewart, A. F. (1998). A new logic for DNA engineering using recombination in *Escherichia coli*. Nature Genetics *20*, 123-128.

Zhang, Y., Muyrers, J. P. P., Testa, G., and Stewart, A. F. (2000). DNA cloning by homologous recombination in *Escherichia coli*. Nature Biotechnology *18*, 1314-1317.

Zhu, Y., Romero, M. I., Ghosh, P., Ye, Z., Charnay, P., Rushing, E. J., Marth, J. D., and Parada, L. F. (2001a). Ablation of NF1 function in neurons induces abnormal development of cerebral cortex and reactive gliosis in the brain. Genes & Development *15*, 849-876.

Zhu, Z., Ma, B., Homer, R., Zhen, T., and Elias, J. A. (2001b). Use of the tetracycline-controlled transcriptional silencer (tTS) to eliminate transgene leak in inducible overexpression transgenic mice. Journal of Biological Chemistry *276*, 25222-25229.

Appendix 1 Primary antibodies. Antibody uses are WB – western blot; IHC – immunohistochemistry; IP – immunoprecipitation. Non-commercial suppliers are Seth Grant, Wellcome Trust Sanger Institute, Cambridge, UK; Masahiko Watanabe, Department of Anatomy, Hokkaido University School of Medicine, Sapporo, Japan and Frank Dunn-Moore, School of Biology, University of St Andrews, St Andrews, UK.

Antigen	Supplier	Antibody type	Working dilution or concentration
NR1	S. Grant	sheep	5 μg per IP
NR1	Upstate	mouse monoclonal	1:1000 (WB)
NR1	Chemicon	mouse monoclonal	5 μg/ml (IHC)
NR2A	Upstate	rabbit polyclonal	1:500 (WB), 5 μg/ml (IHC)
NR2B	BD Biosciences	mouse monoclonal	1:250 (WB), 5 μg/ml (IHC)
GluR1	Upstate	rabbit polyclonal	1:670 (WB)
GluR2	Zymed	mouse monoclonal	1:300 (WB)
GluR6/7	Upstate	rabbit polyclonal	1:500 (WB)
Kv1.4	Upstate	mouse monoclonal	1:667 (WB)
ErbB4	Santa Cruz	rabbit polyclonal	1:200 (WB)
SAP102	Synaptic Systems	rabbit polyclonal	1:5000 (WB)
SAP102	M. Watanabe	rabbit polyclonal	5μg/ml (IHC)
PSD-95	BD Biosciences	mouse monoclonal	1:500 (WB)
PSD-95	Zymed	rabbit polyclonal	10 μg/ml (IHC)
PSD-93	Synaptic Systems	rabbit polyclonal	1:1000 (WB)
PSD-93	Watanabe	rabbit polyclonal	4μg/ml (IHC)
SAP97	BD Biosciences	mouse monoclonal	1:1000 (WB)
SynGAP	Upstate	rabbit polyclonal	1:2000 (WB)
Sec8	BD Biosciences	mouse monoclonal	1:1000 (WB)
Pyk2	BD Biosciences	mouse monoclonal	1:1000 (WB)
Kalirin	Upstate	rabbit polyclonal	1:250 (WB)
Stargazin	Calbiochem	rabbit polyclonal	1:200 (WB)
NrCAM	F. Gunn-Moore	rabbit polyclonal	1:1000 (WB)
MAP2B	BD Biosciences	mouse monoclonal	1 μg/ml (IHC)
ERK 1/2	Cell Signaling	mouse monoclonal	1:1000
phospho-p44/42 ERK 1/2 T202/Y204	Cell Signaling	mouse monoclonal	1:1000

Appendix 2 Oligonucleotide sequences. Sequences are listed 5'→3'.

Name	Sequence	Use
P1	GGTCTCTGAT GAAGCAGTGA TTTTT	SAP102 ES cell genotyping
P2	TGATGACCCA TAGACAGTAG GATCA	SAP102 ES cell genotyping
P3	CTAAAGCGCA TGCTCCAGAC	SAP102 genotyping
P4	CATGTGATGG CTTTACACCG	SAP102 mouse genotyping
P5	CATAGTCTGC TCTGCCTCCC	SAP102 mouse genotyping
P6	AGGACTCTCT TTGGTGGGCA	PSD-95 mouse genotyping
P7	AACCAAGGCG GATCGTGATC CA	PSD-95 mouse genotyping
P8	TGTGGCCGGC TGGGTGTGG	PSD-95 mouse genotyping
P9	AATCGCGGCC GTCTATCTCA T	PSD-95 mouse genotyping
5'PDZfwd	ACAAGCCTTC TTGCTCCAAA	BAC library screen
5'PDZrev	GACTCACTGG AGAGGGCAAG	BAC library screen
5'PDZ2fwd	GGTCTCTGAT GAAGCAGTGA TTTTT	BAC library screen
5'PDZ2rev	TGATGACCCA TAGACAGTAG GATCA	BAC library screen
3'PDZfwd	TTGATGCAAG ACAGGAGTGC	BAC library screen
3'PDZrev	CCACCAGGCA AATTCTCAGT	BAC library screen
SAP5'probefwd	AAGGCATGGA ATGTGGTAGC	5' probe, southern blot
SAP5'proberev	TTACCCGGTG TAAAGCCATC	5' probe, southern blot
SAP3'probefwd	TGCCTAGCAC AGGTGCTTTA	3' probe, southern blot
SAP3'proberev	CTGGAGTTGT TGGTGGGACT	3' probe, southern blot
SAP5'PDZ3fwd	CTTGCCCTCT CCAGTGAGTC	internal probe, southern blot
SAP5'PDZ3rev	GAACTGGCCA GGAGTCTGAG	internal probe, southern blot
L1sense	GCGGCCGCTA TATATATAGG CGCGCCGGAT CCTGATCAAG ATCTGGATCC GTTTAAACTT AATTAATATA TATATATAGT CGAC	linker, pIRESlacZneoflox construction
L1antisense	GTCGACTATA TATATATATT AATTAAGTTT AAACGGATCC AGATCTTGAT CAGGATCCGG CGCGCCTATA TATATAGCGG CCGCACGTC	linker, pIRESlacZneoflox construction
L2sense	GCTTAAGAAT ATTTTTAAAG GATCCGCTAG CAATATTCTT AAGG	Linker, targeting vector construction
L2antisense	AATTCCTTA AGAATATTGC TAGCGGATCC TTTAAAAATA TTCTTAAGCT GCA	Linker, targeting vector construction
AAC+SV40fwd	AACGATCCGC ATCTCAATTA GTC	SV40 polyA signal PCR
AAC+SV40rev	ATCGATCCAG ACATGATAAG ATA	SV40 polyA signal PCR
SAP1A	TCGTTACAAA GTCTGAGGTG CAAACAAAAG TCTCTATCAA GGCAGTACTA AAGGTACCT CCATTCTACC AAACGTCGTG ACTGGGAAAA C	BAC excision I
SAP1B	TCCTCCATTC CTTGGAATAC ATAAAGAGGG ACAAGCATTG GAAGTTGCTT CCCAGTTCT CTCCCTTGAG CGCGGCCGCTT CGACTCTAGT GGATCTGC	BAC excision I
SAP2A	AAATGACTGT GCCCTTCCAC CCCCTTTCAG GGCAACTCTG GCCTTGGCTT CAGTATCGCA GAGCAGAAGC TGATCAGCGA GGAGGACCTG TGATTTAAAC TGATCCCGGG CCGCTCTA	lacZ insertion I
SAP2B	CTCCCGTTCT TCTTGCACTA CTAGAGCACC TGTTAGCACC AGGTTCCTCC TCCACAGAGC TTACAGGCCT GCAGGGCCTG AAGCTTAATA CGCAAACCGC CTCTC	lacZ insertion I
aa1fwd	CCGGGGTACC GGGGGTTGTA TGTGGTGTGT	BAC excision II
aa1rev	AATTGGCGCG CCCCACTCAG AGAAGACCCT GC	BAC excision II
aa2fwd	AATTGGCGCG CCAGCAGCCG TTCATTATTT GG	BAC excision II
aa2rev	CAGCTTGTTT AAACGCATGC TCAAGGGAGA GAAC	BAC excision II
SAP2Afwd	ATAAGAATGC GGCCGCTCCT ATGGATGTTG GGTGTG	lacZ insertion II
SAP2Arev	TTGGCGCGCC TTTAAATCAC AGGTCCTCCT CGCTGATCAG CTTCTGCTCA CCTGCGATAC TGAAGCCAA	lacZ insertion II
SAP2Bfwd	TAAGCTTTGT TTAAACAAGC TTTGTAATCC TGGCCTTTGT CC	lacZ insertion II
SAP2Brev	TATGCCTTAA TTAACCACTG AGAGAGCAGG AACC	lacZ insertion II
SAP5'neofloxfwd	TATACTCGAG GACAGGATGG AGATGAGGGA	neoflox insertion

SAP5'neofloxrev	TATATCTAGA GCTAGCTCCC TTCCATTCAC CTATGG	neoflox insertion
SAP3'neofloxfwd	TATAGGTACC ATGCATGATA TCGAATTCCC AGTCCCAGAT CCTAGCCT	neoflox insertion
SAP3'neofloxrev	TATAAGATCT GCCAAAATGC CTTATCCTGA	neoflox insertion
SAP5'loxPneoflrtfwd	TATATAGCGG CCGCGGGAGG CAGAGCAGAC TATG	loxPneoflrt insertion
SAP5'loxPneoflrtrev	TATAGGCGCG CCTCCTTCAAAG GTCCCAGAAA	loxPneoflrt insertion
SAP3'loxPneoflrtfwd	TATAGTTTAA ACAAGCTTTA AATTACCACT GGCCTTGAAA CC	loxPneoflrt insertion
SAP3'loxPneoflrtrev	TATATAGTCG ACACATCCCTCC CCTTGTATCC	loxPneoflrt insertion

Appendix 3. Full sequences of *TARGETER* plasmids

1. p*TARGETER* (4,673 bp)

tgatcataactagttacatatgtaggtacctacacgtgtaggcgcgcctagtttaaactaaagcttgcatgcggcccggtcgaccgggccgcatctagct
agagtcgatcgaccagcttctgatggaattagaacttggcaaaacaatactgagaatgaagtgtatgtggaacagaggctgctgatctcgttcttcaggc
tatgaaactgacacatttggaaaccacagtacttagaaccacaaagtgggaatcaagagaaaaacaatgatcccacgagagatctatagatctatagatc
atgagtgggaggaatgagctggccctaatttggttttgcttgtttaaattatgatatccaactatgaaacattatcataaagcaatagtaaagagccctt
cagtaaagagcaggcatttatctaatcccaccccacccccacccccgtagctccaatccttccattcaaaatgtaggtactctgttctcaccctttaa
caaagtatgacaggaaaaacttccattttagtggacatctttattgtttaatagatcatcaatttctgcatccctcgactctagtggatctgcattccac
cactgctcccattcatcagttccataggttggaatctaaaatacacaaacaattagaatcagtagtttaacacattatacacttaaaaattttatattta
ccttagagctttaaatctctgtaggtagtttgtccaattatgtcacaccacagaagtaaggttccttcacaaagagatcgcctgacacgatttcctgcac
aggcttgagccatatactcatacatcgcatcttggccacgttttccacgggtttcaaaattaatctcaagttctacgcttaacgctttcgcctgttccca
gttattaatatattcaacgctagaactcccctcagcgaagggaaggctgagcactacacgcgaagcaccatcaccgaaccttttgataaactcttccgtt
ccgacttgctccatcaacggttcagtgagacttaaacctaactctttcttaatagtttcggcattatccacttttagtgcgagaaccttcgtcagtcctg
gatacgtcactttgaccacgcctccagctttccagagagcgggttttcattatctacagagtatcccgcagcgtcgtatttattgtcggtactataaaa
ccctttccaatcatcgtcataatttccttgtgtaccagattttggctttgtatacctttttgaatggaatctacataaccaggtttagtcccgtggtac
gaagaaaagttttccatcacaaaagatttagaagaatcaacaacatcatcaggatccatggcgaggacctgcagggtcgctcggtgttcgaggccacacg
cgtcaccttaatatgcgaagtggacctgggaccgcgccgccccgactgcatctgcgtgttcgaattcgccaatgacaagacgctgggcgggggtttgctcg
acattgggtggaaacattccaggcctgggtggagaggcttttgcttcctcttgcaaaaccacactgctcgacattgggtggaaacattccaggcctggg
tggagaggcttttgcttcctcttgaaaaccacactgctcgagcagctgtccctcctgttcagctactgacggggtggtgcgtaacggcaaaagcaccgc
cggacatcagcgctagcggagtgtatactggcttactatgttggcactgatgagggtgtcagtgaagtgcttcatgtggcaggagaaaaaaggctgcacc
ggtgcgtcagcagaatatgtgatacaggatatattccgcttcctcgctcactgactcgctacgctcggtcgttcgactgcggcgagcggaaatggcttac
gaacgggggcggagatttcctggaagatgccaggaagatacttaacagggaagtgagagggccgcggcaaagccgtttttccataggctccgccccctga
caagcatcacgaaatctgacgctcaaatcagtggtggcgaaacccgacaggactataaagataccaggcgtttccccctggcggctccctcgtgcgctct
cctgttcctgccttttcggtttaccggtgtcattccgctgttatggccgcgtttgtctcattccacgcctgacactcagttccgggtaggcagttcgctcc
aagctggactgtatgcacgaaccccccgttcagtccgaccgctgcgccttatccggtaactatcgtcttgagtccaacccggaaagacatgcaaaagcac
cactggcagcagccactggtaattgatttagaggagttagtcttgaagtcatgcgccggttaaggctaaactgaaaggacaagttttggtgactgcgctc
ctccaagccagttacctcggttcaaagagttggtagctcagagaaccttcgaaaaaccgccctgcaaggcggttttttcgttttcagagcaagagattac
gcgcagaccaaaacgatctcaagaagatcgatcatcttattaatcagataaaatatttctagatttcagtgcaatttatctcttcaaatgtagcacctga
agtcagccccatacgatataagttgtaattctcatgtttgacagcttatcatcgataagctttaatgcggtagtttatcacagttaaattgctaacgcag
tcaggcaccgtgtatgaaatctaacaatgcgctcatcgtcatcctcggcaccgtcaccctggatgctgtaggcataggcttggttatgccggtactgccg
ggcctcttgcgggatatcgtccattccgacagcatcgccagtcactatggcgtgctgctagcgctatatgcgttgatgcaatttctatgcgcacccgttc
tcggagcactgtccgaccgctttggccgccgcccagtcctgctcgcttcgctacttggagccactatcgactacgcgatcatggcgaccacacccgtcct
gtggatcctctacgccggacgcatcgtggccggcatcaccggcgccacaggtgcggttgctggcgcctatatcgccgacatcaccgatggggaagatcgg
gctcgccacttcgggctcatgagcgcttgtttcggcgtgggtatggtggcaggccccgtggccgggggactgttgggcgccatctccttgcatgcaccat
tccttgcggcggcggtgctcaacggcctcaacctactactgggctgcttcctaatgcaggagtcgcataagggagagcgtcgaccgatgcccttgagagc
cttcaacccagtcagctccttccggtgggcgcggggcatgactatcgtcgccgcacttatgactgtcttctttatcatgcaactcgtaggacaggtgccg
gcagcgctctgggtcattttcggcgaggaccgctttcgctggagcgcgacgatgatcggcctgtcgcttgcggtattcggaatcttgcacgccctcgctc
aagccttcgtcactggtcccgccaccaaacgtttcggcgagaagcaggccattatcgccggcatggcggccgacgcgctgggctacgtcttgctggcgtt
cgcgacgcgaggctggatggccttccccattatgattcttctcgcttccggcggcatcgggatgcccgcgttgcaggccatgctgtccaggcaggtagat
gacgaccatcagggacagcttcaaggatcgctcgcggctcttaccagcctaacttcgatcattggaccgctgatcgtcacggcgatttatgccgcctcgg
cgagcacatggaacgggttggcatggattgtaggcgccgccctataccttgtctgcctccccgcgttgcgtcgcggtgcatggagccgggccacctcgac
ctgaatggaagccggcggcacctcgctaacggattcaccactccaagaattggagccaatcaattcttgcggagaactgtgaatgcgcaaaccaaccctt
ggcagaacatatccatcgcgtccgccatctccagcagccgcacgcggcgcatctcgggcagcgttgggtcctggccacgggtgcgcatgatcgtgctcct
gtcgttgaggacccggctaggctggcggggttgccttactggttagcagaatgaatcaccgatacgcgagcgaacgtgaagcgactgctgctgcaaaacg
tctgcgacctgagcaacaacatgaatggtcttcggtttccgtgtttcgtaaagtctggaaacgcggaagtcccctacgtgctgctgaagttgcccgcaac
agagagtggaaccaaccggtgataccacgatactatgactgagagtcaacgccatgagcggcctcatttcttattctgagttacaacagtccgccaccgct
gccggtagctccttccggtgggcgcggggcatgactatcgtcgccgcacttatgactgtcttctttatcatgcaactcgtaggacaggtgccggcagcgc
ccaacagtcccccggccacggggcctgccaccatacccacgccgaaacaagcgccctgcaccattatgttccggatctgcatcgcaggatgctgctggct
accctgtggaacacctacatctgtattaacgaagcgctaaccgtttttatcaggctctgggaggcagaataaa

2. p*IRESlacZneoflox* (7,647 bp)

aacctgcattaatgaatcggccaacgcgcggggagaggcggtttgcgtattgggcgctcttccgcttcctcgctcactgactcgctgcgctcggtcgttc
ggctgcggcgagcggtatcagctcactcaaaggcggtaatacggttatccacagaatcaggggataacgcaggaaagaacatgtgagcaaaaggccagca
aaaggccaggaaccgtaaaaaggccgcgttgctggcgtttttccataggctccgcccccctgacgagcatcacaaaaatcgacgctcaagtcagaggtgg
cgaaacccgacaggactataaagataccaggcgtttccccctggaagctccctcgtgcgctctcctgttccgaccctgccgcttaccggatacctgtccg
cctttctcccttcgggaagcgtggcgctttctcatagctcacgctgtaggtatctcagttcggtgtaggtcgttcgctccaagctgggctgtgtgcacga
accccccgttcagcccgaccgctgcgccttatccggtaactatcgtcttgagtccaacccggtaagacacgacttatcgccactggcagcagccactggt
aacaggattagcagagcgaggtatgtaggcggtgctacagagttcttgaagtggtggcctaactacggctacactagaagaacagtatttggtatctgcg
ctctgctgaagccagttaccttcggaaaaagagttggtagctcttgatccggcaaacaaaccaccgctggtagcggtggttttttttgtttgcaagcagca
gattacgcgcagaaaaaaaggatctcaagaagatcctttgatcttttctacggggtctgacgctcagtggaacgaaaactcacgttaagggattttggtc
atgagattatcaaaaaggatcttcacctagatccttttaaattaaaaatgaagttttaaatcaatctaaagtatatatgagtaaacttggtctgacagtt
accaatgcttaatcagtgaggcacctatctcagcgatctgtctatttcgttcatccatagttgcctgactccccgtcgtgtagataactacgatacggga
gggcttaccatctggccccagtgctgcaatgataccgcgagacccacgctcaccggctccagatttatcagcaataaaccagccagccggaagggccgag
cgcagaagtggtcctgcaactttatccgcctccatccagtctattaattgttgccgggaagctagagtaagtagttcgccagttaatagtttgcgcaacg
ttgttgccattgctacaggcatcgtggtgtcacgctcgtcgtttggtatggcttcattcagctccggttcccaacgatcaaggcgagttacatgatcccc
catgttgtgcaaaaaagcggttagctccttcggtcctccgatcgttgtcagaagtaagttggccgcagtgttatcactcatggttatggcagcactgcat

aattctcttactgtcatgccatccgtaagatgcttttctgtgactggtgagtattattgaagcatttatcagggttattgtctcatgagcggatacatat
ttgaatgtatttagaaaaataaacaaatagggttccgcgcacatttccccgaaaagtgccacctgacgtgcggccgctatatatatagggcgcgccggat
cctgatcccgggccgctctagctagactagtctagctagagaattccgccctctccccccccccccctaacgttactggccgaagccgcttggaataag
gccggtgtgcgtttgtctatatgttattttccaccatattgccgtcttttggcaatgtgagggcccggaaacctggccctgtcttcttgacgagcattcc
taggggtctttcccctctcgccaaaggaatgcaaggtctgttgaatgtcgtgaaggaagcagttcctctggaagcttcttgaagacaaacaacgtctgta
gcgaccctttgcaggcagcggaacccccccacctggcgacaggtgcctctgcggccaaaagccacgtgtataagatacacctgcaaaggcggcacaacccc
agtgccacgttgtgagttggatagttgtggaaagagtcaaatggctctcctcaagcgtattcaacaaggggctgaaggatgcccagaaggtaccccattg
tatgggatctgatctggggcctcggtgcacatgctttacatgtgtttagtcgaggttaaaaaaacgtctaggccccccgaaccacggggacgtggttttc
ctttgaaaaacacgatgataagcttgccacaaccatggaagatcccgtcgttttacaacgtcgtgactgggaaaaccctggcgttacccaacttaatcgc
cttgcagcacatccccctttcgccagctggcgtaatagcgaagaggcccgcaccgatcgcccttcccaacagttgcgcagcctgaatggcgaatggcgct
ttgcctggtttccggcaccagaagcggtgccggaaagctggctggagtgcgatcttcctgaggccgatactgtcgtcgtcccctcaaactggcagatgca
cggttacgatgcgcccatctacaccaacgtgacctatcccattacggtcaatccgccgtttgttcccacggagaatccgacgggttgttactcgctcaca
tttaatgttgatgaaagctggctacaggaaggccagacgcgaattatttttgatggcgttaactcggcgtttcatctgtggtgcaacgggcgctgggtcg
gttacggccaggacagtcgtttgccgtctgaatttgacctgagcgcatttttacgcgccggagaaaaccgcctcgcggtgatggtgctgcgctggagtga
cggcagttatctggaagatcaggatatgtggcggatgagcggcattttccgtgacgtctcgttgctgcataaaccgactacacaaatcagcgatttccat
gttgccactcgctttaatgatgatttcagccgcgctgtactggaggctgaagttcagatgtgcggcgagttgcgtgactacctacgggtaacagtttctt
tatggcagggtgaaacgcaggtcgccagcggcaccgcgcctttcggcggtgaaattatcgatgagcgtggtggttatgccgatcgcgtcacactacgtct
gaacgtcgaaaacccgaaactgtggagcgccgaaatcccgaatctctatcgtgcggtggttgaactgcacaccgccgacggcacgctgattgaagcagaa
gcctgcgatgtcggtttccgcgaggtgcggattgaaaatggtctgctgctgctgaacggcaagccgttgctgattcgaggcgttaaccgtcacgagcatc
atcctctgcatggtcaggtcatggatgagcagacgatggtgcaggatatcctgctgatgaagcagaacaactttaacgccgtgcgctgttcgcattatcc
gaaccatccgctgtggtacacgctgtgcgaccgctacggcctgtatgtggtggatgaagccaatattgaaacccacggcatggtgccaatgaatcgtctg
accgatgatccgcgctggctaccggcgatgagcgaacgcgtaacgcgaatggtgcagcgcgatcgtaatcacccgagtgtgatcatctggtcgctgggga
atgaatcaggccacggcgctaatcacgacgcgctgtatcgctggatcaaatctgtcgatccttcccgcccggtgcagtatgaaggcggcggagccgacac
cacggccaccgatattatttgcccgatgtacgcgcgcgtggatgaagaccagcccttcccggctgtgccgaaatggtccatcaaaaaatggctttcgcta
cctggagagacgcgcccgctgatcctttgcgaatacgcccacgcgatgggtaacagtcttggcggtttcgctaaatactggcaggcgtttcgtcagtatc
cccgtttacagggcggcttcgtctgggactgggtggatcagtcgctgattaaatatgatgaaaacggcaacccgtggtcggcttacggcggtgattttgg
cgatacgccgaacgatcgccagttctgtatgaacggtctggtctttgccgaccgcacgccgcatccagcgctgacggaagcaaaacaccagcagcagttt
ttccagttccgtttatccgggcaaaccatcgaagtgaccagcgaatacctgttccgtcatagcgataacgagctcctgcactggatggtggcgctggatg
gtaagccgctggcaagcggtgaagtgcctctggatgtcgctccacaaggtaaacagttgattgaactgcctgaactaccgcagccggagagcgccgggca
actctggctcacagtacgcgtagtgcaaccgaacgcgaccgcatggtcagaagccgggcacatcagcgcctggcagcagtggcgtctggcggaaaacctc
agtgtgacgctccccgccgcgtcccacgccatcccgcatctgaccaccagcgaaatggatttttgcatcgagctgggtaataagcgttggcaatttaacc
gccagtcaggctttctttcacagatgtggattggcgataaaaaacaactgctgacgccgctgcgcgatcagttcacccgtgcaccgctggataacgacat
tggcgtaagtgaagcgacccgcattgaccctaacgcctgggtcgaacgctggaaggcggcgggccattaccaggccgaagcagcgttgttgcagtgcacg
gcagatacacttgctgatgcggtgctgattacgaccgctcacgcgtggcagcatcaggggaaaacctttatttatcagccggaaaacctaccggattgatg
gtagtggtcaaatggcgattaccgttgatgttgaagtggcgagcgatacaccgcatccggcgcggattggcctgaactgccagctggcgcaggtagcaga
gcgggtaaactggctcggattagggccgcaagaaaactatcccgaccgccttactgccgcctgttttgaccgctgggatctgccattgtcagacatgtat
accccgtacgtcttcccgagcgaaaacggtctgcgctgcgggacgcgcgaattgaattatggcccacaccagtggcgcggcgacttccagttcaacatca
gccgctacagtcaacagcaactgatggaaaccagccatcgccatctgctgcacgcggaagaaggcacatggctgaatatcgacggtttccatatggggat
tggtggcgacgactcctggagcccgtcagtatcggcggaattccagctgagcgccggtcgctaccattaccagttggtctggtgtcaaaaataataataa
ccgggcaggccatgtctgcccgtatttcgcgtaaggaaatccattatgtactatttaaaaaacacaaacttttggatgttcggtttattcttttttctttt
acttttttatcatgggagcctacttcccgtttttcccgatttggctacatgacatcaaccatatcagcaaaagtgatacgggtattatttttgccgctat
ttctctgttctcgctattattccaaccgctgtttggtctgctttctgacaaactcggaacttgtttattgcagcttataatggttacaaataaagcaata
gcatcacaaatttcacaaatttaattaaggccgcgggatcaagatccataacttcgtatagcatacattatacgaagttatcccagatccccgggctgc
aggaattctaccgggtaggggaggcgcttttcccaaggcagtctggagcatgcgctttagcagccccgctgggcacttggcgctacacaagtggcctctg
gcctcgcacacattccacatccaccggtaggcgccaaccggctccgttctttggtggccccttcgcgccaccttctactcctccctagtcaggaagttc
ccccccgccccgcagctcgcgtcgtgcaggacgtgacaaatggaagtagcacgtctcactagtctcgtgcagatggacagcaccgctgagcaatggaagc
gggtaggcctttggggcagcggccaatagcagctttgctccttcgctttctgggctcagaggctgggaaggggtgggtccgggggcgggctcaggggcgg
gctcagggggcggggcgggcgcccgaaggtcctccggaggcccggcattctgcacgcttcaaaagcgcacgtctgccgcgctgttctcctcttcctcatct
ccgggcctttcgaccgatcatcaagctgcacgtgttgacaattaatcatcggcatagtatatcggcatagtataatacgactcactataggagggccacc
atgggatcggccattgaacaagatggattgcacgcaggttctccggccgcttgggtggagaggctattcggctatgactgggcacaacagacaatcggct
gctctgatgccgccgtgttccggctgtcagcgcaggggcgcccggttcttttgtcaagaccgacctgtccggtgccctgaatgaactgcaggacgaggc
agcgcggctatcgtggctggccacgacgggcgttccttgcgcagctgtgctcgacgttgtcactgaagcgggaagggactggctgctattgggcgaagtg
ccggggcaggatctcctgtcatctcaccttgctcctgccgagaaagtatccatcatggctgatgcaatgcggcggctgcatacgcttgatccggctacct
gcccattcgaccaccaagcgaaacatcgcatcgagcgagcacgtactcggatggaagccggtcttgtcgatcaggatgatctggacgaagagcatcaggg
gctcgcgccagccgaactgttcgccaggctcaaggcgcgcatgcccgacggcgaggatctcgtcgtgacccatggcgatgcctgcttgccgaatatcatg
gtggaaaatggccgcttttctggattcatcgactgtggccggctgggtgtggcggaccgctatcaggacatagcgttggctacccgtgatattgctgaag
agcttggcggcgaatgggctgaccgcttcctcgtgctttacggtatcgccgctcccgattcgcagcgcatcgccttctatcgccttcttgacgagttctt
ctgaggttaacgatccgcatctcaattagtcagcaaccatagtcccgcccctaactccgcccatcccgcccctaactccgcccagttccgcccattctcc
gccccatggctgactaatttttttttatttatgcagaggccgaggccgcctcggcctctgagctattccagaagtagtgaggaggctttttggaggccta
ggcttttgcaaaaagctaacttgtttattgcagcttataatggttacaaataaagcaatagcatcacaaatttcacaaataaagcatttttttcactgca
ttctagttgtggtttgtccaaactcatcaatgtatcttatcatgtctggatcgatatccccataacttcgtatagcatacattatacgaagttatggatc
tggatccgtttaaacttaattaatatatatatatagtcgacgtcgac

3. p*neoflox* (4,342bp)

gaactcgagcagctgaagcttgcatgcctgcaggtcgactctagaggatcctgatcaagatccataacttcgtatagcatacattatacgaagttatccc
agatcccccgggctgcaggaattctaccgggtaggggaggcgcttttcccaaggcagtctggagcatgcgctttagcagccccgctgggcacttggcgct
acacaagtggcctctggcctcgcacacattccacatccaccggtaggcgccaaccggctccgttctttggtggccccttcgcgccaccttctactcctcc
cctagtcaggaagttcccccccgccccgcagctcgcgtcgtgcaggacgtgacaaatggaagtagcacgtctcactagtctcgtgcagatggacagcacc
gctgagcaatggaagcgggtaggcctttggggcagcggccaatagcagctttgctccttcgctttctgggctcagaggctgggaaggggtgggtccgggg

gcgggctcaggggcgggctcaggggcggggcgggcgcccgaaggtcctccggaggcccggcattctgcacgcttcaaaagcgcacgtctgccgcgctgtt
ctcctcttcctcatctccgggcctttcgaccgatcatcaagctgcacgtgttgacaattaatcatcggcatagtatatcggcatagtataatacgactca
ctataggagggccaccatgggatcggccattgaacaagatggattgcacgcaggttctccggccgcttgggtggagaggctattcggctatgactgggca
caacagacaatcggctgctctgatgccgccgtgttccggctgtcagcgcaggggcgcccggttctttttgtcaagaccgacctgtccggtgccctgaatg
aactgcaggacgaggcagcgcggctatcgtggctggccacgacgggcgttccttgcgcagctgtgctcgacgttgtcactgaagcgggaagggactggct
gctattgggcgaagtgccggggcaggatctcctgtcatctcaccttgctcctgccgagaaagtatccatcatggctgatgcaatgcggcggctgcatacg
cttgatccggctacctgcccattcgaccaccaagcgaaacatcgcatcgagcgagcacgtactcggatggaagccggtcttgtcgatcaggatgatctgg
acgaagagcatcaggggctcgcgccagccgaactgttcgccaggctcaaggcgcgcatgcccgacggcgaggatctcgtcgtgacccatggcgatgcctg
cttgccgaatatcatggtggaaaatggccgcttttctggattcatcgactgtggccggctgggtgtggcggaccgctatcaggacatagcgttggctacc
cgtgatattgctgaagagcttggcggcgaatgggctgaccgcttcctcgtgctttacggtatcgccgctcccgattcgcagcgcatcgccttctatcgcc
ttcttgacgagttcttctgaggttaacgatccgcatctcaattagtcagcaaccatagtcccgcccctaactccgcccatcccgcccctaactccgccca
gttccgcccattctccgccccatggctgactaatttttttttatttatgcagaggccgaggccgcctcggcctctgagctattccagaagtagtgaggagg
ctttttggaggcctaggcttttgcaaaaagctaacttgtttattgcagcttataatggttacaaataaagcaatagcatcacaaatttcacaaataaag
catttttttcactgcattctagttgtggtttgtccaaactcatcaatgtatcttatcatgtctggatcgatatccccataacttcgtatagcatacatta
tacgaagttatggatctggatccccgggtaccgagctcgaattcatcgatgatatcagatctgccggtctcccttatagtgagtcgtattaatttcgataa
gccaggttaaccggttaacctgcattaatgaatcggccaacgcgcggggagaggcggtttgcgtattgggcgctcttccgcttcctcgctcactgactcg
ctgcgctcggtcgttcggctgcggcgagcggtatcagctcactcaaaggcggtaatacggttatccacagaatcaggggataacgcaggaaagaacatgt
gagcaaaaggccagcaaaaggccaggaaccgtaaaaggccgcgttgctggcgttttccataggctccgcccccctgacgagcatcacaaaaatcgacg
ctcaagtcagaggtggcgaaacccgacaggactataaagataccaggcgtttcccccctggaagctccctcgtgcgctctcctgttccgaccctgccgctt
accggatacctgtccgcctttctcccttcgggaagcgtggcgctttctcatagctcacgctgtaggtatctcagttcggtgtaggtcgttcgctccaagc
tgggctgtgtgcacgaaccccccgttcagcccgaccgctgcgccttatccggtaactatcgtcttgagtccaacccggtaagacacgacttatcgccact
ggcagcagccactggtaacaggattagcagagcgaggtatgtaggcggtgctacagagttcttgaagtggtggcctaactacggctacactagaagaaca
gtatttggtatctgcgctctgctgaagccagttaccttcggaaaaagagttggtagctcttgatccggcaaacaaaccaccgctggtagcggtggttttt
ttgtttgcaagcagcagattacgcgcagaaaaaaaggatctcaagaagatcctttgatcttttctacggggtctgacgctcagtggaacgaaaactcacg
ttaagggattttggtcatgagattatcaaaaggatcttcacctagatccttttaaattaaaaatgaagttttaaatcaatctaaagtatatatgagtaa
acttggtctgacagttaccaatgcttaatcagtgaggcacctatctcagcgatctgtctatttcgttcatccatagttgcctgactccccgtcgtgtaga
taactacgatacgggagggcttaccatctggccccagtgctgcaatgataccgcgagacccacgctcaccggctccagatttatcagcaataaaccagcc
agccggaagggccgagcgcagaagtggtcctgcaactttatccgcctccatccagtctattaattgttgccgggaagctagagtaagtagttcgccagtt
aatagtttgcgcaacgttgttgccattgctacaggcatcgtggtgtcacgctcgtcgtttggtatggcttcattcagctccggttcccaacgatcaaggc
gagttacatgatcccccatgttgtgcaaaaaagcggttagctccttcggtcctccgatcgttgtcagaagtaagttggccgcagtgttatcactcatggt
tatggcagcactgcataattctcttactgtcatgccatccgtaagatgcttttctgtgactggtgagtactcaaccaagtcattctgagaatagtgtatg
cggcgaccgagttgctcttgcccggcgtcaatacgggataataccgcgccacatagcagaactttaaaagtgctcatcattggaaaacgttcttcggggc
gaaaactctcaaggatcttaccgctgttgagatccagttcgatgtaacccactcgtgcacccaactgatcttcagcatcttttactttcaccagcgtttc
tgggtgagcaaaaacaggaaggcaaaatgccgcaaaaaagggaataagggcgacacggaaatgttgaatactcatactcttccttttcaatattattga
agcatttatcagggttattgtctcatgagcggatacatatttgaatgtatttagaaaaataaacaaatagggttccgcgcacatttccccgaaaagtgc
cacctgacgtctaagaaaccattattatcatgacattaacctataaaaatagcgtatcacgaggccctttcgtctcgcgcgtttcggtgatgacggtga
aaacctctgacacatgcagctcccggagacggtcacagcttgtctgtaagcggatgccgggagcagacaagcccgtcagggcgcgtcagcgggtgttggc
gggtgtcggggctggcttaactatgcggcatcagagcagattgtactgagagtgcaccatatggacatattgtcgttagaacgcggctacaattaataca
taaccttatgtatcatacacatacgatttaggtgacactata

4. p*loxPneoflrt* (4,899 bp)

ctgacgcgccctgtagcggcgcattaagcgcggcgggtgtggtggttacgcgcagcgtgaccgctacacttgccagcgccctagcgcccgctcctttcgc
tttcttcccttcctttctcgccacgttcgccggctttccccgtcaagctctaaatcgggggctccctttagggttccgatttagtgctttacggcacctc
gaccccaaaaaacttgattagggtgatggttcacgtagtgggccatcgccctgatagacggtttttcgccctttgacgttggagtccacgttctttaata
gtggactcttgttccaaactggaacaacactcaaccctatctcggtctattcttttgatttataagggattttgccgatttcggcctattggttaaaaaa
tgagctgatttaacaaaaatttaacgcgaattttaacaaaatattaacgcttacaatttccattcgccattcaggctgcgcaactgttgggaagggcgat
cggtgcgggcctcttcgctattacgccagctggcgaaaggggatgtgctgcaaggcgattaagttgggtaacgccagggttttcccagtcacgacgttg
taaaacgacggccagtgagcgcgcgtaatacgactcactatagggcgaattggagctccaccgcggtggcggccgctctagaactagtggatccataact
tcgtatagcatacattatacgaagttatcccagatcggaagttcctatactttctagagaataggaacttcagatccccgggctgcaggaattctaccg
ggtaggggaggcgcttttcccaaggcagtctggagcatgcgctttagcagccccgctgggcacttggcgctacacaagtggcctctggcctcgcacacat
tccacatccaccggtaggcgccaaccggctccgttctttggtggccccttcgcgccaccttctactcctcccctagtcaggaagttcccccccgccccgc
agctcgcgtcgtgcaggacgtgacaaatggaagtagcacgtctcactagtctcgtgcagatggacagcaccgctgagcaatggaagcgggtaggcctttg
gggcagcggccaatagcagctttgctccttcgctttctgggctcagaggctgggaaggggtgggtccgggggcgggctcatgggcgggctcatgggcggg
gcgggcgcccgaagtcctccggaggcccggcattctgcacgcttcaaaagcgcacgtctgccgcgctgttctcctcttcctcatctccgggcctttcgac
cgatcatcaagctgcacgtgttgacaattaatcatcggcatagtatatcggcatagtataatacgactcactataggagggccaccatgggatcggccat
tgaacaagatggattgcacgcaggttctccggccgccttgggtggagaggctattcggctatgactgggcacaacagacaatcggctgctctgatgccgcc
gtgttccggctgtcagcgcaggggcgcccggttctttttgtcaagaccgacctgtccggtgccctgaatgaactgcaggacgaggcagcgcggctatcgt
ggctggccacgacgggcgttccttgcgcagctgtgctcgacgttgtcactgaagcgggaagggactggctgctattgggcgaagtgccggggcaggatct
cctgtcatctcaccttgctcctgccgagaaagtatccatcatggctgatgcaatgcggcggctgcatacgcttgatccggctacctgcccattcgaccac
caagcgaaacatcgcatcgagcgagcacgtactcggatggaagccggtcttgtcgatcaggatgatctggacgaagagcatcaggggctcgcgccagccg
aactgttcgccaggctcaaggcgcgcatgcccgacggcgaggatctcgtcgtgacccatggcgatgcctgcttgccgaatatcatggtggaaaatggccg
cttttctggattcatcgactgtggccggctgggtgtggcggaccgctatcaggacatagcgttggctacccgtgatattgctgaagagcttggcggcgaa
tgggctgaccgcttcctcgtgctttacggtatcgccgctcccgattcgcagcgcatcgccttctatcgccttcttgacgagttcttctgaggttaacgat
ccgcatctcaattagtcagcaaccatagtcccgcccctaactccgcccatcccgcccctaactccgcccagttccgcccattctccgccccatggctgac
taatttttttttatttatgcagaggccgaggccgcctcggcctctgagctattccagaagtagtgaggaggcttttttggaggcctaggcttttgcaaaaa
gctaacttgtttattgcagcttataatggttacaaataaagcaatagcatcacaaatttcacaaataaagcatttttttcactgcattctagttgtggtt
tgtccaaactcatcaatgtatcttatcatgtctggatcgatatcataatttaaacaagcaaaaccaaattaagggccagctcattcctcccactcatgat
ctatagatctggatctgaagttcctatactttctagagaataggaacttcggatccaagcttatcgataccgtcgacctcgaggggggggcccggtaccca

gcttttgttccctttagtgagggttaattgcgcgcttggcgtaatcatggtcatagctgtttcctgtgtgaaattgttatccgctcacaattccacacaa
catacgagccggaagcataaagtgtaaagcctggggtgcctaatgagtgagctaactcacattaattgcgttgcgctcactgcccgctttccagtcggga
aacctgtcgtgccagctgcattaatgaatcggccaacgcgcggggagaggcggtttgcgtattgggcgctcttccgcttcctcgctcactgactcgctgc
gctcggtcgttcggctgcggcgagcggtatcagctcactcaaaggcggtaatacggttatccacagaatcaggggataacgcaggaaagaacatgtgagc
aaaaggccagcaaaaggccaggaaccgtaaaaaggccgcgttgctggcgtttttccataggctccgccccctgacgagcatcacaaaaatcgacgctca
agtcagaggtggcgaaacccgacaggactataaagataccaggcgtttccccctggaagctccctcgtgcgctctcctgttccgaccctgccgcttaccg
gatacctgtccgcctttctcccttcgggaagcgtggcgctttctcatagctcacgctgtaggtatctcagttcggtgtaggtcgttcgctccaagctggg
ctgtgtgcacgaaccccccgttcagcccgaccgctgcgccttatccggtaactatcgtcttgagtccaacccggtaagacacgacttatcgccactggca
gcagccactggtaacaggattagcagagcgaggtatgtaggcggtgctacagagttcttgaagtggtggcctaactacggctacactagaaggacagtat
ttggtatctgcgctctgctgaagccagttaccttcggaaaaagagttggtagctcttgatccggcaaacaaaccaccgctggtagcggtggttttttgt
ttgcaagcagcagattacgcgcagaaaaaaaggatctcaagaagatcctttgatcttttctacggggtctgacgctcagtggaacgaaaactcacgttaa
gggattttggtcatgagattatcaaaaaggatcttcacctagatccttttaaattaaaaatgaagttttaaatcaatctaaagtatatatgagtaaacttt
ggtctgacagttaccaatgcttaatcagtgaggcacctatctcagcgatctgtctatttcgttcatccatagttgcctgactccccgtcgtgtagataac
tacgatacgggagggcttaccatctggccccagtgctgcaatgataccgcgagacccacgctcaccggctccagatttatcagcaataaaccagccagcc
ggaagggccgagcgcagaagtggtcctgcaactttatccgcctccatccagtctattaattgttgccgggaagctagagtaagtagttcgccagttaata
gtttgcgcaacgttgttgccattgctacaggcatcgtggtgtcacgctcgtcgtttggtatggcttcattcagctccggttcccaacgatcaaggcgagt
tacatgatcccccatgttgtgcaaaaaagcggttagctccttcggtcctccgatcgttgtcagaagtaagttggccgcagtgttatcactcatggttatg
gcagcactgcataattctcttactgtcatgccatccgtaagatgcttttctgtgactggtgagtactcaaccaagtcattctgagaatagtgtatgcggc
gaccgagttgctcttgcccggcgtcaatacgggataataccgcgccacatagcagaactttaaaagtgctcatcattggaaaacgttcttcggggcgaaa
actctcaaggatcttaccgctgttgagatccagttcgatgtaacccactcgtgcacccaactgatcttcagcatcttttactttcaccagcgtttctggg
tgagcaaaaacaggaaggcaaaatgccgcaaaaaagggaataagggcgacacggaaatgttgaatactcatactcttcctttttcaatattattgaagca
tttatcagggttattgtctcatgagcggatacatatttgaatgtatttagaaaaataaacaaatagggttccgcgcacatttccccgaaaagtgccac